The Development of Catalytic Enantioselective Additions to Imines

A thesis submitted in partial fulfilment of the requirement for the degree of Doctor of Philosophy (D. Phil.)

Gerard Phillip Robertson

Supervisor: Prof. Darren J. Dixon

Somerville College

University of Oxford

Trinity Term 2017

Great are the works of the Lord, they are pondered by

all those who delight in them. (Psalm 111:2)

To my darling wife, Amanda Nicole Robertson…

Table of Contents

Abstract

The Development of Catalytic Enantioselective Additions to Imines

Gerard P. Robertson Somerville College D.Phil Trinity term 2017

This thesis describes the development and application of catalytic enantioselective additions to imines. **Chapter 2** describes the application of bifuntional iminophosphorane (BIMP) organosuperbases, which are a novel class of bifunctional organocatalyst developed in the group to the first 'unactivated' ketimine phospha-Mannich reaction of diethyl phosphite to afford α-aminophosphonic acid derivatives in excellent yields and moderate enantiocontrol (>99% yield, up to 71% ee).

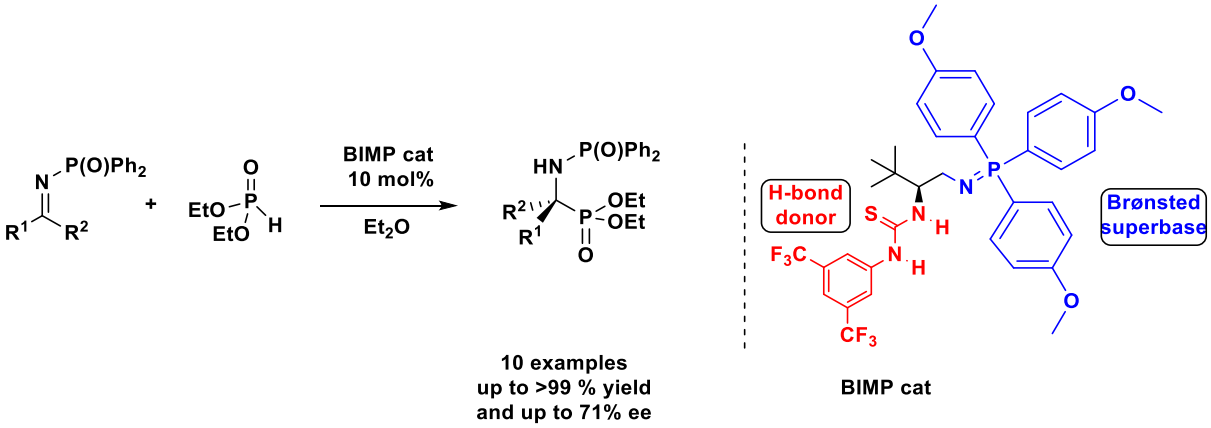

Chapter 3 describes the first silver-catalysed enantioselective Mannich reaction of diazoacetates to *N*-Boc protected aldimines. The reaction proved to be broad in scope with respect to the aldimine; with 14 aromatic aldimines reported and variability on the diazoacetate was also tolerated, giving products with good yields (60-86%) and with very high levels of enantioselectivity (88-98% ee) under the control of the bisphosphine ligand, DM-Segphos. The reaction proved to be scalable as demonstrated on a 5.0 mmol scale with a 1 mol% catalyst loading with respect to silver triflate. The Mannich adduct was derivatised to a few useful products with retention of stereochemical configuration. NMR techniques and non-linear effects studies were used to analyse the catalytic system and gain an insight into the mechanism of this reaction.

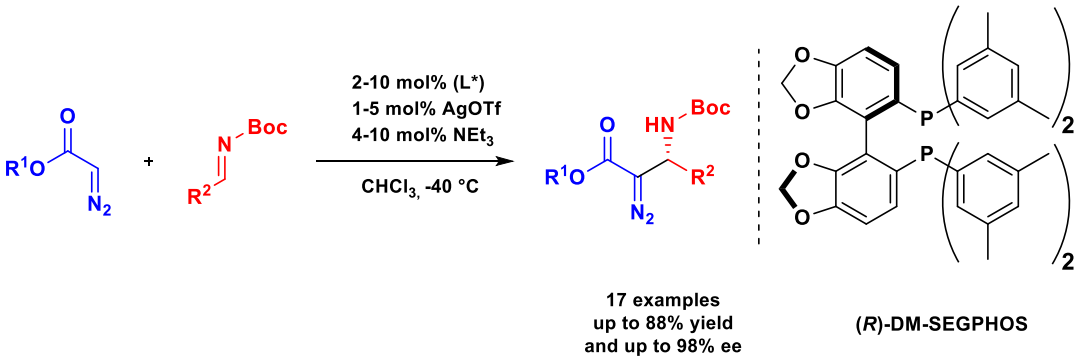

Chapter 4 describes efforts towards the first enantioselective Mannich reaction of ethyl diazoacetate to ketimines. The catalytic system used for this reaction was a modification of the one described in chapter 3, where BEMP was required as a base for reactivity, silver acetate and a chiral aminophosphine ligand made up the catalytic system. Although new reactivity was identified, catalytic turnover was plausibly hampered by reduction of the Ag(I) from the deprotonated diazoacetate. The Mannich adduct was formed in up to 47% yield and up to 42% ee.

Chapter 5 describes the discovery of a novel, practical method for determining the longitudinal relaxation times of low γ spin -1/2 nuclei which are scalar coupled to high γ nuclei. The discovery of this method came about from mechanistic investigations into the catalytic system reported in chapter 3. The method makes it possible to extract T_1 information for the insensitive low γ nucleus from the EXSY spectrum of the observable high γ nucleus. It is shown how the T_1 relaxation constants of Ag can provide valuable insights into the geometrical properties of Ag-bisphosphine complexes. In principle, this method can be applied to any transition metal-ligand system and overcomes the limitations of conventional methods for T_1 determination as it allows for the elucidation of T_1 relaxation time constants of insensitive transition metal nuclei using standard NMR equipment.

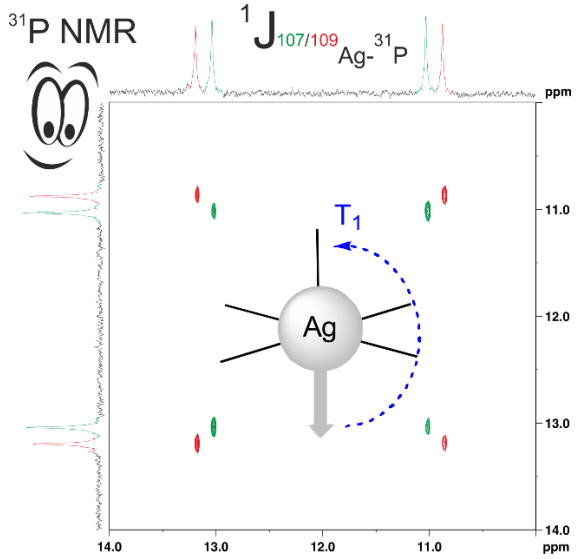

Declarations and Copyright

I declare that thesis has been written by me, that it is the record of work carried out by me and that it has not been submitted in any previous application for a higher degree at this or any other university or institute of learning. Work that was done as part of a collaboration with a research colleague has been fully acknowledged and referenced within the text.

I was admitted as a probationary research student in October 2013 and as a candidate for the degree of Doctor of Philosophy in October 2014; the higher study for which this is a record was carried out in the University of Oxford between 2013 and 2017.

Gerard P. Robertson

Date 11 Jun 2018 Signature of candidate 

In submitting this thesis to the University of Oxford, I understand that I am giving permission for it to be made available for use in accordance with the regulations of the University Library for the time being in force, subject to any copyright vested in the work not being affected thereby. I also understand that the title and the abstract will be published, and that a copy of the work may be made and supplied to any *bona fide* library or research worker, that this thesis will be electronically accessible for personal or research use, and that the library has the right to migrate this thesis into new electronic forms as required to ensure continued access to the thesis. I have obtained any third-party copyright permissions that may be required in order to allow such access and migration.

Acknowledgements

Firstly, I would like to thank Darren for taking me on as a DPhil student and giving me the opportunity to study the exciting chemical systems that are unique to his group and for the challenge that come with this. Thank you for your mentorship throughout my DPhil, your passion for chemistry has been ingrained within me and it is for this that I am most thankful as it is my passion for chemistry that makes my research meaningful. Secondly, I must thank Dr. Barbara Odell from the bottom of my heart for all the times we had together trying to make sense of our NMR data despite that it seemed as if we were on a wild goose chase at first! Thank you for your enthusiasm and diligence which rubbed off on me so very easily and thank you for being an inspiration to me, not just in my scientific endeavours but also in my life. I must also thank Prof. Dr. Timothy. D. W. Claridge for your ingenious insight; predicting the results and applications of the unique properties of the EXSY spectra of our silver-bisphosphine complexes. Thanks to Dr. Alistair J. M. Farley for your advice and insight. Thanks also for being a great friend to me and for that time we worked day in day out to get our paper out. That was an enjoyable, albeit tiring time and it is a memory which will stay with me for the rest of my life. Special thanks go to Heyao Shi for your humility, patience and companionship and thanks most of all for being so inspirational to me in all areas of my life, but most notably in chemistry. You are my number one nickoice. Thanks go to Angel Fuentes, Heyao Shi, Sam Ellis and Alistair Farley for proofreading this thesis. Thanks to Mum, Dad and Andrew for being the best family I could ever ask for. Thank you, Dad for your wise words and advice which will remain with me for the rest of my life and have shaped me as a person, as a man. I would not be the man I am today if it were not for you. Lastly, but not least, I must thank my beautiful wife, Amanda Robertson for your encouragement and listening to me talk on and on about chemistry, despite it boring you somewhat. Thanks also for listening to me practice my presentation talks, even though you fell asleep, I appreciated having an audience. Thanks most of all for your undying love and endless perseverance. Truly, a cord of three strands is not easily broken.

Abbreviations

Å	Angstrom
Ac	Acetyl
aq.	Aqueous
Ar	Aryl
BEMP	2-*tert*-butylimino-2-diethylamino-1,3-dimethylperhydro-1,3,2-diazaphosphorine
BIMP	Bifunctional IMinoPhosphorane
BINAP	2,2'-Bis(diphenylphosphino)-1,1'-binaphthalene
BINOL	1,1'-bi-2,2'-naphthol
Bn	Benzyl
Boc	*tert*-Butyloxycarbonyl
BOX	Bisoxazoline
BTMG/Barton's base	2-*tert*-Butyl-*N*,*N*,*N*',*N*'-Tetramethylguanidine
Bu	Butyl
Cbz	Carboxybenzyl
CPME	Cyclopentylmethyl ether
Cy	Cyclohexyl
DABCO	1,4-Diazabicyclo[2.2.2]octane
DBU	1,8-Diazabicyclo[5.4.0]undec-7-ene
DIAD	Diisopropyl azodicarboxylate
DMAP	4-(Dimethylamino)pyridine
DMF	Dimethylformamide
DMSO	Dimethylsulfoxide
DOSY	Diffusion Ordered Spectroscopy
dr	Diastereomeric ratio
ee	Enantiomeric excess
equiv	Equivalents
Et	Ethyl
EWG	Electron Withdrawing Group
EXSY	Exchange Spectroscopy
HOMO	Highest Occupied Molecular Orbital
HPLC	High Performance Liquid Chromatography

HRMS	High Resolution Mass Spectrometry
Im	Imidazole
IR	Infrared
LRMS	Low Resolution Mass Spectrometry
LUMO	Lowest Unoccupied Molecular Orbital
Me	Methyl
Mes	Mesityl
MS	Molecular sieves
N-DPP	*N*-diphenylphosphoryl
NOESY	Nuclear Overhauser effect spectroscopy
NMI	1-Methylimidazole
Np	Naphthyl
PG	Protecting group
Ph	phenyl
PMB	para-methoxybenzyl
PMP	para-methoxyphenyl
Pr	Propyl
PS-BEMP	Polystyryl 2-tert-butylimino-2-diethylamino-1,3-dimethylperhydro-1,3,2-diazaphosphorine
PyBOP	Benzotriazol-1-yl-oxytripyrrolidinophosphonium hexafluorophosphate
RBF	Round bottom flask
RDS	Rate Determining Step
rt	Room temperature
SSSE	Spin-state satellite exchange
TBAF	Tetra-*n*-butylammonium fluoride
TBS	*tert*-Butyldimethylsilyl
tBu	*tert*-Butyl
Tf	Trifluoromethanesulfonyl
TFA	Trifluoroacetic acid
TfOH	Trifluoromethanesulfonic acid
THF	Tetrahydrofuran
TMG	*N*,*N*,*N*',*N*'-Tetramethylguanidine
t_{mix}	Mixing time

TMS	Trimethylsilyl
TOF	Turnover frequency
TON	Turnover number
TS	Transition state
Ts	Tosylate

1. Introduction

1.1 Introduction to Chiral Amines

Chiral amines can be defined as any compound containing an amine (primary, secondary, tertiary or quaternary) motif attached to a stereogenic carbon atom in a molecule. Chiral amines are present in many synthetically relevant compounds, from alkaloid natural products to drug compounds. The precise 3-dimensional configuration of chiral amine moieties is an important facet of these compounds (Figure 1). Therefore, there is a need for the discovery and development of new, efficient, enantioselective methodologies for the synthesis of compounds containing chiral amine functionalities.

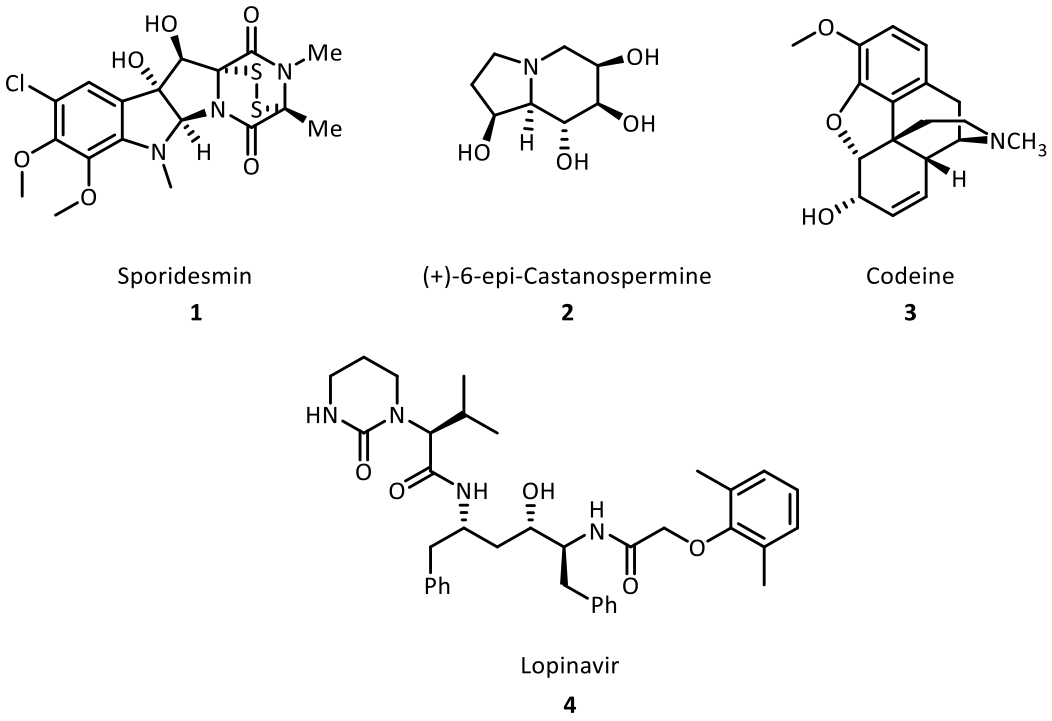

Figure 1: Natural products and drug molecules possessing chiral amine motifs.

The 1,2-addition of nucleophiles to imine electrophiles is a powerful synthetic tool for the synthesis of chiral amines. Facial selectivity on the imine electrophile can be achieved in a variety of different ways, most notably using a chiral catalyst which not only serves to impart stereoselectivity in the product, but also serves to activate the imine electrophile, resulting in the lowering of the LUMO (lowest unoccupied molecular orbital) and consequently the activation energy, resulting in C-C bond formation with the nucleophile. This chapter aims to provide an overview of some of the relevant

catalytic enantioselective 1,2-addition reactions to imines for the synthesis of chiral amines. The examples presented herein are most closely related to the work presented in this thesis.

1.2 Additions using Organometallic Reagents

1.2.1 Lewis base Activation

The use of Lewis bases to activate organometallics such as organolithiums is well known. Organolithiums are known to form aggregates with each other and coordinating ethereal solvents. Any ligand that can coordinate to the lithium centre deaggregates the organolithium, consequently making it more reactive. Recently, dimeric and higher aggregate mechanisms for reactivity of organolithiums with Lewis bases have been elucidated.[1]Tomioka and co-workers[2], in the early 1990s reported one of the first examples where a chiral Lewis basic ligand was used to induce asymmetry in the product as a result of a 1,2-addition reaction of an organolithium to an imine electrophile (derived from benzaldehyde **5a** and cinnamaldehyde **5b**) utilising 30 mol% of chiral ligand **6** as a Lewis base (Scheme 1).

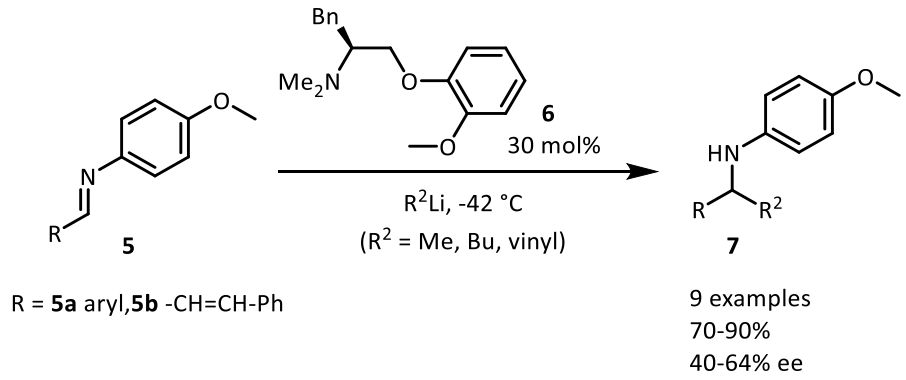

Scheme 1: Tomioka's enantioselective organolithium addition into aldimine electrophiles.

The reaction afforded the product, amine **7** in good yields and moderate to good enantioselectivity. Soon after, Soai[3] *et al.* reported the enantioselective alkylation of *N*-diphenyl phosphinoyl aldimines using a dialkyl zinc species with chiral β-amino alcohols (**9a** or **9b**) as chiral ligands (Scheme 2).

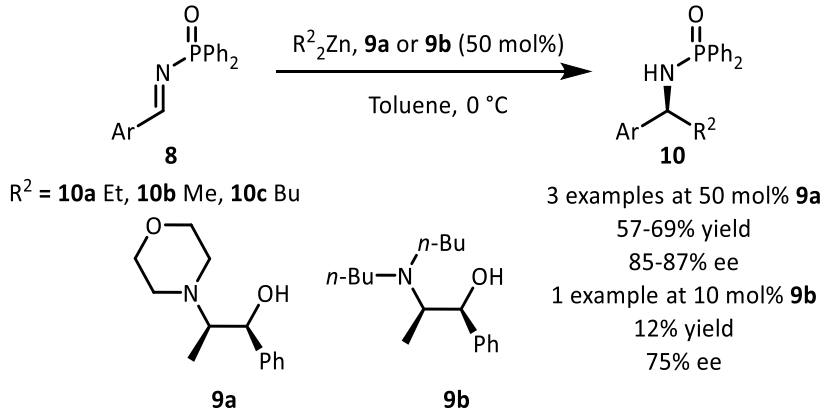

Scheme 2: Soai's enantioselective addition of diethyl zinc to *N*-DPP aldimines utilising chiral β-amino alcohol chiral ligands.

High catalyst loadings of 50 mol% were required for reactivity, with one example being reported at 10 mol% of **9b** for the addition of an ethyl group from diethyl zinc to the aldimine derived from benzaldehyde. Although reactivity was poor using this latter condition, enantioselectivity was not attenuated significantly compared with the results obtained with 50 mol% β-amino alcohol loadings. Overall, the high catalyst loadings required for reactivity had practicality issues associated with it, but nevertheless served as a foundation for further work.

Denmark *et al.* reported a highly enantioselective method for the reaction of organolithiums with *N*-anisyl imines.[4] The reaction utilised a chiral, *C*-2 symmetric bisoxazoline (BOX) ligand (Scheme 3) and was conducted in a non-coordinating solvent such as toluene to improve the interaction between the organometallic and the ligand.

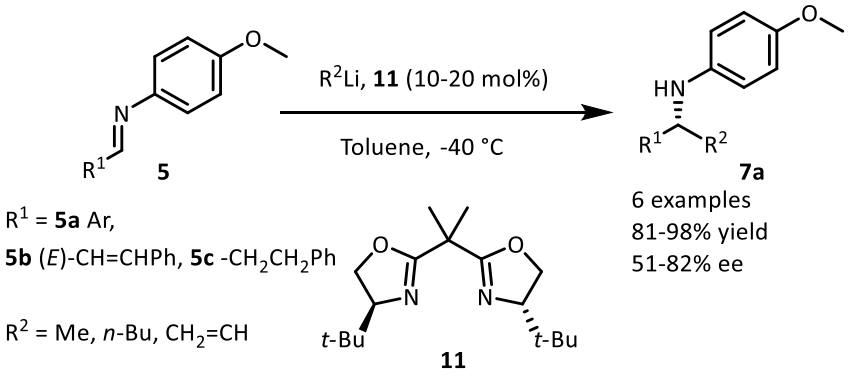

Scheme 3: Denmark's bisoxazoline (BOX) catalysed addition of organolithiums to aldimines.

The reaction gave excellent yields and moderate to high levels of enantioselectivity of the desired product under catalytic organolithium. It was shown that in the absence of bisoxazoline ligand **11**, the reaction barely proceeded with methyllithium as the organometallic and the benzaldehyde derived imine substrate (R^1 = ph). As was mentioned above, Lewis base additives change the aggregation properties of organolithium reagents to render them more reactive as was shown by extensive studies

of phenyllithium and butyllithium solutions in the presence of Lewis basic additives.[5,6] Therefore, as there was little background reaction with MeLi, the ligand could induce attack from the complexed organometallic on to one face of the aldimine substrate. This was reflected in their results; with significant erosion in enantioselectivity being observed when background reactions associated with the use of other organolithium species were in operation.

In a similar manner, in 2005, Alexakis found good yields and moderate enantioselectivities for the addition of methyl lithium to a range of aromatic aldimines bearing an *N*-*para*-methoxyphenyl protecting group.[7] The reaction was catalysed by 20 mol% of *C2*- symmetric diamine **12a** (Scheme 4), and was broadly tolerant of electron-rich and electron-poor aromatic aldimines (12, examples, 42-98% yield, 4-68% ee). It was found that sterically demanding R-substituents on the stereogenic nitrogen atoms of the ligand led to an increase in enantioselectivity.

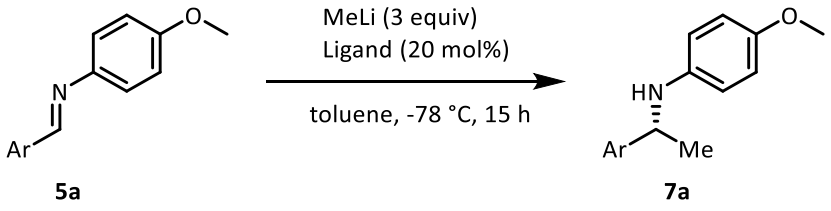

5a **7a**

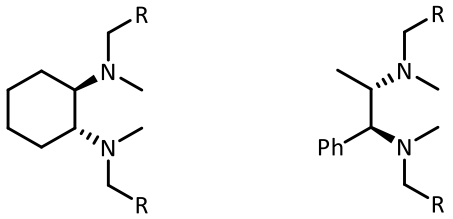

12a **12b**

R = CH_2Ph, CH_2t-Bu	R = CH_2Ph
12 examples	6 examples
42-90% yield	17-91% yield
4-68% ee	30-69% ee*

Scheme 4: Alexakis' enantioselective addition of methyl lithium to *N*-*p*-methoxy phenyl aldimines. *Product obtained with (*S*)-configuration.

Further work involved evaluation of ligand **12b**, derived from (1*S*, 2*S*)-pseudoephedrine, which generally gave rise to comparable levels of reactivity and enantiocontrol in contrast to the analogous diamine ligand **12a** (6 examples, 17-91% yield, 30-69% ee).[8]

1.2.2 Additions of Organozinc reagents using Lewis acid Activation

Lewis acids can be employed to activate imine electrophiles on coordination of the imine to the electron deficient Lewis acid through the lone pair of electrons on the nitrogen atom. This donation

of electron density from the imine makes its carbon more electron deficient and thereby increases its electrophilicity. In 2000, Tomioka[9] developed a novel copper(II)-amidophosphine catalysed asymmetric addition of diethylzinc into *N*-sulfonylimines in excellent yields and enantioselectivities, with catalyst loadings as low as 1 mol% being achieved (Scheme 5).

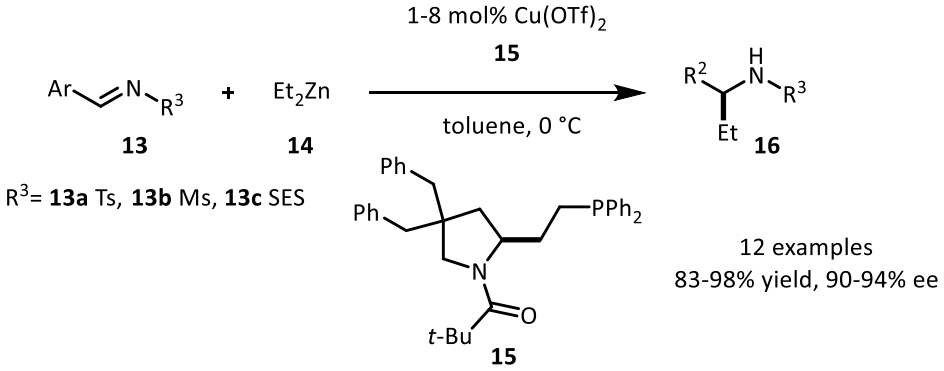

Scheme 5: Tomioka's copper-catalysed asymmetric addition of diethylzinc to *N*-sulfonyl aldimines.

Later, modifications to the amidophosphine ligand allowed application of the chemistry to enolizable imines of alkanals[10], which were poor substrates in previous organolithium methods. Wang[11] and co-workers reported a similar method for the enantioselective addition of diethylzinc (**14**) with *N*-diphenylphosphinoyl (*N*-DPP) aldimines using planar, chiral ferrocene ligands (Scheme 6). The products were obtained in excellent enantioselectivities overall.

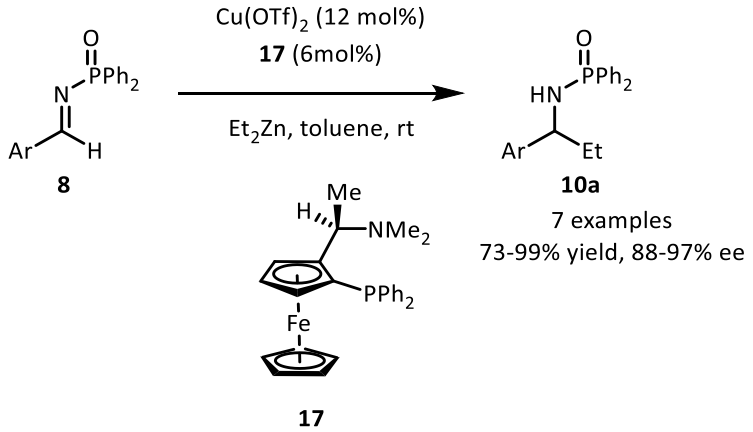

Scheme 6: Wang's Copper-catalysed addition of diethylzinc to *N*-DPP aldimines.

However, Wang's method was not applicable to enolizable *N*-DPP aldimines due to their instability under the reaction conditions. This problem was circumvented by Charette and co-workers who formed the aldimines *in situ* under the basic conditions employed, from amidosulfone precursors **18** (Scheme 7).[12]

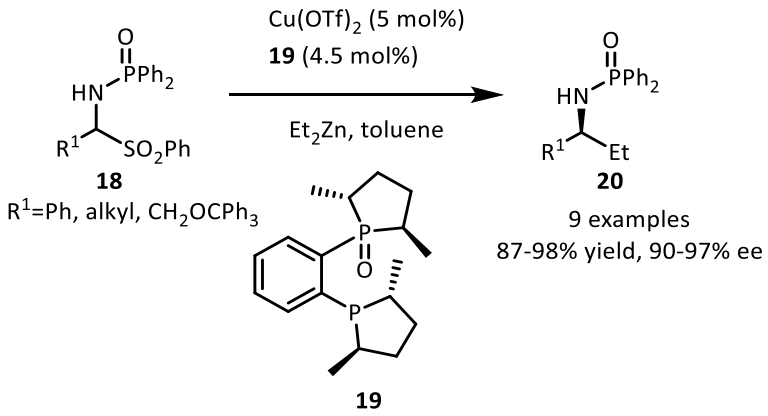

Scheme 7: Charette's copper-catalysed addition of diethylzinc to *N*-DPP aldimines formed *in situ* from amidosulfone precursors.

Hoveyda and Snapper reported the highly enantioselective addition of dialkylzincs to imines in the presence of a chiral peptide based ligand and a Lewis acid from Zr(O-*i*Pr)$_4$ with alkyl, aryl, alkenyl and alkynyl imines all being well tolerated (Scheme 8). The reaction afforded the desired product in good yields and excellent enantioselectivities and was a very general application, as exemplified by the very broad substrate scope.[13] Interestingly, the use of less Lewis acidic Hf(O-*i*Pr)$_4$ resulted in improved reactivity and similar selectivities when compared with zirconium activation.[14] It was elucidated that the AA2 region (see Scheme 8) of the peptide ligand coordinated to the organozinc through the carbonyl of the electron-rich amide and thereby was acting as a Lewis base. Reactivity was facilitated by this effect as the coordination of a Lewis base to an organozinc reduces the bond order of Zn-C bonds and thereby increases the nucleophilicity of the organozinc. The transition metal centre was proposed to activate the imine electrophile through coordination.

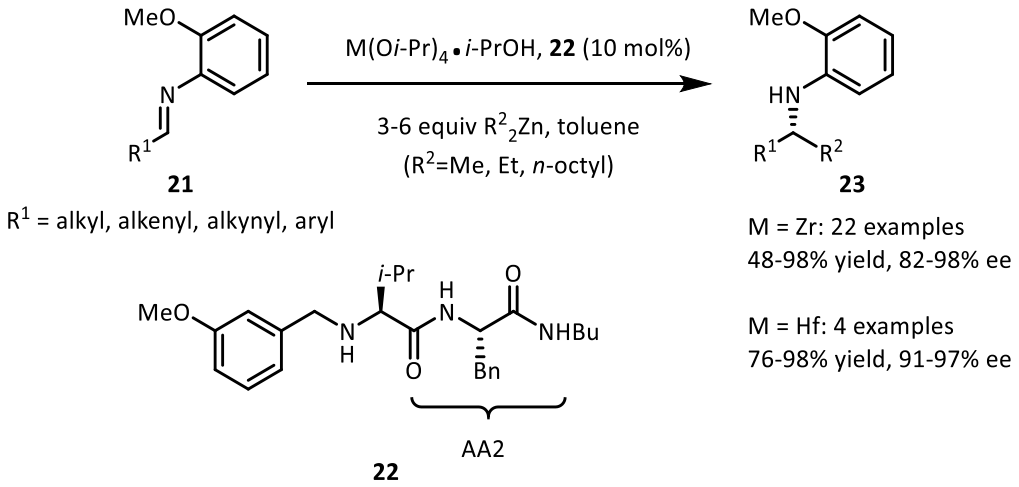

Scheme 8: Hoveyda's zirconium catalysed asymmetric addition of diethyl zinc to aldimines utilising a chiral peptide ligand.

Despite this, the main drawback in using organozinc reagents is the limited scope with respect to the zinc reagent; only alkyl groups can be used as nucleophiles.

1.2.3 Transmetallation strategies

Transmetallation involves the transfer of the nucleophilic component of an organometallic to a main group transition metal *prior* to C-C bond formation with the substrate. This became a popular approach to circumvent the problems associated with using organozincs as it is not limited to the addition of alkyl groups. It also overcomes the problems associated with the use of organolithiums in asymmetric transformations; namely the need for high catalyst loadings required to suppress background reactions. An early example of this comprised of Rh-catalysed additions of arylstannanes[15], aryltitanium species[16] and arylboroxines[17] to aldimines all reported by Hayashi.

De Vries, Feringa and Minaard reported a highly efficient enantioselective arylation of *N,N*-dimethyl sulfamoyl aldimines using a Rhodium-monodentate phosphoramidite ligand system and 1.3 equiv of aryl boronic acid (Scheme 9).[18]

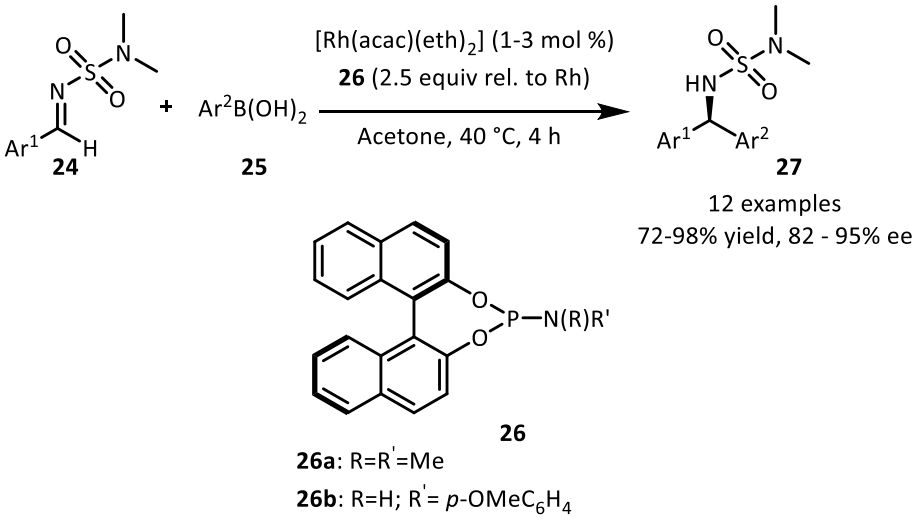

Scheme 9: Feringa's enantioselective arylation of *N,N*-dimethyl sulfamoyl aldimines.

Excellent enantioselectivities were obtained and the reaction proved to be broad in scope with respect to the imine. The protecting group on the resulting amine product **27** was removed under relatively mild conditions; heating under microwave irradiation with 1,3-diaminopropane effected transamination and subsequent deprotection to afford the chiral amine.

1.2.4 Asymmetric Synthesis of Propargylic and Allylic Amines

The synthesis of chiral propargylic and allylic amines are attractive as they serve as useful 'handles' to enable further synthetic manipulation of the product. Li and co-workers reported a copper-catalysed, enantioselective propargylation reaction of aldimines (Scheme 10).[19] The reaction surprisingly

performed well when water was used as solvent. Their catalytic system utilised a tridentate pyridine bisoxazoline (pyBOX) ligand. The aldimine substrates were synthesised *in situ* from the aldehyde and the corresponding amine. The reaction proved to have a broad application over a range of aryl aldimines with good yields and excellent enantioselectivites of the desired product being obtained.

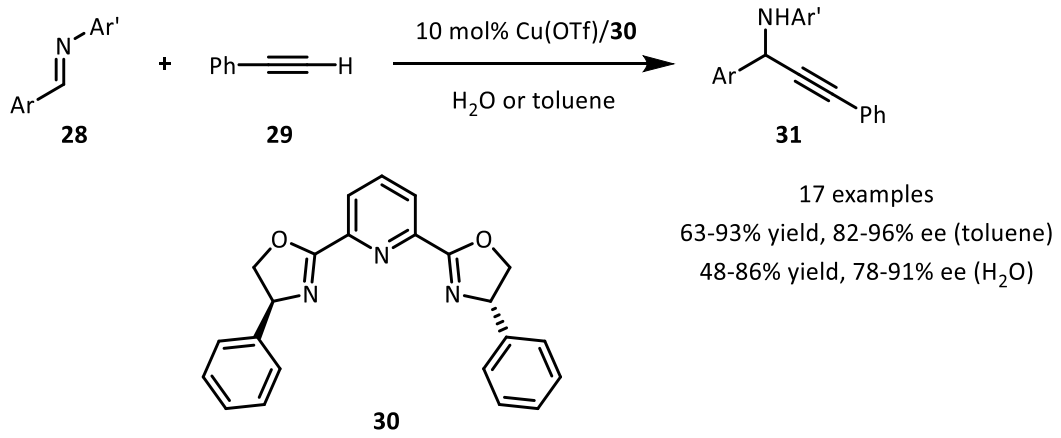

Scheme 10: Li's copper-catalysed enantioselective propargylation of *N*-aryl aldimines utilising a pyBOX chiral ligand.

Another important C-C bond forming reaction to imine substrates are enantioselective allylations. For example, Yammamoto reported the π-allyl palladium catalysed enantioselective allylation of aldimines using allyl trimethylsilane **33** with TBAF as a co-catalyst (Scheme 11).[20] The reaction resulted in excellent yields and good enantioselectivities of the desired product and had the advantage of avoiding the use of the less stable, more toxic allylstannanes. Almost racemic products were obtained where an aryl protecting group featured on the imine substrate (Ph and 4-$MeOC_6H_4$). It was proposed that coordination of the nitrogen atom of the imine to the palladium metal centre was prohibited due to an increase in the local steric bulk around the nitrogen atom bearing *N*-aryl protecting groups. The reaction did not proceed in the absence of palladium catalyst and it was therefore postulated that the role of fluoride ions in this reaction was not to generate free allyl anions, which could be trapped by the imine electrophile. Rather, the role of the fluoride ions from TBAF was to coordinate to the allyl silane to generate the pentacoordinate allyl silicate which could then undergo facile transmetallation with Pd(II).

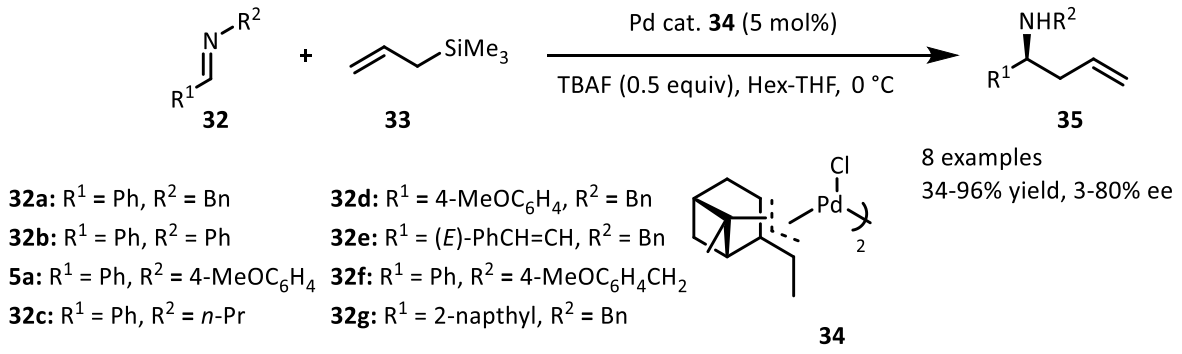

Scheme 11: Yammamoto's palladium-catalysed asymmetric allylation of aldimines.

Asymmetric allylations of ketimines (imines derived from ketones) with the formation of a quaternary stereogenic centre is a particularly challenging synthetic problem due to the unreactive nature of ketimines compared to their aldimine counterpart. Furthermore, discrimination between the two pro-chiral faces on ketimine electrophiles becomes more difficult due to the greater similarity (in terms of steric and electronic properties) of the two substituents attached to the imine, which makes enantioselective transformations of ketimines more challenging compared with aldimines.[21,22] Shibasaki has addressed this problem to some extent using a transmetallation approach with a copper-catalysed addition of allyl boronic acid pinacol esters to a range of ketimines (Scheme 12).[23]

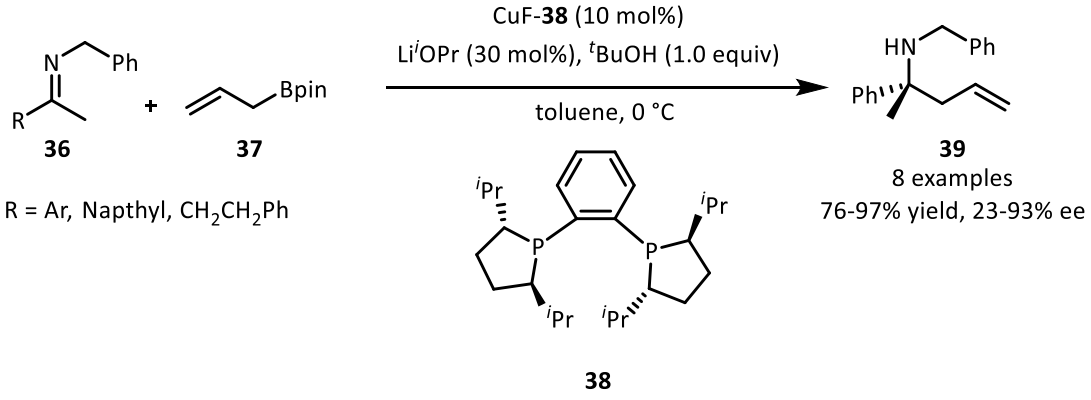

Scheme 12: Shibasaki's copper-catalysed asymmetric allylation of ketimines.

The catalytic system was composed of a CuF-DuPHOS system with a catalytic amount of Li^{i}OPr and stoichiometric *t*-BuOH. The substrate scope with respect to the aromatic ketimine substrate proved to be broad, with electron-rich and electron-poor aryl ketimines giving rise to high yields and enantioselectivities in their respective products. A limitation to this method, however, was that aliphatic ketimines were not well tolerated and resulted in low enantioselectivities. Extensive mechanistic investigations revealed that using Li^{i}OPr as a co-catalyst increased the rate of the reaction by increasing the concentration of the active, allyl copper nucleophile. Stoichiometric *t*-BuOH increased catalytic turnover by acting as a proton source, enabling dissociation of the product from

the copper metal centre, which would otherwise serve as a deactivation pathway for the metal catalyst.

1.3 Enantioselective Mannich Reactions

Mannich reactions are important C-C bond forming reactions for the synthesis of β-amino carbonyl compounds, particularly β-amino acid derivatives which are found in natural products and are precursors to β-lactams.[24] For example, β-amino acids are prevalent in drug compounds such as cispentacin **40**, which exhibits antifungal properties and Bestatin **42**, which is an metallo-aminopeptidase inhibitor (Figure 2)[25,26]. It is also found in many natural products such as (*R*)-β-Dopa **41** which gives the mushroom *cortinarius violaceous* its blue colour, as part of the Fe(III) catechol complex.[27]

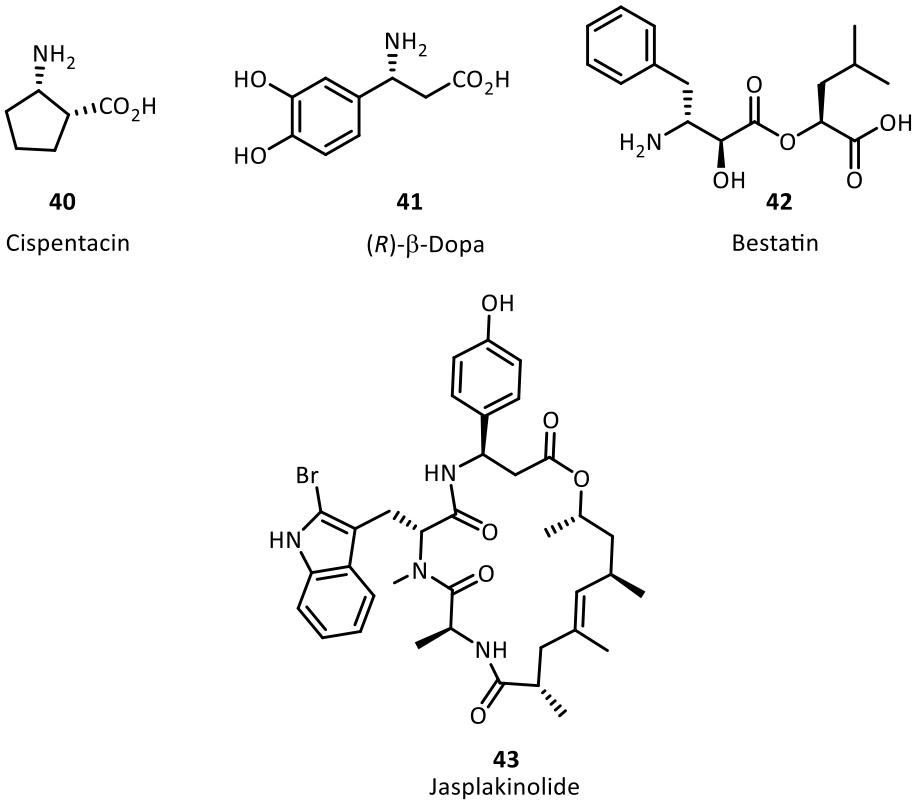

40 Cispentacin

41 (*R*)-β-Dopa

42 Bestatin

43 Jasplakinolide

Figure 2: Drug compounds and naturally occurring bioactive compounds containing β-amino acid functionalities.

Jasplakinolide **43** is a natural product isolated from a marine sponge, which exhibits selective anti-microbial activity against *Candida albicans*.[28] Due to the prevalence of β-amino carbonyl motifs in drug molecules and natural products, there is a need for their synthesis.

1.3.1 Metal-Based Approaches

In 1997, Kobayashi reported the first enantioselective Lewis acid mediated Mukaiyama Mannich-type reaction which involved the addition of silyl enolates to aldimines (Scheme 13). The reaction was mediated by a zirconium-BINOL catalyst **46** with *N*-methyl imidazole as an additive. The reaction afforded the product in good to high yields and excellent enantiomeric excess. The reaction tolerated electron-rich and electron-poor aryl aldimines as well as a heteroaryl aldimine; derived from furfural. Furthermore, the reaction also tolerated the aliphatic aldimine derived from cyclohexyl carboxaldehyde; resulting in only a moderate yield (56%), whilst enantioselectivity remained high (80% ee) for this substrate. Mechanistic insights revealed the transfer of the TMS group to the nitrogen atom of the imine after C-C bond formation allowed for dissociation of the product from the catalyst and thereby aided catalytic turnover.[29] The reaction was later applied to α-alkoxy silyl enolates for the synthesis of both *syn* and *anti* β-amino alcohols.[30]

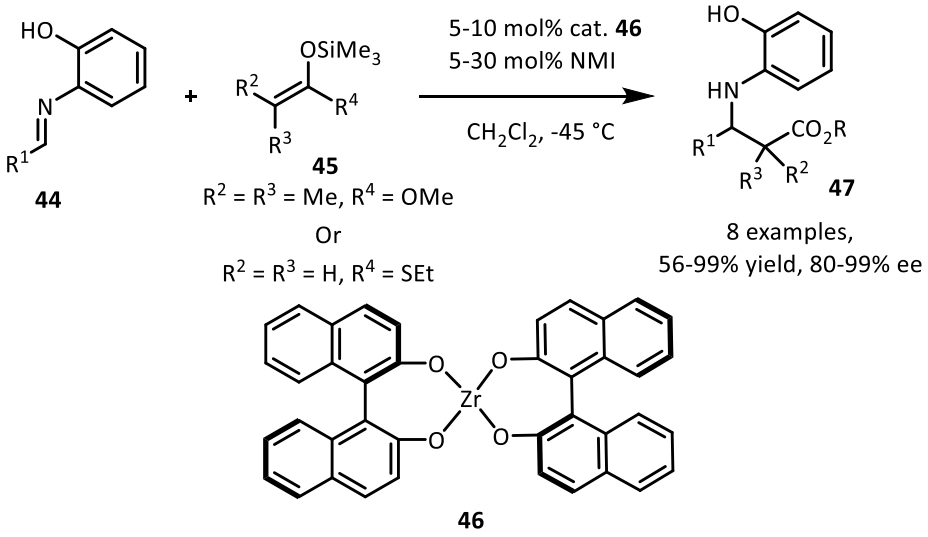

Scheme 13: Kobayashi's Lewis acid mediated enantioselective Mukaiyama Mannich reaction of aldimines.

Later on, Hoveyda and co-workers reported a general, highly enantioselective silver-catalysed Mukaiyama Mannich reaction of silyl enol ethers to aryl, alkyl, alkenyl and alkynyl imines (Scheme 14).[31]

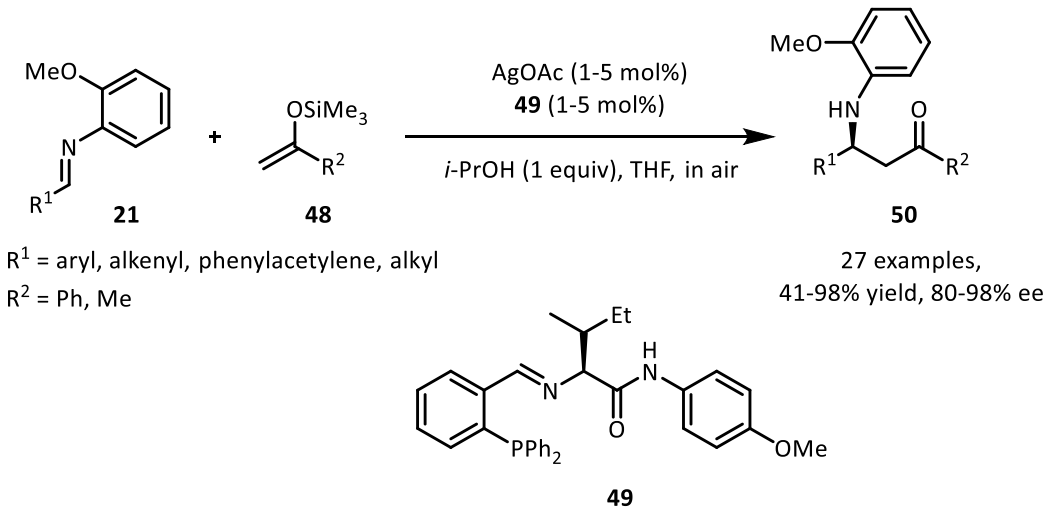

Scheme 14: Silver(I)-catalysed asymmetric Mukaiyama Mannich reaction of aldimines.

The reaction was catalysed by ligand **49** and it was found that 1 equivalent of *iso*propanol was required for high reactivity. The products were obtained in good yields and excellent enantioselectivities. Furthermore, the synthetic utility of this method was demonstrated through its application to the synthesis of natural product, (-)-*sedamine* which was obtained in 40% yield (over 4 steps).

Biologically relevant structures such as α-hydroxy-β-amino acids can be easily generated through a Mannich reaction (see section 3.6.5). For example, Trost used the dinuclear Zn catalyst **53** (Scheme 15) for the enantioselective Mannich reaction of α-hydroxyketones to aldimines. Overall, the reaction afforded the desired product in good yields, excellent enantioselectivities and moderate diastereoselectivities, with aliphatic aldimines being tolerated well. Diastereoselectivity was controlled by altering the protecting group on the imine between *N*-DPP to *N*-Boc, where *N*-DPP imines favoured the *anti* product, whereas *N*-Boc imines favoured the *syn* product.[32]

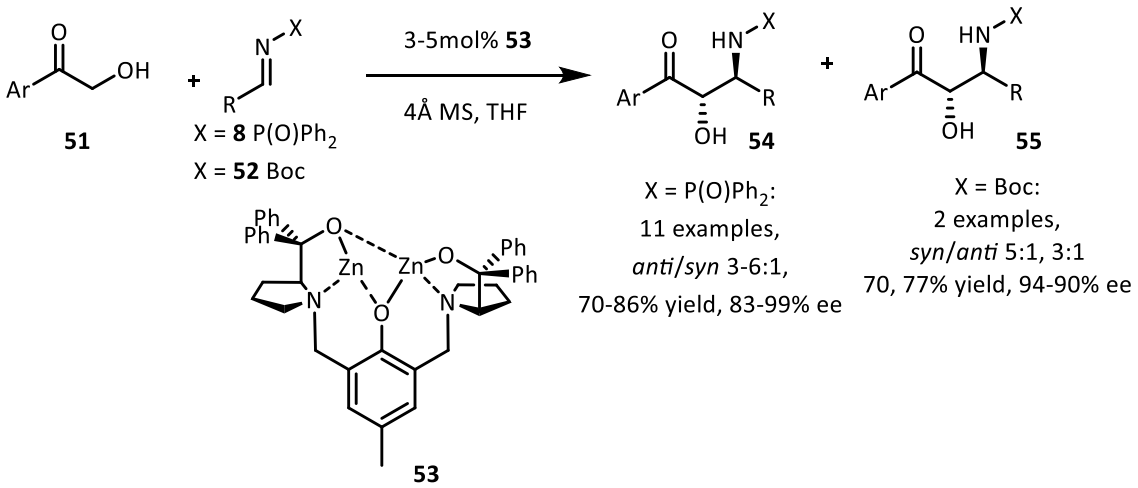

Scheme 15: Trost's enantioselective Mannich reaction of α-hydroxyketones to *N*-DPP and *N*-Boc aldimines.

1.3.2 Organocatalytic Approaches

Organocatalysis can be broadly divided into two distinct categories: covalent catalysis and non-covalent catalysis. Covalent catalysis describes the activation of substrates by the organocatalyst through the formation of covalent bonds. An early example of this type of catalysis came from List and co-workers who reported an organocatalyzed Mannich reaction of hydroxyacetone **57** with imines of **56**, formed *in situ* on condensation with *p*-anisidine **59**. Reaction of the imine was initiated by enamine formation of hydroxyacetone after condensation with (*S*)-proline catalyst **58**. This resulted in the formation of *syn*-1,2-amino alcohols in good yields, good diastereoselectivities and excellent enantioselectivities (Scheme 16).[33] The reaction tolerated electron-rich and electron-poor aromatic aldimines. One aliphatic aldimine possessing an isopropyl group was also reported, however, a reduction in reactivity was observed (57%), whilst enantioselectivity was moderate (65% ee) and diastereoselectivity was high (17:1 dr). Barbas[34], Cordova[35] and many others quickly built on this early work for enantioselective Mannich reactions mediated by a chiral amine organocatalyst.

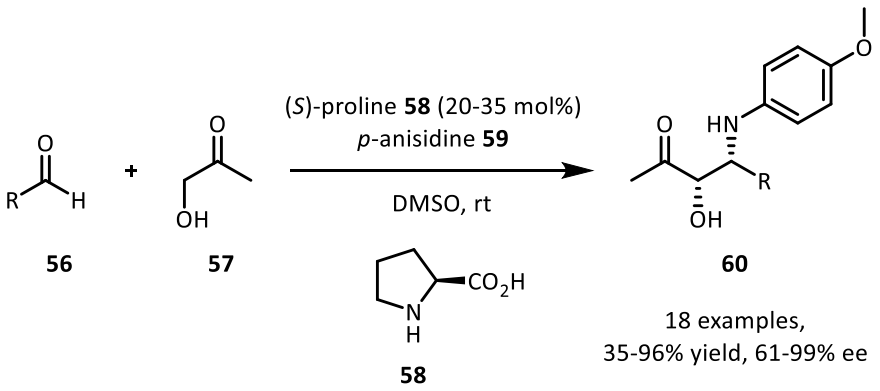

Scheme 16: List's proline-catalysed Mannich reaction of α-hydroxyketones to aldehydes.

On the other hand, non-covalent organocatalysis describes the activation of substrates in a non-covalent manner through hydrogen-bonding from the organocatalyst. Typically, this class of organocatalyst is 'bifunctional' in that it contains a Brønsted base to activate the nucleophile by deprotonation and a hydrogen bond donor group to activate the electrophile, both of which occur in a synergistic manner. The two functionalities are linked together over a chiral scaffold (Figure 3).

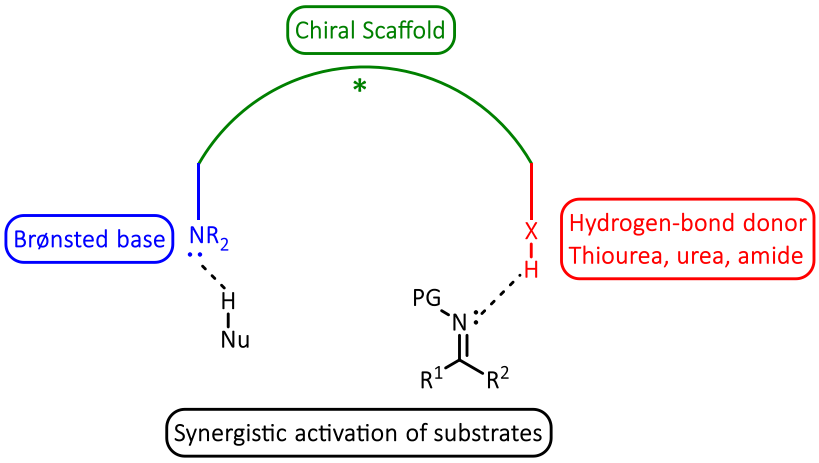

Figure 3: Bifunctional organocatalysis concept.

An example of non-covalent catalysis came from Dixon and co-workers who reported the highly enantioselective Mannich reaction of dimethyl malonate to a range of aromatic aldimines. The reaction was catalysed by a bifunctional cinchonine alkaloid derived organocatalyst **63**, bearing a Schreiner-type thiourea (see section 2.4) hydrogen bond-donor group (Scheme 17).[36]

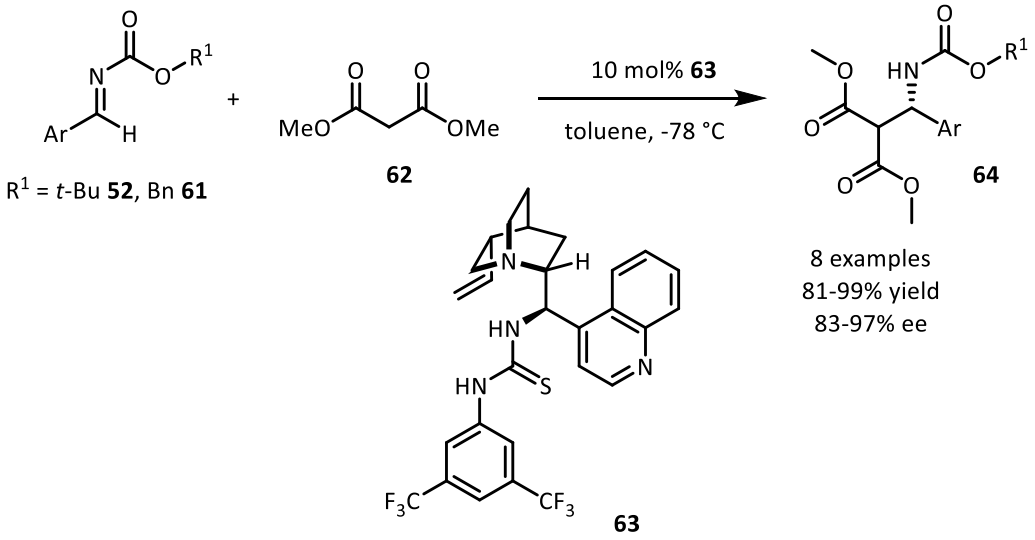

Scheme 17: Dixon's enantioselective Mannich reaction of dibenzyl malonate to *N*-Boc protected aldimines using a thiourea cinchona alkaloid derived bifunctional organocatalyst.

The reaction proved to be applicable to a both *N*-Boc and *N*-Cbz protected aldimines. Heteroaromatic aldimines were also tolerated well; affording the desired products in very high yields (81-99%) and excellent enantioselectivities (83-97% ee).

1.3.3 Nitro-Mannich

The addition of a nitro-alkyl substrate to an imine, (nitro-Mannich reaction), allows for the synthesis of useful products bearing a nitro functionality which allows for further synthetic modification. Early work from Shibasaki[37] included the addition of nitromethane to *N*-DPP aldimines (Scheme 18).

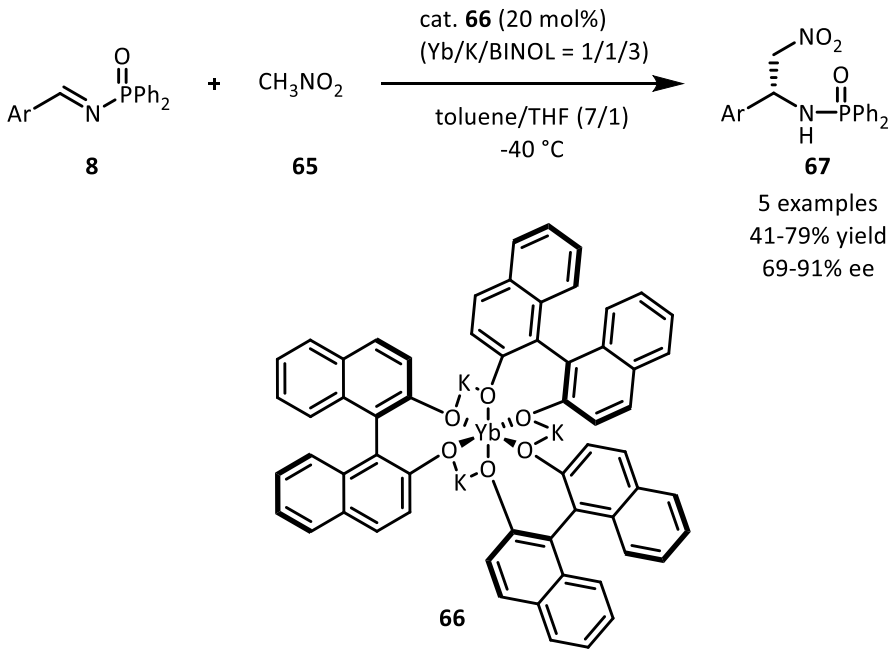

Scheme 18: Shibasaki's nitro-Mannich reaction of nitromethane with aryl *N*-DPP aldimines catalysed by a heterobimetallic catalyst.

The reaction was catalysed by heterobimetallic catalyst **66** to afford the product **67** in good yields and high enantioselectivities. It was found that electron-rich aryl aldimines required long reaction times and gave rise to lower yields and enantioselectivities of the product in contrast to electron-deficient aryl aldimines. This limited somewhat the scope of this method.

Takemoto reported a highly enantioselective nitro-Mannich reaction of a range of nitroalkanes to aryl *N*-Boc aldimines (Scheme 19).[38] The reaction was catalysed by a bifunctional catalyst possessing a Schreiner-type thiourea as the hydrogen-bond donor group and a tertiary amine as the Brønsted base over a chiral scaffold derived from *trans*-1,2-diaminocyclohexane **69**. Furthermore, prochiral nitroalkanes resulted in high diastereoselectivities and excellent enantioselectivities, giving rise to *syn*-β-nitroamines as the major product.

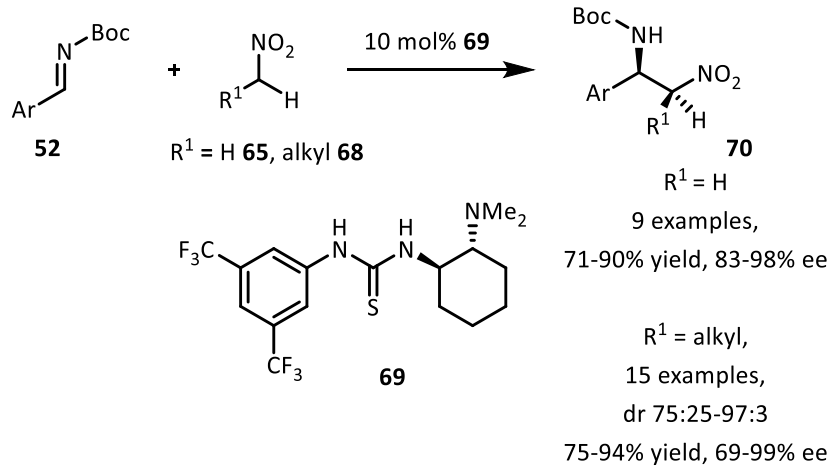

Scheme 19: Takemoto's enantioselective aza-Henry reaction catalysed by a bifunctional thiourea organocatalyst.

This was a very general application, with nitro-alkanes bearing electrophilic substituents such as mesylate and tosylate functionalities also being tolerated. The synthetic utility of this reaction was demonstrated when it was applied to the synthesis of the biologically important piperidine CP-99,994, a neurokinin-1 (NK-1) receptor[39] antagonist (Scheme 20).

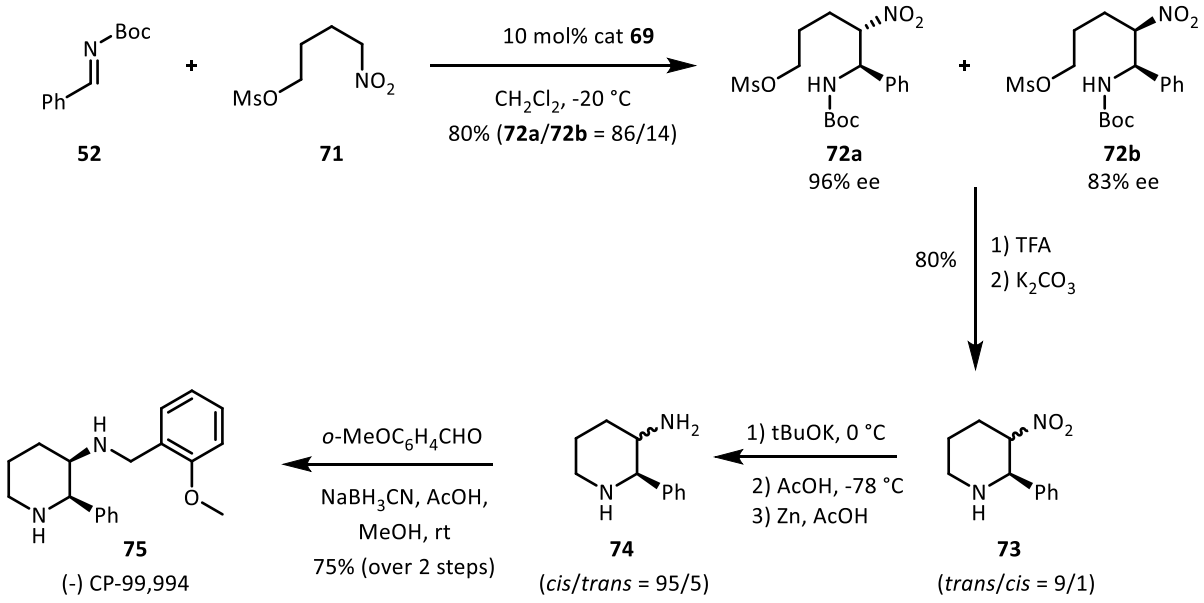

Scheme 20: Synthesis of neurokinin-1 antagonist (-) CP-99,994, using the enantioselective nitro-Mannich reaction as a key step.

Mesylate **71** was reacted with aldimine **52**, mediated by thiourea catalyst **69** (10 mol%) to afford nitro-Mannich adduct **72** as a mixture of diastereoisomers (**72a**/**72b** = 86/14) in 80% yield. The enantiomeric excess of **72a** and **72b** was 96% ee and 83% ee respectively. Treatment of **72** with TFA effected removal of the *N*-Boc group and cyclised products **73** were obtained in the presence of K_2CO_3 as a 9/1 mixture of *trans* and *cis* isomers in 80% yield. The C3 position of **73** was successfully epimerised in the presence of *t*-BuOK (2.0 equiv) and then AcOH at -78 °C followed by reduction of the nitro group which was

carried out with Zn in AcOH to afford diamine *cis*-**74** as the major product (*cis*/*trans* = 95/5). Finally, reductive amination afforded the desired compound **75** in 75% yield (over 2 steps).

Jørgensen successfully combined both methods of catalysis: metal-based catalysis and non-covalent organocatalysis in a co-operative manner for the reaction of 2-nitro propanoic acid *tert*-butyl ester **77** with *N*-PMP glyoxylate imine **76**. The reaction featured a quinine organocatalyst **79** and a Cu(II)-Box complex and afforded the product bearing a quaternary stereocentre in good yields, high diastereoselectivity with excellent enantioselectivity (Scheme 21).[40]

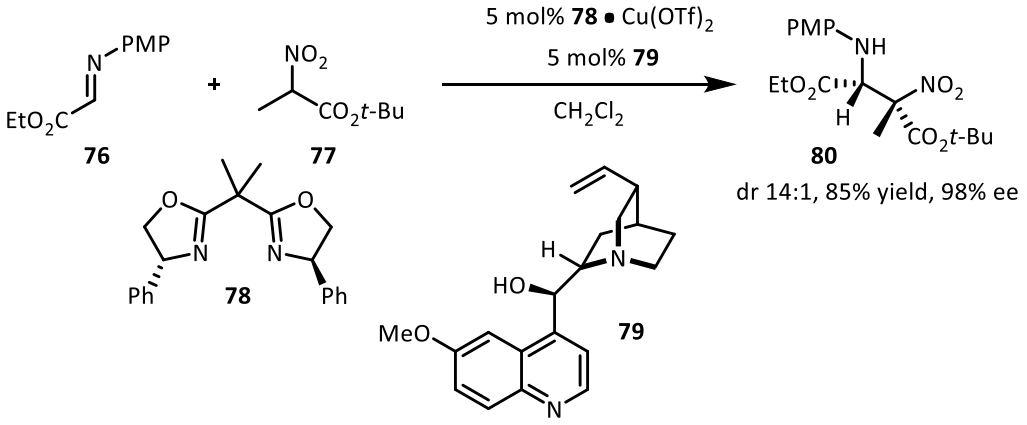

Scheme 21: Jørgensen's enantioselective aza-Henry reaction catalysed by a quinine organocatalyst and a Cu(I)-BOX complex in a cooperative manner.

A series of control experiments established that the enantioselectivity of this reaction was controlled by the chiral copper complex, where diastereoselectivity was controlled largely by the quinine organocatalyst. Nitroamine **80** was readily transformed into the corresponding chiral diamine on reduction of the nitro group using Ra-Ni.

1.4 Aims of the Thesis

The reactions presented above are a brief overview for the synthesis of chiral amines and highlight metal catalysis and organocatalysis as effective synthetic tools to achieve this. Our aim was to develop new synthetic methodologies for the enantioselective addition of pro-nucleophiles to imine substrates to afford the chiral amine products in high enantioselectivities. We envisioned the development and application of both an organocatalytic system and a metal-ligand based system for these studies. We were particularly interested in studying the reactivity of imines derived from ketones (ketimines) which have been scarcely reported under current organo and metal-based catalysis. We believed that our chiral BIMP organosuperbase catalysts had the potential to provide a solution to this synthetic problem and thereby sought to apply these organocatalysts to the discovery of novel reactivity. We

also aimed to explore alternative metal-ligand based catalytic systems for these reactions. These would be interesting from a mechanistic point of view; to elucidate the binding modes of the chiral ligand and how this could potentially influence reactivity and/or enantioselectivity.

2. Bifunctional Iminophosphorane Catalysed Enantioselective Ketimine Phospha-Mannich Reaction

2.1 Chapter Overview

This chapter describes the first general organocatalytic, enantioselective hydrophosphonylation reaction of 'unactivated' ketimines using diethyl phosphite as the pro-nucleophile. The reaction is catalysed by a bifunctional iminophosphorane (BIMP) superbase organocatalyst which is a novel class of bifunctional organocatalysts developed in the Dixon group. The reaction tolerates ketimines bearing electron-rich and electron-poor aryl substituents resulting in excellent yields and modest enantioselectivities under mild reaction conditions.

2.2 Bifunctional Iminophosphorane Organocatalysts

In section 1.3.2 bifunctional Brønsted base/H-bond donor organocatalysts, namely catalysts bearing a tertiary amine moiety as the Brønsted base were discussed. The main limitation of these types of organocatalyst is that pro-nucleophiles bearing sufficiently acidic protons to enable acid/base activation with the tertiary amine moiety on the organocatalyst is required. Moreover, there are ample reports of asymmetric additions to imines derived from aldehydes (aldimines) under tertiary amine based catalysis in the literature,[41] whereas additions to imines derived from ketones (ketimines) are scarce. To circumvent this problem, in 2013, the Dixon group developed Bifunctional iminophosphorane (BIMP) organocatalysts which represent a new class of bifunctional organocatalysts to enable enantioselective transformations between pro-nucleophiles bearing less acidic protons and electrophiles which are inherently less electrophilic such as ketimines, that are inaccessible by means of current organocatalytic technologies. As was aforementioned, bifunctional organocatalysts are composed of two main components: 1) hydrogen bond donor group and 2) Brønsted base (Scheme 22).

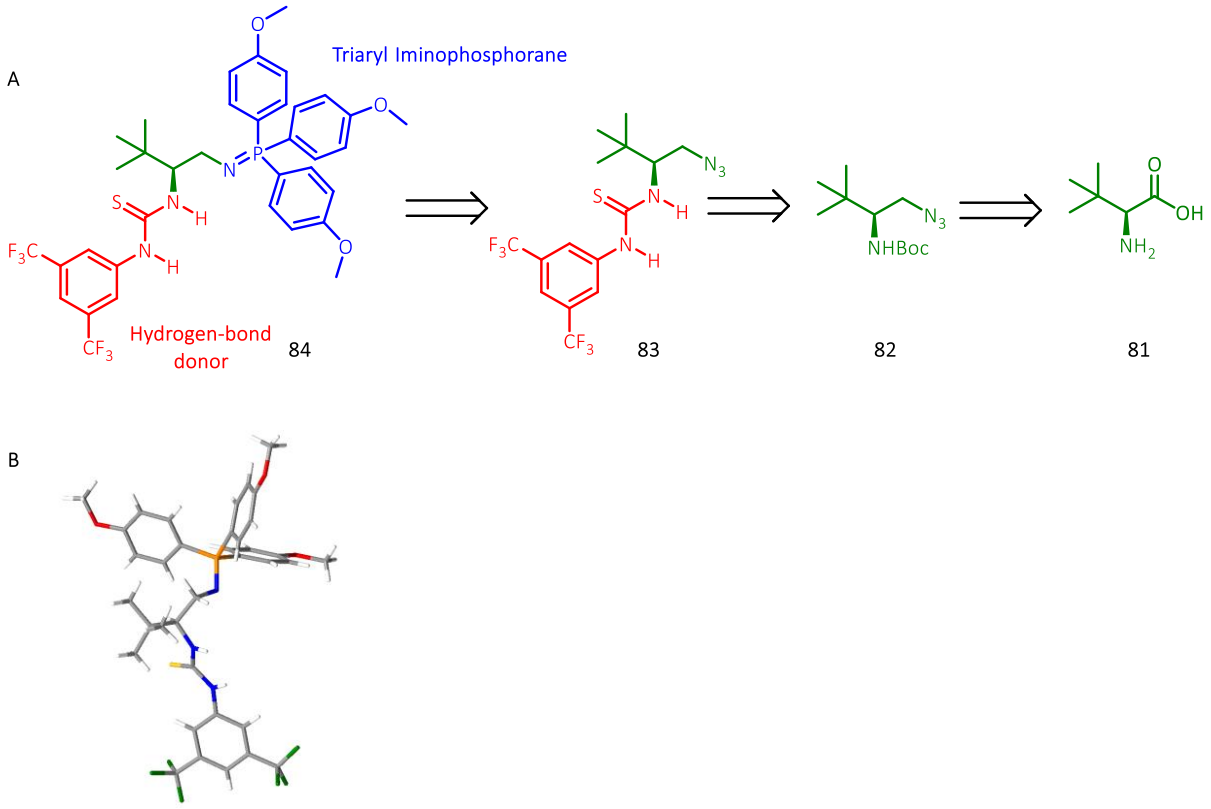

Scheme 22: (A) BIMP 84 derived from L-*tert*-leucine (B) Single crystal X-ray structure of 84.

The retrosynthetic strategy for the synthesis of BIMP **84** (scheme 22, A), the structure of which was confirmed by a single crystal X-ray structure (Scheme 22, B) involves a late-stage Staudinger reaction between azide **83** and a triarylphosphine. Azide **83** could be synthesised from the corresponding *N*-Boc protected amino azide **82** with the corresponding isothiocyanate (for a thiourea hydrogen bond donor) following *N*-Boc deprotection. Amino azide **82** can be taken back in a retrosynthetic manner to the amino acid from which it is derived as exemplified here with L-*tert*-leucine **81**. The Brønsted base in catalyst **84** is the iminophosphorane moiety. Investigations into the basicity of the iminophosphorane derived from cyclohexyl azide and triphenylphosphine determined the pK_{BH+} to be 22.7 in acetonitrile, where a guanidine such as BTMG gives rise to a pK_{BH+} of 23.6.[42] However, the iminophosphorane derived from cyclohexyl azide and *tris*(4-methoxyphenyl phosphine) gives rise to a pK_{BH+} of 25.0; around 2 orders of magnitude more basic than the iminophosphorane derived from triphenylphosphine.[42] This demonstrates that the basicity of the iminophosphorane can be 'tuned' by employing either electron-rich or electron-deficient phosphines in the Staudinger reaction.

The juxtaposition of Brønsted base and hydrogen bond donor group over a chiral scaffold is of critical importance for successful enantioselective catalysis. The chiral scaffold here can be altered by changing the amino acid from which it is derived (see section 2.4). Furthermore, the hydrogen-bond donor group can also be modified by coupling the amino azide **82** with an isocyanate (for urea) or acyl chloride (for

amide) after *N*-Boc deprotection. This modular nature of the catalyst allows for a rapid library generation from azide catalyst precursors with a range of triarylphosphines and enables the expedient screening of catalysts for reaction optimisation.

Previous work from our laboratory demonstrated the applicability of this class of organocatalyst to the first general ketimine nitro-Mannich reaction (Scheme 23) involving the addition of nitromethane **65** to *N*-diphenyl phosphinoyl (*N*-DPP) protected ketimines. The reaction was catalysed by BIMP catalyst **86** to afford the product in excellent yields and enantioselectivities.[42]

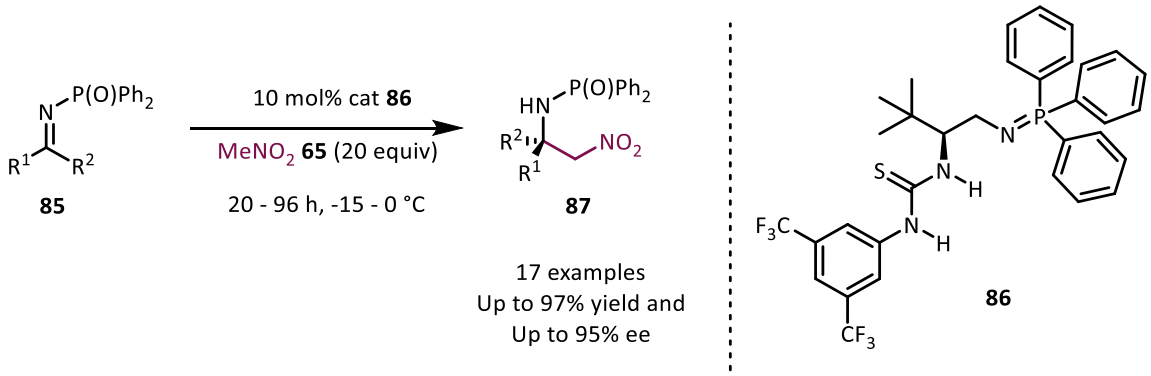

Scheme 23: The first general nitro-Mannich ketimine reaction of nitromethane to *N*-DPP ketimines.[42]

It was thereby demonstrated that BIMP organocatalysts make unreactive electrophiles such as imines derived from ketones (ketimines) accessible in catalytic enantioselective synthesis. In the same vein, we wanted to show that pro-nucleophiles containing heteroatoms were also productive using BIMPs by developing a method for the enantioselective hydrophosphonylation of ketimines.

2.3 Hydrophosphonylation of Ketimines

2.3.1 Introduction

The hydrophosphonylation of ketimines allows for easy access to α-aminophosphonic acid derivatives, which have been found to be bioisosteres of α-amino acids[43] and have exhibited antibacterial[44], anti-HIV[45], and protease inhibition[46] activities. Often, the physiological profiles of these compounds are dependent on the stereochemical configuration of one or more stereogenic centres in the α-aminophosphonic acid compound. For example, (*R*)-phospholeucine **88** proves to be a more powerful inhibitor of leucine aminopeptidase than its enantiomer (Figure 4). Similarly, (*S*,*R*)-alafosfalin **89** shows a higher anti-bacterial profile against both Gram-positive and Gram-negative bacteria than its other three diastereoisomers.[41]

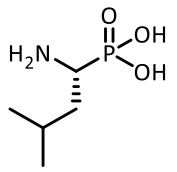

(*R*)-phospholeucine, **88**

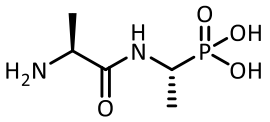

(*S,R*)-alafosfalin, **89**

Figure 4: α-amino phosphonic acids (*R*)-phospholeucine and (*S,R*)-alafosfalin.

The absolute configurations of α-aminophosphonic acids are therefore important for their biological profiles, which makes their enantioselective synthesis desirable.[47] Direct access to such compounds can be achieved through a 1,2-addition of phosphite pro-nucleophiles to imines.

2.3.2 Organocatalytic Approaches for the Hydrophosphonylation of Aldimines

Much attention has been focussed on asymmetric hydrophosphonylation of imines derived from aldehydes (aldimines). In 2006, Pettersen *et al.* reported the enantioselective Mannich reaction of diethyl phosphite **90** to a range of *N*-Boc protected aryl aldimines to afford the α-aminophosphonic acid derivative **91** in good yields and good to excellent enantioselectivities (Scheme 24).[48] The reaction was catalysed by quinine **79**, which bears a quinuclidine nitrogen as the Brønsted base and a hydroxyl motif attached to a stereogenic carbon as part of the chiral scaffold as the hydrogen bond donor. Although reaction times proved to be long; a limitation of tertiary amine-based organocatalysis, enantioselectivity was typically found to be good to excellent.

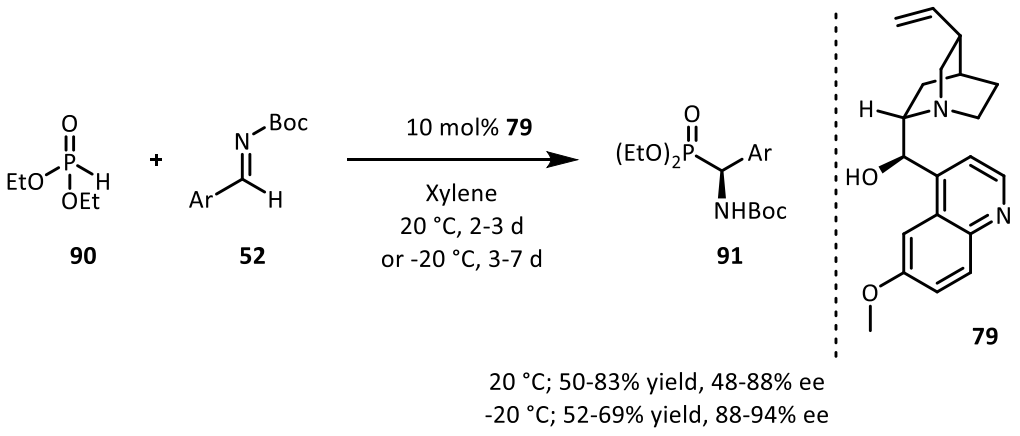

Scheme 24: Enantioselective quinine catalysed phospha-Mannich reaction of diethyl phosphite to *N*-Boc protected aryl aldimines.

Interestingly, enantioselectivity was moderate at 20 °C, however this was greatly augmented on lowering the temperature of the reaction to -20 °C. The subsequent reduction in reactivity on lowering the temperature of the reaction meant longer reaction times were required.

Jacobsen reported the highly enantioselective phospha-Mannich reaction utilising phosphite **92** to *N*-Bn protected aldimines. The reaction was catalysed by organocatalyst **93**, bearing a Schiff base moiety as the Brønsted base and a thiourea hydrogen-bond donor over a *trans* 1,2-diaminocyclohexyl scaffold. This proved to be a very general application with aryl as well as alkyl aldimines being tolerated well, and afforded the product in good yields and excellent enantioselectivities (Scheme 25).[49]

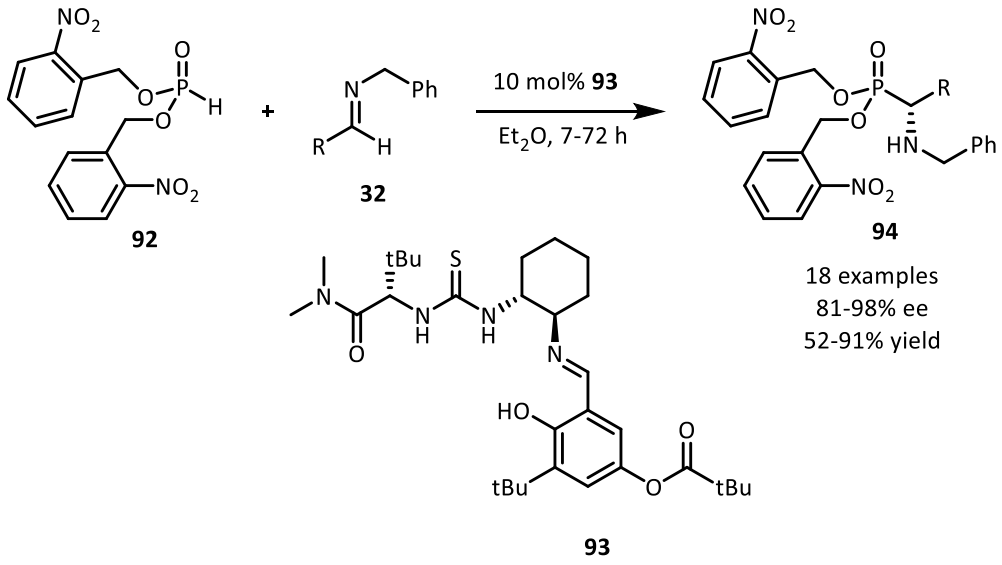

Scheme 25: Jacobsen's phospha-Mannich reaction of phosphite 92 to *N*-benzyl protected aldimines catalysed by 93.

A limitation of this method is that a very specific phosphite was required for reactivity and/or enantioselectivity; which limited the generality of this method. These limitations typically associated with organocatalytic methods were overcome using metal-based methods.

2.3.3 Metal-Based Approaches for the Hydrophosphonylation of Aldimines

For example, in 2007, Katsuki and co-workers developed a metal-catalysed asymmetric hydrophosphonylation of aromatic and aliphatic aldimines using dimethyl phosphite **97**. The reaction utilised the optically active aluminium salalen complex **98** as a catalyst (Scheme 26).[50]

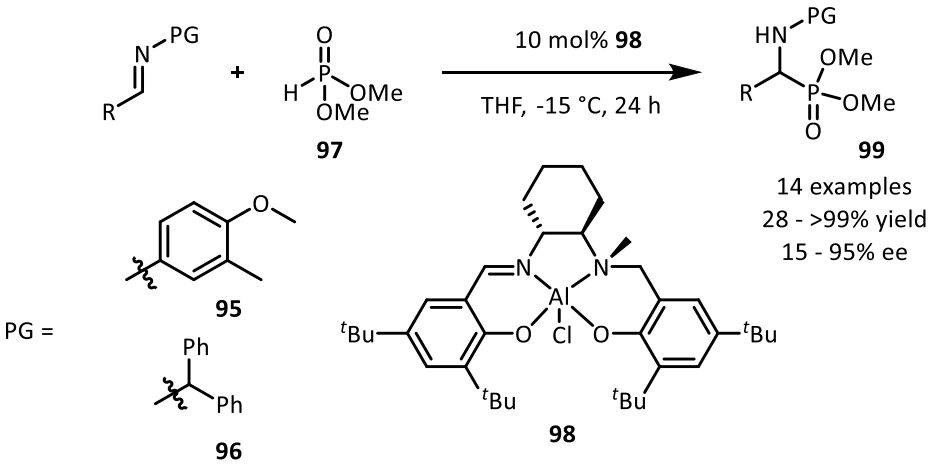

Scheme 26: Katsuki's aluminium salalen catalysed hydrophosphonylation of aromatic and aliphatic aldimines.

Due to their instability, the aliphatic aldimines were formed *in situ* on condensation of the aliphatic aldehyde with the amine in one pot. The reaction proved to be very broad in substrate scope with good reactivity and high levels of enantioselective induction being obtained overall.

Shibasaki and co-workers reported the first method for the enantioselective catalytic hydrophosphonylation of cyclic imines (thiazolines) **100** using heterobimetallic lanthanoid complex **66** as the catalyst (Scheme 27).[50] The reaction afforded pharmaceutically relevant cyclic α-aminophosphonates **101** in good yields and excellent enantioselectivities.

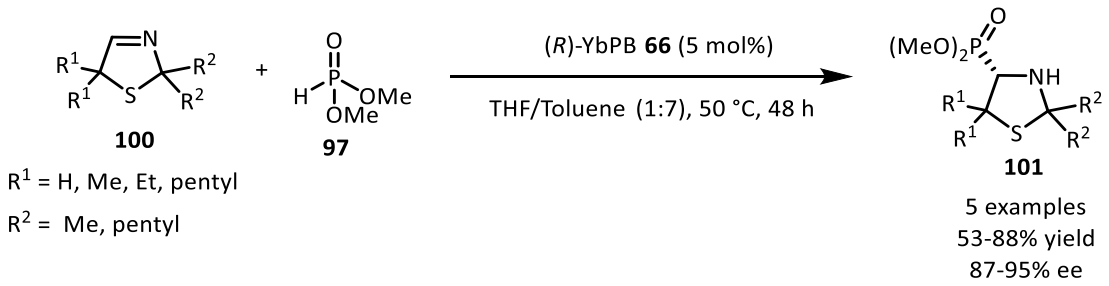

Scheme 27: Shibasaki's asymmetric hydrophosphonylation of thiazolines, catalysed by heterobimetallic lanthanoid complex.

2.3.4 Hydrophosphonylation of Ketimines

Organocatalytic approaches for the hydrophosphonylation of ketimines remained relatively scarce due to the unreactive nature of these electrophiles and poor catalyst-enabled substrate activation; a problem which necessitates the use of metal ion catalysis. This was exemplified by the work of Shibasaki and co-workers (Scheme 28)[51], who reported the highly enantioselective phospha-Mannich reaction of phosphite pro-nucleophiles with *N*-diphenyl thiophosphinoyl ketimines under copper(I) catalysis.

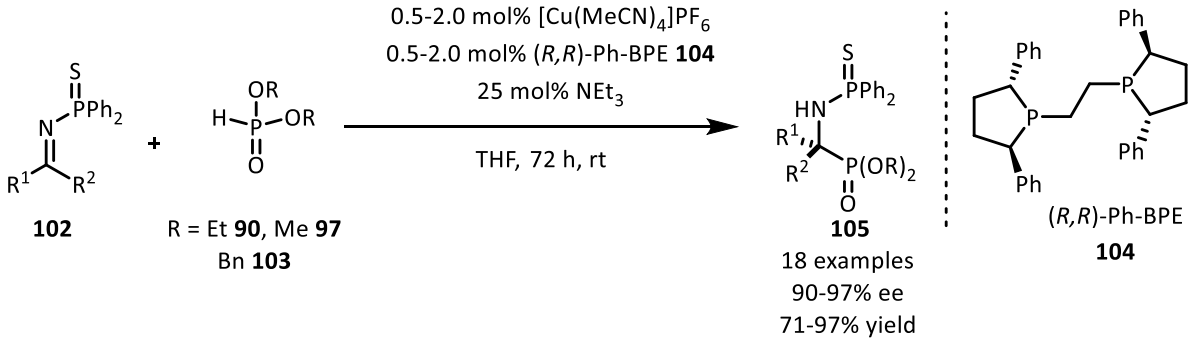

Scheme 28: Shibasaki's copper-catalysed asymmetric hydrophosphonylation of *N*-thiodiphenylphosphinoyl ketimines.

The use of a copper(I) metal centre as part of the catalytic system resulted in good reactivity and excellent enantioselectivities with *N*-diphenyl thiophosphinoyl ketimine. The sulfur atom on the thio-DPP protecting group was proposed to bind the copper to allow for a favourable 'soft-soft' interaction, which led to activation of the ketimine. Use of *N*-diphenyl phosphinoyl ketimines resulted in little reactivity with this catalytic system due to the proposed unfavourable 'hard-soft' interaction of the oxygen atom with the copper metal centre.

Organocatalytic approaches came from the work of Nakamura *et al.* who reported the enantioselective hydrophosphonylation of mesitylene sulfonyl ketimines using diphenyl phosphite **107** as the nucleophile, catalysed by hydroquinine **108a** or hydroquinidine **108b** organocatalysts (Scheme 29).[52]

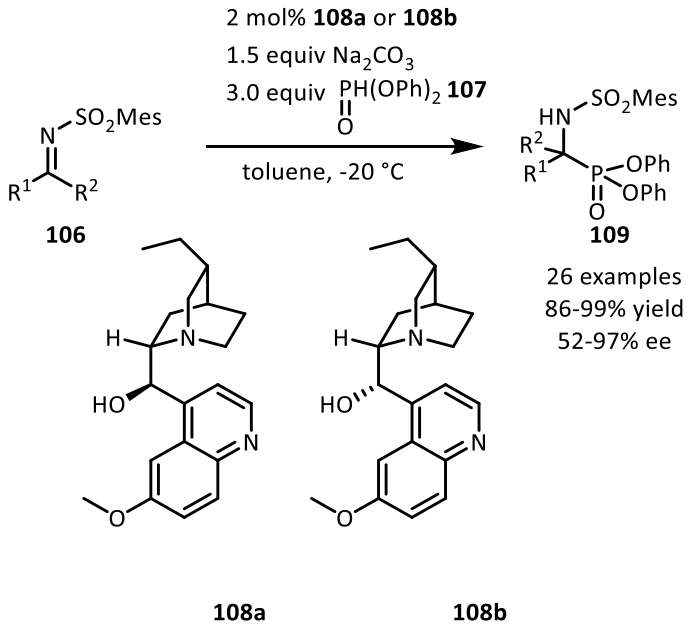

Scheme 29: Enantioselective hydrophosphonylation of mesitylene sulfonyl ketimines.

The reaction was very broad in substrate scope and afforded the product in excellent yields and enantioselectivities, where super stoichiometric quantities of Na_2CO_3 were required for reactivity.

Recently, Chimni and co-workers[53] and Reddy and co-workers[54] documented the enantioselective hydrophosphonylation of reactive isatin derived ketimines using diphenyl phosphite **107** as the pro-nucleophile, catalysed by cinchona-alkaloid derived thiourea **111** and squaramide **113** catalysts respectively (Scheme 30).

Chimni's cinchona alkaloid catalysed phospha-Mannich reaction (Scheme 30, A) resulted in good yields overall and high enantioselectivities. However, relatively high catalyst loadings were required. In comparison, Reddy's quinine derived squaramide variant (Scheme 30, B) proved to have a larger scope with respect to the isatin derived ketimine; with lower catalyst loadings being tolerated, affording the products in excellent yields and good to excellent enantioselectivities. The main limitation of both organocatalytic methods was that they were not applicable to dialkyl phosphites due to their lower reactivities, which limited their generality.

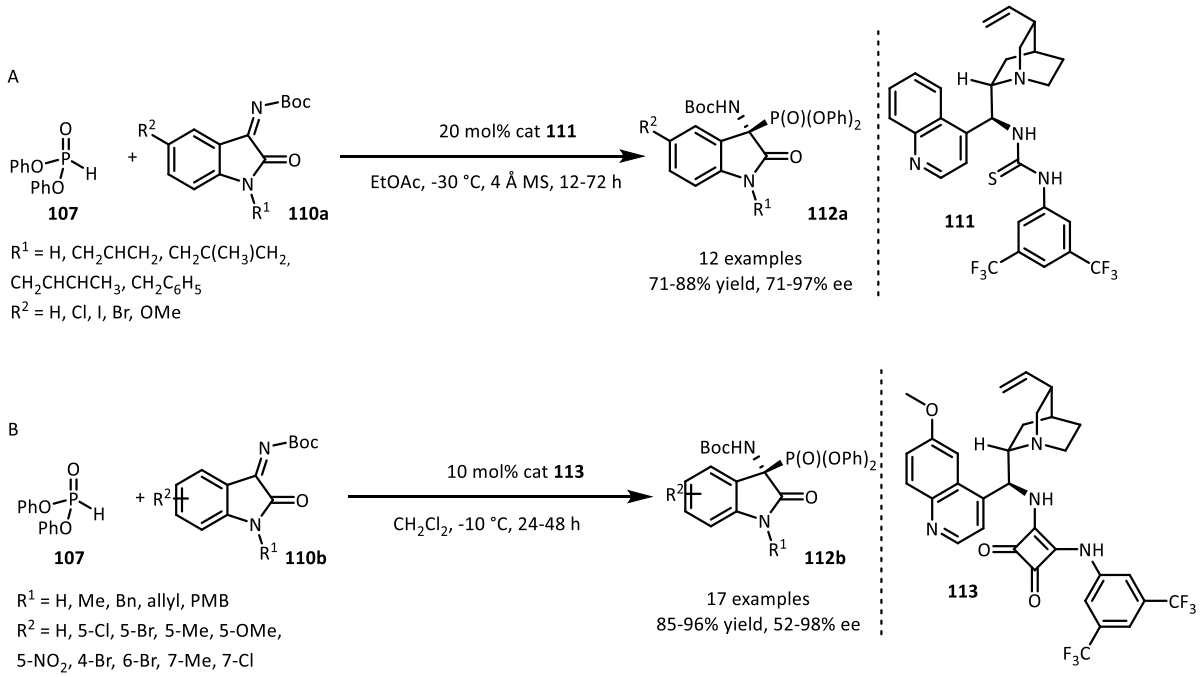

Scheme 30: Asymmetric hydrophosphonylation of isatin derived *N*-Boc ketimines utilising (A) Chimni's cinchona alkaloid thiourea organocatalyst (B) Reddy's squaramide organocatalyst.

We therefore sought to address the limitations encountered using tertiary amine based organocatalytic methods for the enantioselective hydrophosphonylation of ketimines. We aimed to do this through the use of our BIMP organocatalyst family to the end of developing an organocatalytic method which tolerated a dialkyl phosphite pro-nucleophile and an unactivated ketimine electrophile; with low reaction times under relatively mild reaction conditions.

2.4 Synthesis of BIMP Catalysts

The hydrogen bond donor group used on the BIMP organocatalysts in the following section is a Schreiner-type thiourea. Schreiner effectively demonstrated the usefulness of thiourea organocatalyst **116** in 2001 for the Diels Alder reaction between cyclopentadiene **115** and oxazolidinone **114** (Scheme 31).[55] It was shown that in the presence of thiourea catalyst **116**, the Diels-Alder reaction could be carried out at 23 °C; affording the product in good yield after 48 h with a comparable diastereomeric excess to the use of $TiCl_4$ as a Lewis acid. Upon computational analysis, it was found that oxazolidinone **114** can exist in two different conformers; **114a** and **114b**, where **114b** was the ground state configurational preference. It was clear that Lewis acid and hydrogen-bonded complexed oxazolidinone complexes preferred the **114a** conformation.

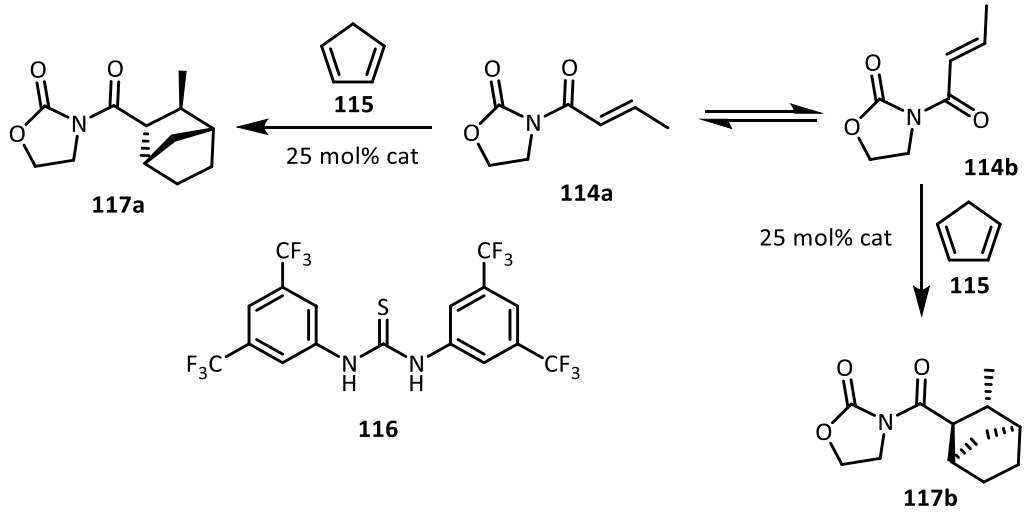

Entry	Catalyst	T/°C	t/h	Yield/%	117a/117b
1	$AlCl_3$	-78	1	95	92:8
2	$TiCl_4$	-78	1	92	89:11
3	**116**	23	48	78	81:19

Scheme 31: Diels Alder reaction catalysed by Schreiner thiourea catalyst 116 compared with $AlCl_3$ and $TiCl_4$ Lewis acids.

A range of BIMP catalysts bearing a Schreiner-type thiourea hydrogen-bond donor group were synthesised. The amino acid starting material was varied with the aim of evaluating the effect different substituents attached to the stereogenic centre would have on reactivity and selectivity in the BIMP catalysed ketimine phospha-Mannich reaction.

2.4.1 L-Phenyl Alanine Derived BIMP

The synthesis of the catalyst precursor bearing a benzyl group at the stereogenic centre began as reduction of the carboxylic acid of **118** using BH_3 generated *in situ*; a method adapted from the work of McKennon *et al.* and subsequent *N*-Boc protection of the amine resulted in compound **119** which was used crude in the next step (Scheme 32).[56] The primary alcohol of **119** was then activated through

tosylation and substitution with sodium azide afforded aminoazide **121** as a key intermediate in 63% yield.

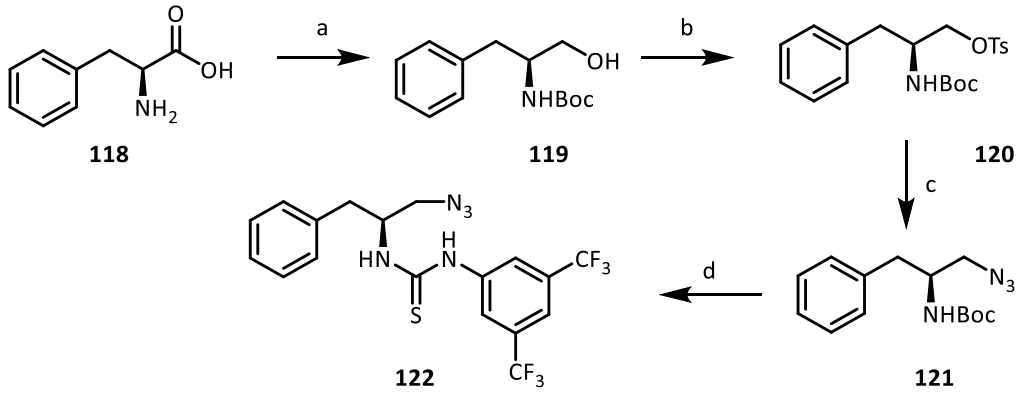

Scheme 32: (a) $NaBH_4$, I_2, THF, reflux, 18 h then Boc_2O, NEt_3, CH_2Cl_2, RT, 12 h, quant; (b) TsCl, NEt_3, DMAP, CH_2Cl_2, RT, 8 h, 35%; (c) NaN_3, DMF, 45 ºC, 14 h, 63%; (d) TFA, then 3,5-bis (trifluoromethyl)phenyl isothiocyanate, THF, RT, 12 h, 74%.

N-Boc deprotection proceeded smoothly using neat TFA and coupling of the free amine (formed on workup with sodium hydroxide solution) with the isothiocyanate furnished the thiourea pre-catalyst **122** in 74% isolated yield. (For further details on iminophosphorane formation, see section 2.7.1)

2.4.2 L-tert-Leucine Derived BIMP

The synthesis of the catalyst precursor bearing a *tert*-butyl group as part of the stereogenic centre began with reduction of the carboxylic acid of L-*tert*-leucine **81** using BH_3 generated *in situ* and subsequent *N*-Boc protection of the amine resulted in **123** in 60% yield over 2 steps (Scheme 33). Initially, activation of the primary alcohol through tosylation and subsequent substitution with sodium azide in the same manner as before was attempted previously.[i] However, the tosylated product led to the formation of an oxazolidinone side product, from degradation of the *N*-Boc protecting group in the presence of sodium azide. The formation of the oxazolidinone by-product could not be stopped with this scaffold.

Accordingly, another synthetic route was exploited which involved a Mitsunobu-Gabriel sequence to afford the primary amine **125**. Conversion of the amine to an azide was effected using a diazo transfer process. Thus, **123** was then subjected to Mitsunobu conditions with phthalimide as the nucleophile, to afford compound **124** in 90% isolated yield. A subsequent Gabriel reaction with hydrazine monohydrate afforded the diamine **125** in 90% yield. At this point the diazotransfer reagent was synthesised by reaction of imidazole **126** with sulfuryl chloride to form **127** in 80% yield (Scheme 34).

[i] **Degradation of *N*-Boc protecting group to form oxazolidinone by-product from *O*Ts or *O*Ms protected 123 was observed by Alistair Farley.**

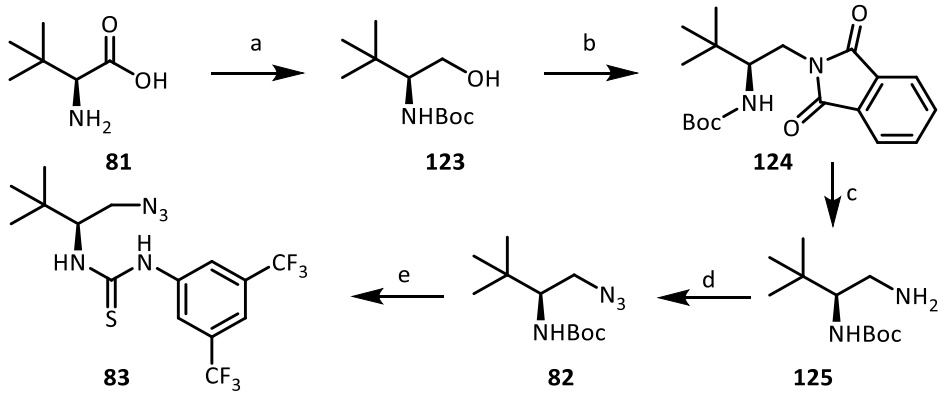

Scheme 33: (a) $NaBH_4$, I_2, THF, reflux, 18 h then Boc_2O, NEt_3, CH_2Cl_2, RT, 10 h, 60%; (b) DIAD, PPh_3, phthalamide, RT, 72 h, 80%; (c) $N_2H_4.H_2O$, EtOH, reflux, 5 h, 90%; (d) diazotransfer reagent 129 in EtOAc, 2 mol% $CuSO_4.5H_2O$, MeOH, 10 h, 62%; (e) TFA then 3,5-bis(trifluoromethyl)phenyl isothiocyanate, THF, 12 h, 51%.

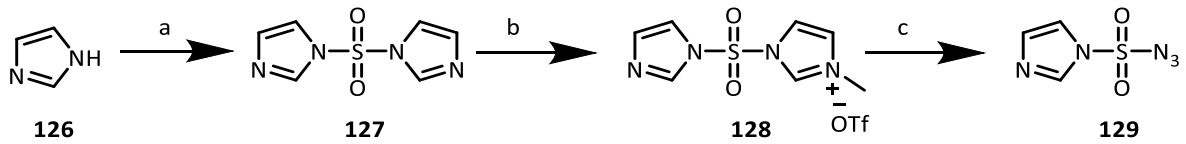

Scheme 34: (a) SO_2Cl_2, CH_2Cl_2, 0 °C to rt, overnight, 80%; (b) MeOTf, CH_2Cl_2, 0 °C, 2.5 h, 97%; (c) NaN_3, H_2O/EtOAc, 0 °C, 2 h, crude product left in EtOAc and transferred to reaction d in scheme 33.

Quaternization of the nitrogen atom on the imidazole ring of **127** was effected using one equivalent of methyl triflate to form triflate salt **128** in quantitative yield. The 3-methyl imidazolium triflate was then substituted with an azide group using sodium azide to afford diazo transfer reagent **129** which was used immediately with diamine **125** to convert the primary amine into an azide using catalytic copper sulfate pentahydrate to form aminoazide **82** in 62% yield. *N*-Boc deprotection using trifluoroacetic acid and coupling of the resulting amine with 3,5-*bis*(trifluoromethyl)phenyl isothiocyanate afforded the desired catalyst precursor **83** in 51% yield, bearing a Schreiner-type thiourea as the hydrogen-bond donor group.

2.4.3 L-Valine Derived BIMP

Synthesis of the catalyst precursor containing an isopropyl substituent at the stereogenic centre started with reduction of the carboxylic acid of L-valine in the same way as was performed for **81** and **118**. Initially, *N*-Fmoc was chosen as a bulky protecting group to avoid the formation of an organoazide of low molecular mass which could potentially be explosive.

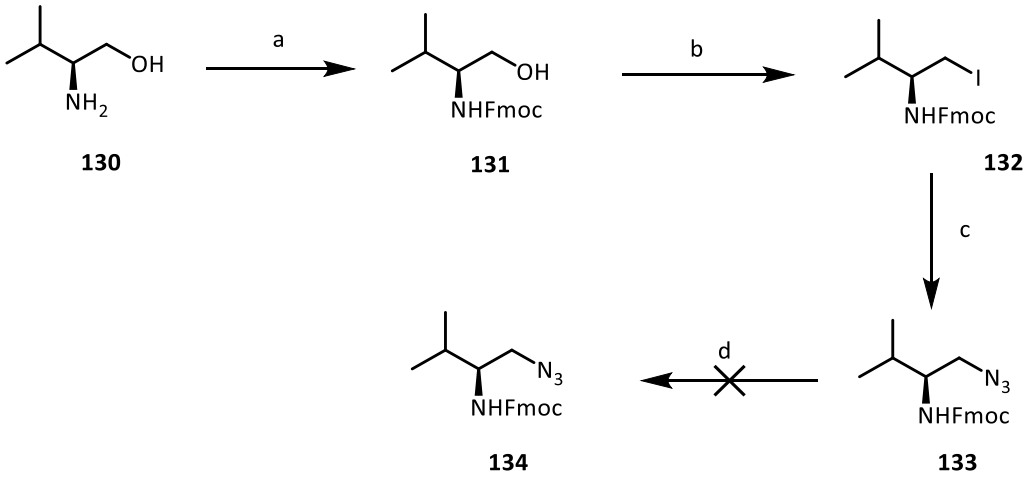

130 **131** **132** **133** **134**

Scheme 35: (a) FmocCl, 5% K_2CO_3, THF, 2h, 83%; (b) PPh_3, I_2, Imidazole, DCM, 90%; (c) NaN_3, DMF, 77%; (d) Et_2NH, THF then bis(3,5-trifluoromethyl)phenyl isothiocyanate, 0%.

The Fmoc protected amino alcohol **131** was produced in 83% yield (Scheme 35). An Appel reaction efficiently afforded the iodide **132** in 90% yield and subsequent treatment with sodium azide afforded the azidoamine **133** in 77% yield. Deprotection of the Fmoc functional group using diethylamine and subsequent reaction of the resulting amine with *bis*(3,5-trifluoromethyl)phenylisothiocyanate was attempted. Purging of the residual diethylamine by azeotropic removal with toluene proved to be unsuccessful due to the volatile nature of the free azidoamine**.** Furthermore, instability of the azidoamine to silica gel and acid meant that these two methods of purification were not viable.

Due to the problems that this synthetic route presented, the synthetic pathway detailed for the L-phenyl alanine derived scaffold (*vide* supra) was evaluated for the L-valine derived scaffold (Scheme 36).

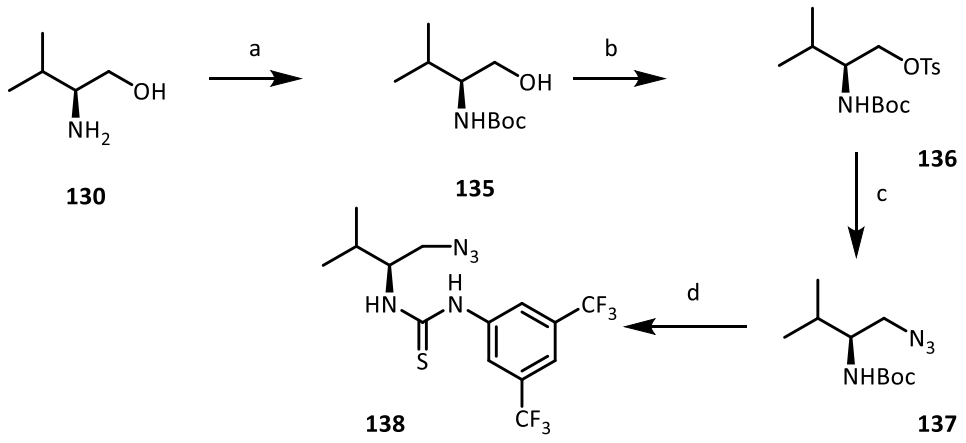

130 **135** **136** **137** **138**

Scheme 36: (a) Boc_2O, NEt_3, CH_2Cl_2, RT, 12 h, quant; b: TsCl, NEt_3, CH_2Cl_2, RT, 8 h, 64%; (c) NaN_3, DMF, 45 ºC, 14 h, 51%; (d) TFA, then 3,5-bis (trifluoromethyl)phenyl isothiocyanate, THF, RT, 12 h, 61%.

The *N*-Boc protected azidoamine **137** was formed in 51% yield. *N*-Boc deprotection and coupling with the isothiocyanate afforded the desired L-valine derived catalyst precursor **138** in 61% yield.

2.5 Proof of Concept

2.5.1 Initial reactivity

A study was initiated to explore whether there was a correlation between reactivity and the basicity of organocatalyst in the reaction of 1.0 equiv of diethyl phosphite **90** with 2.0 equiv of *N*-DPP ketimine **139a**, derived from commercially available acetophenone. A series of NMR experiments were conducted using 10 mol% of different achiral bases where conversion[ii] was measured as a function of time (Figure 5). Triisopropyl Verkade superbase **141** performed very well (blue line, Figure 5) and displayed the highest reactivity. Second, BEMP **142**, bearing an iminophosphorane moiety was the achiral base of choice to represent BIMPs and reactivity was promising (black line, Figure 5). DBU **143** (green line, Figure 5) was comparable to BEMP, but displayed a slightly attenuated reactivity profile.

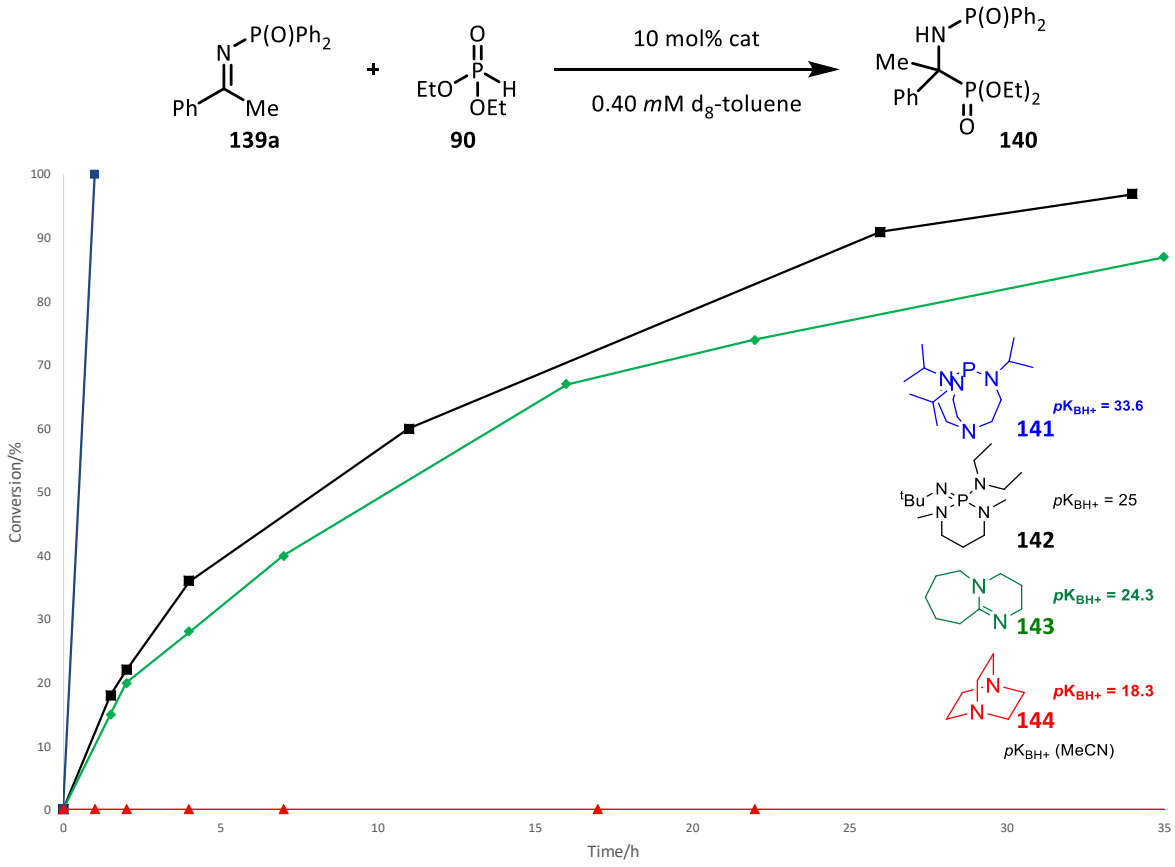

Figure 5: Measurement of conversion with respect to reaction time for ketimine phospha-Mannich reaction using achiral bases: (blue) tri-isopropyl Verkade's base, (black) BEMP, (green) DBU, (red) DABCO.

[ii] **Conversion measured with respect to ketimine starting material.**

DABCO **144**, the base of choice to represent the tertiary amine based organocatalysts displayed no reactivity (red line, Figure 5). The conclusion of this investigation was that strength of base is indeed proportional to reactivity and that this phospha-Mannich ketimine reaction, utilising diethyl phosphite as the pro-nucleophile could be accessible using our chiral BIMP organosuperbase family of catalysts.

2.6 Synthesis of *N*-Diphenylphosphinoyl (*N*-DPP) Ketimines

The synthesis of *N*-DPP ketimines was achieved in two steps, where the oxime was first synthesised on condensation of hydroxylamine hydrochloride and ketones **145a-c** (Scheme 37). This afforded the oxime intermediates **146a-c**, which was used crude in the next step. The second step of the synthesis involved reaction of the oxime with chlorodiphenylphosphine in the presence of triethylamine at -45 °C, which was then slowly warmed to room temperature and stirred at this temperature for an overnight period to afford the desired ketimine products **139a-c**.[57] The unreactive nature of *N*-DPP ketimines means that they were less susceptible to hydrolysis and were therefore more stable to silica gel than their aldimine counterparts; making flash column chromatography a viable means of purification.

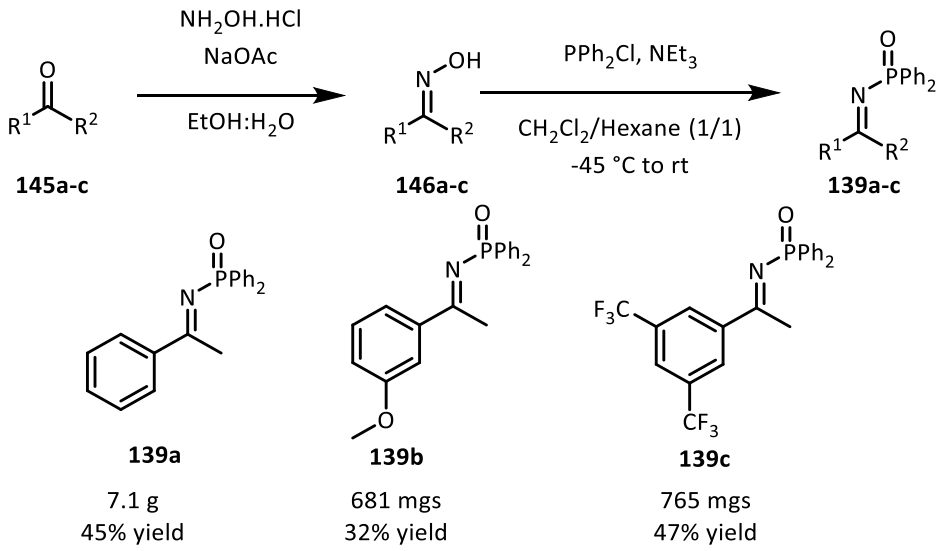

Scheme 37: Synthesis of *N*-DPP ketimines over two-steps. Isolated yields reported were determined with respect to the oxime.[iii]

The low isolated yields of Ketimines **139a-c** is reflective of their partial instability to silica. After flash column chromatography (FCC), pure ketimines were obtained by trituration with Et_2O. Alternative means of purification such as recrystallization proved to be unreliable.

2.7 Optimisation of Reaction

[iii] **Ketimines 139d-j were synthesised by Alistair Farley.**

The Mannich reaction of diethyl phosphite **90** with ketimine **139a**, from acetophenone was chosen to be our model system for this reaction. The effect of solvent on the catalysis was evaluated using 10 mol% of first generation BIMP catalyst **84** (Table 1).

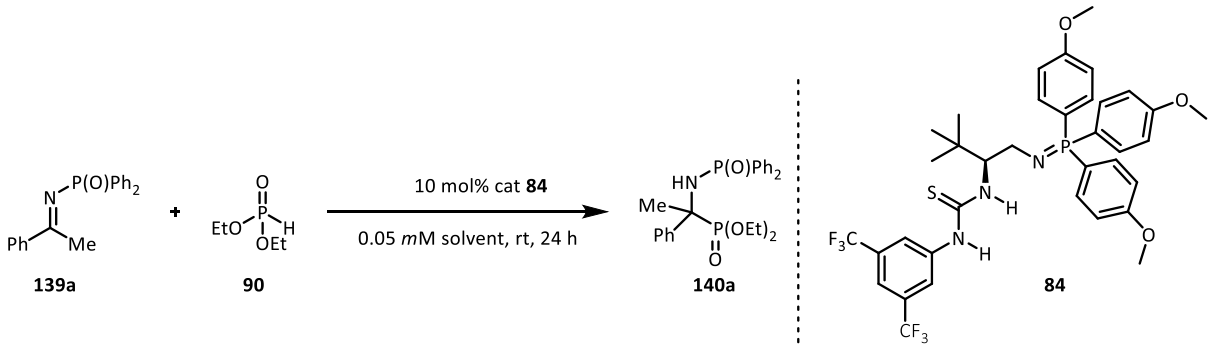

139a **90** **140a** **84**

Entry	Solvent	Yield/% (153)	ee/%
1	Toluene	95	45
2	Et_2O	99	58
3	THF	99	45
4	MeCN	62	0
5	MeOH	0	-

Table 1: Solvent screen for BIMP catalysed ketimine phospha-Mannich reaction.

Use of toluene as a solvent led to a good isolated yield of adduct **140a** and moderate enantioselectivity (Table 1, entry 1). It was shown that ethereal solvents such as THF and Et_2O were favourable for reactivity and enantioselectivity (Table 1, entries 2 & 3). Employment of polar aprotic and polar protic solvents as exemplified with acetonitrile and methanol respectively led to moderate reactivity with the former (Table 1, entry 4) and no reactivity with the latter (Table 1, entry 5). The inferior results on employment of these two solvents suggest that in a polar medium, interactions between the organocatalyst and substrates are not as strong compared to a non-polar medium. With this knowledge in hand, investigations into the optimum components of the BIMP catalyst for this reaction followed.

2.7.1 Optimisation of Catalyst Scaffold

To allow for an expeditious screening process, the catalysts were synthesised *in situ* from the corresponding aminoazide precursor and an equimolar amount of *tris*(4-methoxyphenyl)phosphine in Et_2O for 24 hours, after which the solvent was removed. Ketimine, solvent (that had been degassed *prior* to use) and diethyl phosphite were subsequently added. Reactivity was good on using catalyst **86**, where the iminophosphorane derived from triphenylphosphine resulted in a good yield of 74% being obtained after 24 hours and a moderate ee of 56% (Figure 6). On using more basic catalyst **84**,

reactivity was augmented (as reported in Table 1) and a slight increase in enantioselectivity (99% yield, 58% ee) was observed.

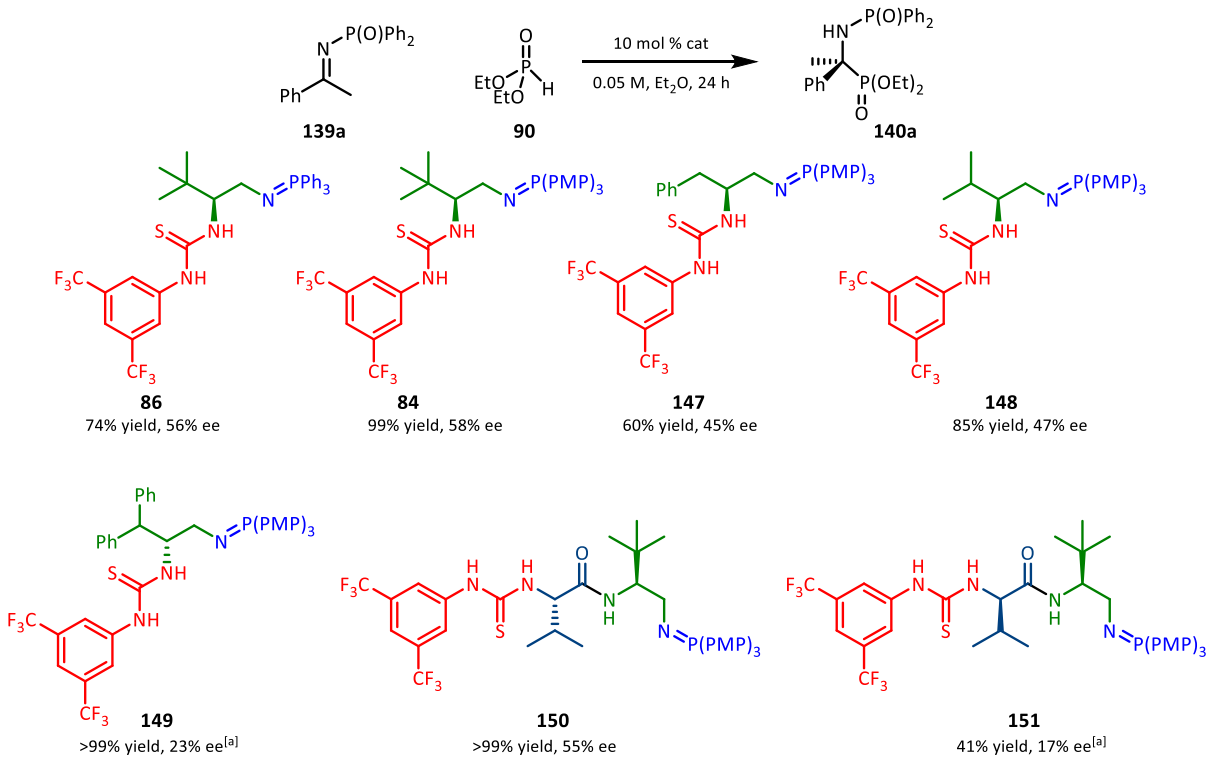

Figure 6: Optimisation of chiral scaffold of catalyst, PMP=*para*-methoxyphenyl. [a]Opposite enantiomer obtained.

Catalysts derived from L-phenylalanine and L-valine, **147** and **148** respectively resulted in lower reactivity and selectivity. Catalyst **149**, featuring a diphenylmethyl moiety resulted in quantitative formation of product with lower enantioselectivity (23% ee). Interestingly, catalysts **150** and **151** featuring a valine residue in between the iminophosphorane and Schreiner thiourea group allow for diastereoisomers to be synthesised from both L- and D-valine. Taken together, these two catalysts demonstrated that the valine residue was playing a critical role in governing both the reactivity and selectivity of this reaction. Catalyst **150** afforded the product in 55% ee and quantitative isolated yield, whereas catalyst **151** afforded the product in a significantly lower yield of 41% and only 17% ee of the opposite enantiomer of product. From these results, the optimum catalyst scaffold was the L-*tert*-Leucine derived scaffold featuring a *tris*(4-methoxyphenyl) phosphine as part of the iminophosphorane **84**. The hydrogen-bond donor group was then assessed.

2.8 Optimisation of the Hydrogen-Bond Donor Group

Accordingly, use of a urea hydrogen-bond donor group instead of a thiourea in catalyst **152**[iv] resulted in a small drop in enantioselectivity of the product (51% ee), whilst reactivity was retained compared with the Schreiner-type thiourea hydrogen bond donor (Scheme 38).

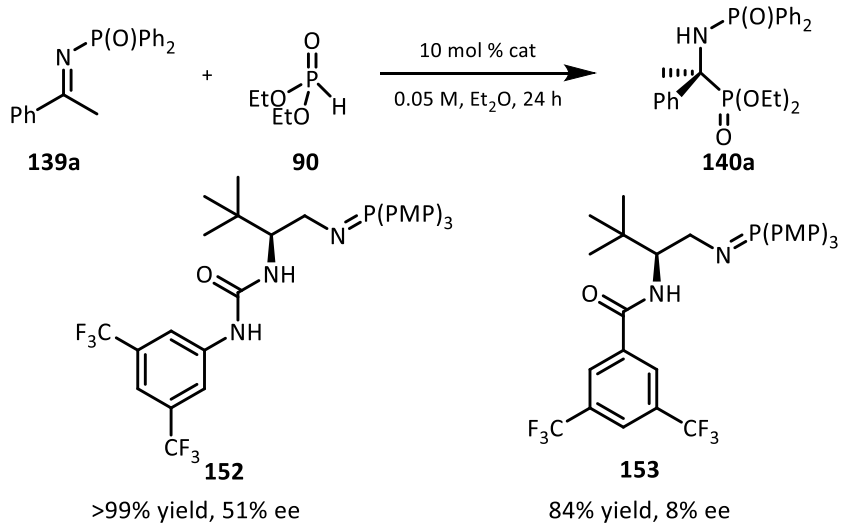

Scheme 38: Screening urea and amide hydrogen-bond donor groups.

Catalyst **153**, featuring an electron-deficient amide resulted in attenuated reactivity (84% yield) and poor enantioselectivity (8% ee). On the basis of these experiments, we concluded that acidic hydrogen-bond donor groups were favourable for both reactivity and selectivity. In 2009, Ellman and co-workers reported the use of an *N*-sulfinyl thiourea hydrogen-bond donor group in catalyst **156** for the highly efficient enantioselective addition of thioacetic acid **155** to nitroolefins (Scheme 39).[48]

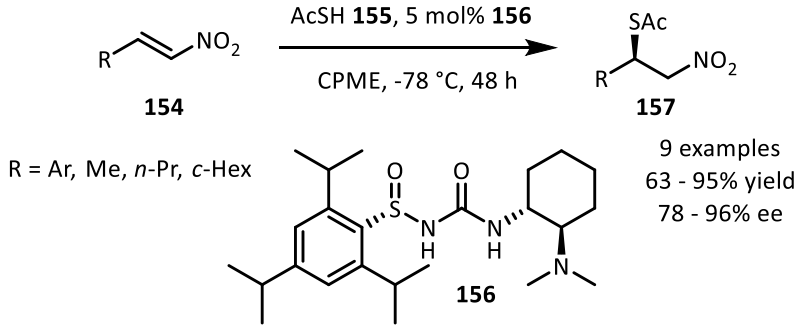

Scheme 39: Ellman's enantioselective addition of thioacetic acid to nitroolefins catalysed by Takemoto's catalyst bearing an *N*-sulfinylthiourea hydrogen-bond donor group.

[iv] **Catalysts 152 and 153 were prepared by Alistair Farley.**

Aliphatic and aromatic nitroolefins were tolerated well, with good reactivities and excellent enantioselectivities. It was shown that use of Takemoto's catalyst, bearing a Schreiner thiourea hydrogen-bond donor group resulted in a significantly lower enantiomeric excess of the product contrasted with the same catalyst bearing an *N*-sulfinyl thiourea hydrogen bond donor group.

Catalytic precursor **161**, derived from L-*tert*-leucine bearing an *N*-sulfinyl thiourea hydrogen-bond donor was thereby synthesised (Scheme 40).

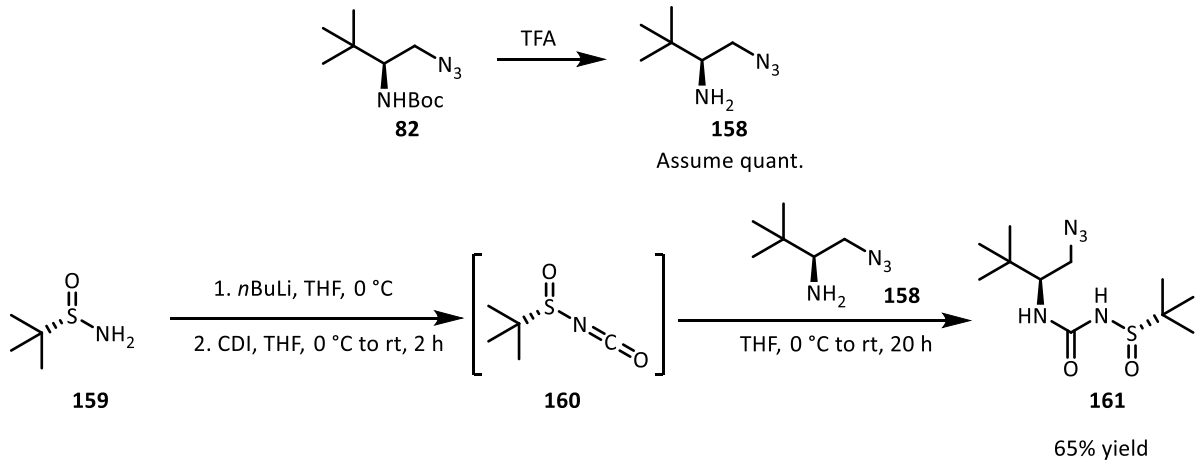

Scheme 40: Synthesis of catalyst precursor 161 bearing an *N*-sulfinyl thiourea hydrogen-bond donor group. Catalyst containing *N*-sulfinyl thiourea derived from (*R*)-sulfinamide was also synthesised in the same way as presented here.

Synthesis of **161** was adapted from the work of Ellman[58] and co-workers. Initially, deprotonation of chiral sulfinamide **159** was performed using *n*BuLi and subsequent reaction with carbonyldiimidazole, followed by rearrangement afforded the proposed isocyanate intermediate **160**. This was then trapped with azidoamine **158** to afford the desired product **161** in moderate yield over two steps. Iminophosphoranes derived from *tris*(4-methoxyphenyl)phosphine of catalysts **161a** and **161b** bearing *N*-sulfinyl thioureas derived from (*S*)-sulfinamide and (*R*)-sulfinamide respectively were synthesised as outlined in section 2.7.1 and were screened using the best conditions obtained thus far (Figure 7).

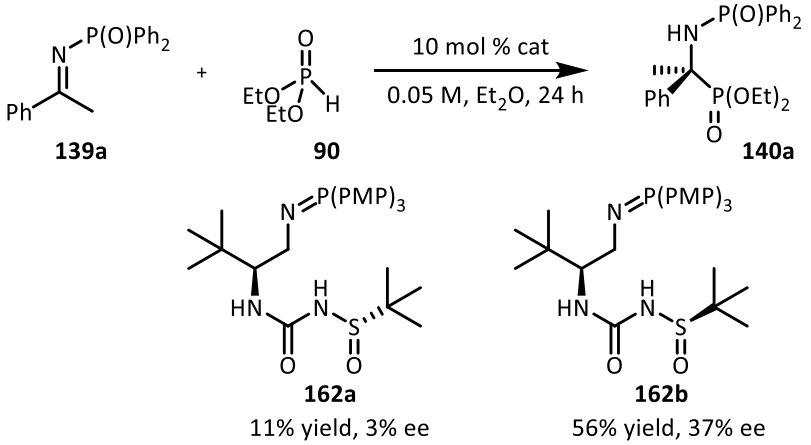

Figure 7: Evaluation of catalysts 162a and 162b (synthesised from catalytic percursors 161a and 161b) bearing an *N*-sulfinyl thiourea derived from (*S*)-2-methylpropane-2-sulfinamide and (*R*)-2-methylpropane-2-sulfinamide respectively.

The stereogenic centre on the sulfur atom exhibited a significant effect on both reactivity and selectivity with catalyst **162b** affording the product in 56% yield and 37% ee. Use of diastereoisomeric catalyst **162a** afforded the product in a significantly lower yield and enantioselectivity (11% and 3% ee).

However, this investigation indicated that the Schreiner thiourea hydrogen-bond donor group was the best for both reactivity and selectivity. A brief optimisation for reaction concentration and temperature using 10 mol% cat **84** disappoingtingly saw no improvement in enantioselectivity. With these conditions in hand, the substrate scope of the reaction was then evaluated.

2.9 Substrate Scope

Examination of the scope of ketimines for this reaction revealed that electron-rich and electron-poor aromatic ketimines were well tolerated (Figure 8). Reactivity was typically high, with yields of >99% being obtained. Enantioselectivities were moderate (41-71% ee) with the highest enantioselectivity being obtained with the ethyl homologue **140j** (71% ee and >99% yield).

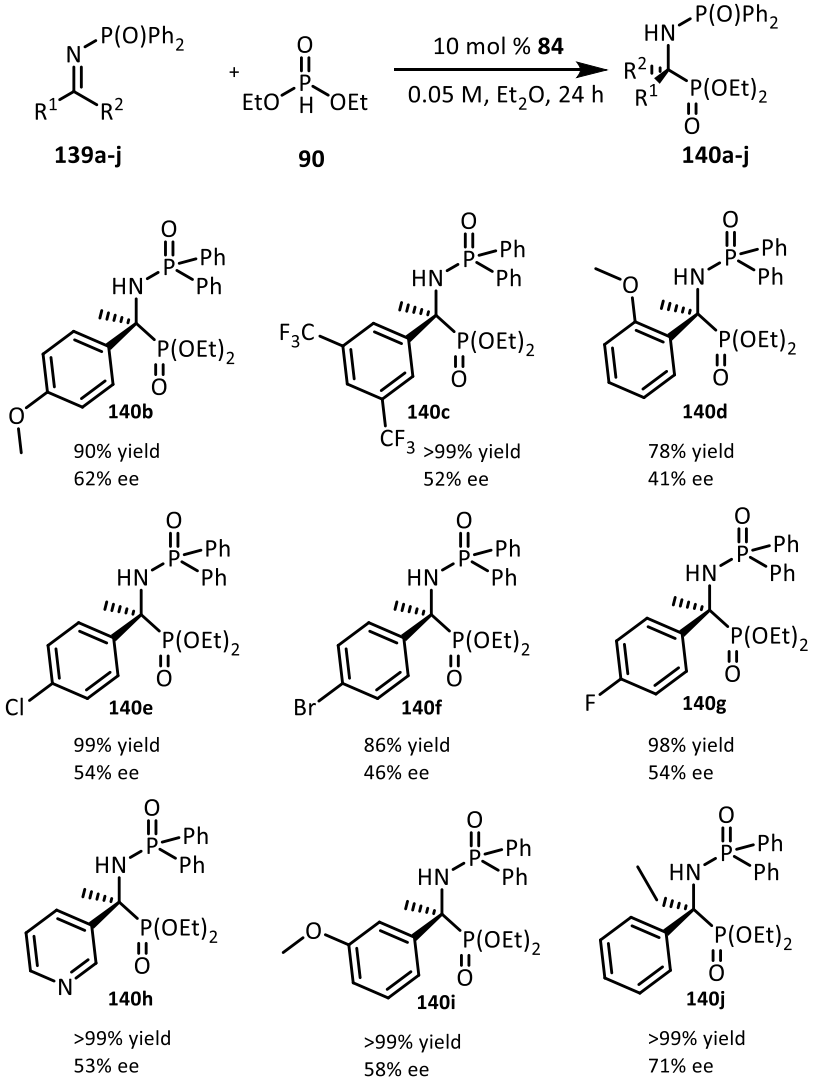

Figure 8: Substrate scope for the bifunctional iminophosphorane catalysed ketimine phospha-Mannich reaction.[59]

Pleasingly, the 3-pyridyl substrate performed well and the product **140h** was obtained in >99% yield and 53% ee.

2.9.1 Determination of Absolute Configuration

The absolute configuration of **140** was determined by derivatisation to a known compound and the specific optical rotation compared with the literature (Scheme 41). The diphenylphosphinoyl protecting group was cleaved under HCl generated *in situ* by dropwise addition of acetyl chloride to ethanol. The absolute configuration of the chiral amine **163** was thus determined to be *S*.

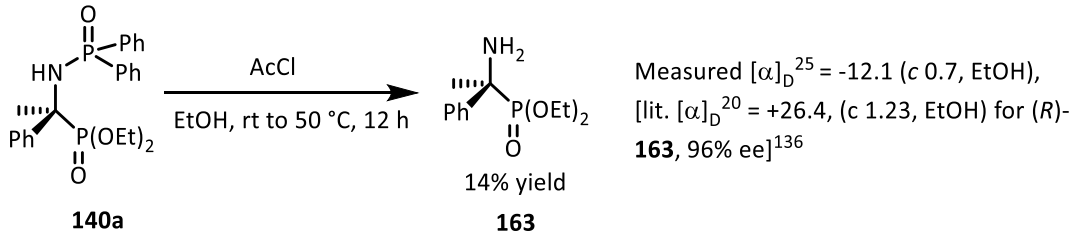

Scheme 41: Derivatisation of phospha-Mannich adduct for proof of absolute stereochemical configuration.

2.9.2 Reaction Mechanism

The prototropic tautomerism of organophosphorous compounds containing a phosphinylidene moiety is well documented.[60] Prototropic tautomerism can be best defined as the movement of a proton from one atom in a molecule to another (Scheme 42, A). The best example of this kind of tautomerism is keto-enol tautomerism. Prototropic tautomerism can be induced by a catalytic amount of Brønsted base. Tan[61] and co-workers reported the highly efficient, enantioselective phospha-Michael reaction of a phosphine oxide nucleophile **164** with nitroolefin electrophiles in the presence of a bicyclic guanidine as catalyst **165** (Scheme 42, B).

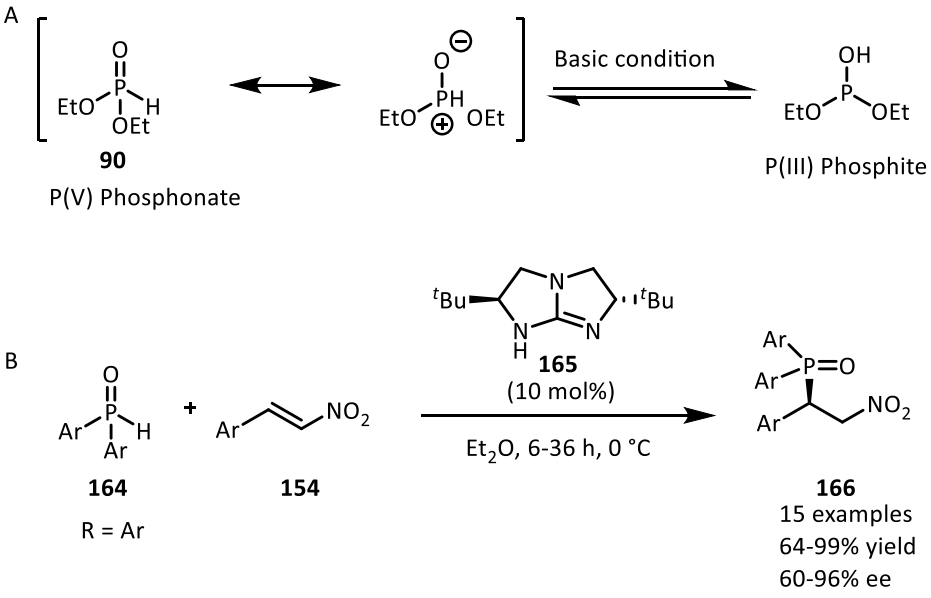

Scheme 42: (A) Prototropic tautomerism of diethyl phosphite 90 where base catalyses the interconversion of the phosphonate form to the phosphite form; (B) Tan's phospha-Michael reaction of phosphine oxide pro-nucleophiles with nitroolefins.

Furthermore, theoretical investigations into this reaction[62] revealed that the bicyclic guanidine organocatalyst played a crucial role in catalysing the interconversion of the phosphine oxide nucleophile into the phosphinic acid form. The nucleophile in the phosphinic acid form can then take part in P-C bond formation with the activated nitroolefin electrophile, which was elucidated to be the

rate determining step. The final stage of the reaction is the abstraction of the N-H proton on the catalyst by the α-anion of the nitroolefin to liberate the product.

A catalytic cycle is thereby proposed whereby the bifunctional iminophosphorane catalysed ketimine phospha-Mannich reaction proceeds in a similar manner (Figure 9).

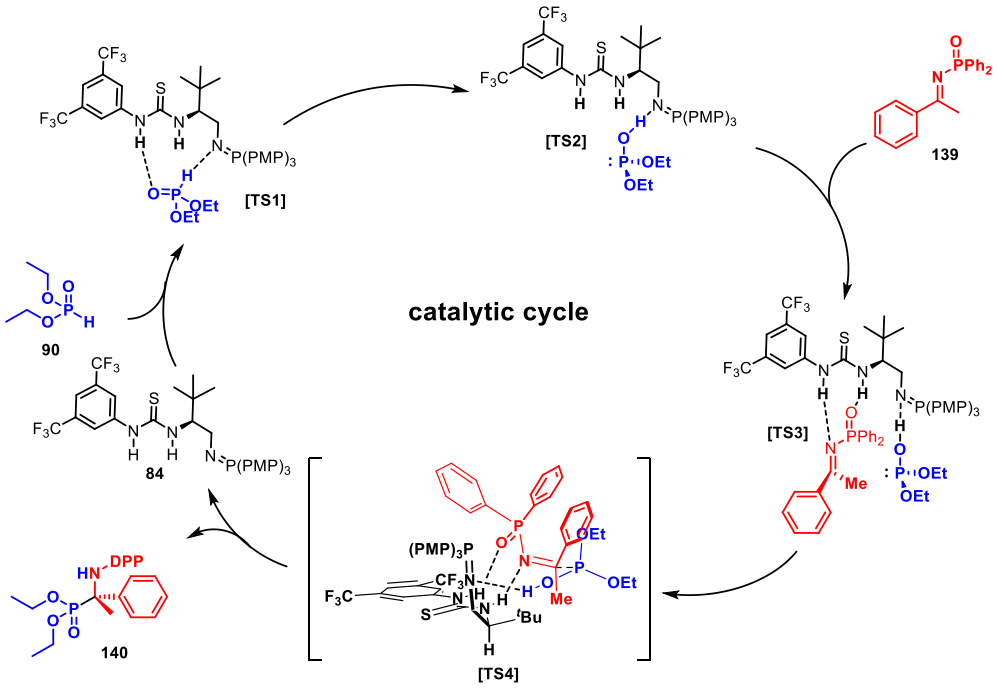

Figure 9: Proposed catalytic cycle for the enantioselective BIMP catalysed ketimine phospha-Mannich reaction. Charges on the catalyst and ketimine have been omitted for clarity.

Coordination of the phosphite in the more stable phosphonate form to the BIMP catalyst leads to a complex stabilised by hydrogen-bonding interactions (**TS1**). This pre-transition state complex allows for a simultaneous proton abstraction by the iminophosphorane moiety on the catalyst and proton donation from the acidic Schreiner-type thiourea moiety to effect tautomerization to yield the phosphite nucleophile (**TS2**). Subsequently, the ketimine electrophile is activated by hydrogen-bonding from both the Schreiner thiourea and/or the newly formed protonated iminophosphorane (**TS3**). This complex brings both the phosphite nucleophile and activated ketimine electrophile into close proximity whereby P-C bond formation can take place on to the *si*-face of the ketimine (**TS4**). Proton transfer from the protonated catalyst to the product leads to liberation of the product with *S*-stereochemistry and regeneration of the catalyst.

2.10 Conclusions and Future Work

In conclusion, the first organocatalytic ketimine phospha-Mannich reaction with *N*-DPP ketimines has been reported. The reaction tolerates both electron-rich and electron-deficient aromatic ketimines, with heteroaryls proving to be accessible under our reaction conditions resulting in excellent yields and moderate enantioselectivities (78-99% yield, 41-71% ee) throughout. Future work involves the synthesis and evaluation of a larger library of BIMP organocatalysts for this reaction in the hope of improving enantioselectivity.

3. Silver-Catalysed Enantioselective Mannich Reaction of Diazoacetates to *N*-Boc protected Aldimines

3.1 Chapter Overview

This chapter describes the first highly enantioselective silver-catalysed Mannich reaction of diazoacetate esters with *N*-Boc protected aldimines. We chose to explore this reaction as it allows for the synthesis of β-amino acid derivatives with the added value of the possibility of further synthetic potential of the diazo motif. Metal-based approaches for this reaction have been limited, possibly due to the high lability of the diazo moiety in the presence of many metal ions; liberating a carbenoid intermediate with the concomitant evolution of dinitrogen gas.[63] This renders a Mannich reaction of diazoacetate esters with aldimines impossible using many metal ions. A Lewis acid mediated catalytic system was quickly discovered in the form of Ag(I) in combination with an atropisomeric chiral bisphosphine ligand. The scope was broadly tolerant of electron-rich and electron-poor substituents on the aryl component of the aldimine as well as displaying good tolerance for heterocycles. To demonstrate the generality of our method compared with previous methods, variations on the ester component of the diazoacetate ester was also tolerated. Investigations into the scalability of this reaction was performed as well as derivatisations of the adduct. It is shown that this catalytic system addresses the reactivity and selectivity problems encountered thus far with metal-catalysed approaches for this reaction.

3.2 Introduction and Previous Work

The reaction of diazoacetate esters with aldimines features the diazoacetate ester acting as a carbon-centred nucleophile (Scheme 43) and can produce two possible outcomes, where **168** is a common intermediate. One outcome is the Mannich reaction, where the diazo group remains intact in the product **170**. The other outcome is formation of the aziridine product **169** through an intramolecular cyclisation, where the resulting anion residing on the nitrogen atom in intermediate **168** can function as a nucleophile and cyclise with the α-position liberating dinitrogen gas.

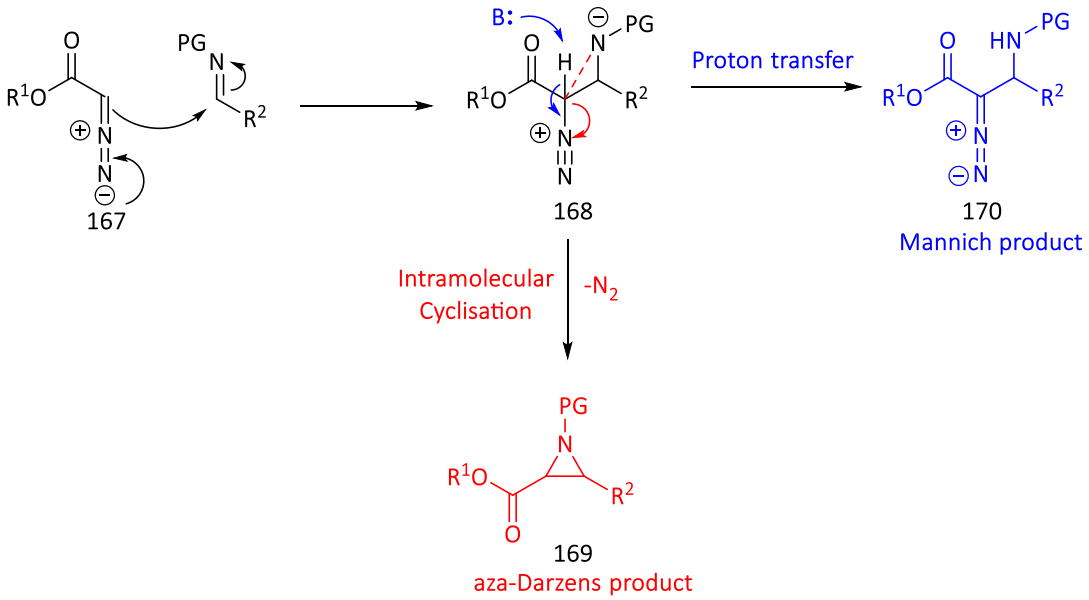

Scheme 43: Reaction profiles for both Mannich (blue) and aza-Darzen (red) reactions which proceed *via* intermediate 168.

The Mannich reaction pathway would involve deprotonation of the α-proton after C-C bond formation, thus reforming the diazo motif. This deprotonation can be effected using either a basic catalyst or by the addition of a basic additive. Subsequent proton transfer yields the Mannich-type product.

3.2.1 Metal-based Approaches for Mannich Reaction

To the best of our knowledge, there has been only one report of a metal-catalysed Mannich type reaction of ethyl diazoacetate **171** (EDA) with the *N*-Boc aldimine of furfural **52c** reported by Kumaraswamy in 2010.[64] The catalytic system employed here consisted of 5 mol% of Trost ligand *S*,*S*-prophenol **172**/10 mol% of Et_2Zn in THF which afforded the Mannich adduct in a moderate yield of 62% and an ee of 84% (scheme 44).

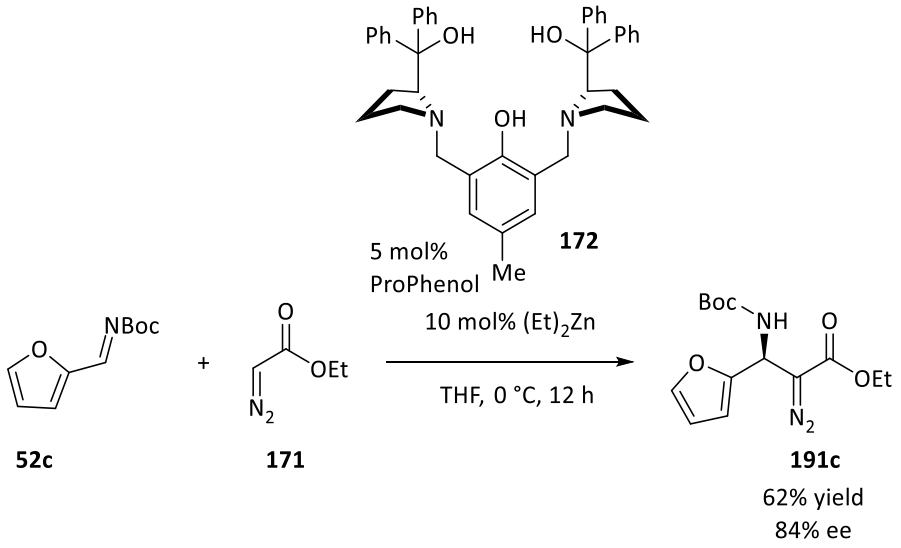

Scheme 44: Kumaraswamy's Mannich reaction of EDA with *N*-Boc imine of furfural.

Furthermore, Trost and co-workers attempted this reaction utilising their dinuclear Mg-based chiral catalytic system, however it resulted in low reactivity and enantioselectivity. Their catalytic system proved to be more oxyphilic and was successfully applied to the addition reaction where aldehydes were employed as the electrophile for the synthesis of β-hydroxy-α-diazoesters.[65] The limited scope and only moderate reactivity was a limitation of the prophenol-zinc catalytic system for the synthesis of Mannich adducts using diazoacetate ester pro-nucleophiles.

3.2.2 Organocatalytic Approaches for Mannich Reaction

Organocatalytic examples of this reaction have been more successful. For example, in 2005, Terada[66] reported the highly enantioselective Mannich reaction of *tert*-butyl diazoacetate **174** with aldimines (Scheme 45).

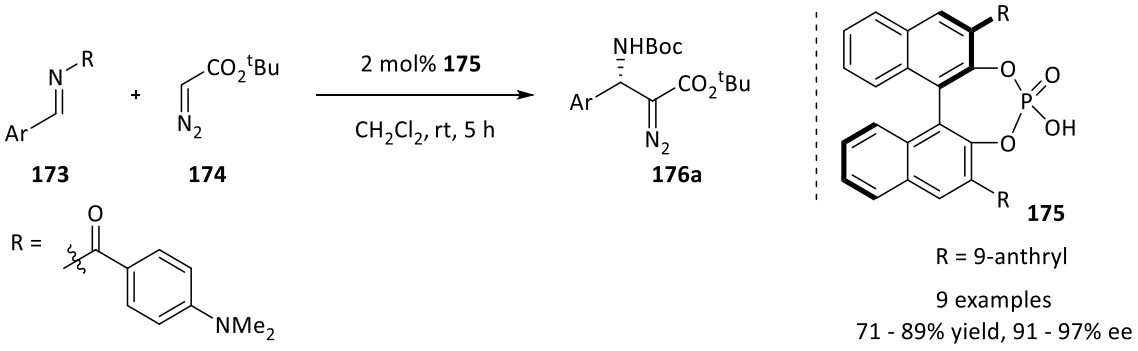

Scheme 45: Terada's enantioselective Mannich reaction of *tert*-butyl diazoacetate with aldimines, catalysed by a chiral phosphoric acid catalyst.

The highest enantioselectivities were achieved using *para*(dimethylamino)benzoyl protected aldimines. The reaction afforded the desired Mannich adducts in excellent yields and

enantioselectivities with only 2 mol% of organocatalyst **175**. It was found that *tert*-butyl diazoacetate ester **174** gave rise to the highest enantioselectivities, with ethyl diazoacetate **171** resulting in only moderate enantioselectivity (79% ee). This limited the scope somewhat and generality of this method.

Shortly afterwards, in 2007, Maruoka[67] reported a highly enantioselective Mannich reaction of *tert*-butyl diazoacetate **174** with *N*-Boc protected aldimines mediated by a chiral dicarboxylic acid catalyst **177** (Scheme 46).

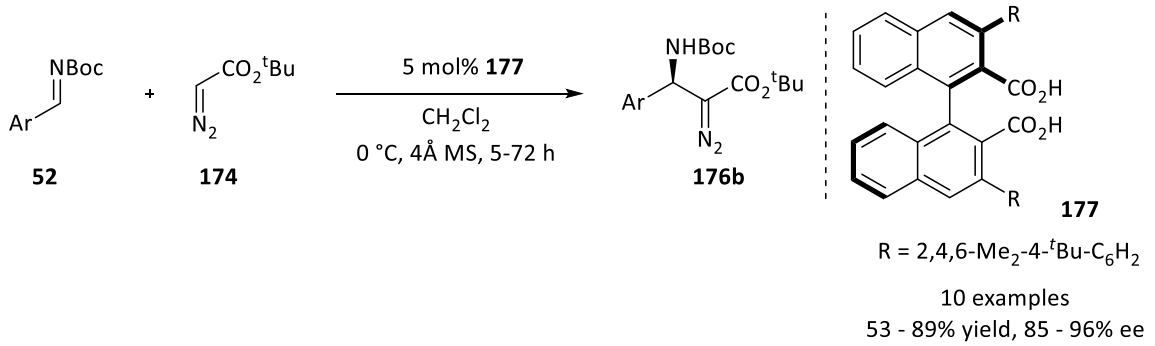

Scheme 46: Maruoka's dicarboxylic acid catalysed reaction of tert-butyl diazoacetate with *N*-Boc protected aldimines.

The reaction afforded the product in good yields and typically excellent enantioselectivities. The scope of the reaction proved to be broad with respect to the aldimine substrate; tolerating electron-rich and electron-poor aryl aldimines well. A limitation of this method was that long reaction times were required for electron-rich aldimines such as the *o*-tolyl substrate; requiring 72 hours to generate the product in only 53% yield. Furthermore, heteroaryl aldimines in form of the furyl substrate resulted in diminished enantioselectivity of 85% ee.

3.2.3 Lewis Acid and Brønsted Acid Approaches for Aziridine synthesis (aza-Darzens)

Lewis acid mediated reactions of diazoacetate esters with aldimines typically lead to aza-Darzen products. In 2007, Wulff and co-workers reported the highly enantioselective and *cis*-selective aziridination reaction of ethyl diazoacetate **171** to *N*-dianisylmethyl (*N*-DAM) aldimines (Scheme 47).[68]

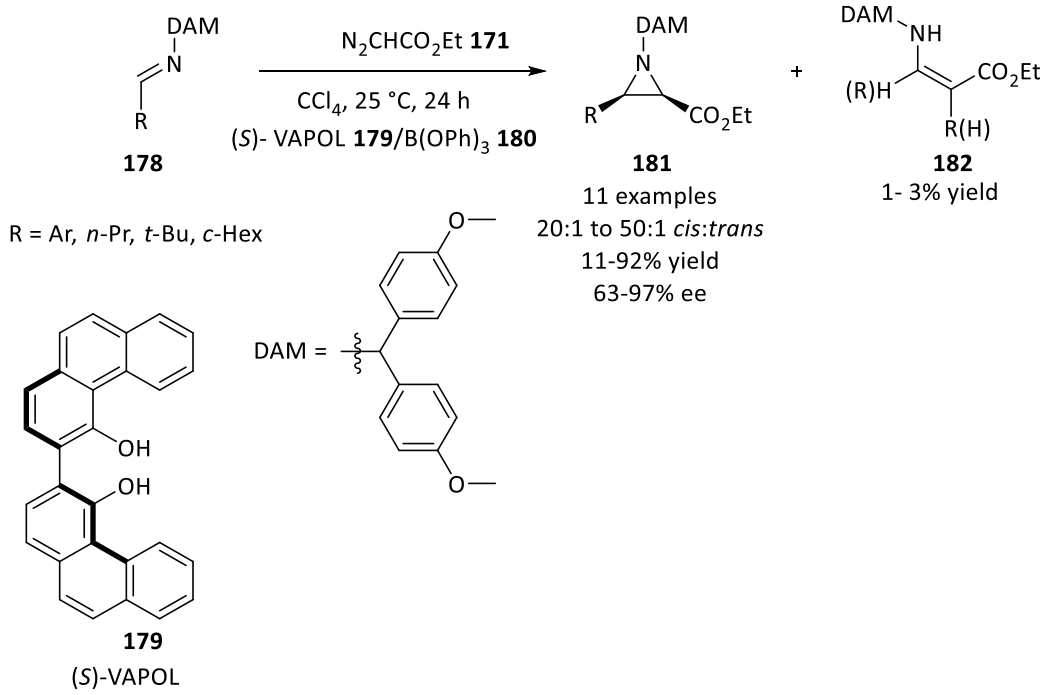

Scheme 47: Wulff's enantioselective aziridination reaction of ethyl diazoacetate with *N*-DAM aldimines for the formation of the *cis*-selective aziridine product.

The reaction was mediated by a chiral catalyst formed from triphenyl borate **180** and VAPOL ligand **179**. High enantio and diasteroselectivities were obtained for both aliphatic and aromatic aldimines with carbon tetrachloride as a reaction solvent. Only small quantities of enamine side product **182** were generated in the reaction (*vide infra*).

Brønsted Acid organocatalysts can also be used to afford aza-Darzen products from diazoacetate esters and aldimines. For example, Johnston reported the highly diastereoselective aza-Darzens reaction of ethyl diazoacetate with *N*-$CHPh_2$ imines mediated by a triflic acid catalyst (Scheme 48).[69] The reaction afforded the *cis*-configured product in good yields and excellent diastereoselectivities. Aromatic as well as aliphatic aldimines were tolerated. A limitation of this method was that electron-deficient aromatic aldimines gave rise to the desired product in higher yields and diastereoselectivities contrasted with products from aliphatic or electron-rich aromatic aldimine substrates.

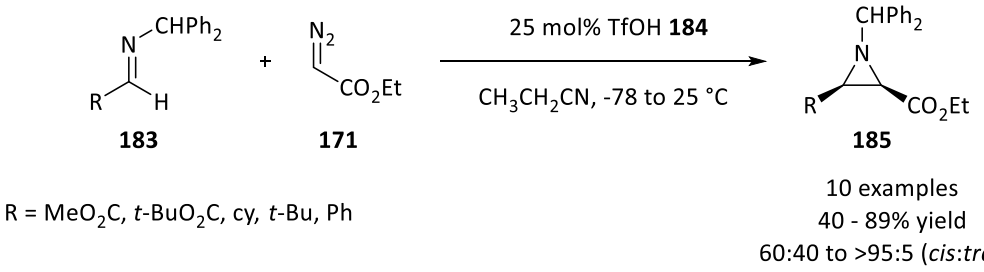

Scheme 48: Johnston's highly diastereoselective, triflic acid mediated aza-Darzens reaction of ethyl diazoacetate with *N*-$CHPh_2$ aldimines.

In a similar manner, Bew and co-workers identified pyridinium triflate as an efficient Brønsted Acid organocatalyst for the synthesis of *cis*-configured *N*-alkyl and *N*-arylaziridine carboxylates from aryl or aliphatic aldimines with ethyl or *tert*-butyl diazoacetate.[70]

Following on from the work of Terada (*vide supra*), Akiyama reported the highly enantioselective aza-Darzens reaction of ethyl diazoacetate **171** with *N*-PMP protected phenyl glyoxal derived aldimines (Scheme 49).[71,72] The aldimines could be formed *in situ* by condensation of the glyoxal derivative and *p*-anisidine **59** in the presence of $MgSO_4$.

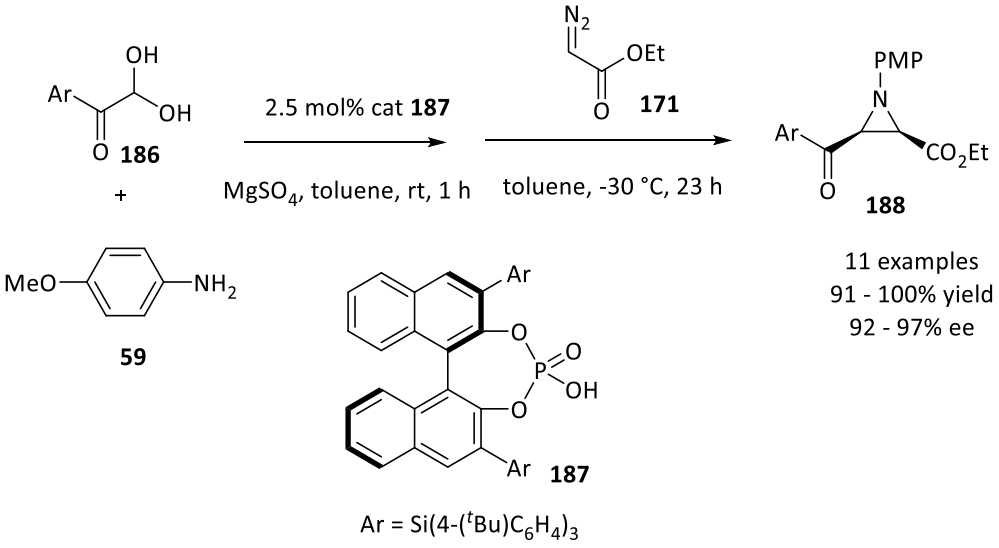

Scheme 49: Akiyama's enantioselective, phosphoric acid catalysed aza-Darzens reaction.

The reaction furnished the *cis*-product, as a single diastereoisomer in excellent yields and enantioselectivities. It was proposed that the electron-donating *N*-PMP protecting group promoted aziridine formation, whereas in Terada's Mannich reaction (Scheme 45), the electron-withdrawing *N*-acyl protecting group renders the nitrogen atom sufficiently less nucleophilic to favour the formation of the Mannich product. The different product distributions obtained on varying the protecting group on the aldimine highlights the bifunctional nature of the chiral phosphoric acid organocatalysts **175** and **187**. In the Mannich reaction pathway, the catalyst must be acting as a Brønsted acid to activate

the aldimine as well as a Brønsted base to rediazotise the product according to Figure 10. The same argument can be made for the axially chiral carboxylic acid catalyst **177**.

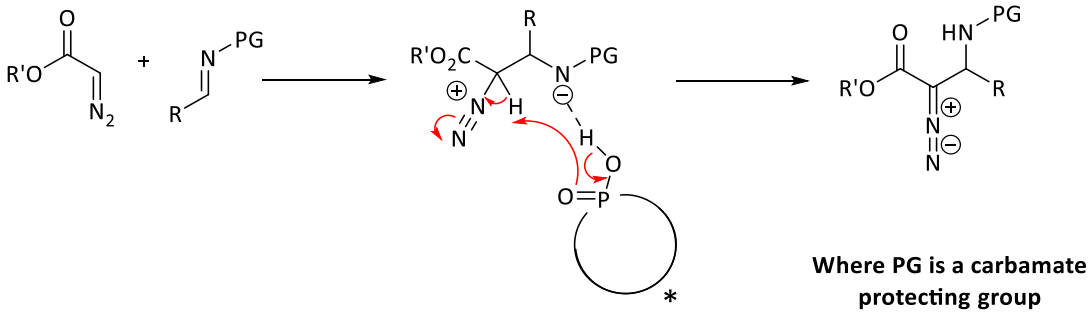

Figure 10: Bifunctional nature of chiral phosphoric acid catalyst to allow for formation of the Mannich-type product.

Clearly, the chemistry of the reaction of diazoacetate esters with aldimines is diverse. However, due to the limitations described above for the synthesis of Mannich products using current organo and metal-based catalytic methods, we saw an opportunity to develop our own catalytic system for a more general, enantioselective Mannich reaction of diazoacetate esters with aldimines.

3.3 The Discovery of the Ag(I) Catalytic System for the Synthesis of Mannich Products

Accordingly, we wanted to develop a catalytic system comprising of a main group transition metal (Ag, Cu, Au), the salts of which can be obtained inexpensively from commercial sources. We chose to focus our attention on silver to begin with.

3.3.1 Insight from the Literature

Given reports in the literature on carbene transfer reactions using silver salts and diazo compounds as the carbenoid precursor[73,74,75], it seemed unlikely that a Mannich reaction of diazoacetates with aldimines could be catalysed by Ag(I). However, the initial discovery of the Ag(I) catalytic system came from the work of Schöllkopf and Rieber[76] who reported the alkylation of ethyl diazoacetate with a range of alkyl halides (Scheme 50).

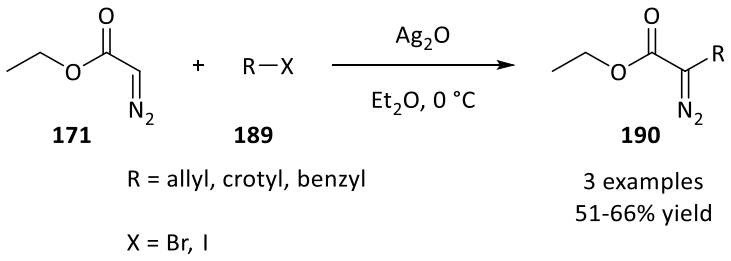

Scheme 50: Schöllkopf and Rieber's Ag_2O mediated alkylation of ethyl diazoacetate.

The reaction was performed using stoichiometric silver(I) oxide and this afforded the desired products in moderate yields. Interestingly, from a mechanistic viewpoint, they speculated the generation of a

silver organometallic diazoacetate ester intermediate on mixing diazoesters and diazo ketones with stoichiometric silver(I) oxide (Figure 11).

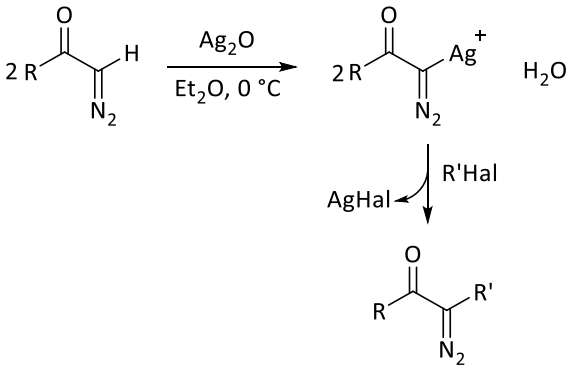

Figure 11: Schöllkopf and Rieber's alkylation of diazo compounds using silver(I) oxide – mechanistic rationale.

Schöllkopf showed that the diazo moiety of ethyl diazoacetate can survive in the presence of Ag(I) and does not form a metal-carbenoid species at 0 °C. This unique reactivity of diazoesters in the presence of silver(I) oxide led us to believe that the proposed silver organometallic complexes of diazoacetates could be trapped with other electrophilic species such as aldimines. Moreover, a chiral ligand associated with the silver ion as part of a metal-ligand complex could allow for an enantioselective transformation.

3.3.2 Proof of Concept and Initial Screening

Accordingly, we chose Ag(I) to be the metal centre for our catalytic system. Ethyl diazoacetate **171** and aldimine **52** were chosen to be our model substrates for the reaction. A preliminary screen for reactivity involved using catalytic silver(I) oxide with ethyl acetate as a solvent (Scheme 51).

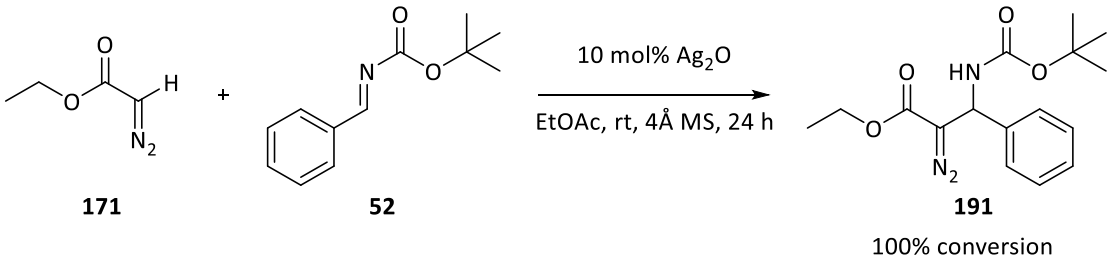

Scheme 51: Mannich reaction of ethyl diazoacetate and aldimine 52, catalysed by silver(I) oxide.

To our delight reactivity was observed; with complete conversion being attained in 24 hours. With this pleasing reactivity established on using silver(I) oxide to afford the Mannich product **191**, it was found that a catalytic amount of triethylamine improved the reactivity greatly, with the reaction going to completion in just 7 hours at room temperature (Scheme 52, A).

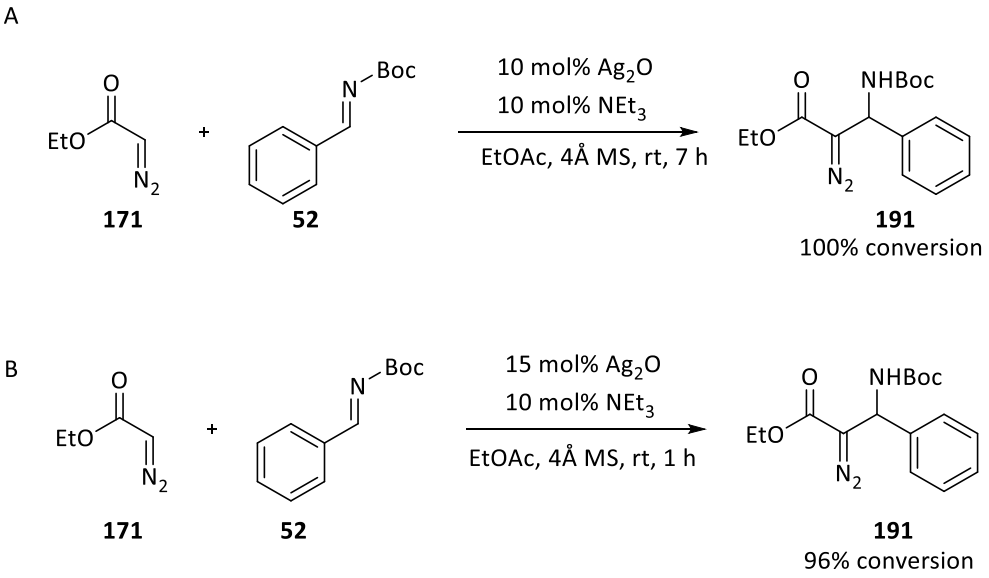

Scheme 52: Mannich reaction of ethyl diazoacetate and aldimine 52, catalysed by silver(I) oxide with the addition of catalytic triethylamine (A) 1 : 1 of Ag_2O : NEt_3 (B) 1.5 : 1 of Ag_2O : NEt_3.

With this knowledge in hand, we then varied the relative stoichiometries of silver(I) oxide : triethylamine and found that a small excess of silver(I) oxide over triethylamine resulted in a faster rate of reaction; with 96% conversion being obtained in just 1 hour at room temperature (Scheme 52, B). The improvement in reactivity with the use of triethylamine is possibly due to the triethylamine acting as a ligand to the silver(I) cation. This effect might not be due to a change in the electronic properties of silver but rather that there are more soluble silver(I) ions available in solution as silver(I) oxide is only partially soluble in ethyl acetate. With this initial reactivity established, we then sought to make the transformation enantioselective.

3.3.3 Initial Ligand and Solvent Screen

The chiral ligand creates a discrete pocket through which the pro-nucleophile and electrophile can be brought into close proximity; adopting a well-defined transition state for bond formation to occur selectively on to one face of the pro-chiral electrophile. The aminophosphine ligand system derived from cinchona alkaloids have been developed and applied by the Dixon group. Dixon and co-workers have developed Ag(I) mediated methods for the enantio and diastereoselective Mannich reaction for the addition of α-substituted isocyanoacetates to ketimines, ketones and aldehydes using chiral aminophosphine ligands.[77] Accordingly, these ligands were evaluated first (Table 2, Entry 1). Pleasingly on using a 1 : 1 stoichiometry of aminophosphine ligand **200** : Ag_2O, a non-zero ee and good reactivity was obtained (81% yield, 9% ee).

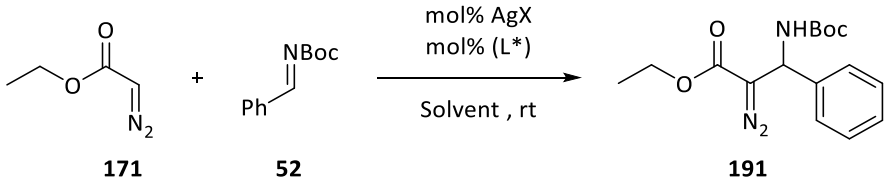

171 **52** **191**

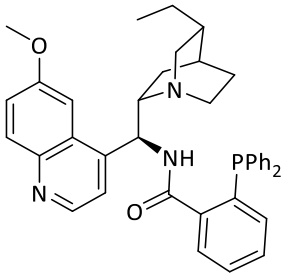

192

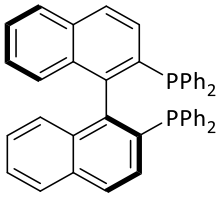

193a

Entry	Ligand (mol%)	Solvent	Silver Salt (mol%)	Time/h	Yield/%	ee/%
1	**192** (10 mol%)	EtOAc	Ag_2O (10 mol%)	15	81	9
2	**192** (20 mol%)	EtOAc	Ag_2O (5 mol%)	24	32	9
3	**192** (10 mol%)	Et_2O	Ag_2O (10 mol%)	24	58	0
4	**192** (10 mol%)	toluene	Ag_2O (10 mol%)	44	13	9
5	**193a** (10 mol%)	EtOAc	Ag_2O (10 mol%)	5	87	24
6	**193a**(10 mol%)	EtOAc	AgOTf (10 mol%)	4	74	37
7	**193a** (10 mol%)	EtOAc	AgOTf (5 mol%)	4	71	39
8	**193a**(10 mol%)	EtOAc	AgOTf (20 mol%)	4	52	35
9	**193a** (10 mol%)	CH_2Cl_2	AgOTf (5 mol%)	6	38	49
10	**193a** (10 mol%)	Et_2O	AgOTf (5 mol%)	6	28	21
11	**193a** (10 mol%)	CH_2Cl_2	AgOTf (5 mol%)	4	50	49[a]

Table 2: All reactions carried out on a 0.10 mmol scale, 0.08 M concentration. [a]Reaction with 10 mol% NEt_3 as additive.

We first evaluated the relative stoichiometries of ligand to silver salt using aminophosphine ligand **192**. It was clear that a 1:1 ratio was best for reactivity (Table 2, entries 1 and 2). Use of an ethereal solvent as represented by diethyl ether led to a decrease in reactivity and 0% ee (Table 2, entry 3). Toluene gave a remarkably low yield compared to ethyl acetate with no improvement in ee (Table 2, entry 4).

At this point, we moved away from the aminophosphine ligand **192** and evaluated other classes of ligands. An obvious class of ligand to study were the bisphosphine ligands, represented here by the

atropisomeric (*S*)-BINAP **193a**. On using this electron-rich ligand, the reactivity increased greatly as did the enantioselectivity (Table 2, entry 5). Silver(I) oxide is quite basic, and with *prior* knowledge from our preliminary investigations that the reaction can be catalysed by silver(I) oxide alone, we decided to evaluate different silver salts with the aim of stopping any background reaction that might be eroding ee. Silver triflate was found to give a boost in enantioselectivity (from 24% to 37% ee) compared to silver(I) oxide (Table 2, entry 6). Optimisation of the relative amounts of silver triflate to ligand then followed, with a 2 : 1 ratio of ligand : silver triflate resulting in a marginal increase in enantioselectivity from 37% ee to 39% ee (Table 2, entry 7). An excess of ligand was desirable to avoid the formation of unligated Ag(I) ions, which could potentially result in the formation of catalytically competent species and consequently lead to a background reaction with erosion of ee of the product.

Use of dichloromethane seemed to be highly favourable for enantioselectivity (Table 2, entry 9), however the reaction was not clean and catalyst turnover was problematic. The addition of 10 mol% triethylamine was necessary to promote catalytic turnover in this solvent (Table 2, entry 11). With all the components of our catalytic system established, optimisation of the chiral ligand followed.

3.3.4 Optimisation of the Ligand

Accordingly, a range of atropisomeric bisphosphine ligands were screened, of which the most significant results are reported (Figure 12). Use of (*R*)-MeO-BIPHEP **194** resulted in a faster rate of reaction compared with (*S*)-BINAP **193a** and gave a small increase in enantioselectivity (from 49% ee to 51% ee). Next, use of (*R*)-SEGPHOS **195** resulted in a lower rate of reaction compared with MeO-BIPHEP **194** however, a significant augmentation in enantioselectivity was observed with **195**. The difference in reactivity between MeO-BIPHEP **194** and SEGPHOS **195** might be due to a combination of steric and electronic properties on the ligand. Optimisation (in terms of sterics and electronics) of the substituents on the phosphorous atoms of **195** then followed.

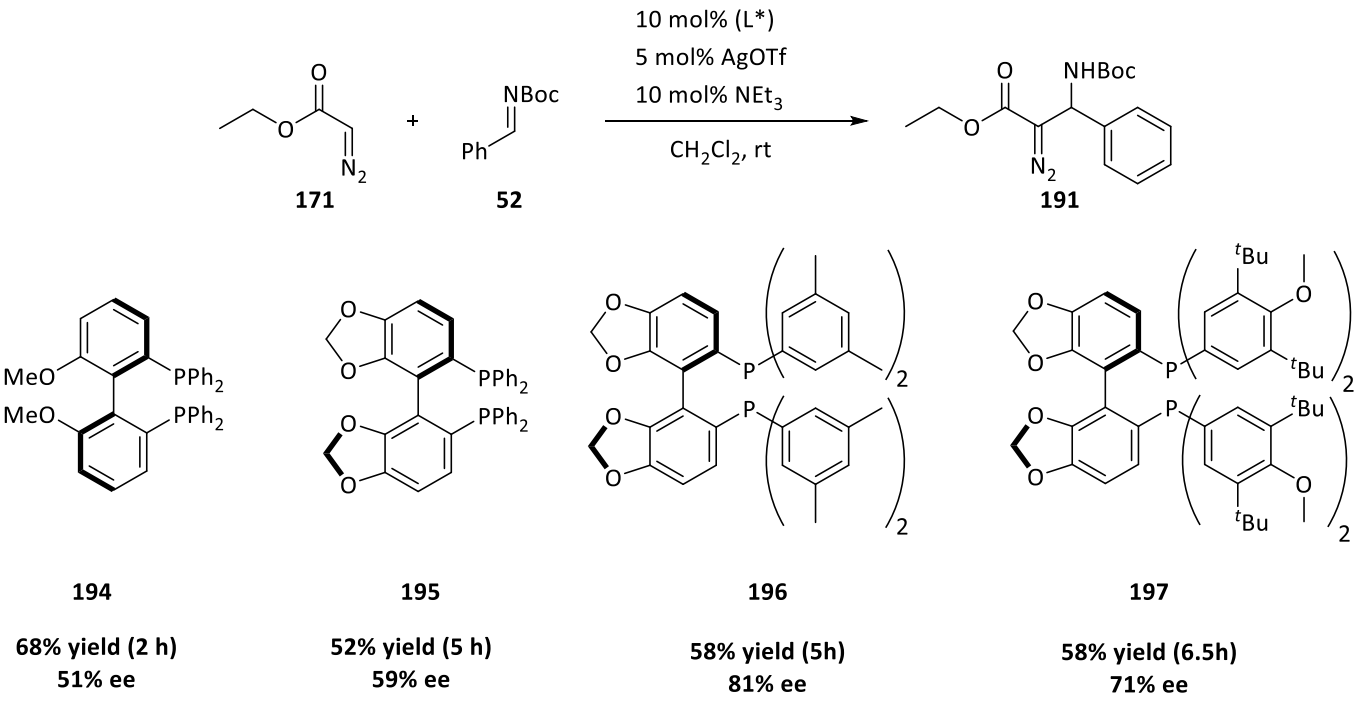

Figure 12: Screening atropisomeric bisphosphine ligands.

Pleasingly, a 3,5-dimethyl substituted bis-aryl diphosphine on SEGPHOS, (*R*)-DM-SEGPHOS **196** resulted in a significant increase in enantioselectivity. A bulkier and more electron-rich di-*tert*-butyl 4-methoxy bis-aryl diphosphine in **197** also resulted in an increase in enantioselectivity compared with SEGPHOS **195**, but a reduction in ee was observed compared with DM-SEGPHOS **196**. With this result in hand, solvent, concentration and temperature were then optimised to further improve enantioselectivity.

3.3.5 Optimisation of Solvent, Concentration and Temperature

A few chlorinated solvents were evaluated, starting with chlorobenzene (Table 3, Entry 1) and carbon tetrachloride (Table 3, entry 2), but no change in enantioselectivity was observed when compared with the result obtained on using dichloromethane. However, an increase in enantioselectivity was observed with chloroform[v] as a solvent (Table 3, entry 3). At this point, the temperature of the reaction was lowered to -20 °C whereby the ee increased further to 91% (Table 3, entry 4). However, the reactivity (as measured by isolated yield after 16 h) was poor and thereby the concentration of the reaction was doubled to 0.16 *m*M, which led to an increase in reactivity (68% yield) with only a small attenuation in enantioselectivity being observed (Table 3, entry 5).

[v] **Solvent had to be purified before use to remove ethanol stablilser. See Supporting Information for further details.**

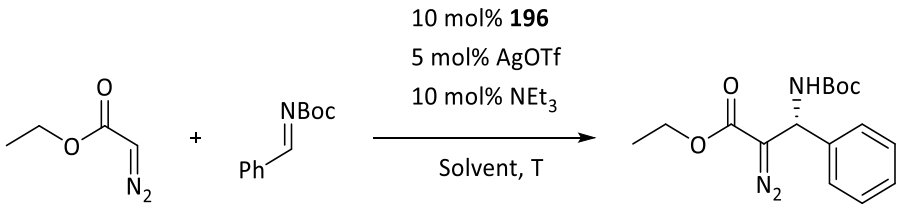

171 52 191

Entry	Temperature/°C	Conc/mM	Solvent	Time/h	Yield/%	ee/%
1	RT	0.08	ClC_6H_5	6	65	75
2	RT	0.08	CCl_4	6	77	25
3	RT	0.08	$CHCl_3$	6	48	85
4	-20	0.08	$CHCl_3$	24	32	91
5	-20	0.16	$CHCl_3$	16	68	88
6	-40	0.16	$CHCl_3$	24	77	97
7	-50	0.16	$CHCl_3$	24	68	97
8	-40	0.08	$CHCl_3$	72	40	91
9	-40	0.12	$CHCl_3$	24	40	95
10	-40	0.20	$CHCl_3$	17	70	97

Table 3: All reactions performed on a 0.10 mmol scale. Absolute configuration was determined by derivatisation *vide infra*.

The temperature was then lowered further to -40 °C, which resulted in a 97% ee (Table 3, entry 6), with good reactivity. Lowering the temperature further to -50 °C saw no increase in enantioselectivity but a drop in reactivity was witnessed (Table 3, entry 7). Subsequent iterations on varying the concentration (Table 3, Entries 8 to 10) proved that 0.16 *m*M was the optimum concentration for both reactivity and enantioselectivity.

3.4 Scope of Silver-Catalysed Enantioselective Mannich reaction of Diazoacetates with *N*-Boc protected Aldimines

3.4.1 Synthesis of a range of *N*-Boc protected Aldimines

With the optimal conditions for the reaction in hand, a broad range of *N*-Boc protected aldimines were prepared to investigate how generally our catalytic system could be applied to this reaction. The aldimines were prepared according to a method developed by Greene *et al.* in 1993[78] where the amidosulfone precursor **201** was initially prepared through reaction of benzene sulfinic acid sodium salt **199**, *tert*-butyl carbamate **198** and the corresponding aldehyde in the presence of formic acid **200**. In all cases, the amidosulfone precipitated out and was filtered, whereby the filter cake was washed with diethyl ether. The aldimine was then generated by refluxing the requisite amidosulfone in THF in

the presence of stoichiometric potassium carbonate and stoichiometric sodium sulfate, which served as a dessicant. Accordingly, using this two-step procedure, 14 aldimines presenting variations to the aromatic component were prepared in excellent yields (92-98%) (Scheme 53).

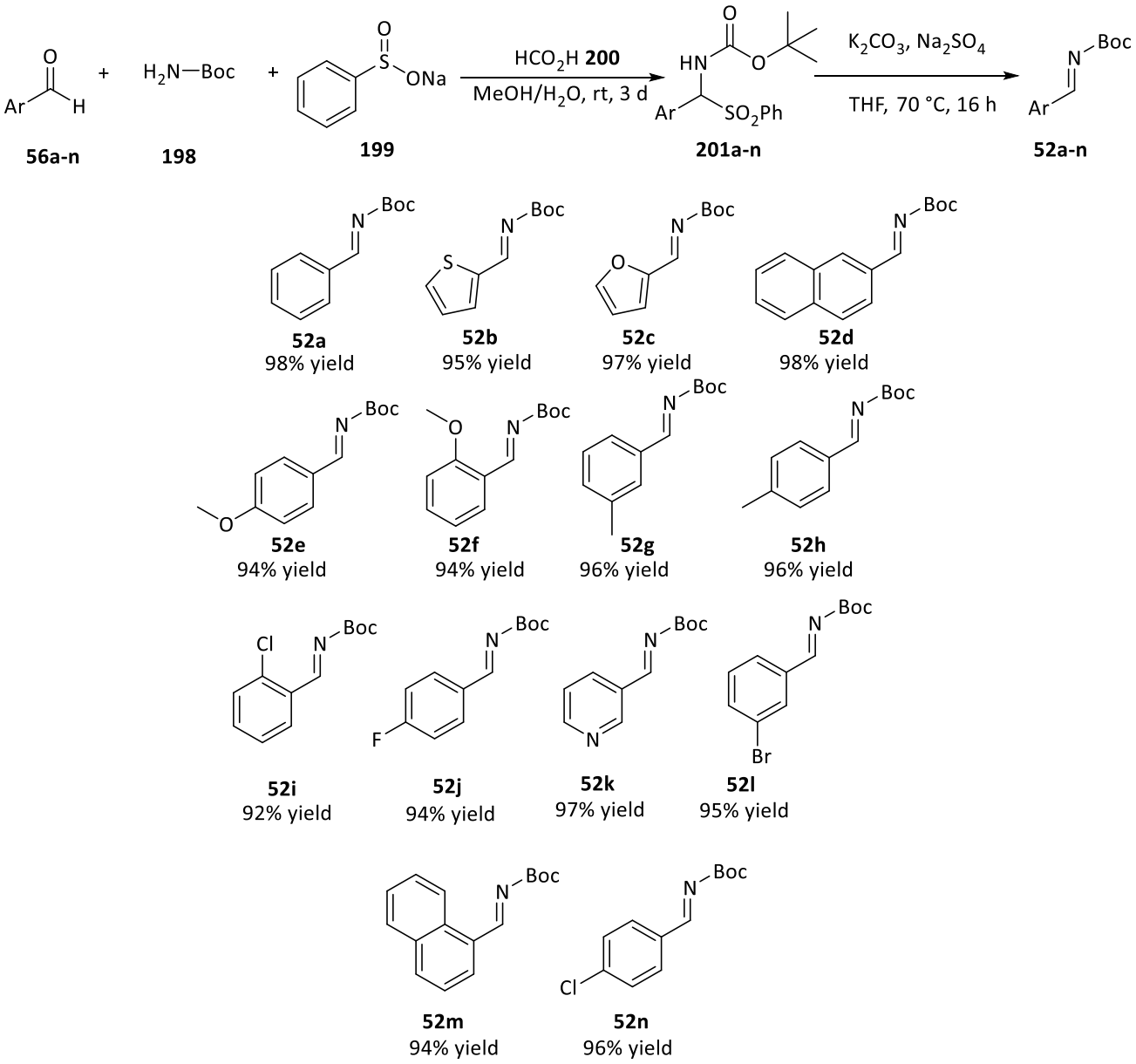

Scheme 53: Two-step synthesis of *N*-Boc protected aldimines.

Although this method was good for synthesising aromatic aldimines from the amidosulfone precursors, it was not amenable to aliphatic aldimines. For example, cyclohexyl aldimine **52o** proved to be too unstable at 70 °C due to tautomerization to the enamine product. As a result of this, Deng's method was successfully employed as an alternative; the elimination reaction was carried out in refluxing dichloromethane in the presence of a stronger base such as Cs_2CO_3 to furnish the corresponding aldimine in excellent yield (Scheme 54).[79]

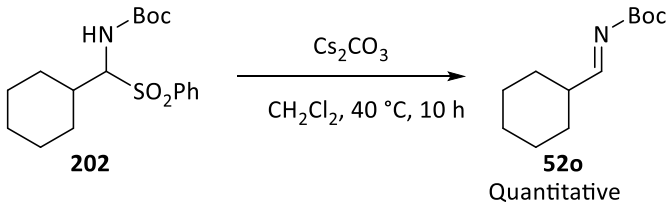

202 **52o** Quantitative

Scheme 54: Deng's method for the synthesis of aliphatic *N*-Boc aldimines.

3.4.2 Substrate Scope of the Silver-Catalysed Enantioselective Mannich reaction of Diazoacetate esters with *N*-Boc Aldimines

With a range of aldimines in hand, we then proceeded to evaluate their performance in the Mannich reaction. Under the optimised conditions, the reaction showed a broad tolerance for all 14 aromatic aldimines (Figure 13).

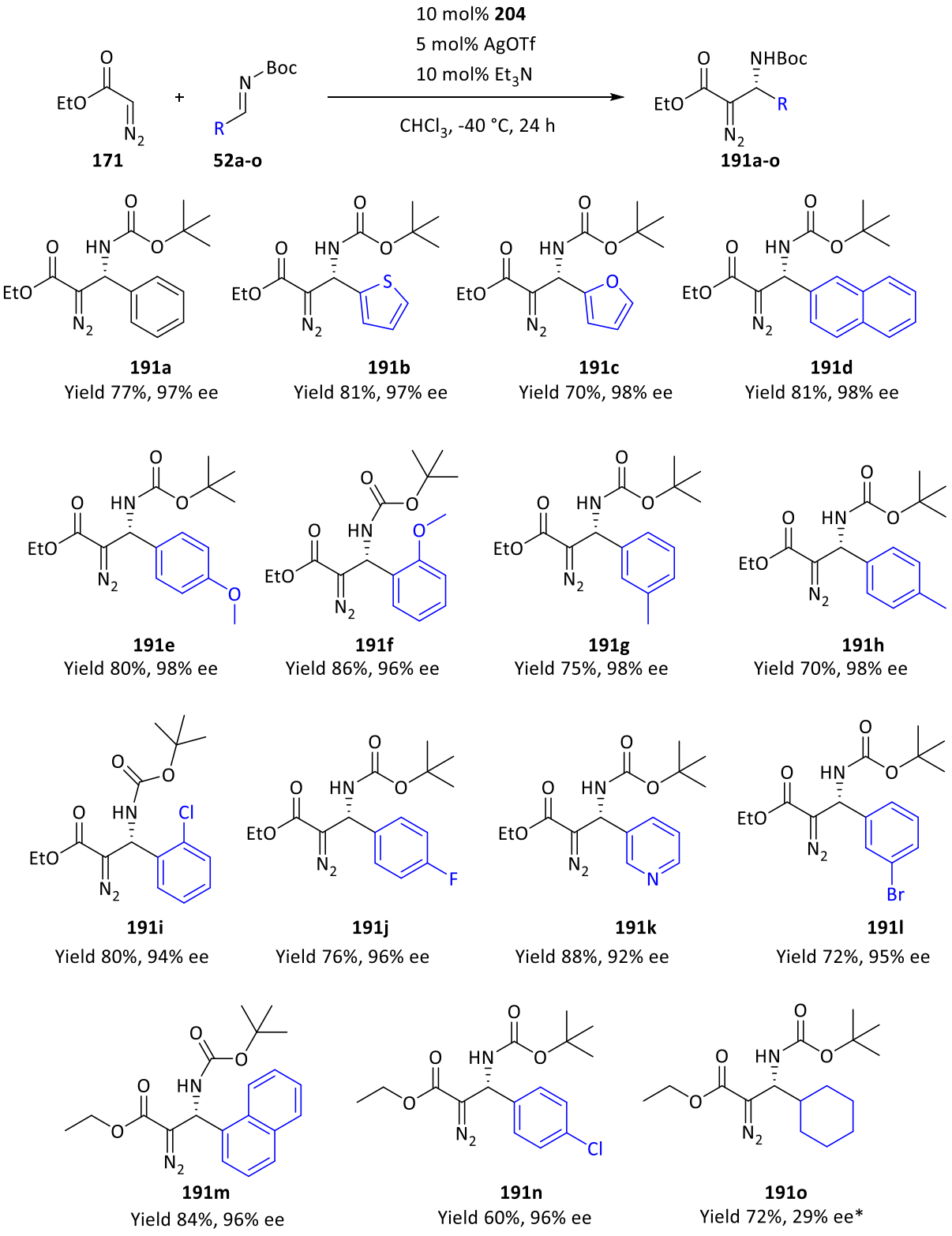

Figure 13: Scope of silver-catalysed asymmetric Mannich reaction of diazoacetate esters with a range of *N*-Boc Aldimines.*20 mol% 196/10 mol% AgOTf used.

Aldimines containing 2-thienyl and 2-furyl heterocycles **191b** and **191c** were tolerated well with good yields and excellent enantioselectivities being obtained. Furthermore, 3-pyridyl aldimine **191k** was

also tolerated well; good reactivity was maintained and enantiocontrol remained high. Pleasingly, 1- and 2-naphthaldehyde derived imines gave rise to Mannich adducts **191m** and **191d** with good yields and excellent enantioselectivities. Electron-rich and electron-poor aromatic aldimines bearing substitution in *ortho*, *meta* and *para* positions afforded Mannich adducts **191e**-**191n** with enantioselectivities of 96-98% ee and good yields, demonstrating the reaction is tolerant of significant variations to both steric and electronic effects.

Aliphatic aldimine **52o** afforded Mannich adduct **191o** in a low yield of 33% and only moderate enantioselectivity. The low yield of this adduct is possibly due to the inherently less reactive cyclohexyl aldimine. The moderate enantiocontrol on using this substrate could suggest the importance of π- π stacking between the aromatic aldimine and the ligand which might be of importance in facial discrimination and thus enantioocontrol. Doubling the catalyst loading for this particular substrate afforded Mannich adduct **191o** in 72% yield and 29% ee. Further optimisation of the reaction with this aldimine was not pursued at this point. Taken together, we successfully demonstrated that this first silver-catalysed enantioselective Mannich reaction of ethyl diazoacetate to *N*-Boc protected aldimines could be broadly applied to a range of aromatic aldimines. Investigations into whether significant levels of enantiocontrol could be achieved by using different diazoacetate nucelophiles was then pursued.

3.4.3 Evaluation of Diazoacetate Esters

Diazoacetate esters **209a-c**, were synthesised in a two-step manner from bromoacetyl bromide **207** (Figure 14)**.** Treatment with the corresponding alcohol in the presence of either sodium hydrogencarbonate or potassium phosphate tribasic, furnished bromoacetates **208a-c** in quantitative yields which were separately reacted with *N,N*-ditosylhydrazine **205** in the presence of stoichiometric DBU **143**. This afforded the respective diazoacetate esters[80] with yields ranging from 45-52% with respect to the bromoacetate intermediate.

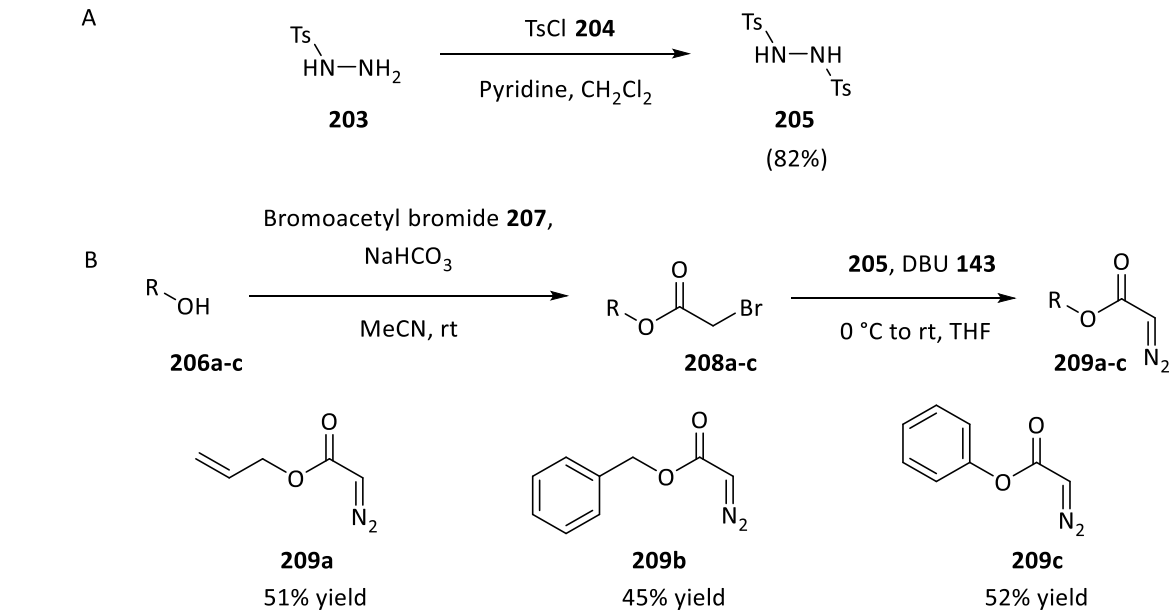

Figure 14: (A) Synthesis of *N*,*N*-ditosylhydrazine.[81] (B) Synthesis of diazoacetates from bromoacetylbromide.

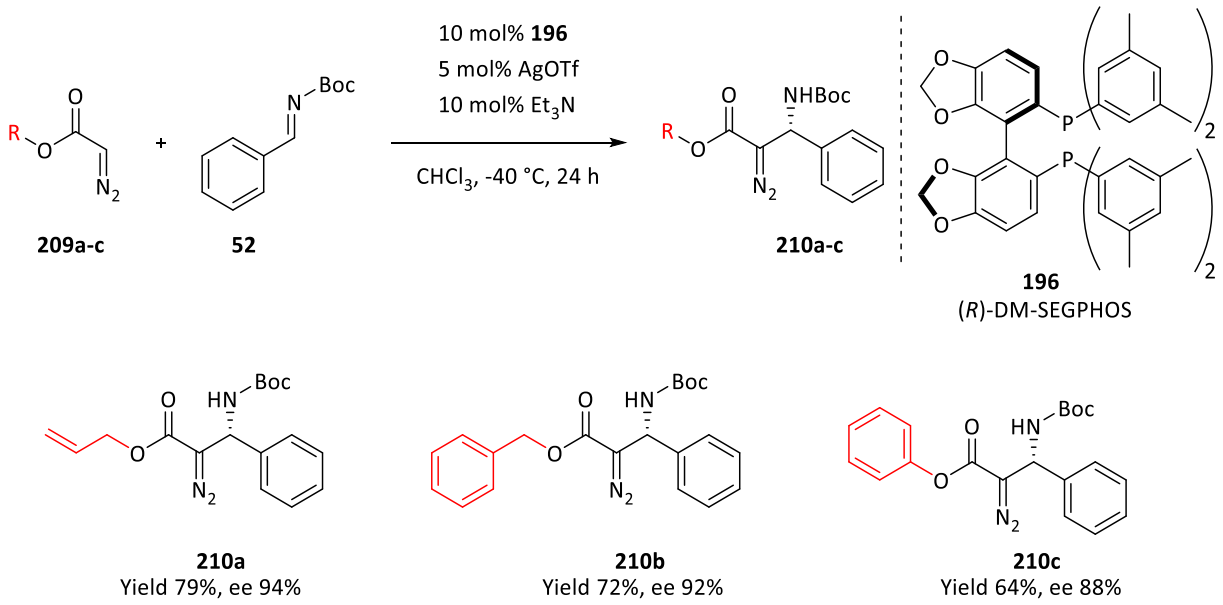

Figure 15: Scope of the silver-catalysed asymmetric Mannich reaction with respect to the diazoacetate ester.

Gratifyingly, diazoacetate esters other than ethyl diazoacetate were well tolerated (Figure 15). The Mannich adduct from allyl diazoacetate **210a** gave a comparable yield to the ethyl variant with only a small decrease in ee of 94%. A bulkier group such as a benzyl **210b** also gave good reactivity and pleasingly the enantioselectivity was not diminished significantly compared to the allyl group. Phenyl diazoacetate furnished the product **210c** with only a small decrease in reactivity where enantioselectivity remained high (64% yield, 88% ee).

3.5 Scale-up Studies

Up until this point, all reactions had been performed on a 0.10 or 0.20 mmol scale using 10 mol% of chiral ligand **196**, 5 mol% AgOTf and 10 mol% of NEt_3. To prove the usefulness of this methodology, a demonstration that this reaction could be performed on larger scales was necessary. Low catalyst loadings are desirable on scale due to the costs associated with using a commercially available atropisomeric bisphosphine ligand, catalyst loading studies were initially performed (Table 4).

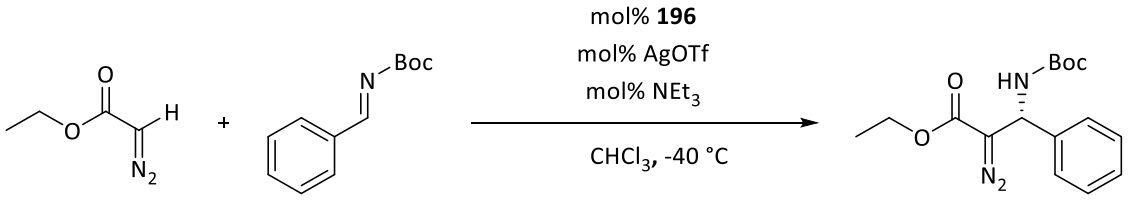

171 **52** **191**

Entry	Cat. Loading/mol% (196/AgOTf/NEt_3)	Concentration/mM	Time/h	Scale/mmol	Yield/%	ee/%
1	5/2.5/5	0.167	24	0.40	33	96
2	5/2.5/5	0.334	24	0.40	64	96
3	2/1/2	0.835	24	1.0	55	93
4	2/1/2	0.835	48	1.0	57	92

Table 4: Initial scale-up studies

Firstly, the catalyst loading was halved (5 mol% of **196**, 2.5 mol% AgOTf, 5 mol% NEt_3) and the scale of the reaction was increased to 0.40 mmol (Table 4, entry 1). As expected, this resulted in the product being obtained in a lower isolated yield (33%, T.O.N[vi] = 13.2) and no change in enantioselectivity compared with the optimised condition (77%, T.O.N = 15.4); where the reaction time was the same. The concentration was then doubled (Table 4, entry 2) and the isolated yield of the product also went up by factor of 2 (64%, T.O.N = 25.6). Subsequently, the catalyst loading was dropped to 2 mol% with respect to the ligand, the concentration was increased proportionally to 0.835 *m*M and the scale of the reaction was increased to 1.0 mmol (Table 4, entry 3). The enantioselectivity diminished slightly and the reactivity was reduced significantly compared to entry 2. On repeating the reaction with a longer reaction time of 48 hours (Table 4, entry 4), no change to both the reactivity and enantioselectivity was observed, suggesting that something was poisoning the catalyst, rendering it inactive. This problem was circumvented through the addition of molecular sieves in the reaction vessel and pleasingly levels of both reactivity and enantioselectivity were restored (Scheme 55).

[vi] **T.O.N is turnover number of catalyst with respect to silver triflate.**

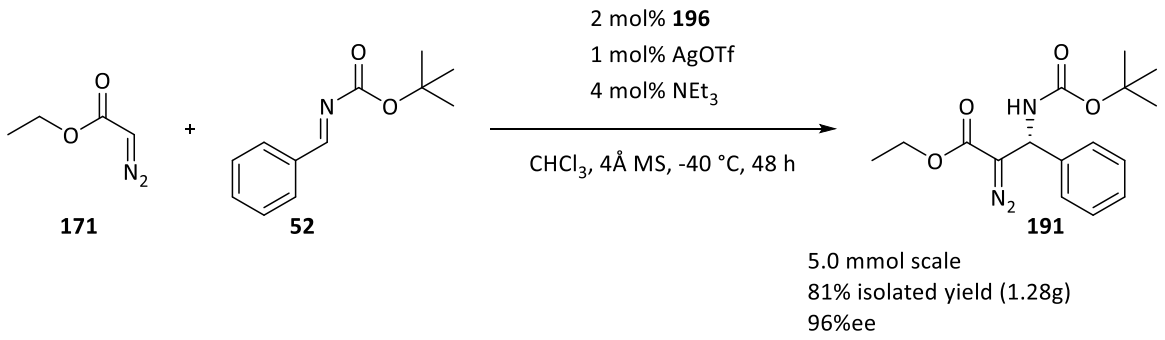

Scheme 55: Scale-up condition for silver-catalysed asymmetric Mannich reaction of diazoacetates with *N*-Boc protected aldimines.

This experiment suggested water was the inhibitor of the catalyst and showed that at larger scales and with lower catalyst loadings, molecular sieves are required for both reactivity and enantioselectivity. Pleasingly, an isolated yield of 81% (T.O.N = 81) was obtained on 5.0 mmol scale after 48 hours and the ee of the reaction returned to 96%, which is what was expected as the effective concentration of the catalyst at a concentration of 0.835 *m*M is the same with 10 mol% ligand : 5 mol% AgOTf catalyst loading at a concentration of 0.167 *m*M. It was also observed that having a small excess of triethylamine with respect to **196** (4 mol%) resulted in a slight increase in yield with this loading of catalyst. Due to this study, we were able to successfully demonstrate that the catalytic system for this reaction is scalable, with catalyst loadings as low as 2 mol% ligand : 1 mol% AgOTf being achieved to afford the product in good yield and excellent enantioselectivity.

3.6 Product Derivatisation

To further demonstrate the synthetic utility of our method, we sought to transform Mannich adduct **191a** into a range of useful products.

3.6.1 Synthesis of β-Amino Acid Derivative and Determination of Absolute Configuration

The absolute stereochemical configuration was determined by treatment of **191a** with Pd/C under 1 atmosphere of hydrogen gas, which afforded β-amino acid derivative **211** in a good yield with retention of stereochemical configuration (Scheme 56).

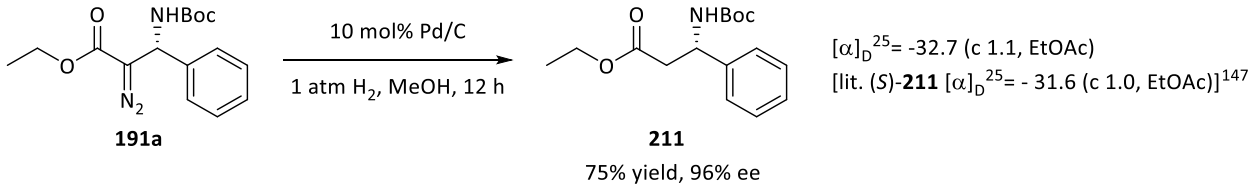

Scheme 56: Hydrogenation of 191a using Pd/C, 1 atm H_2 to determine the absolute configuration.

The specific optical rotation of **211** was found to be ($[\alpha]_D^{25}$= - 32.7 (c 1.1, EtOAc)). Comparison with literature values of the same compound (*S*)-**211** lit. $[\alpha]_D^{25}$= - 31.6 (c 1.0, EtOAc).[147] Therefore, the (*S*)-**211** had been obtained in the hydrogenation and thus it follows that the (*R*)-**191a** adduct had been obtained in the enantioselective Mannich reaction.

3.6.2 Carbene Chemistry of Diazo Compounds

It is well precedented that treatment of a diazo compound with a metal complex will lead to insertion of the metal into the diazo moiety forming a metal-carbenoid intermediate with concomitant evolution of dinitrogen gas. The mechanism of this insertion involves nucleophilic attack of the diazo group onto the electrophilic metal to form a metal-stabilised carbene or carbenoid (Figure 16)[63]. This carbene intermediate can be trapped with electron-rich compounds to form a variety of different products of varying complexity with regeneration of the metal catalyst.[82,83]

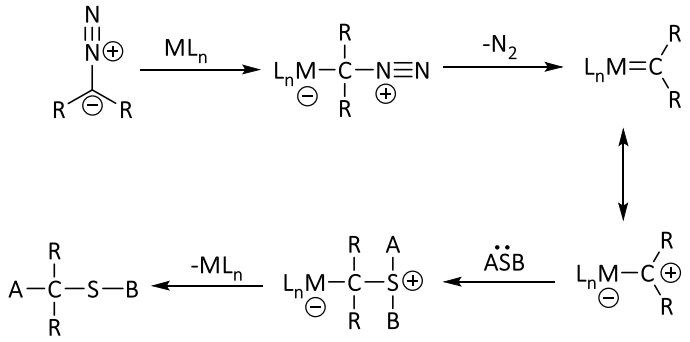

Figure 16: General mechanism for decomposition of diazo compounds in the presence of a metal and subsequent trapping of the carbenoid species with an electron-rich compound (ASB).

Accordingly, we evaluated the carbene chemistry of Mannich adduct **191a**. Zhou and co-workers have reported a copper(I)-catalysed method for the O-H, N-H and S-H insertions of alcohols, anilines and thiols respectively with α-diazo esters.[84]

Building on this precedent, an S-H insertion reaction was attempted using 1.0 equiv of thiophenol **212** and **191a** of 97% ee with 5 mol% of copper tetrakis acetonitrile hexafluorophosphate in dichloromethane (Scheme 57).

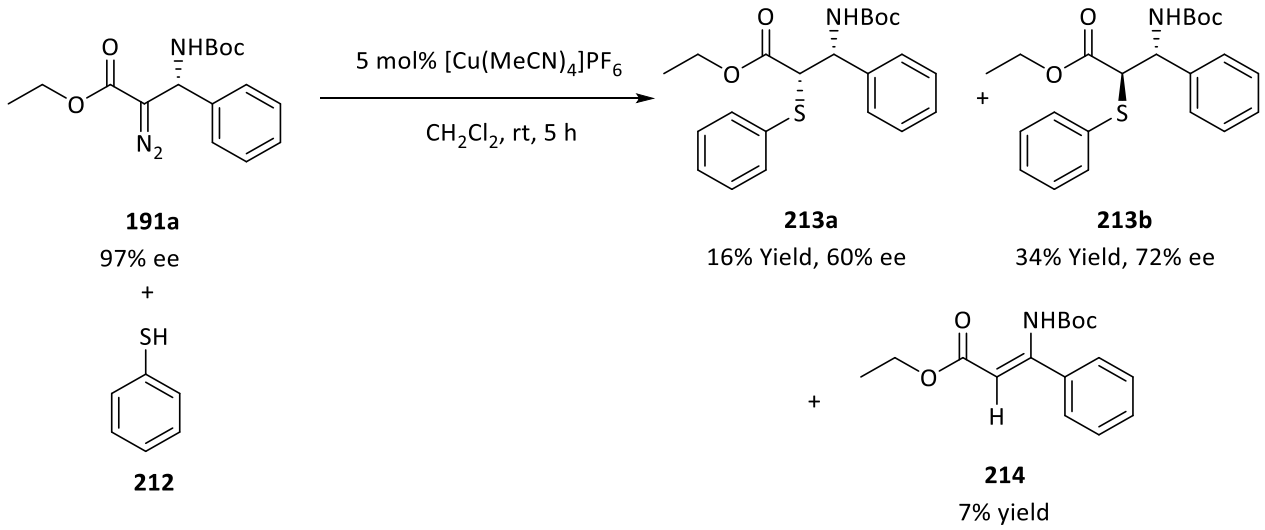

Scheme 57: Attempted S-H insertion of thiophenol with Mannich-adduct 191a.

The reaction was complete within 5 hours and initially proceeded with the disappearance of the yellow colour which is characteristic of many diazo compounds in solution and significant evolution of dinitrogen gas was observed. The reaction afforded the desired product **213a** and **213b**, as a mixture of diastereoisomers; which proved to be separable by FCC and were isolated in a roughly 2 : 1 (*anti* : *syn*). A by-product in this reaction was enamine **214**, the formation of which was the result of a 1,2-hydride shift in the carbenoid state *prior* to enamine formation (Figure 17). It was attempted to stop this side reaction by performing the reaction with a large excess of thiophenol (10.0 equiv), however it still remained prevalent. Furthermore, to our surprise, the enantioselectivity of the two diastereoisomers differed and were lower than the starting material.

The mechanism and underlying kinetics of this reaction are complicated and we do not fully understand how the result reported in scheme 57 was obtained. Given that the enantioselectivities of diasteroisomers **213a** and **213b** differed, it is plausible that a stepwise mechanism is operative whereby nucleophilic attack of Mannich adduct **191a** on Cu(I) occurs to form ylide **Int-1**. Subsequently, back-bonding from the metal d-orbitals to the empty p-orbital on the α-carbon of Mannich adduct **191a** affords the copper carbenoid species **Int-2**.

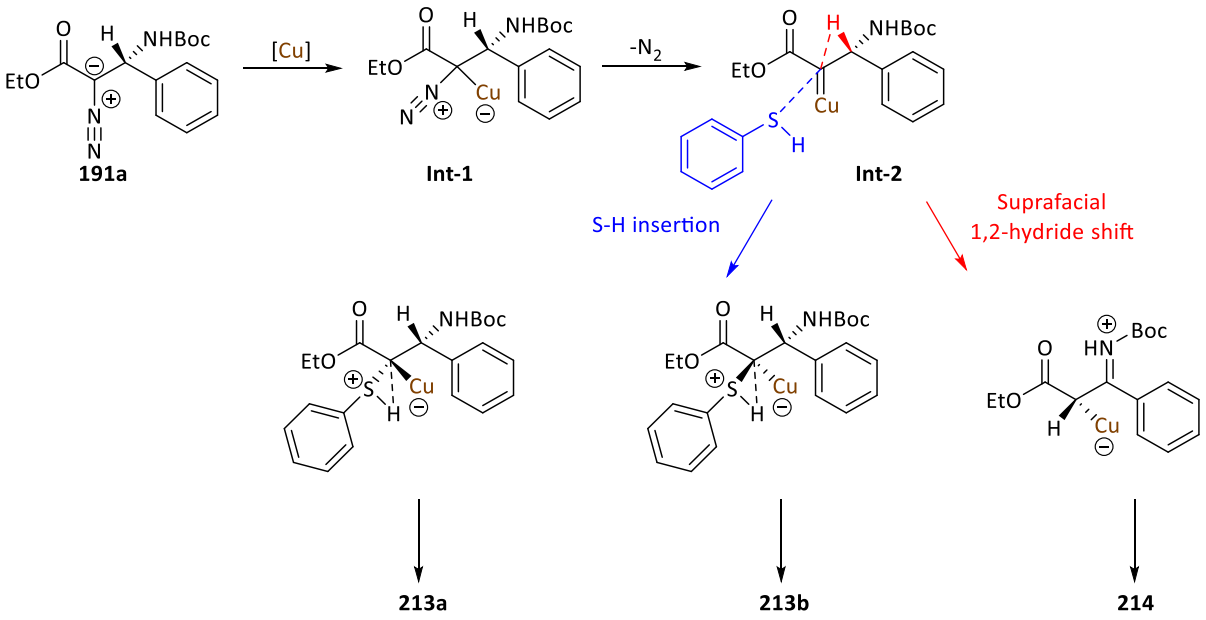

Figure 17: Postulated mechanistic *rationale* for S-H insertion reaction highlighting the two plausible mechanistic pathways from carbenoid intermediate Int-2: S-H insertion (in blue), 1,2-hydride migration (in red).

Copper carbenoids have been characterised by single crystal X-ray structures and NMR spectroscopy. Hofmann and co-workers found that copper(I) carbenes were electrophilic in nature and thus displayed Fischer-type carbene character.[85] Therefore, from **Int-2** the reaction can proceed through one of two routes. Firstly, the thiophenol (Figure 17, blue arrow) can attack the carbenoid through the *si*-face or the *re*-face to generate products **213a** and **213b** respectively. Secondly, from **Int-2** a suprafacial 1,2-hydride shift can take place from the β-position (Figure 17, red arrow). The shift can be aided by donation of electron density from the lone pair of electrons on the nitrogen atom; forming an imine intermediate with loss of stereochemical integrity at this position, which goes on to generate the more stable enamine by-product **214** as depicted in Figure 17. Although this proposed mechanism accounts for how products **213a-b** and **214** were obtained, it is not adequate to account for why the two diastereoisomers differ in enantioselectivity.

3.6.3 Metalloradical Chemistry

With the aim of avoiding the formation of the enamine by-product, we attempted to form a radical at the alpha position of our Mannich adducts; trapping the subsequent reactive intermediate with a suitable compound to hopefully obtain the desired product. Accordingly, in 2007, Zhang and co-workers developed a method for an asymmetric cyclopropanation reaction between diazoacetates and styrenes (Scheme 58).[86] Their catalyst was a chiral porphyrin ligated to a Co(II) metal ion.

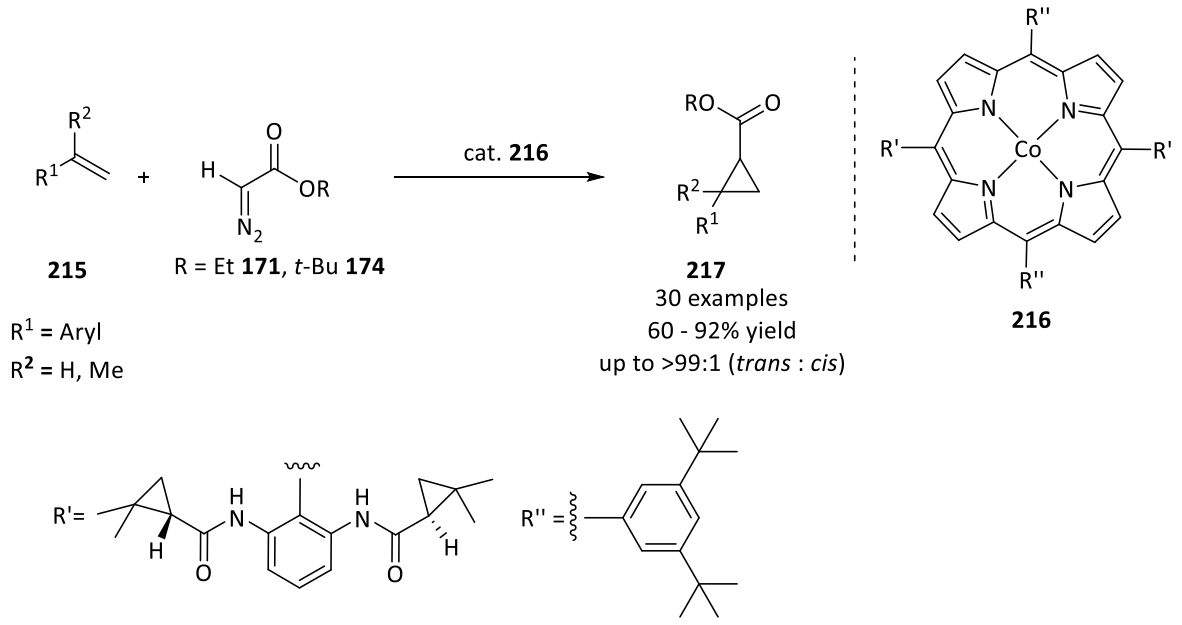

Scheme 58: Zhang's asymmetric cyclopropanation utilising a Co(II)-TPP porphyrin complex as the catalyst.

The scope of the reaction proved to be broad with variability on both the styrene and diazoacetate ester being tolerated to furnish the respective products in good to excellent yields, excellent enantioselectivities with *trans* selectivity being favoured. Zhang later speculated that a metalloradical or carbene radical is formed at the α-position of the diazoacetate; formed by donation of an electron from the $3dz^2$ metal orbital to the empty $2P_y$ molecular orbital on the terminal α-carbon of the diazoacetate ester which is acting as a ligand. This results in the formation of a Co^{III} (d^6) metal centre and the terminal radical on the diazoacetate ester can then undergo cyclopropanation with olefins.[87,88] It was hoped that the formation such a radical species at the α-position of the diazoacetate adduct would not undergo a 1,2-radical shift, racemising the adjacent β-stereocentre. Diazo adduct **191a** was subjected to the cyclopropanation conditions with styrene **218** reported by Zhang and co-workers using achiral Co(TPP) **219** in toluene (Scheme 59).

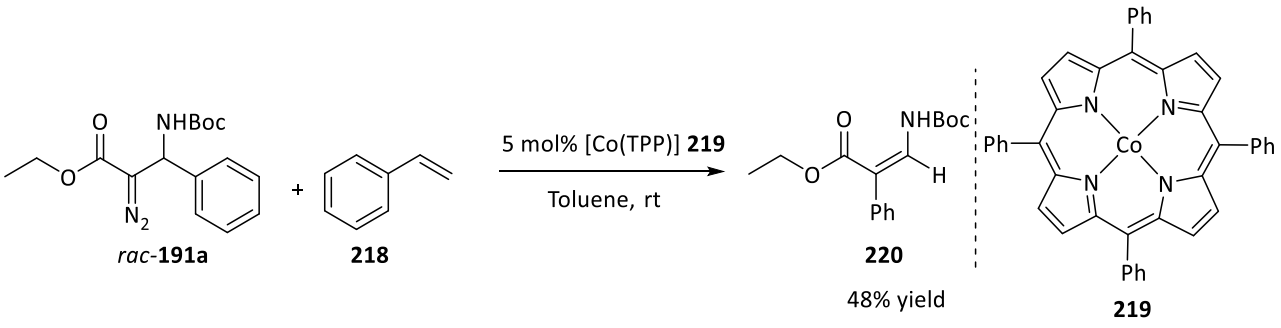

Scheme 59: Attempted Co(TPP) catalysed cyclopropanation of *rac*-191a with styrene.

Disappointingly, no desired cyclopropanation product was observed. Enamine **220** was isolated along with starting materials. The formation of enamine **220** (from a 1,2-aryl shift) possibly provides an insight into the mechanism of metalloradical formation. Given this result, it is suggestive that the mechanism of metalloradical formation is possibly 'stepwise' in that a singlet (Fischer-type) carbene is formed first, through which 1,2-aryl migration takes place forming the enamine product; precluding the formation of a (Schrock-type) metalloradical intermediate and prohibiting further reactivity. Interestingly, selective migration of the aryl group was observed, and isomeric enamine product **214** was not observed in the reaction.

3.6.4 Synthesis of Triazoline

The synthesis of other, useful compounds was subsequently attempted. 1,4,5-triazolines are precursors to aziridines[89], triazoles[90] and have also been found to be biologically relevant as anti-convulsants.[91] Typically, triazolines are synthesised by 1,3-dipolar addition of azides with activated olefins.[92] Mannich adduct **191a** was transformed into the respective triazoline **221** in the presence of sodium hydride, effecting an intramolecular 1,3-addition of the nitrogen nucleophile onto the terminal *N* of the diazo group. Trapping of the resulting anion at the α-carbon after cyclisation with a suitable electrophile; exemplified here with benzyl bromide - furnished the triazoline product in good yield and not comprimising stereochemical integrity as a single diastereoisomer (Scheme 60). This method was adapted from the work of Gevorgyan and co-workers.[93]

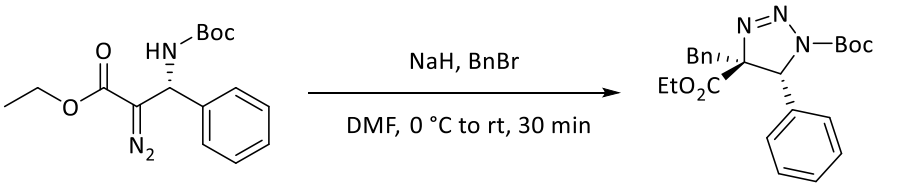

191a
97% ee

221
79% yield, 96% ee

Scheme 60: Intramolecular 1,3-addition of nucleophilic and electrophilic species across the diazo moiety to furnish substituted triazoline 221.

3.6.5 Synthesis of α-hydroxy-β-amino acid derivative

Hydroxy-β-amino acid derivatives are biologically relevant and have been found to be important functionalities in protease inhibitors.[94] More specifically, α-hydroxy-β-amino acid derivatives are important components of naturally occurring molecules such as the side chain present in Taxol **222** (Scheme 61).

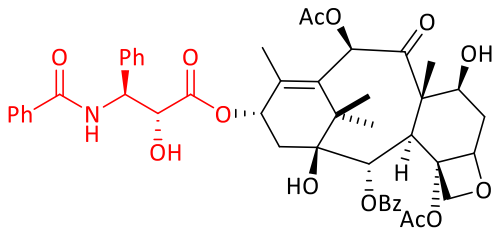

222

Scheme 61: Taxol (highlighted in red is the α-hydroxy-β-amino acid side chain).

Synthesis of α-hydroxy-β-amino acid derivative from Mannich adduct **191a** (Scheme 62) was brought about by oxidation of the diazo moiety to a ketone using Oxone® and subsequent reduction of the ketone with sodium borohydride which furnished the product **223** in a 58% yield (over 2 steps) in an 8 : 1 d.r. (*anti* : *syn*)[vii].

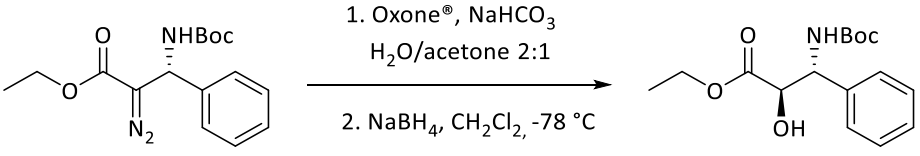

191a
97% ee

223
8:1 d.r. (*anti:syn*)
58% yield

Scheme 62: Synthesis of α-hydroxy-β-amino acid derivative from Mannich adduct 191a.

3.6.6 Facile Synthesis of Hydrazone Motif

Transformations of the diazo moiety into other, synthetically useful functional groups was explored. Hydrazone functional groups are useful 'handles' in synthesis. Tri-butyl phosphine was found to partially reduce the diazo moiety in Mannich adduct **191a** into the hydrazone **224** (Scheme 63) in good yield with retention of stereochemistry.

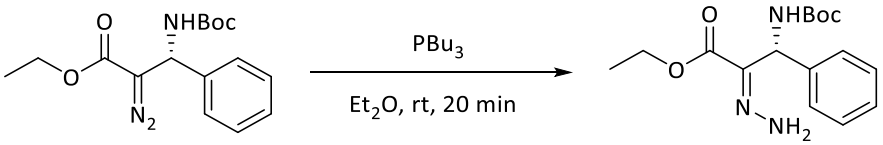

191a
97% ee

224
97% ee, 88% yield

Scheme 63: Synthesis of hydrazone 224 from Mannich adduct 191a.

[vii] **Diastereoisomers proved to be impossible to separate by FCC. Diastereomeric ratio was determined by analysis of ^{1}H-NMR.**

3.7 Mechanistic Studies on the Catalytic System

3.7.1 Identification of the 'Active' Catalytic species by NMR

The work of Schöllkopf was presented in section 3.3.1, and provided the basis for our discovery of the silver(I) catalytic system for the asymmetric Mannich reaction of diazoacetates with *N*-Boc protected aldimines. Schöllkopf assumed that an organometallic of the diazoacetate was formed in the presence of Ag(I) by exchange of the acidic α-proton with a Ag(I) ion. Investigations were carried out to gain an insight into what the active catalytic species was in the reaction. More specifically, these experiments were carried out to elucidate the structural nature of the catalytic species. Fundamentally, it was believed that an understanding of the mechanistic details of this catalytic system and how it behaves under the reaction conditions would allow us to evaluate the applicability of this catalytic system to other reactions with reasonable confidence.

The nature of the silver-phosphorous interaction in our catalytic system was investigated using ^{31}P-NMR. Yamamoto and co-workers published work on the elucidation of the coordination properties of BINAP complexes with silver triflate through the $^{1}J_{^{107}Ag\text{-}^{31}P}$ coupling constant.[95] The catalytic species was formed on mixing **196** (14.4 mgs, 0.02 mmol) with silver triflate (2.6 mgs, 0.01 mmol) in $CDCl_3$ (0.8 mL); two complexes were observed (Figure 18). A 2 : 1 stoichiometry of ligand : AgOTf was chosen to mimick the optimised reaction condition.

The first complex (Figure 18, highlighted in blue) is a trigonal-planar complex **225** consisting of a SEGPHOS ligand occupying two coordination sites on the silver(I) cation and the remaining coordination site is occupied by the triflate counterion, characterised by $^{1}J_{^{107}Ag\text{-}^{31}P}$ = 408.7 Hz which is characteristic of an sp^2 hybridised Ag(I) metal centre.[96] The second complex (Figure 18, highlighted in red) is a tetrahedral dimer **226** consisting of two SEGPHOS ligands with the triflate counterion occupying an outer sphere coordination position, $^{1}J_{^{107}Ag\text{-}^{31}P}$ = 225.3 Hz that is characteristic of an sp^3 hybdridised Ag(I) metal centre.[41,96]

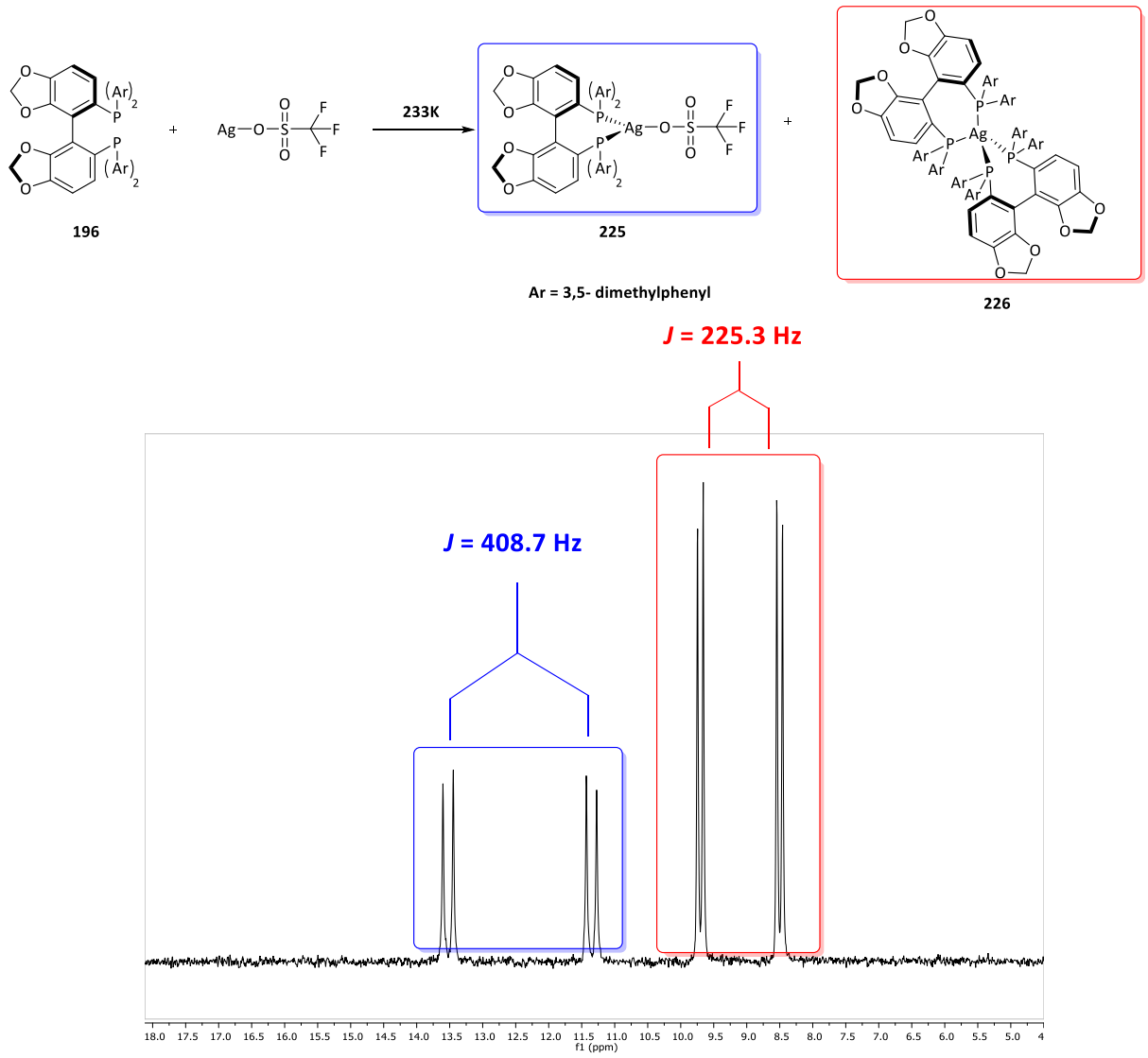

Figure 18: Trigonal planar complex 225 (blue) and Tetrahedral dimer complex 226 (red) formed on mixing DM-SEGPHOS 196 with silver (I) triflate (2 : 1) in $CDCl_3$ at 233K, Ar = 3,5-dimethylphenyl.

Having identified these two species, investigations into how they behaved in the presence of substrates (primarily the aldimine electrophile) were conducted. In the same manner as before, the first step involved formation of the trigonal-planar and tetrahedral species by mixing **196** with silver triflate (Figure 19, inset 1). The second step involved addition of 10 mol% triethylamine relative to aldimine **52** (0.20 mmol) (Figure 19, inset 2). Here, the peaks corresponding to the trigonal planar complex broadened and shifted upfield. This was attributed to a ligand exchange reaction, whereby the triethylamine displaced the labile triflate counterion from inner sphere coordination to outer sphere coordination.

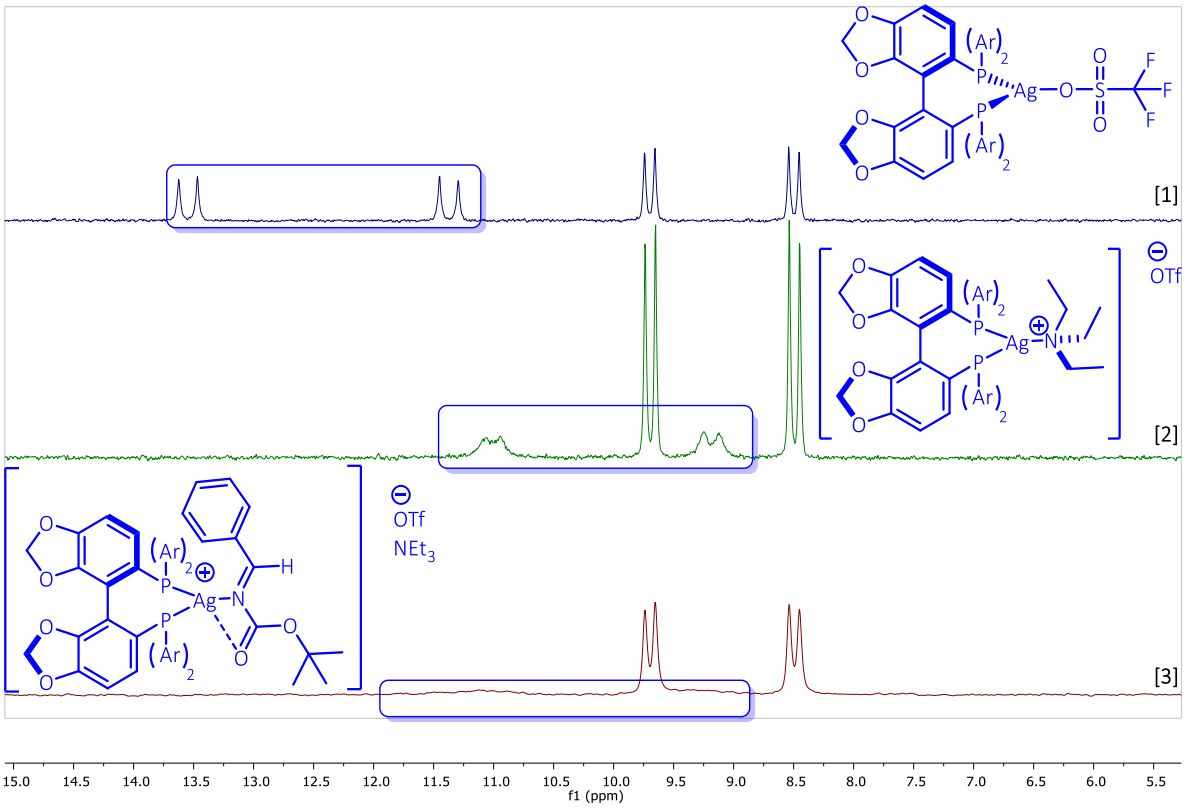

Figure 19: ^{31}P-NMR spectra at 233K [1] on mixing SEGPHOS (10 mol%) with silver(I) triflate (5 mol%); [2] Addition of 10 mol% NEt_3; [3] Addition of 1.0 equiv of aldimine 52.

The change in the chemical shift of these peaks is possibly due to the greater σ-bonding ability of triethylamine by virtue of it being more electron-rich compared with triflate as a ligand. Thus, the silver(I) ion will be more electron-rich, resulting in greater shielding of ^{31}P-nuclei. The line-broadening is possibly reflective of a shorter T_2-relaxation time constant (spin-spin relaxation) of the ^{31}P-nuclei due to chemical exchange. Furthermore, when stoichiometric aldimine was added (Figure 19, inset 3), further broadening was observed. This was again attributed to a ligand exchange process, where the triethylamine was displaced from an inner sphere position to an outer sphere position by the aldimine which is present in excess. Coordination of the aldimine to the silver(I) ion 'activates' it, which leads to a more electron-deficient aldimine, ready for C-C bond formation.

Based on these preliminary NMR studies, it seemed that the tetrahedral complex **226** was an inactive dimer as no evidence of interaction with the imine substrate was observed on an NMR timescale. Conversely, the trigonal-planar complex **225** appeared to be the 'active' catalytic species in the reaction. The relative stoichiometries of **196** : AgOTf is of crucial importance for the generation of the 'active' trigonal planar catalytic species **225**. Any positive deviation from a 2 : 1 stoichiometry to a 3 : 1 stoichiometry for example, results in the exclusive formation of tetrahedral species **226** and the

reaction shuts down. This was demonstrated by an NMR experiment similar to the one described in Figure 19.

3.7.2 EXSY experiments

Initially, we believed that the tetrahedral complex **226** functioned as a reservoir for the trigonal planar complex **225**. So, although the tetrahedral complex did not interact with the substrates directly, it could interconvert into the trigonal-planar complex and *vice versa*. To test this, a series of proton decoupled ^{31}P-^{31}P NMR EXSY experiments were conducted. EXSY or exchange spectroscopy NMR experiments use a modified NOESY pulse sequence and can be used to monitor chemical exchange. Chemical exchange is any chemical process which takes a nucleus from one chemical environment to another, different chemical environment. Rotation around the C-N bond in *N,N*-dimethylformamide is a classic example of this, where the proton nuclei of the methyl groups are placed in two distinct chemical environments due to the anisotropy of the carbonyl functionality. This chemical exchange process can be observed as cross peaks on the ^{1}H-^{1}H-EXSY of *N,N*-dimethylformamide.

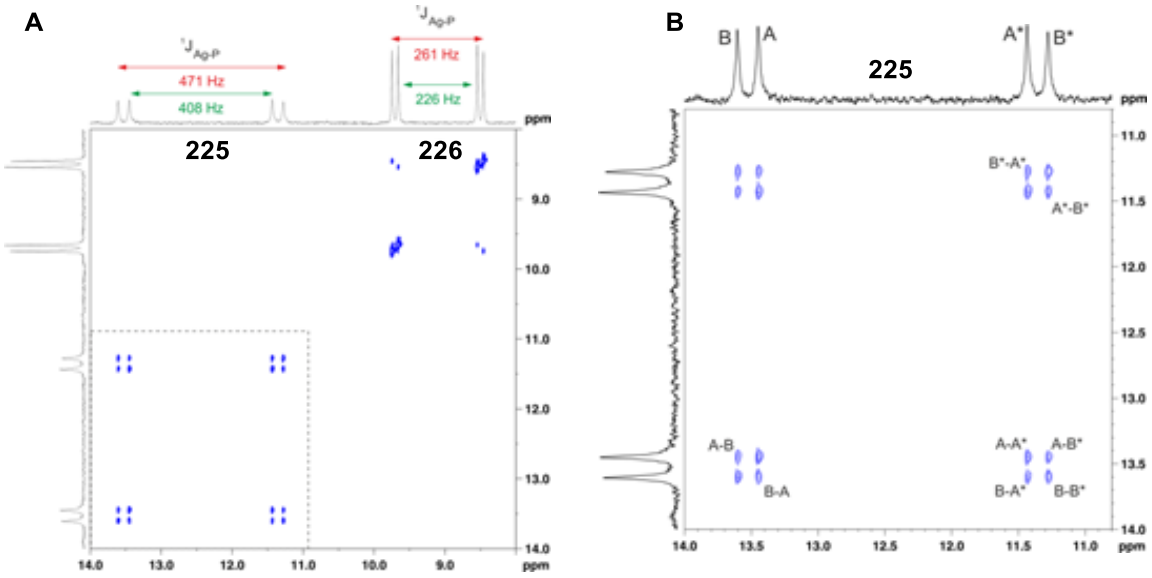

Figure 20: (A) ^{31}P-^{31}P-{^{1}H}- EXSY of complexes 225 and 226 showing the absence of cross-peaks between the trigonal-planar complex 225 and the tetrahedral complex 226 (t_{mix}=800msec, 233K, $CDCl_3$); one-bond Ag-P coupling constants for each metal isotope (red ^{109}Ag, green ^{107}Ag) are indicated on the 1D phosphorus spectrum. (B) Region of EXSY spectrum boxed in A, highlighting the trigonal planar complex 225.

Interestingly, the EXSY spectrum (Figure 20, A) showed that there was no interchange between the trigonal-planar species and the tetrahedral species; with no cross-peaks being observed between the two. It was concluded that there is no interconversion between the trigonal-planar complex **225** and the tetrahedral complex **226**, at least on an NMR timescale, which would correspond to the T_1-relaxation time constant of the ^{31}P-nuclei in this case.

However, the ^{31}P-^{31}P EXSY did show that the active, trigonal-planar complex **225** had some interesting dynamic properties in solution. Closer inspection revealed that chemical exchange was occurring in the trigonal-planar complex, namely dissociation-association of the ligand with the metal; as characterised by peaks A-B, B-A, B-A*, A-B*, B*-A* and A*-B* which correspond with mixing of ^{31}P-nuclei with both ^{107}Ag-nuclei and ^{109}Ag-nuclei. (Figure 20, B). In contrast, these chemical exchange cross-peaks were not observed for the tetrahedral complex **226**, which suggested that this complex was relatively stable and exhibited no such dynamic behaviour in solution. Despite many efforts, a crystal structure of the trigonal-planar complex **225** was unobtainable possibly due to its labile nature in solution however, the tetrahedral complex **226** was obtained exclusively with the concomitant formation of Ag(0) (Figure 21).

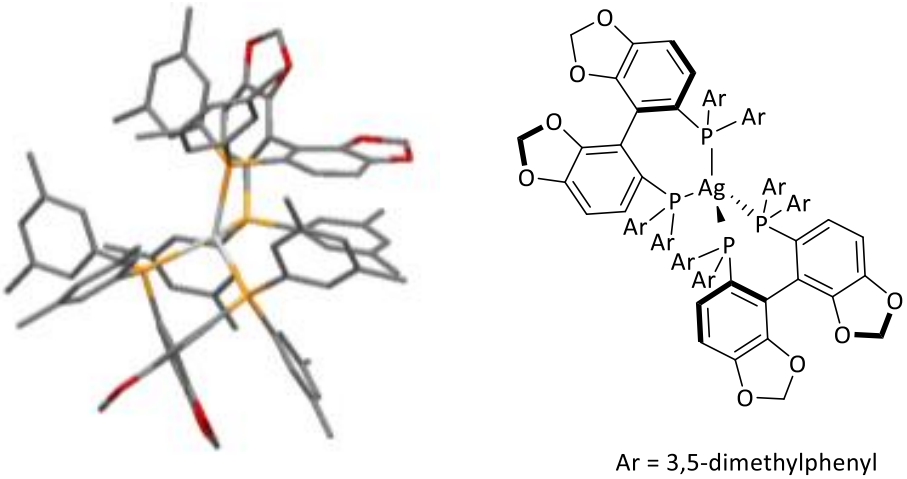

Figure 21: Single crystal X-ray structure of tetrahedral complex 226.

From the ^{31}P-^{31}P-EXSY (Figure 20), the cross peaks that remained in both complexes were those correlating satellites arising from either ^{107}Ag or ^{109}Ag; characterised by peaks A-A* and B-B* (Figure 23, B) and were due to a phenomenon known as spin-state satellite exchange (see Chapter 5 for details). The intensities of these cross-peaks for both complexes were found to be dependent on mixing time[viii] (t_{mix}) and the intensities of the peaks corresponding to chemical exchange in complex **226** were also found to have a dependence on mixing time. Both sets of cross peaks; those arising from chemical exchange in trigonal-planar complex **225** and those arising from spin-state satellite exchange in both **225** and **226** were not observed in the ^{31}P-^{31}P-COSY. This was due to the absence of a mixing time period (t_{mix}) in the COSY pulse sequence, where chemical exchange and spin-state satellite exchange can take place.

[viii] **For volume integral dependence of cross peaks with mixing time (t_{mix}), see chapter 5.**

3.7.3 Proposed Catalytic Cycle

In light of these NMR studies, the following catalytic cycle was proposed (Figure 22). Mixing a 2 : 1 ratio of ligand to silver(I) triflate in $CHCl_3$ produces the trigonal planar complex **225** and tetrahedral complex **226**. Addition of 10 mol% triethylamine results in a ligand exchange reaction, whereby the triethylamine is coordinated to the Ag metal centre. Subsequent addition of the aldimine leads to a further ligand exchange reaction, whereby the aldimine is coordinated to the silver metal centre and is thereby 'activated'. Finally, addition of ethyl diazoacetate allows for carbon-carbon bond formation on to the *si*-face of the 'activated' aldimine. This step is enantiodetermining and the steric bias of the ligand allows for facial discrimination on the aldimine. The α-proton can be abstracted by triethylamine to form a triethylammonium species and thereby re-diazotise the substrate. Subsequent dissociation and proton transfer from the triethylammonium to the product allows for liberation of the enantioenriched Mannich product, with the vacant coordination site on the catalyst being filled by triethylamine to regenerate the catalytic species and hence the cycle can progress. It is not necessary to invoke exchange of the α-proton of the diazoacetate with Ag(I) here as there was no evidence of this exchange on the NMR timescale when ethyl diazoacetate was added to **225** and **226** instead of aldimine addition.

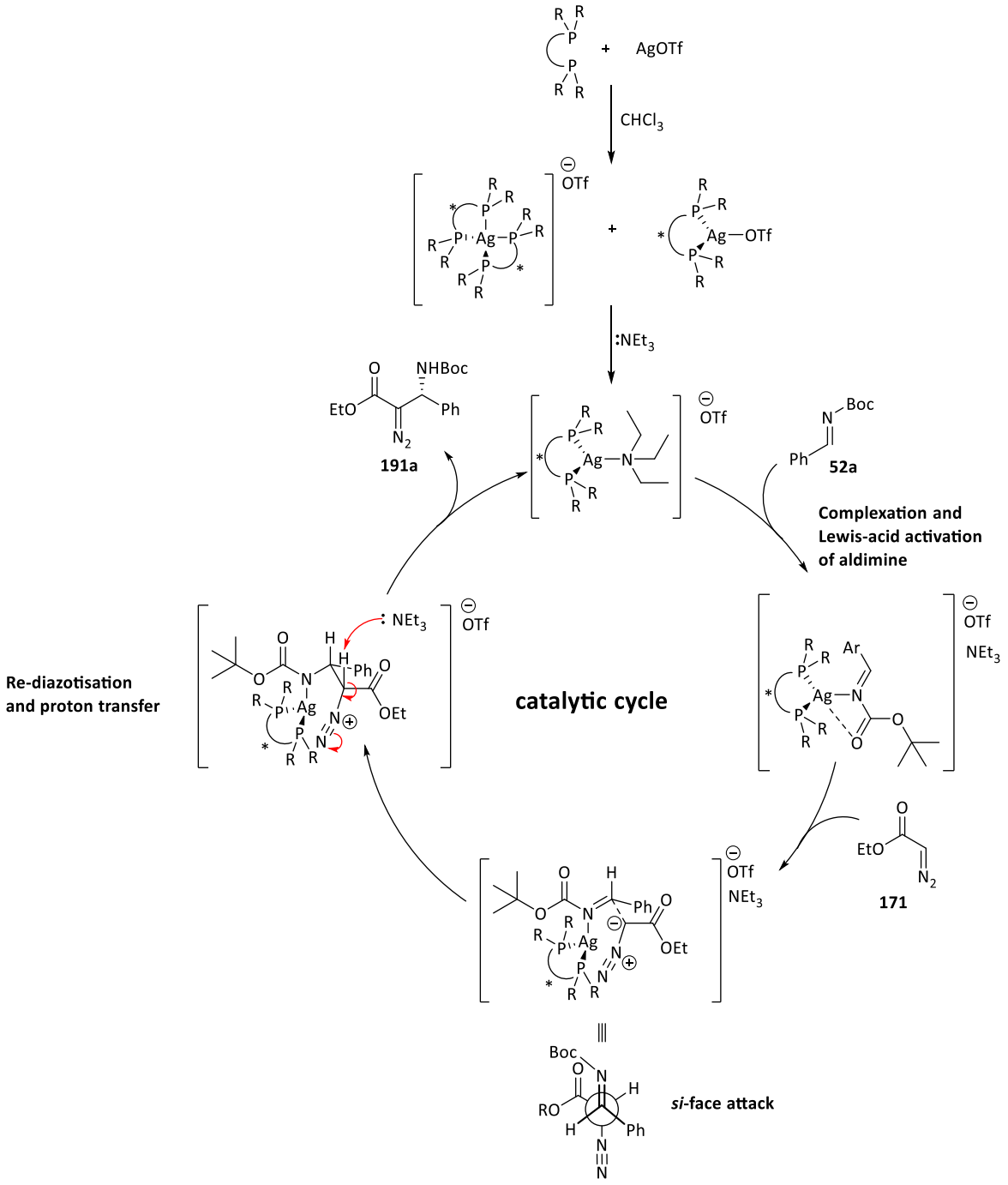

Figure 22: Proposed catalytic cycle for silver-catalysed asymmetric Mannich reaction of diazoacetates with *N*-Boc aldimines (R = 3,5-dimethylphenyl).

The proposed catalytic cycle infers that the active catalytic species (complex **225**) is monomeric in nature. However, as this was only postulated, a study of the non-linear effects of this catalytic system was conducted.

3.7.4 Non-linear effects study

Kagan, in 1986 first reported the study of the non-linear relationship between the enantiopurity of the catalyst with the enantioselectivity of the product as a means to gain insight into the mechanism

of enantioselective reactions.[97] Non-linear effects are particularly characteristic of metal-ligand catalytic systems in which the catalytic species contains two ligands. The theoretical ee for an asymmetric reaction (ee_{max}) is determined using equation 1, which shows a linear correlation between $ee_{product}$ and $ee_{catalyst}$ (Figure 23, line a).

$$ee_{max} = \frac{ee_{product}}{ee_{catalyst}} \quad [1]$$

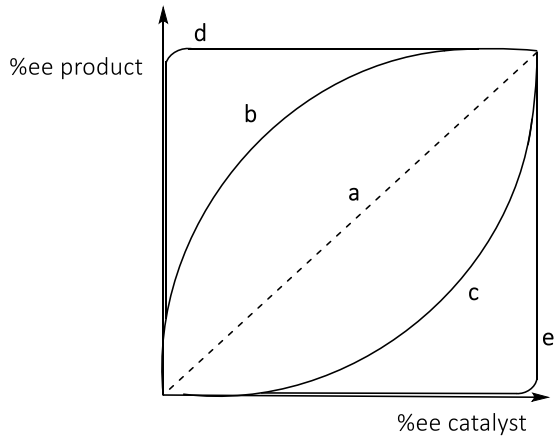

Figure 23: Graph showing a) linear relationship between ee of product and ee of catalyst; b) positive non-linear effect; c) negative non-linear effect; d) strong positive non-linear effect; e) strong negative non-linear effect.

This formulation is applicable if the catalytic species in an enantioselective reaction is of the form: ML* (i.e. monomeric), where L* is any chiral ligand. However, this formulation is not applicable to catalytic systems of the form: ML^*_2 where an enantiomerically impure ligand will yield three catalytic species: 1) ML_RL_R (homochiral) 2) ML_SL_S (homochiral) 3) ML_RL_S (heterochiral). Kagan proposed a model to account for this type of catalytic system (Figure 24).

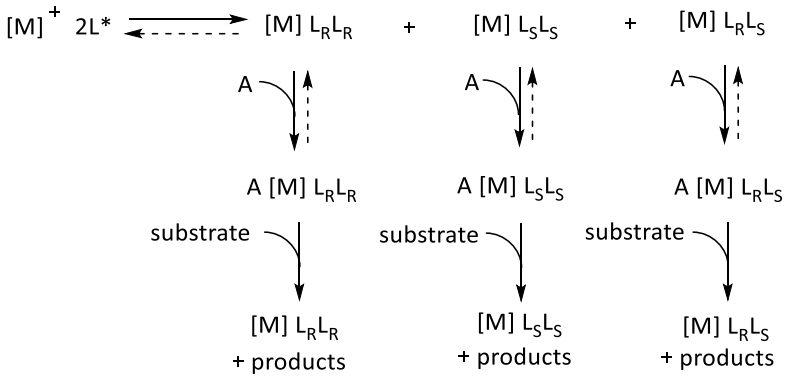

Figure 24: Kagan's model for an ML_2 catalytic system.

Any observed deviation from linearity according to this model would be due to the relative reactivities of the homochiral complexes with respect to the heterochiral, *meso* complex or if the reactivities of all complexes are the same, the ligand distribution is not an even one giving rise to different concentrations of the three complexes. As mentioned above, equation 1 is not adequate in describing an ML_2 catalytic system. Therefore, a correction factor (*f*) is required:

$$ee_{product} = ee_{max} \times ee_{catalyst} \cdot f \quad [2]$$

$$\Rightarrow ee_{product} = ee_{max} \times ee_{catalyst} \left(\frac{1+\beta}{1+g\beta}\right) \quad [3]$$

From equations 2 and 3, β is the amount of *meso* species : homo chiral species and *g* is the relative reactivity of meso species : homo chiral species. Linearity in such a catalytic system will be obtained if (β=0, or *g*=1) and that means if the *meso* complex is absent or if the *meso* complex has the same reactivity with respect to the homochiral species. If the homochiral species is more reactive (g<1) than the meso species, then asymmetric amplification will result and an observed positive deviation from linearity will be observed (Figure 23, curve b). Conversely, if the heterochiral meso species is more reactive (g>1) than the homochiral species then asymmetric depletion will result and will give rise to an observed negative deviation from linearity (Figure 23, curve c).

Experiments were performed on varying the enantiopurity of the catalyst to determine whether non-linear effects were operative in our Ag(I)-SEGPHOS catalytic system[ix]. From our NMR studies in section 3.7.1, we would expect to observe complete linearity due to the monomeric nature of the proposed 'active', trigonal planar catalytic species **225**.

[ix] **See Supporting Information for further details.**

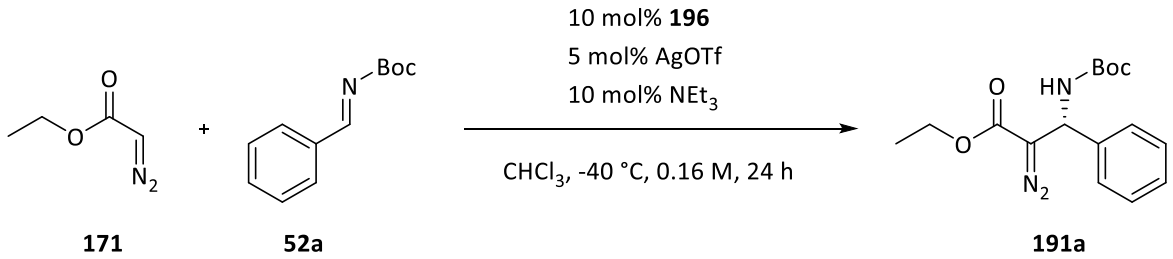

171 **52a** **191a**

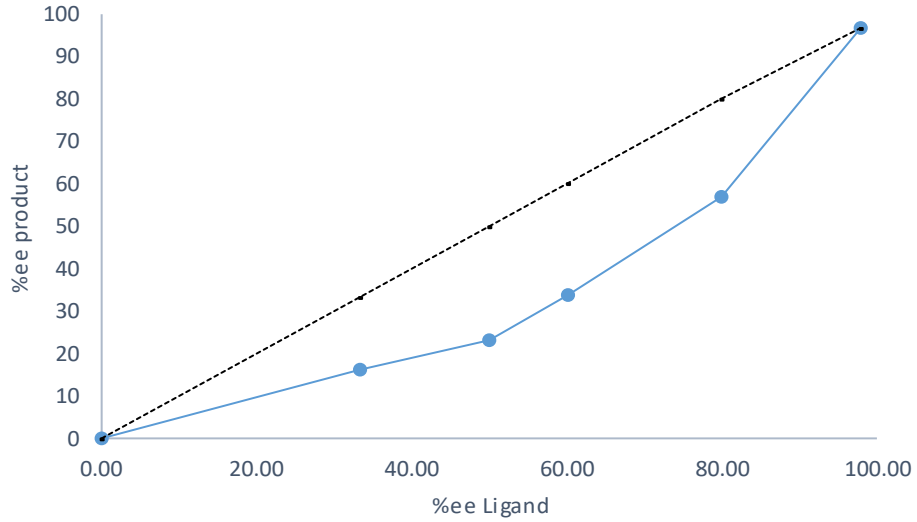

Figure 25: Non-linear effects study of silver(I) catalysed Asymmetric Mannich reaction of diazoacetates with *N*-Boc aldimines; (dashed black line) linearity; (blue line) non-linear effects data.

Interestingly, a negative non-linear effect was observed (Figure 25). There are at least two mechanistic scenarios that can lead to this result and the data presented in this work is not sufficient to elucidate which mechanistic scenario is operative in this system. One mechanistic scenario arises when the tetrahedral dimer complex **226** is much lower in energy compared to the monomeric trigonal planar complex **225**. In this case, the tetrahedral complex acts as a reservoir for the ligand and there would be much less ligand available for the active monomeric trigonal planar complex **225**, which would give rise to the observed negative non-linear effect. Another explanation for the observed negative non-linear effect would be if two ligands were involved in C-C bond formation (enantiodetermining step) between the diazoacetate and aldimine, in the transition state, whereby the heterochiral species is more reactive than the homochiral species. This would be in accord with the labile nature of the trigonal planar complex **225** as demonstrated by ^{31}P-^{31}P-EXSY NMR experiments (Section 3.7.2). In order to elucidate which of these mechanistic scenarios is operative, further experimentation is required. Namely, conducting the non-linear experiment again but with a higher catalyst loading; if a reservoir effect is operative then the non-linear effect should be dependent on the concentration of catalyst. Secondly, kinetic experiments to elucidate the order of the reaction with respect to the

catalyst needs to be conducted; an order less than 1 in catalyst would suggest that most of the active catalyst is present as the tetrahedral dimer. A follow up experiment would be to find the order of catalyst with a 1 : 1 stoichiometry of **196** : AgOTf and subsequently perform the non-linear experiments with this stoichiometry. These experiments would give a clearer mechanistic picture of the reaction.

Further analysis of complex **225** was carried out to verify that it was monomeric and not binuclear at silver with a symmetry element to allow for equivalent chemical environments at the phosphorous atoms on the bisphosphine ligand. A ^{31}P-DOSY experiment (Figure 26) was performed on complexes **225** and **226**, which showed that complex **225** has a marginally larger diffusion coefficient (*D*) than complex **226**. This suggests that complex **225** is smaller and moves more rapidly through solution than complex **226** which is what we would expect if it was monomeric.

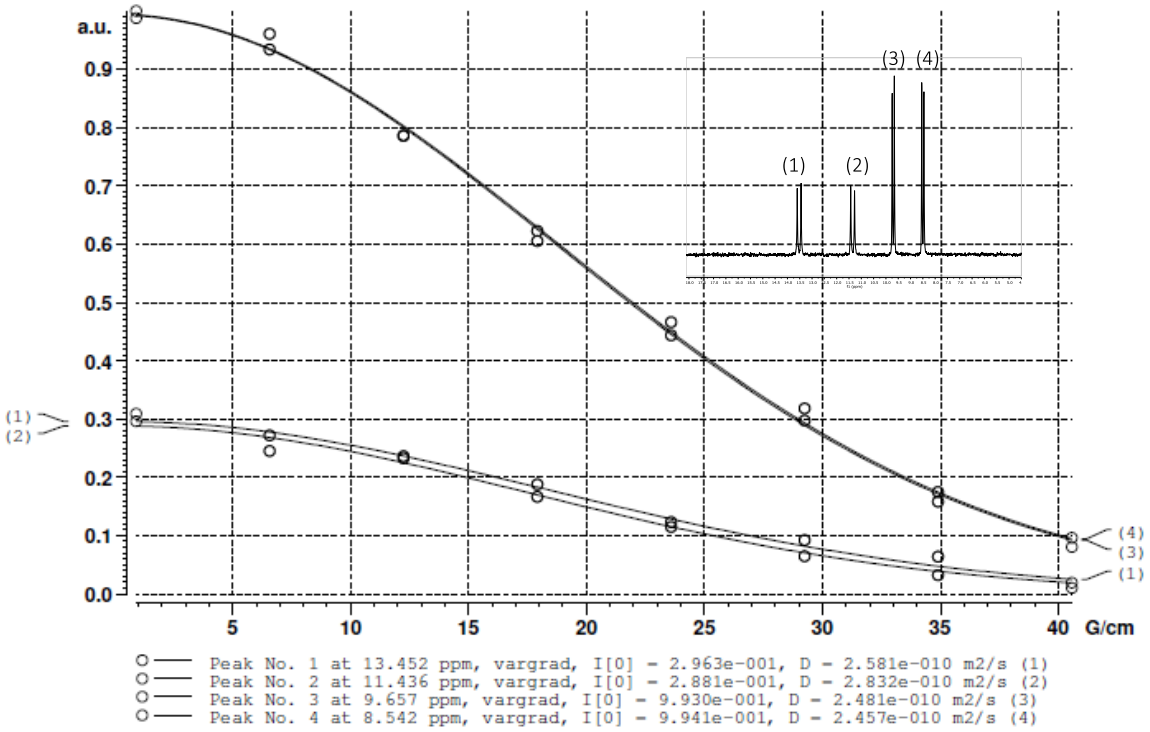

Figure 26: ^{31}P-DOSY experiment at 233K using 14.4 mg of (*R*)-DM-SEGPHOS and 2.6 mg of AgOTf.

3.8 Conclusions and Future Work

In conclusion, the first enantioselective silver-catalysed Mannich reaction of diazoacetate esters with *N*-Boc protected aldimines has been developed. The catalytic system for the reaction is comprised of 2 : 1 ratio of chiral, atropisomeric bisphosphine ligand (*R*)-DM-Segphos **196**: silver triflate, with catalyst loadings ranging from 1-5 mol% with respect to silver triflate to afford Mannich adducts in good yields and excellent enantioselectivities. Investigations into the reaction mechanism, using a variety of NMR

techniques led to identification of two main species: 1) trigonal planar complex **225**, which appears to catalyse the reaction and 2) tetrahedral complex **226** which appears to be an inactive dimer at least on the NMR timescale. ^{31}P-^{31}P-EXSY NMR showed that these two complexes do not interconvert in solution. Furthermore, it was observed that the trigonal planar complex **225** is very dynamic in solution; ligand exchange was observed by the presence of the quadrant cross-peaks on the 2D spectrum, which corresponded to mixing of ^{31}P nuclei with both isotopes of silver nuclei. A negative non-linear effect was observed, which showed the underlying kinetics and mechanistic aspects of the reaction are complicated and further mechanistic studies are required to the end of developing a more complete mechanistic picture for this reaction so that the catalytic system can be applied to other, novel enantioselective transformations.

4. Silver-Catalysed Mannich Reaction of Diazoaceatates with *N*-DPP Ketimines

4.1 Chapter Overview

This chapter describes work towards the development of the first enantioselective Mannich reaction of diazoacetate esters with imines derived from unactivated ketones. Catalytic enantioselective synthesis of tetrasubstituted stereogenic centres is a challenge.[98] Due to the formation of the quaternary, chiral stereocentre in the product, it was anticipated that this class of Mannich adduct would be amenable to carbene chemistry. The catalytic system for this reaction was developed by logical extension from the previous methodology detailed in Chapter 3 describing the silver(I)-catalysed Mannich reaction of diazoacetates with *N*-Boc aldimines. The poor electrophilicity of the ketimine electrophile necessitated the use of an organosuperbase as part of the catalytic system, however low reactivity remained an issue. Ultimately, low catalytic turnover was the main limitation of this methodology, a problem that could not be overcome in the presence of strong base.

4.2 Extension of Previously Established Catalytic System

We sought to apply the catalytic system developed in Chapter 3 to the reaction of diazoacetate esters with ketimines. On employing the same system and conditions with an *N*-DPP ketimine derived from acetophenone **139a**, no product was observed and only starting materials were returned (Scheme 64).

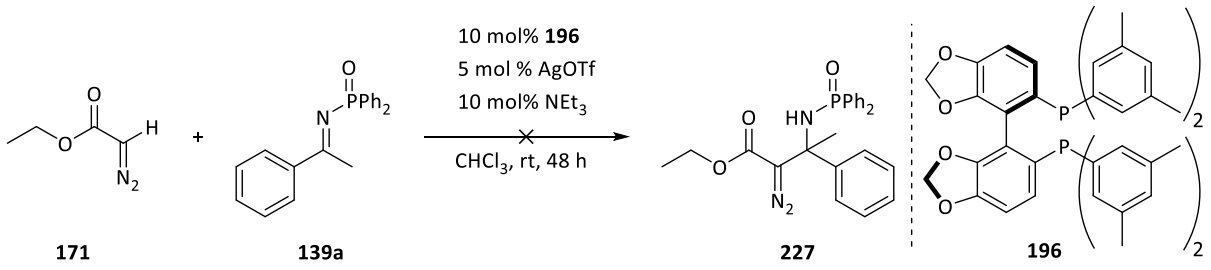

Scheme 64: Reaction of ethyl diazoacetate (EDA) with *N*-DPP ketimine 139a under the optimised conditions presented in Chapter 3.

The formation of no product is reflective of just how unreactive ketimines are compared to their aldimine counterparts. It was clear at this point that different conditions were required to initiate this reaction and inspiration was taken from literature precendent.

For example, Shibasaki and co-workers developed a protocol utilising a strong Brønsted Base with a metal-ligand system in a cooperative manner for the enantioselective alkynylation of ketimines (Scheme 65).[99]

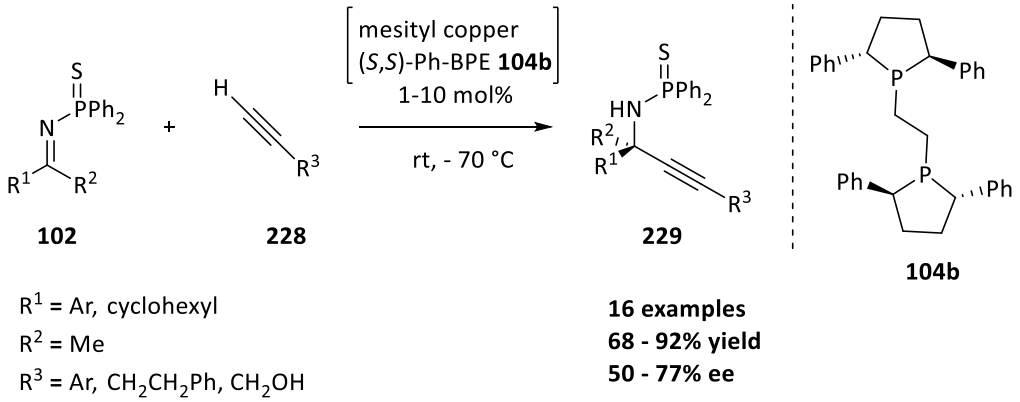

Scheme 65: Shibasaki's copper-catalysed asymmetric alkynylation of *N*-thiodiphenyl phosphinoyl ketimines.

The reaction proved to be broad in substrate scope; with variability on both the ketimine and terminal alkyne being tolerated well. The desired product was furnished in good yields and moderate enantioselectivities. The catalytic system consisted of a hard and strong Brønsted Base in the form of mesityl copper, with the copper(I) acting as a soft Lewis-acid. It was shown that the sulfur atom on the thiophosphinoyl protected ketimine **102** was crucial for reactivity; with the phosphinoyl ketimine variant resulting in no reactivity. This was explained by a proposed 'soft-soft' interaction between the sulfur atom and the copper(I) metal ion being favourable and therefore activation of the ketimine electrophile is only achieved in this manner. Once the ketimine electrophile is activated, carbon-carbon bond formation can then take place with the copper acetylide nucleophile, with facial selectivity being achieved through the use of the chiral phosphine ligand to bind the copper.

4.2.1 Proof of Concept

Therefore, as a logical modification to our previously established catalytic system for the enantioselective Mannich reaction of diazoacetate esters with *N*-Boc aldimines, it appeared that the natural nucleophilicity of the diazoacetate ester was not sufficient for reactivity with ketimines and we required a stronger base as a replacement for triethylamine to allow for an initial deprotonation of the diazoacetate ester pro-nucleophile at the α-position. This is a different mechanism to the silver-catalysed enantioselective Mannich reaction of diazoacetate esters with *N*-Boc protected aldimines reported in chapter 3 (*vide supra*), where triethylamine was a necessary component of the catalytic system; its role was to abstract the proton at the α-position of the Mannich adduct after C-C bond formation had occurred to reform the diazo moiety. It was hoped that forming the α-anion of the diazoacetate ester would make it more nucleophilic towards the ketimine electrophile. Our initial choice of ligand was the aminophosphine ligand **230**, which was utilised in a previously developed isocyanoacetate Mannich reaction of ketimines for the enantio and diastereoselective synthesis of substituted imidazolines.[100]

Initial reactivity was explored using a 1.2 : 1 stoichiometry of ethyl diazoacetate **171** : ketimine **139a** and a 2 : 1 stoichiometry of ligand **230** : silver salt was maintained to avoid the possibility of unligated silver(I). Tetramethylguanidine (TMG) was used as the base to begin with and reactivity was observed (albeit with low catalytic turnover after 48 h) and a non-zero ee of 20% was obtained (Scheme 66).

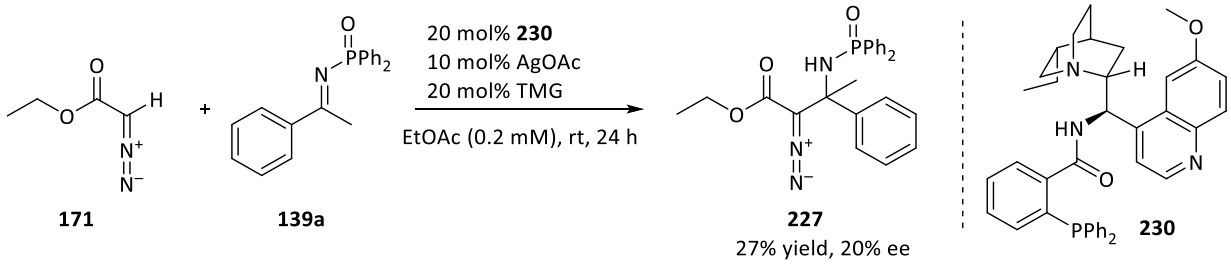

Scheme 66: Proof of concept for silver(I) catalysed Mannich reaction of diazoacetates with *N*-DPP ketimines.

The poor catalytic turnover was an issue that needed to be addressed. It was observed that after 24 h a silver precipitate collected around the bottom of the reaction vessel which hadn't been observed previously. We speculated that the reduction of silver(I) to silver(0) was connected to the base; the TMG was not compatible with Ag(I) under these conditions.

To establish that a base-catalysed background reaction was not occurring, the relevant control experiments were performed (scheme 67). The reaction was performed in the presence of 20 mol% TMG (Scheme 67, A) and 20 mol% TMG and 10 mol% AgOAc (Scheme 67, B).

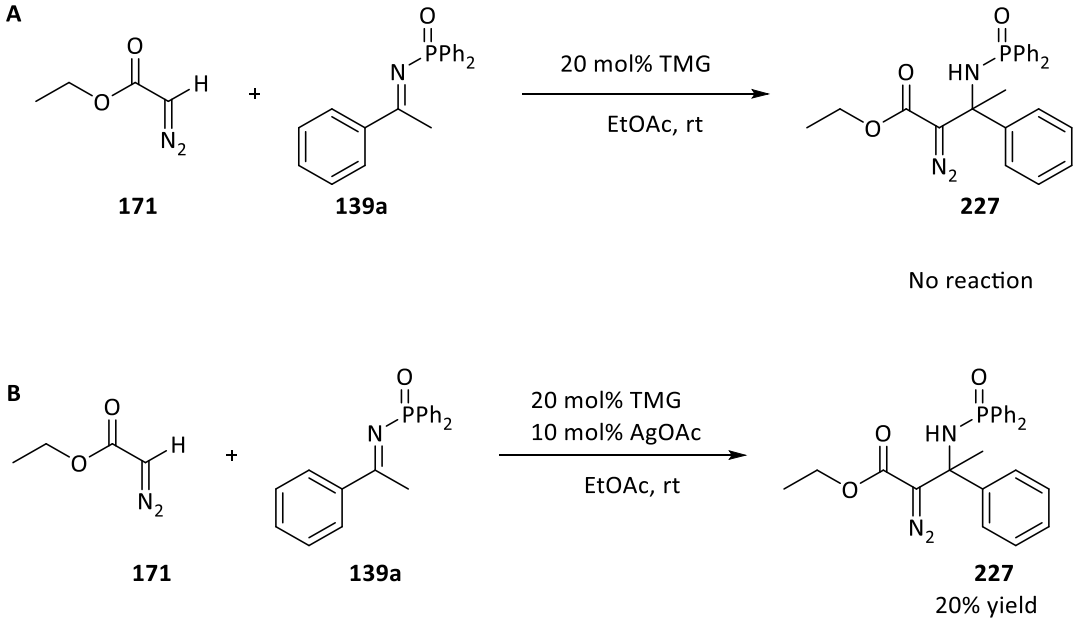

Scheme 67: Control reactions: (A) ethyl diazoacetate with *N*-DPP ketimine 139a in the presence of TMG; (B) ethyl diazoacetate with *N*-DPP ketimine 139a in the presence of TMG and silver acetate.

The control experiments showed that the reaction could not be catalysed by TMG alone (Scheme 67, A). However, it was shown that TMG in combination with silver acetate could catalyse the reaction with a yield equivalent to that obtained with ligand **230** (Scheme 67, B). This suggests that the unison of the silver salt (Lewis acid) and TMG (Brønsted base) is necessary for the formation of a catalytically active system. Another, similar base to TMG, presenting an *N*-*tert*-butyl group at the 2-position on the guanidine, Barton's base (BTMG) was screened (Scheme 68).

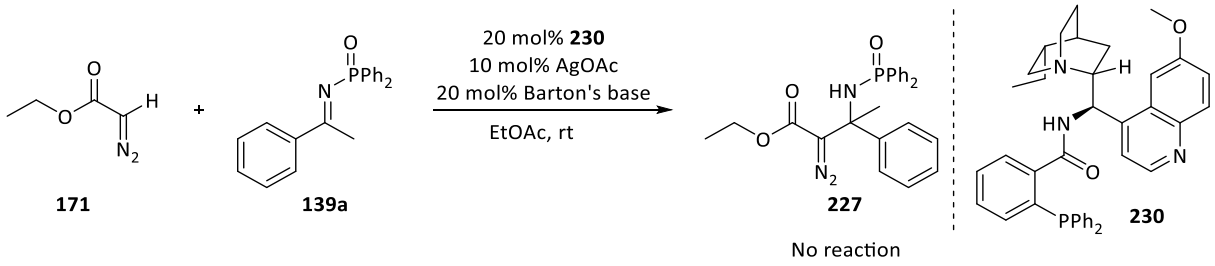

Scheme 68: Silver-catalysed Mannich reaction of ethyl diazoacetate with *N*-DPP ketimine 146a in the presence of Barton's base (BTMG).

Interestingly, no reaction was observed when Barton's base was used. This result is suggestive that the substrates and/or the silver(I)-**230** complex is being activated by TMG where no such activation occurs with bulky bases such as BTMG. Clearly, an alternative base was required to reduce the background reaction and thereby maximise enantioselectivity. The base would need to be of a smilar basicity as TMG.

Before different bases were evaluated, a ligand screen was conducted where the bisphosphine ligands were evaluated (Figure 27).

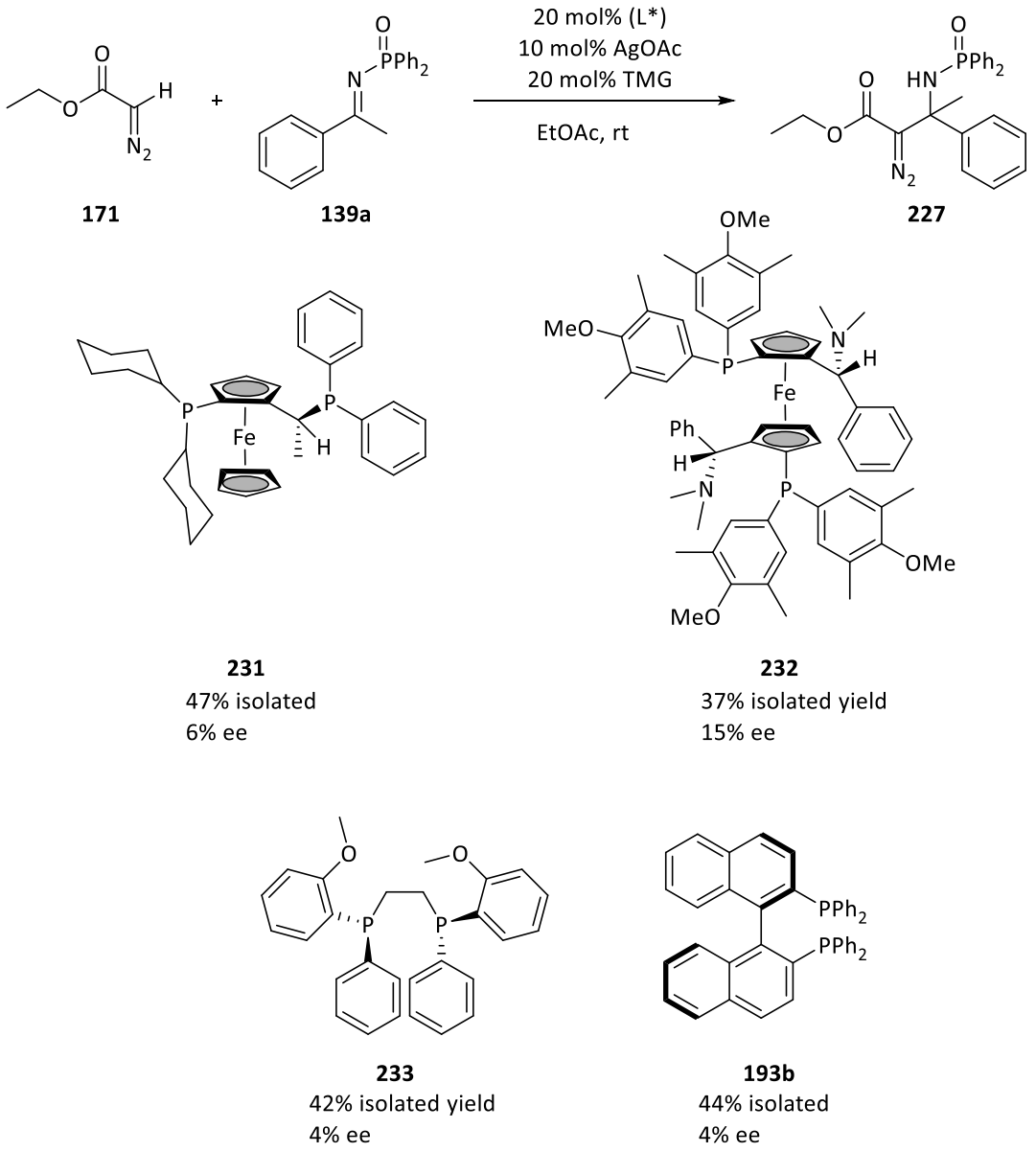

Figure 27: Evaluation of bisphosphine ligands. Reactions were performed on a 0.10 mmol scale.

Overall, an increase in reactivity was observed on using the more electron-rich bisphosphine ligands compared to the aminophosphine ligand **230**. However, enantioselectivity was poor except for MandyPhos ligand **232** (15% ee). Josiphos ligand **231** gave the best reactivity obtained hitherto; the product was obtained with an isolated yield of 47%, however, the ee was only 6%. Interestingly, atropisomeric ligand (*R*)-BINAP **193b** resulted in a very low ee of 4%.

The differences in enantioselectivities on using the aminophosphine ligand contrasted with the bisphosphine ligands could be attributed to the amide functionality on the aminophosphine ligand. The *N*-H of the amide functionality on the aminophosphine ligand **230** is potentially important in facial selectivity of the ketimine electrophile. Previous work in the Dixon group elucidated the binding mode of this ligand with silver acetate by means of single crystal X-ray diffraction studies.[100] In the solid state

it was shown that the silver(I) ion adopts a tetrahedral geometry where the ligand coordinates through the quinuclidine *N*-atom and the phosphine to form a 9-membered macrocycle. The other coordination sites on the silver(I) ion are occupied by the acetate counterion and a quinolone unit of another, adjacent ligand allowing for the formation of polymeric chains of ligand-silver units in the solid state. It was also observed that the π-system of the amide is oriented towards the silver, suggesting possible coordination. Such coordination would make the *N*-H more acidic and thereby improve the hydrogen-bonding capabilities of the ligand.

Using aminophosphine ligand **230** as the most selective ligand, an evaluation of a few different achiral bases was performed in the hope of reducing the background reaction as well as increasing catalytic turnover. Polystyrene supported BEMP performed better than TMG in terms of enantioselectivity but with an attenuation in reactivity; adduct **227** was formed in 16% yield and with 34% ee (Scheme 69, A). This result suggested that the background reaction was reduced on using polystyrene supported BEMP. The second base evaluated was a lithium phenoxide derived from *para*-methoxy phenol, which was prepared as a 0.1 M stock solution in THF and used without delay. This base was pioneered by Shibasaki for enantioselective catalytic applications.[101] This gave a similar yield to PS-BEMP, but enantioselectivity was lower (Scheme 69, B). Both reactions led to the formation of a 'silver mirror', suggesting reduction of silver(I) to silver(0) was the main reason for low conversion. At this point, a few other parameters were evaluated using PS-BEMP as the base.

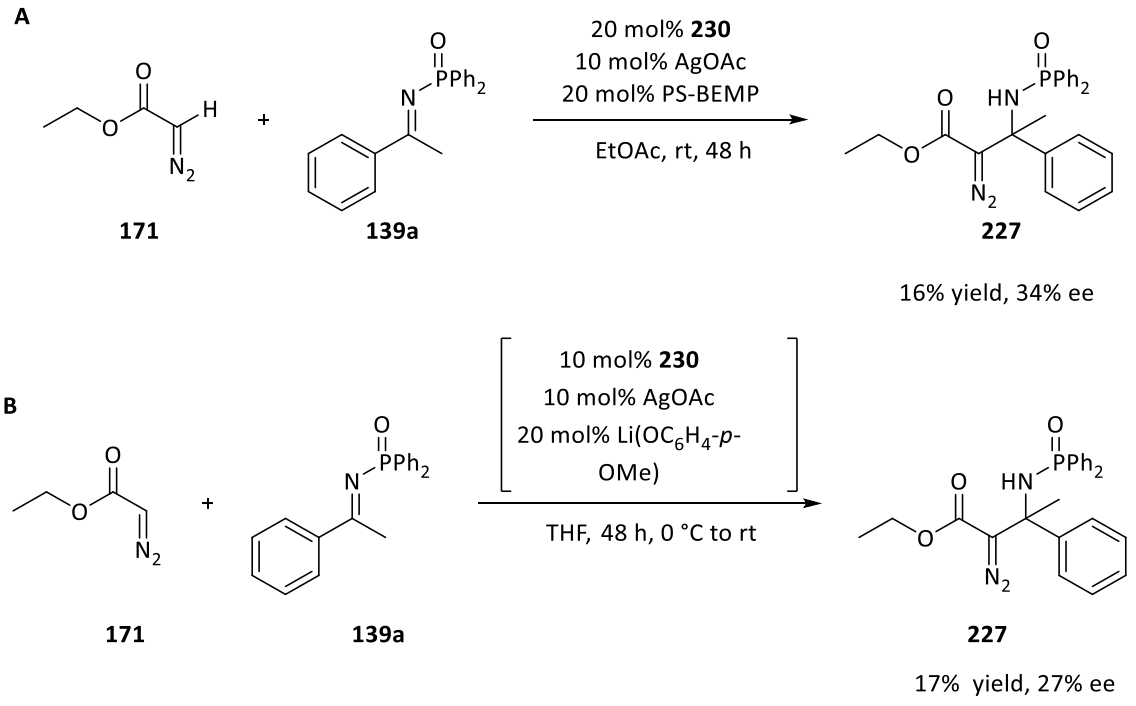

Scheme 69: Evaluation of (A) PS-BEMP and (B) Li(OC_6H_4-*p*-OMe) in the Mannich reaction of diazoacetates to *N*-DPP ketimines.

4.2.2 Silver Salt Screen

Screening of the silver salt was conducted in the hope of increasing enantioselectivity and reactivity. Silver carbonate gave a similar yield to silver acetate but with no improvement in enantioselectivity (Table 5, entry 1). Silver oxide gave no improvement in yield, however a slight augmentation in enantioselectivity was observed (Table 5, entry 2). Silver triflimide gave an improvement in the yield (*ca.* 3 catalytic turnovers) and a small augmentation in enantioselectivity compared with silver acetate (Table 5, entry 3).

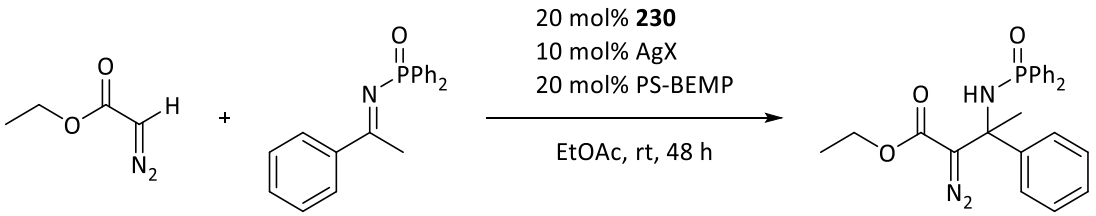

171 **139a** **227**

Entry	AgX	Yield/%	ee/%
1	Ag_2CO_3	23	34
2	Ag_2O	19	36
3	$AgNTf_2$	31	36

Table 5: Silver salt screen. All reactions were performed on a 0.20 mmol scale.

Solvent plays a key role in many reactions, for example, in section 3.3.5 it was observed that use of chlorinated solvents, namely chloroform resulted in a significant increase in the enantioselectivity of the silver-catalysed Mannich reaction of diazoacetate esters with *N*-Boc aldimines. At this point, it was decided to conduct a solvent screen using silver acetate as opposed to its more expensive counterpart, silver triflimide.

4.2.3 Solvent Screen

Accordingly, a solvent screen was performed to assess the main classes of solvent on reactivity and enantioselectivity: polar aprotic, polar protic, non-polar and chlorinated. Interestingly, use of dichloromethane resulted in no product formation (Table 6, entry 1). Use of toluene resulted in augmentation in enantioselectivity to 44% ee (Table 6, entry 2) but poor reactivity was still an issue; 16% yield of adduct **227** was obtained. Methanol gave no product (Table 6, entry 3). Acetonitrile also gave no reactivity, possibly due to the ligating ability of the nitrile group, thereby poisoning the Ag(I) metal centre (Table 6, entry 4).

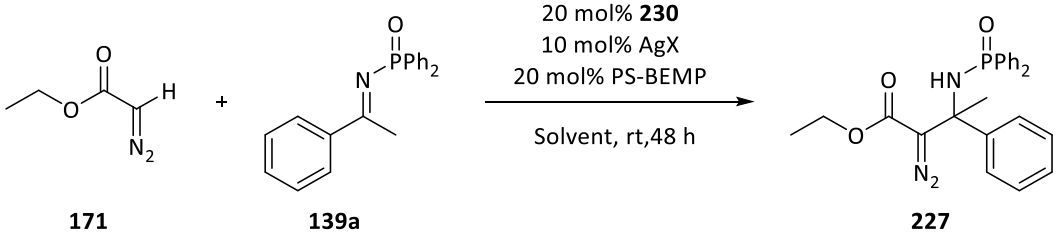

171 **139a** **227**

Entry	Solvent	Yield/%	ee/%
1	CH_2Cl_2	-	-
2	Toluene	16	44
3	MeOH	-	-
4	MeCN	-	-

Table 6: Solvent screen. All reactions were performed on a 0.20 mmol scale.

With these results in hand, use of soluble BEMP was explored in the hope that the ligating properties of this form of BEMP would result in an increase in reactivity. Use of BEMP as a base resulted in an increase in reactivity with only a small erosion in enantioselectivity (Scheme 70).

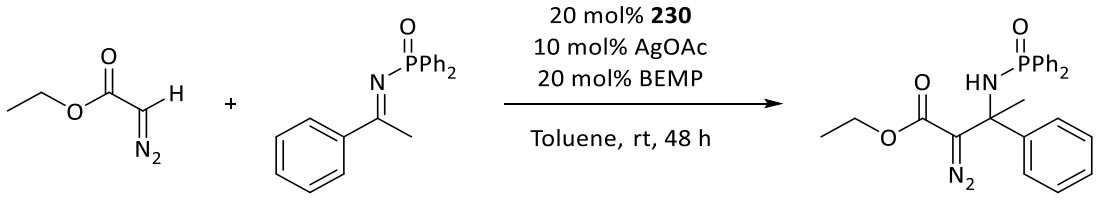

Scheme 70: Silver(I)-catalysed Mannich reaction of diazoacetates to *N*-DPP ketimines using BEMP as the Brønsted base.

4.3 Investigations into Improving Catalytic Turnover

The main limitation for further optimisation of this method was the poor catalytic turnover which we speculated to be linked to the formation of the silver mirror. Without identifying the underlying cause for the reduction of silver(I), there were two options to investigate: 1) increasing the electrophilicity of the ketimine and 2) increasing the nucleophilicity of the diazoacetate nucleophile. Both routes were explored (*vide infra*) with the aim of increasing the rate of reaction significantly.

4.3.1 Increasing the Electrophilicity of the Ketimine

Synthesis of ketimine **238** bearing a trifluoromethyl functionality as well as an *N*-Boc protecting group was conducted by Boc protection of hydrazine to afford **235** in good yield (Scheme 71). This was then treated with acetic acid and sodium nitrite to afford Boc azide as an intermediate which was then reacted with triphenyl phosphine to afford the iminophosphorane **236** *via* a Staudinger reaction in good yield. Reaction of **236** with trifluoroacetophenone **237** in an aza-Wittig process afforded the desired ketimine in good yield (81%).

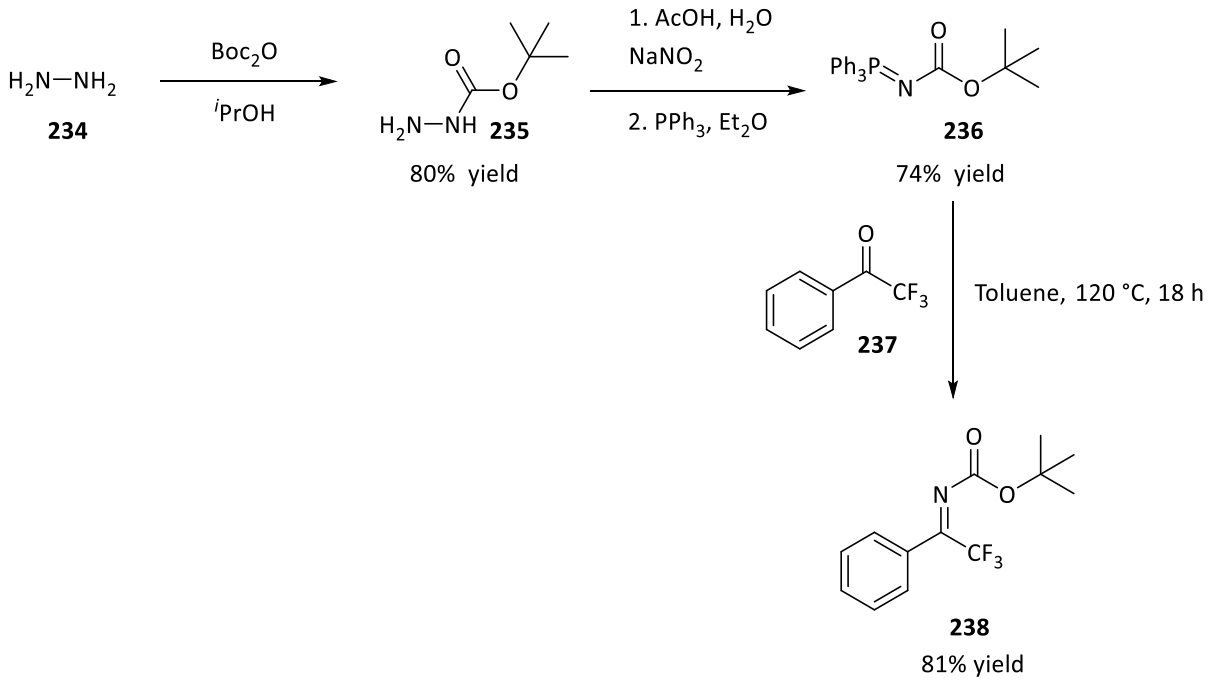

Scheme 71: Synthesis of *N*-Boc protected Ketimine derived from trifluoroacetophenone by an aza-Wittig process.

Ketimine **238** was then subjected to the best reaction conditions with silver acetate as the silver salt (Scheme 72), but disappointingly no reaction was observed.

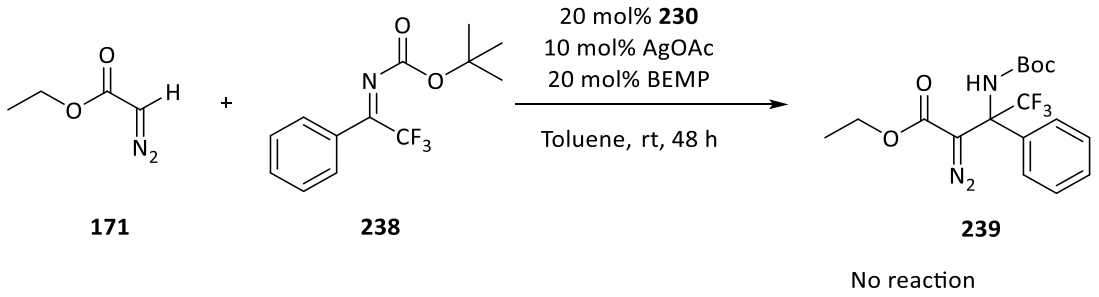

Scheme 72: Attempted silver(I)-catalysed Mannich reaction of ethyl diazoacetate to *N*-Boc ketimine 238 derived from trifluoroacetophenone.

According to Mayr, *N*-DPP aldimines are less electrophilic than *N*-tosyl aldimines (Figure 28).[102, 103]

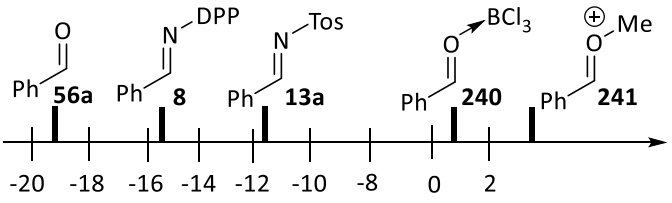

Figure 28: Herbert Mayr's electrophilicity table for aldehydes and aldimines.

It was hoped that this trend would extend to ketimine substrates. Accordingly, *N*-tosyl ketimine **243** was synthesised by a gold-catalysed hydroamination of phenylacetylene which afforded the desired imine product in good yield (Scheme 73).[104]

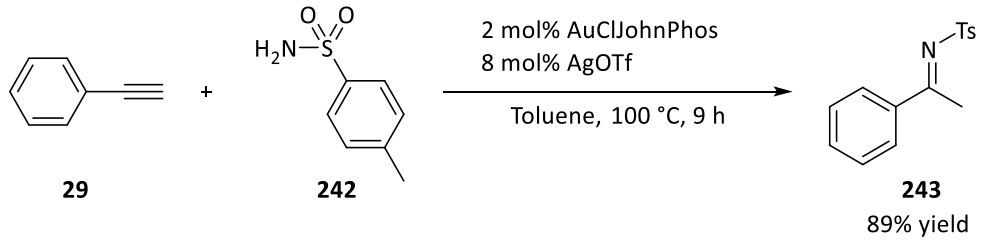

Scheme 73: Gold-catalysed reductive amination of phenylacetylene 29.

Ketimine **243** was then subjected to the reaction conditions but surprisingly, no reaction was observed (Scheme 74).

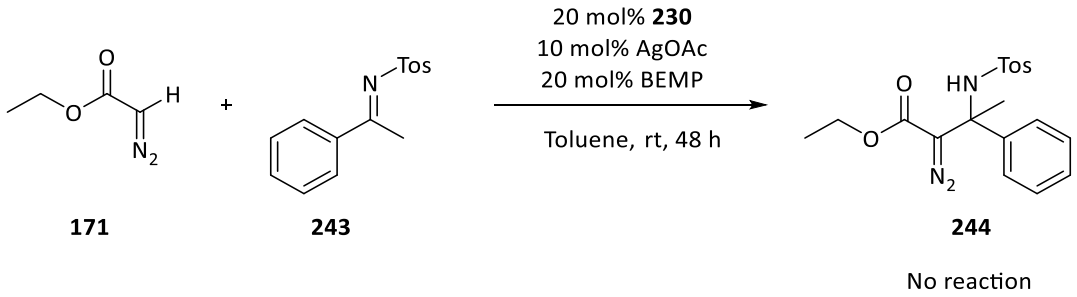

Scheme 74: Silver(I)-catalysed Mannich reaction of diazoacetates to *N*-tosyl ketimine 243 derived from acetophenone.

Although disappointing, this result potentially highlights the importance of the *N*-DPP protecting group as an activating group with the aminophosphine ligand-Ag system.

4.3.2 Synthesis and Evaluation of 2,2,2-trifluoroethyl-2-diazoacetate

The trifluoromethyl variant of ethyl diazoacetate **171** was previously used by Zhu and co-workers for the asymmetric allylic alkylation of diazoacetates on reaction of **248** with Morita Baylis-Hillman carbonates in the presence of a Lewis-base.[105] In a deuterium experiment, they observed a significantly higher deuterium incorporation in trifluoroethyl diazoacetate **248** compared with ethyl diazoacetate **171** which is reflective of the more acidic α-position in **248**. It was hoped that under our conditions, the presence of a more acidic α-proton in the pro-nucleophile would circumvent the reactivity problems observed thus far. Synthesis of diazoacetate **248** started with reaction of 2,2,2-trifluoroethanol **246** with 2,2,6-trimethyl-4H-1,3-dioxin-4-one **245** with the concomitant evolution of acetone to afford trifluoroethyl acetoacetate **247** in modest yield (Scheme 75). The diazoacetate was formed by reacting trifluoroethyl acetoacetate **247** with tosyl azide followed by base workup. The

product was not stable to silica and was thus purified by vacuum distillation which proved to be difficult due to the volatile nature of diazoacetate **248**.

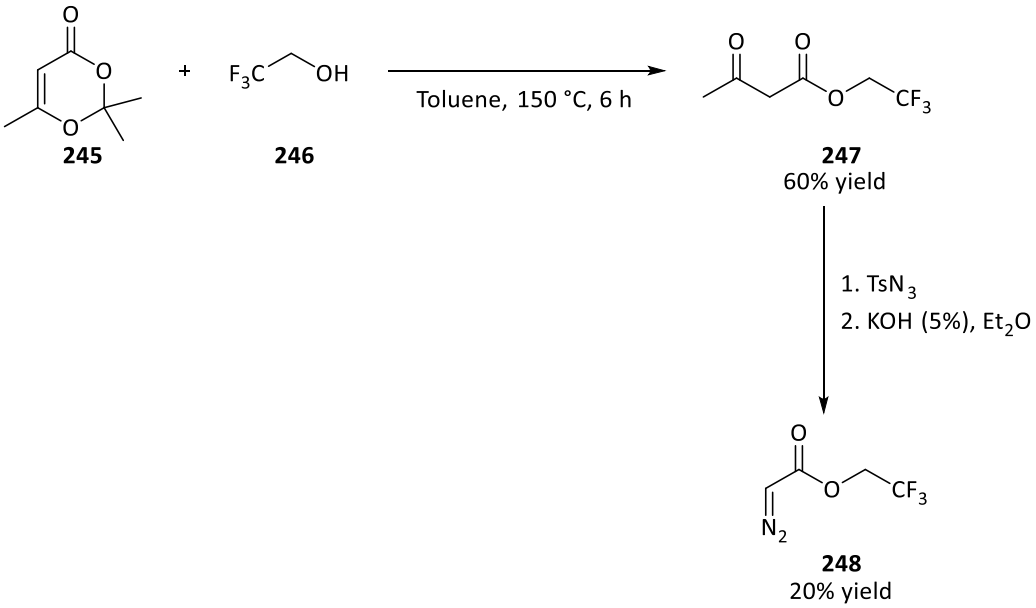

Scheme 75: Synthesis of 2,2,2-trifluoroethyl 2-diazoacetate.

Diazoacetate **248** was subjected to the reaction conditions with ketimine **139a** and no reaction was observed. This result suggests that a nucleophile containing more acidic protons does not necessarily infer greater nucleophilicity and thus reactivity.

4.3.3 Investigation into the Reducing Agent

Little was known as to what component of the reaction system was involved in the reduction of silver(I) to silver(0), resulting in poor catalytic turnover and thus low conversion. As the main limitation to this method, investigations were carried out to elucidate what was causing this reduction and whether it could be stopped. A clue to this problem came from the work of Newman and Beal who described their novel method of using silver benzoate and triethylamine in methanol for performing a Wolff rearrangement of diazo ketones in 1950.[106] They proposed that when the diazo ketone is deprotonated, the resulting anion undergoes single-electron transfer (SET) with the silver(I) ion to form silver metal and the corresponding diazo ketone radical intermediate. To test this hypothesis, two control experiments were performed (Scheme 76).

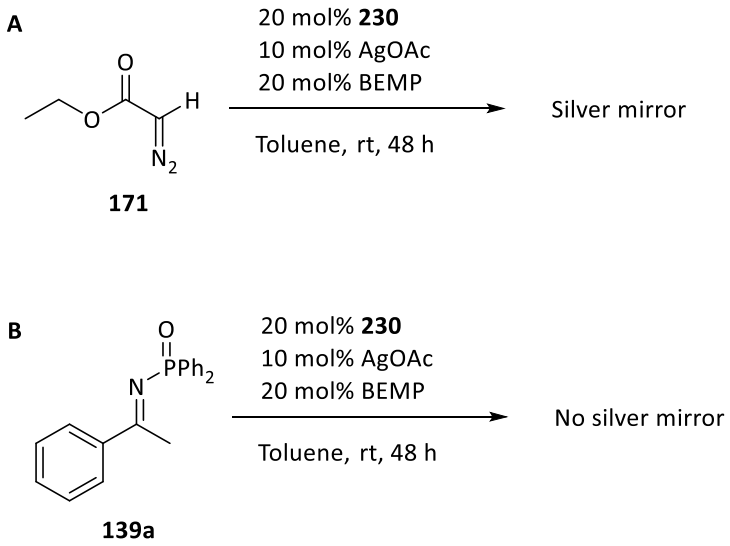

Scheme 76: Control experiments (A) in the absence of ketimine 139a (B) in the absence of ethyl diazoacetate.

Where ethyl diazoacetate in the absence of ketimine **139a** was subjected to the reaction conditions (Scheme 76, A), a silver mirror was formed after 48 hours. However, when ketimine **139a** in the absence of ethyl diazoacetate was subjected to the same conditions, no silver mirror was observed after 48 hours. A third control experiment was performed with just aminophosphine ligand **230**, silver acetate and BEMP and no silver mirror was observed after 48 hours. These results suggest that it was the deprotonated diazoacetate that was the reducing the silver(I) ion to silver (0) and thus destroying the catalytic species.

4.4 Conclusions and Future Work

In conclusion, a new method for the enantioselective Mannich reaction of ethyl diazoacetate with *N*-DPP ketimines has been explored with novel reactivity being documented and enantioselectivity of up to 44% ee being obtained. High reactivity (using chiral aminophosphine ligand **230**) was unattainable due to poor catalytic turnover; a problem that was unavoidable on deprotonating the diazoacetate pro-nucleophile as our investigations led us to conclude that the deprotonated diazoacetate was responsible for the reduction of the silver(I) metal centre. This problem likely necessitates the use of a different metal ion in future studies into this reaction.

5. Novel NMR Method for Determining the Longitudinal Relaxation Times of Low Gamma Nuclei by Indirect Detection *via* Spin-State Satellite Exchange

5.1 Chapter Overview

This chapter follows on from the work reported in chapter 3 and describes a practical method for determining the spin-lattice or longitudinal relaxation time constants (T_1) of nuclei with low magnetogyric ratios. The discovery of this method stemmed from mechanistic studies into the silver-bisphosphine system reported in chapter 3. Direct measurement of T_1 for low γ nuclei is not possible using standard NMR instruments equipped with broadband, resonance or triple resonance probes due to the problematic sensitivity of low γ nuclei. The T_1 measurement of nuclei with low magnetogyric ratios (γ) necessitates the use of expensive probes. A practical method is presented herein, which proposes to overcome these limitations and make T_1 relaxation times of low γ nuclei obtainable using standard NMR equipment. The method is applicable to any scalar (*J*) coupled two-spin system AX, where X is the low γ nucleus of interest and both nuclei are of spin-1/2. It makes use of the exchange spectroscopy (EXSY) NMR experiment of the directly observable high γ nucleus and uses a theoretical description of spin relaxation to help interpret the experimental results. EXSY NMR has traditionally been used to elucidate kinetic parameters relating to chemical exchange[107,108,109], however the indirect extraction of T_1 data of a scalar coupled nucleus from EXSY spectra has been hitherto unreported. We propose that this method is applicable to any transition metal-ligand system, where the transition metal is of low γ (such as Rh, Ag, W).

5.2 Introduction

Nuclear spin is fundamental to NMR and is a property common to all nuclides possessing a non-integer spin quantum number (I). A spinning nucleus has charge and angular momentum (P) associated with it. The charge is not static as the nucleus spins, but dynamic and this gives rise to a magnetic moment (μ) (equation 4).

$$\mu = \gamma . P \qquad [4]$$

The magnetogyric ratio[110] (γ) is a measure of how sensitive a nucleus is. Angular momentum and magnetic moment are vector quantities in that they possess both magnitude and direction. When

placed in an external magnetic field (B_0), the magnetic moments of all the nuclei adopt specific, discrete orientations that are dependent on spin quantum number. For an (I=1/2) nucleus, there are two different states the spins of the nuclei could adopt: with the applied magnetic field or against the applied magnetic field, the latter being higher in energy. If we consider a number of nuclides in solution placed within a magnetic field, statistically, at equilibrium, there will be a larger proportion of total nuclides adopting spins parallel to the external magnetic field. This can be formulated by means of the Boltzmann distribution, (equation 5) where N_α is the number of nuclides in the α spin state (spins parallel to the external magnetic field) and likewise, N_β is the number of nuclides in the β spin state (spins anti-parallel to the external magnetic field).

$$\frac{N_\alpha}{N_\beta} = e^{\Delta E/RT} \quad [5]$$

The imposition of a radio frequency pulse on this sample causes perturbation in the nuclear spins from their lowest energy state to a higher energy state. Over a given period of time, thermal equilibrium will be restored by relaxation. Knowledge of the time that this process takes is required for the effective execution of the NMR experiment for a clearly resolved spectrum.[111]

5.2.1 Longitudinal Spin-Lattice Relaxation (T_1)

Upon imposition of a radio frequency pulse on a sample, the magnetisation at thermal equilibrium (M_0) is displaced from the +z-axis along with a change in the spin states of the nuclides in the sample. After a period of time, the bulk magnetisation vector returns to the +z-axis and the system thereby re-establishes thermal equilibrium. The energy absorbed by the sample is re-emitted to the surroundings (the lattice) in the form of thermal energy. The time taken for this process to happen is dictated by the spin-lattice relaxation time constant T_1. The Bloch equations for NMR describes this return of the bulk magnetisation vector (M_0) to the +z-axis (M_z) (equation 6) and is generally complete after a period of $5T_1$.

$$\frac{dMz}{dt} = \frac{(M_0 - Mz)}{T_1} \quad [6]$$

The Bloch equations for relaxation theory illustrate that the recovery of the bulk magnetisation vector to the +z-axis is exponentially related to time and can be formulated as shown in equation 7.

$$M_Z = M_0(1 - e^{-t/T_1}) \quad [7]$$

Longitudinal relaxation time constants (T_1) have been found to be a useful tool in organic synthesis. For example, Hall and co-workers used Longitudinal relaxation times as a probe for the structural assignment of oligosaccharide derivatives. In summary it was found that at the anomeric position, axially oriented protons had shorter longitudinal relaxation times compared with equatorially oriented protons at the same position.[112] In addition to this, spin-lattice relaxation times have been used for a variety of different analytical purposes such as the derivation of molecular parameters such as bond distances[113] and studies of local molecular dynamics in solution.[114]

5.2.2 Difficulty in Measuring T_1s of Transition Metals

There seems to be a paucity of spin-lattice relaxation data pertaining to organometallic compounds containing transition metals in the literature; particularly transition metals of low magnetogyric ratio. As a result, the relaxation properties of transition metals as part of complexes has not been fully explored. This is due to a number of factors, namely the problematic sensitivity of low γ nuclei and the need for specialised NMR probes operating at low frequencies (often <20 MHz for a 500 MHz instrument). Measurement of the spin-lattice relaxation times (T_1) provides valuable information for transition metal complexes relating to their geometry, oxidation states and re-orienational properties.[115] Standard modern NMR instruments with broadband, inverse or triple resonance probes are not equipped for measuring T_1s of transition metal nuclei with very low magnetogyric ratios such as Ag and Rh. INEPT[116] sequences for transferring magnetisation from scalar-coupled high gamma nuclei to low gamma nuclei require specialised probes. This often makes the T_1s of such nuclei difficult or impossible to obtain directly. Accordingly, we recognised that these limitations could be overcome by using an indirect method which uses the EXSY spectrum of the high γ-nucleus A to which the low γ X-nucleus of interest is scalar coupled; such a two-spin system is particularly characteristic of a metal-ligand complex.

5.3 Spin-State Satellite Exchange of a Two-Spin System using an EXSY Pulse Sequence

We discovered that during the EXSY of a scalar coupled AX spin system, the phenomena of spin-state satellite exchange is observed. Spin-state satellite exchange is due to a change in the spin-states of the X nucleus during the EXSY pulse sequence of the A nucleus, characterised by off-diagonal cross peaks. Typically, a 1-D spectrum of the A nucleus will give rise to a doublet multiplicity pattern, which is reflective of the two-different spin-states of the X nucleus and this gives rise to two different resonance frequencies of A. The frequency difference between the two resonance frequencies represents the scalar coupling constant (Figure 29, A). During the mixing time of the 2-D EXSY sequence (which is usually when chemical exchange would occur), the X nuclei change spin states (X_α

to X_β and X_β to X_α) through natural longitudinal relaxation processes, observed as off diagonal cross peaks in the 2-D spectrum (Figure 29, B).

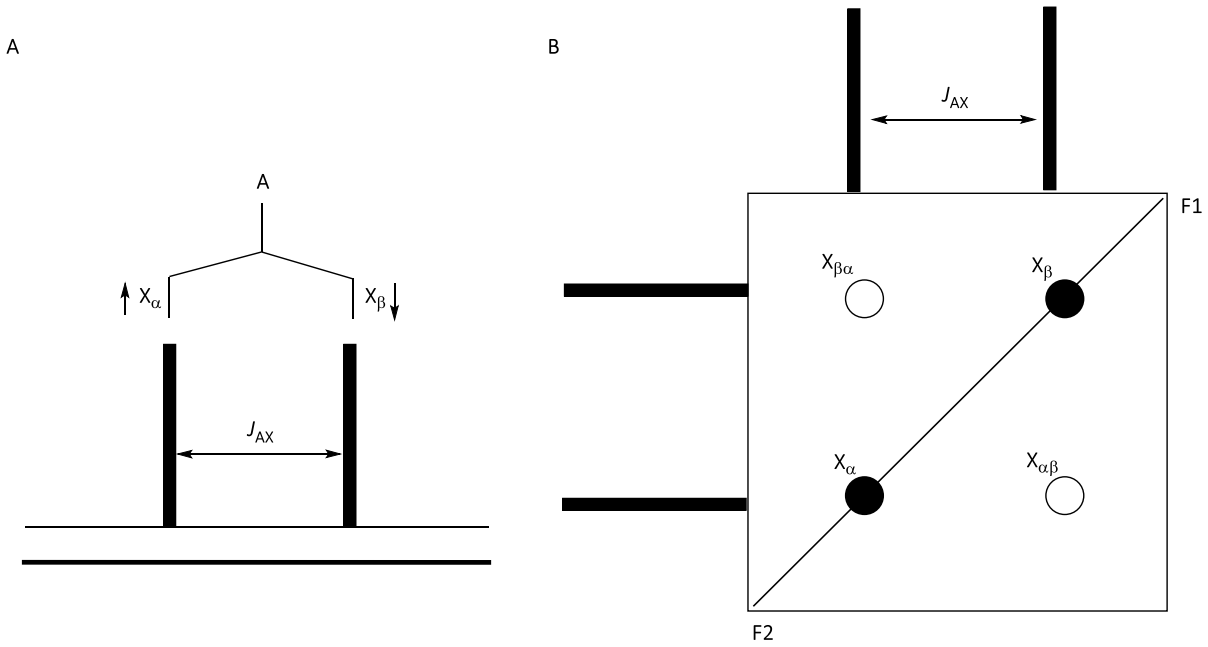

Figure 29: General scheme for underlying cause of spin-state satellite exchange of a two-spin AX system (A) 1-D spectrum of A nucleus which is scalar coupled the X nucleus (B) 2-D EXSY spectrum of A nucleus showing cross peaks arising from spin-state satellite exchange.

Spin-state satellite exchange occurs as a result of the internal energy of the system (i.e. molecular tumbling) and therefore does not require a radio frequency pulse to initiate it. This is due to the small energy difference between the α and β states of a nuclide. The change in spin-states of the X nucleus can be observed in the EXSY spectrum of the A nucleus, observed as off-diagonal cross peaks in the EXSY NMR spectrum. This phenomenon may be prevalent in any scalar coupled system. We have demonstrated that this effect can be observed in a ^{1}H-^{1}H EXSY of a ^{13}C-labelled sodium acetate; spin-state satellite exchange of ^{13}C nuclides were observed.[x]

We envisaged that the volume integrals of satellite cross peaks arising from spin-state satellite exchange during the EXSY sequence with respect to mixing time (t_{mix}) could be correlated with the T_1 of the (X) nuclide ($T_1(X)$). This can only happen if the volume intensity of the satellite cross-peaks is dependent on the $T_1(X)$. To rationalise why this might be the case, the underlying mechanisms that underpin relaxation need to be understood. The two main mechanisms which contribute to relaxation

[x] **See Appendix for spectrum.**

are: 1) dipole-dipole interaction and 2) chemical shift anisotropy (CSA). The dipole-dipole contribution[117] to relaxation in a two-spin AX system can be defined by the following expression:

$$\frac{1}{T_1} = \frac{{\gamma_A}^2 {\gamma_X}^2 \hbar \tau_c}{r^6} \quad [8]$$

$1/T_1$ – Longitudinal relaxation rate; γ_A – Magnetrogyric ratio of A nucleus; γ_X – Magnetrogyric ratio of X nucleus; $\hbar = h/2\pi$; τ_c – correlation time; r – radius separating two dipoles/nuclei.

In situations where strong CSA exists, as is likely to be the case in many transition metal systems, it is reasonable to assume that the dipole-dipole driven relaxation will be negligible. In such a situation, the relaxation of both nuclides should be dominated by chemical shift anisotropy. CSA occurs as the electron distribution in chemical bonds is not symmetrical, thus the local field and chemical shift of a nucleus as part of a chemical bond will depend on its orientation with respect to the applied magnetic field. The tumbling of molecules in solution averages out the CSAs that only one frequency is observed for a chemically distinct nucleus as part of a chemical bond. However, this dynamic magnetic field of a chemical bond can contribute to relaxation significantly for nuclei that exhibit large chemical shifts such as ^{31}P, ^{19}F and metal nuclides. A salient feature of relaxation dominated by CSA is its square dependence on the applied magnetic field. From equation 9, there is a linear dependence of $1/T_1$ with respect to B_0^2, where CSA is the dominant mechanism for relaxation.

$$\frac{1}{T_1} = \frac{2}{15} {\gamma_A}^2 {B_0}^2 \Delta\sigma^2 \tau_c \quad [9]$$

The analysis outlined in this chapter utilises a mathematical model described using *Spinach*[118], which is based on the assumption that the main mechanism for relaxation of transition metal nuclides in metal complexes is chemical shift anisotropy (CSA). Indeed, Soulié and co-workers have proposed that CSA was the dominant relaxation mechanism in the ^{195}Pt nucleus of platinum complexes and will likely be the case for metals that exhibit large chemical shift ranges.[119] The model does not conform to systems where dipole-dipole (DD) interaction has a significant contribution to relaxation.

5.4 Results and Discussion

5.4.1 Mathematical Model

Given the assumptions specified above, a complete *ab initio* relaxation theory treatment of a two spin (I=1/2) AX system in a liquid medium was conducted.[xi] It is worth noting that $k_{x\ indirect}$ is indirectly, the longitudinal relaxation rate of the X nucleus, obtained from satellite exchange NMR spectroscopy. Mathematical manipulation of $k_{x\ indirect}$ is required to obtain the longitudinal relaxation rate for the X nucleus, $k_{X\ direct}$. Equations 10 and 11 describe the longitudinal relaxation rates of the X spin in a direct and indirect sense respectively. There are clearly two terms present in both equations for longitudinal relaxation; the CSA term (highlighted in blue) and the DD (dipole-dipole) interaction term (highlighted in red).

$$k_{x\ direct} = -\frac{\Delta^2{}_{CSA-x}}{30} J(\tau_c, \omega_x) - \frac{\Delta^2{}_{DD}}{360}[3J(\tau_c, \omega_x) + J(\tau_c, \omega_a - \omega_x) + 6J(\tau_c, \omega_a - \omega_x)] \quad [10]$$

$$k_{x\ indirect} = -\frac{\Delta^2{}_{CSA-x}}{60} J(\tau_c, \omega_x) + \frac{\Delta^2{}_{DD}}{720}[3J(\tau_c, \omega_x) + J(\tau_c, \omega_a - \omega_x) + 6J(\tau_c, \omega_a - \omega_x)] \quad [11]$$

k_n – longitudinal relaxation rate of spin *n*; Δ^2 – squared modulation depth parameters; J – spectral power density function; τ_c – correlation time; ω_n – resonant frequency of spin *n*.

Where dipole-dipole contributions are negligible to relaxation, we obtain the following expressions:

$$k_{xdirect} = -\frac{\Delta^2{}_{CSA-x}}{30} J(\tau_c, \omega_x) \quad [12]$$

$$k_{xindirect} = -\frac{\Delta^2{}_{CSA-x}}{60} J(\tau_c, \omega_x) \quad [13]$$

It is clear from equations 12 and 13 that there is a factor of 2 difference between $k_{x\ direct}$ and $k_{x\ indirect}$. More specifically, **$k_{x\ direct} = k_{x\ indirect} \times 2$**. With this knowledge in hand, it was envisaged that if we could obtain indirectly, the longitudinal relaxation rate of the X-spin from the EXSY spectrum of the high γ nucleus by measuring the volume integrals of the peaks corresponding to spin-state satellite exchange as a function of mixing time and subsequently determine the initial rate of longitudinal relaxation, then it would be mathematically trivial to calculate the T_1 of the direct low γ X-spin.

[xi] **Formulation reported (equations 10-13) was derived by Ilya Kuprov, professor of chemical physics, university of Southampton.**

5.4.2 *Cis*-dichlorobis(triphenylphosphine) platinum(II)

Before testing this method on the silver complexes reported in Chapter 3, a model system was chosen whereby the T_1 of the X-nucleus could be measured directly using inversion recovery, to determine whether there was a correspondence between experimentally determined values from spin-state satellite exchange and directly determined values from inversion recovery. *Cis*-dichlorobis(triphenylphosphine) platinum(II) **249** (Figure 30) was chosen as an appropriate model, due to the relatively high sensitivity of ^{195}Pt compared to $^{107/109}$Ag for example.

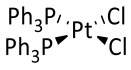

249

Figure 30: *Cis*-dichlorobis(triphenylphosphine) platinum(II).

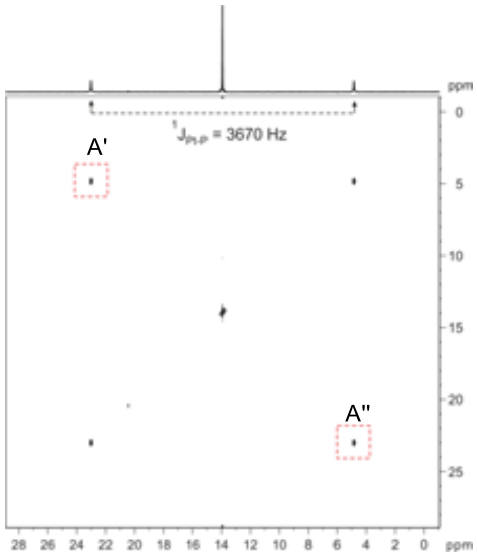

Figure 31: 202 MHz 2-D ^{31}P-^{31}P-{^{1}H}-EXSY NMR spectrum of *cis*-dichlorobis(triphenylphosphine) platinum(II) 0.05 M (t_{mix} = 800msec) in CD_2Cl_2 at 298K showing the ^{195}Pt satellite cross-peaks for spin-state satellite exchange (boxed in red).

In the proton decoupled ^{31}P-^{31}P-EXSY spectrum of **249**, the off-diagonal cross peaks arising from spin-state satellite exchange were clearly visible (Figure 31). Although these have been previously observed (for example see the EXSY spectra of platinum aminophosphine complexes reported by Sadler[120] and co-workers), their significance was not realized.

The net relaxation rate of the ^{195}Pt satellite nucleus was measured by plotting the normalised volume integrals; the ratio of the volume integrals of the satellite cross peaks to the volume integral of the diagonal peak ($I_{cross\text{-}peak}/I_{diagonal}$) against mixing time, t_{mix} (Figure 32). Interestingly, the build-up profile

of **249** from spin-state satellite exchange had an initial linear part in accordance with first-order kinetics and then plateaued. This was particularly indicative of a relaxation effect and suggested we could obtain the net relaxation rate of the Pt nucleus from the gradient of the linear part of the curve.

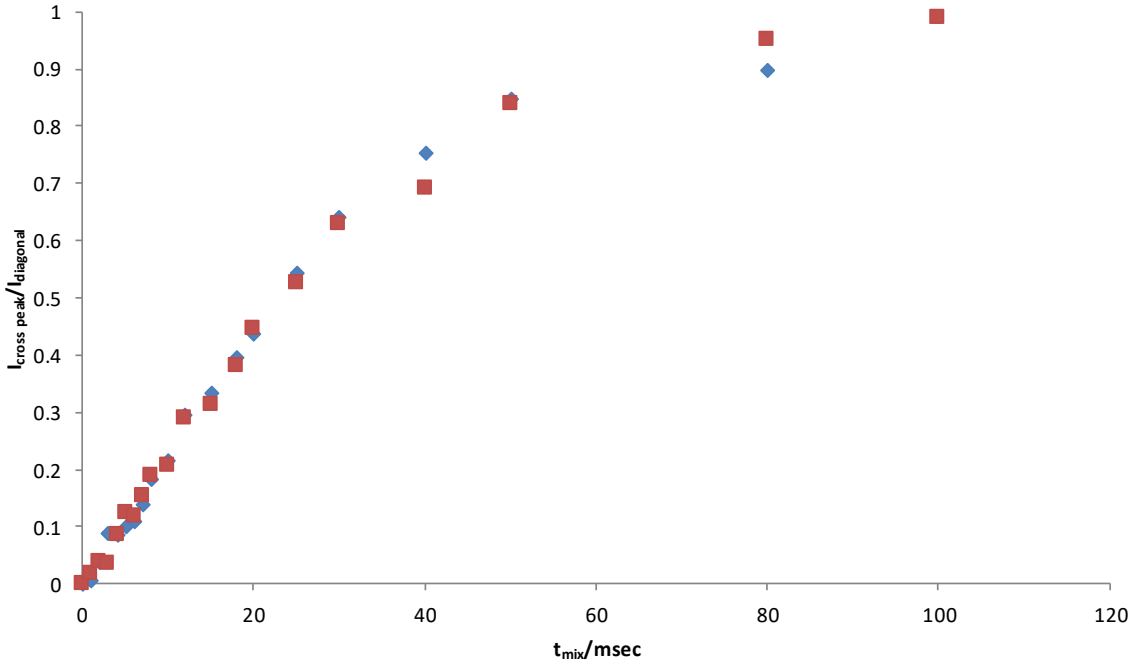

Figure 32: Build-up profile t_{mix}= 0 - 180 msec of of ^{195}Pt-satellites in complex 249; volume integral of A' satellite cross-peak (blue); volume integral of A'' satellite cross-peak (red); 298K in CD_2Cl_2, using ^{31}P-^{31}P-{^{1}H}-EXSY spectra of 249 on a Bruker Avance III HD 500 Mhz.

To test the prediction from the mathematical model, the build-up profiles were elucidated in the manner discussed above at fields of 400 and 600 MHz and the initial rates were measured by measuring the gradient of the slopes produced from the points corresponding to t_{mix} = 0 - 15 msec (Figure 33).

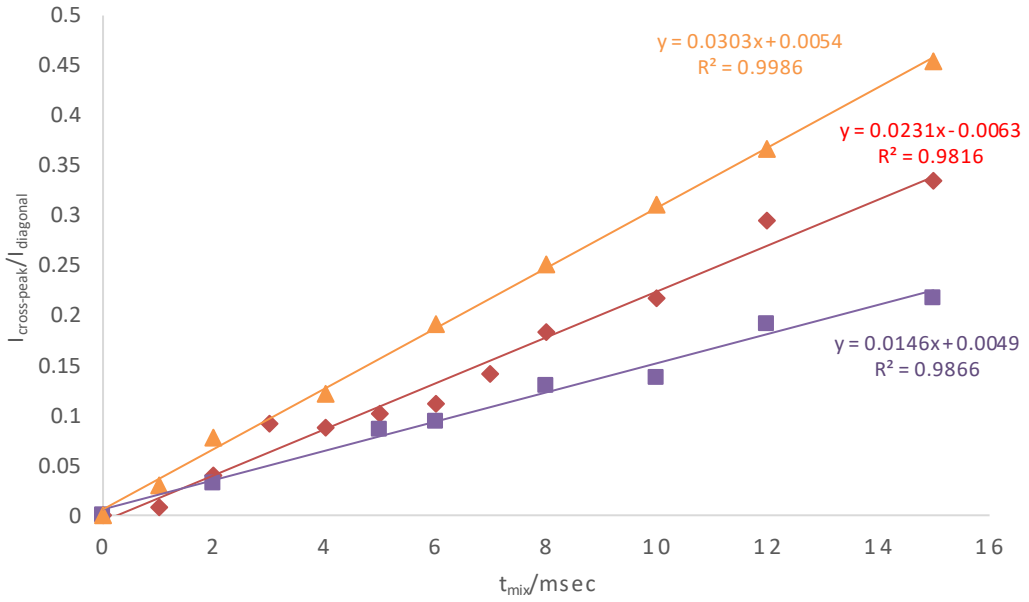

Figure 33: Cross relaxation rate of ^{195}Pt-satellites (A') in complex 249 at 600 MHz (yellow), 500 MHz (red) and 400 MHz (purple). ^{195}Pt-satellite peaks were measured as volume integral ratio of satellite cross peaks: diagonal peak $I_{cross\text{-}peak}$ / $I_{diagonal}$ from ^{31}P-^{31}P EXSY over a range of mixing times (t_{mix}= 0 - 15 msec); 298K in CD_2Cl_2.

The application of our method in determining the T_1(^{195}Pt) of **249** proceeded as follows: the initial relaxation rate at 500 MHz (red line) was determined to be 0.0231 msec^{-1} from the slope of the graph, which is indirectly the longitudinal relaxation rate of the X spin ($k_{xindirect}$). From equations 11 and 12, this gives a longitudinal relaxation rate of the X spin, ^{195}Pt ($k_{Xdirect}$) of 0.0462 msec^{-1} (0.0231×2). Thus, the longitudinal relaxation time for ^{195}Pt would be 21.6 msec (1/0.0462) at 500 MHz. The T_1s of ^{195}Pt in complex **249** were determined in the same manner by spin-state satellite exchange at different field strengths. Due to the relatively high sensitivity of ^{195}Pt, it was possible to directly measure the T_1 of this nuclide in complex **249** at 400, 500 and 600 MHz using inversion recovery and these directly measured T_1s were compared with the indirectly determined T_1s obtained using the method outlined above from spin-state satellite exchange (Table 7).

B_0/T (^{1}H MHz)	**T_1(^{195}Pt)/msec (from spin-state satellite exchange method)**	**T_1(^{195}Pt)/msec (measured directly using inversion recovery)**
9.40 (400MHz)	34.2	34.4
11.77 (500MHz)	21.6	20.7
14.09 (600 MHz)	16.5	15.3

Table 7: ^{195}Pt Longitudinal relaxation times as a function of B_0 measured indirectly by ^{31}P-^{31}P-{^{1}H}-EXSY from build-up curve of satellite exchange cross peaks compared with direct measurement of T_1 using inverse recovery.

Gratifyingly, our model favourably predicted the T_1s for complex **249** over different field strengths (within experimental error). As was aforementioned, the distinguishing feature of CSA relaxation is its square dependence on the magnetic field (B_0).

It was shown that the cross-relaxation of ^{195}Pt satellites in complex **249** were linearly dependent on B_0^2 at 400, 500 and 600 MHz[xii] (Figure 34) with the concomitant line broadening of ^{195}Pt satellite peaks in the 1-D ^{31}P spectra[xiii] and thus it could be concluded that platinum relaxation in complex **249** was primarily dominated by CSA.

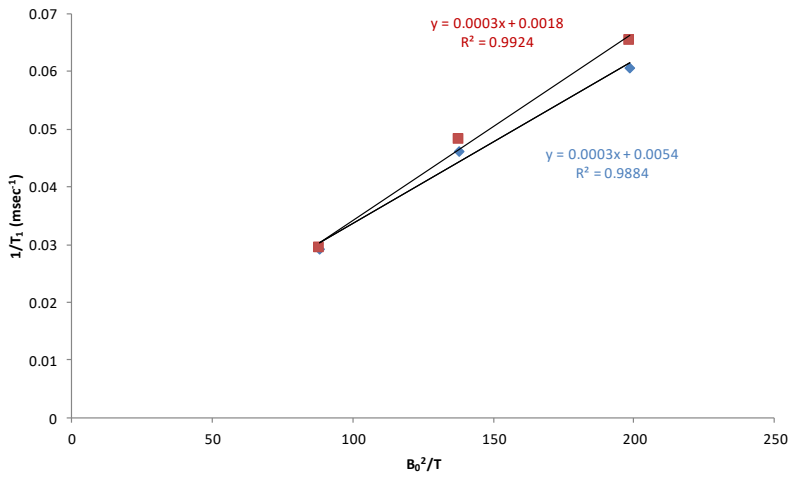

Figure 34: T_1 values as measured indirectly from the spin-state satellite exchange cross peaks (blue) compared with directly measured values (red) against square of field strength (B_0^2).

5.4.3 Silver Complexes from Chapter 3

With our method for measuring the T_1 relaxation rate for indirect X-nuclei established, complexes **225** and **226** from Chapter 3 were thus tested using this method.

[xii] **The measured T_1(^{31}P) in complex 249 using inverse recovery also showed a linear dependence with respect to B_0^2, indicating that the relaxation of both ^{195}Pt and ^{31}P nuclei are governed by CSA exclusively as was expected (See Supporting Information).**

[xiii] **See supporting information for spectra.**

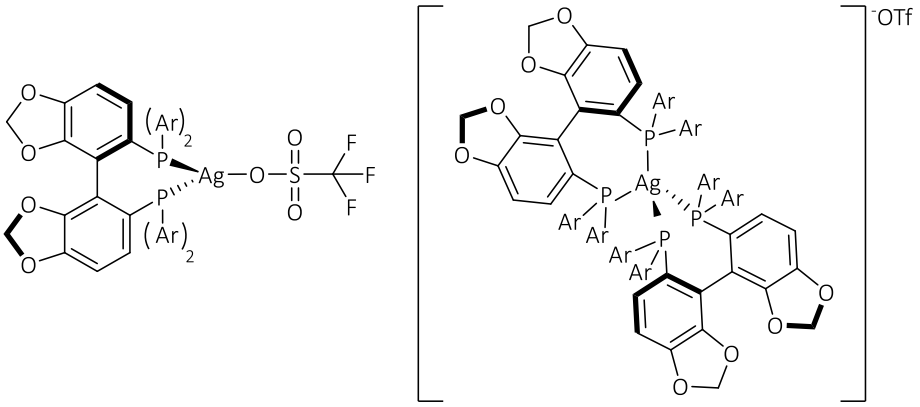

225 226

Figure 35: Trigonal-planar silver(I) complex 225 and tetrahedral silver(I) complex 226 from chapter 3, Ar = 3,5-dimethylphenyl.

The T_1s of $^{109/107}$Ag could not be measured directly on our instruments due to the insensitivity of silver and inefficient relaxation mechanisms for $^{107/109}$Ag nuclei.[121] Thus, indirectly determined values from spin-state satellite exchange are only presented here. Complexes **225** and **226** have sufficiently different geometrical properties that they will be expected to exhibit different magnetic properties with respect to chemical shift anisotropy (CSA). Complex **226**, exhibiting a distorted tetrahedral geometry is more symmetrical than complex **225**, displaying a trigonal-planar geometry. Therefore, we speculated that the Ag-P bonds in complex **226** are likely to be less anisotropic and CSA will contribute less to the relaxation of the silver nuclei and was expected to result in a longer T_1($^{109/107}$Ag) in contrast to the trigonal planar complex **225**. As was discussed in section 3.7.2, on performing the ^{31}P-^{31}P-EXSY experiment at 233K in $CDCl_3$, chemical exchange was inferred in the labile trigonal planar complex as characterised by quadrant cross peaks for the trigonal species. Cross peaks A-B, B-A, A*-B*, B*-A*, B-A* and A-B* suggested exchange of ^{31}P with both ^{107}Ag and ^{109}Ag isotopes at 233K (Figure 20).

Such a feature was not observed in the more stable tetrahedral complex **226**. It was suspected that the chemical exchange mechanism could affect the relaxation of Ag in trigonal planar complex **225** and thus a means was sought to stop, or at least slow down the chemical exchange observed in this species to such an extent that it would not be observed on an NMR timescale. Indeed, it was possible to 'freeze' the chemical exchange exhibited by the trigonal-planar complex **225** by cooling the sample to 203K (Figure 36). Significantly, for both **225** and **226** the cross-peaks corresponding to spin-state satellite exchange (A-A* and B-B* in **225**) remained under these conditions. This suggested that the rate of the chemical exchange process is slower than the rate of spin-state satellite exchange. In principle, these cross-peaks could be generated by ligand dissociation; providing the ligand dissociates from a silver isotope of a given spin-state and then associates with the same silver isotope of the

opposite spin-state. This process, however, does not apply for the non-labile complex **226** or for complex **225**; where at 203K, all peaks corresponding to other ligand exchange processes are not visible.

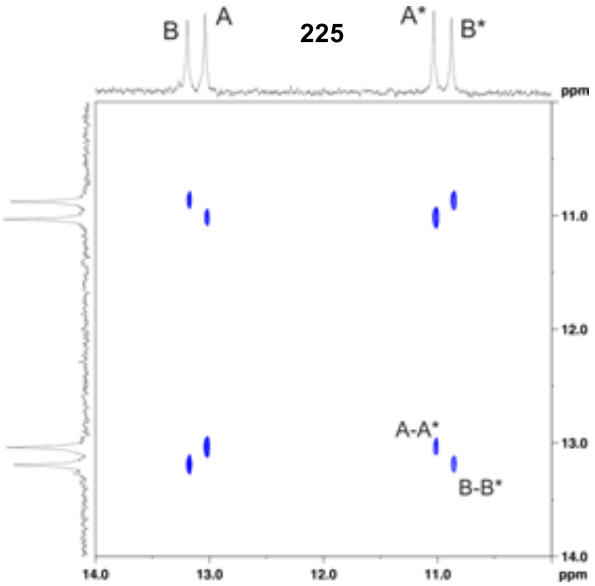

Figure 36: ^{31}P-^{31}P-{^{1}H}- EXSY of 225 without chemical exchange, cross-peaks A-A* and B-B* arise from spin-state satellite exchange (t_{mix} = 800 msec, 203K, CD_2Cl_2).

In the same manner as before, from the ^{31}P-^{31}P-EXSY at 203K, volume integral ratios $I_{cross\text{-}peak}/I_{diagonal}$ for ^{109}Ag (use of the ^{107}Ag cross peak gave similar results) in complexes **225** and **226** were plotted against t_{mix} (Figure 37).

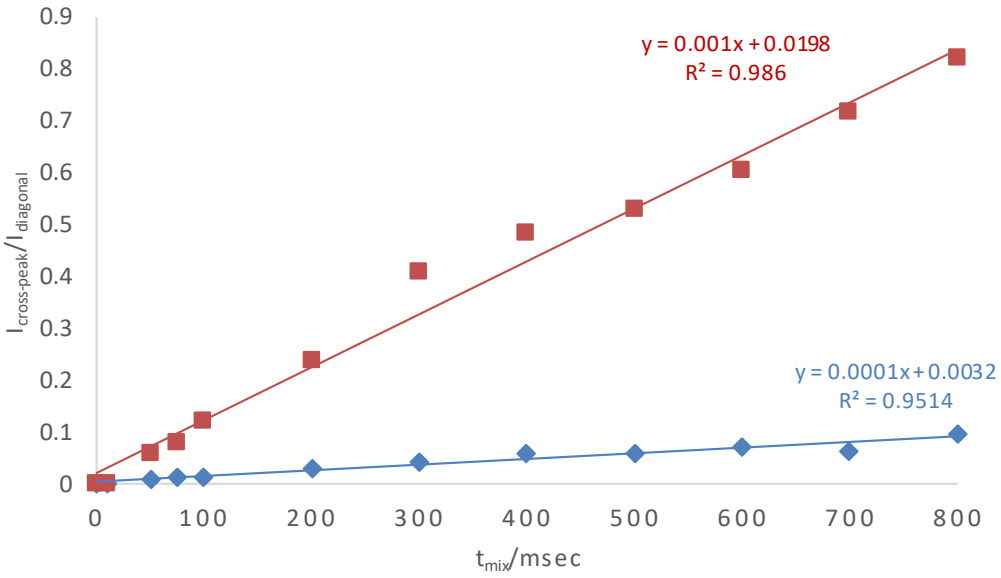

Figure 37: Plots of $I_{cross\text{-}peak}$ / $I_{diagonal}$ from ^{31}P-^{31}P-{^{1}H}-EXSY experiments at 203K in CD_2Cl_2; satellite exchange rate of ^{109}Ag satellite in complex 226 (blue); satellite exchange rate of ^{109}Ag satellite in complex 225 (red) (tmix = 0-800 msec).

For complex **226** the initial relaxation rate was determined to be 0.0001 $msec^{-1}$ ($k_{xindirect}$) from the slope of the graph. This gives a direct longitudinal relaxation rate of the Ag spin of 0.0002 $msec^{-1}$($k_{xdirect}$), which translates to a $T_1(^{109}Ag)$ of 5 sec for the tetrahedral Ag complex **226**. Likewise, for complex **225**, the initial relaxation rate was determined to be 0.001 $msec^{-1}$ ($k_{xindirect}$) from the slope of the graph. This gives a direct longitudinal relaxation rate of the Ag spin ($k_{xdirect}$) of 0.002 $msec^{-1}$and thus a $T_1(^{109}Ag)$ of 500 msec for the trigonal-planar Ag complex **225**, assuming CSA dominates relaxation. The large difference between T_1 s of **226** 5sec and **225** 500msec reflects significant differences in the CSA is between the two complexes due to their inherent geometrical differences. The greater symmetry in complex **226** correlates with a larger T_1-relaxation time constant due to the inefficiency of CSA as a relaxation mechanism at silver in a tetrahedral environment, contrasted with the lower symmetry and greater anisotropy in the trigonal-planar environment of complex **225**, which leads to a much smaller T_1-relaxation time constant.

5.5 Conclusions and Future Work

In conclusion, a method for determining the longitudinal relaxation time constants for indirect X nuclei with low γ has been documented. The X nucleus of interest comprises one component of a scalar coupled AX system, where A is the observable high γ gamma nucleus and both nuclei are of spin -1/2. The method makes use of the EXSY spectrum of A, where cross-peaks are observed which arise from spin-state satellite exchange of the X nucleus. The intensities of these cross peaks are a function of mixing time (t_{mix}) and the initial build-up rates of these cross-peaks are primarily dependent on the T_1 of the X nucleus. The mathematical description details a practical means of how $T_1(X)$ can be extracted from these initial build-up rates. We have demonstrated that the method is applicable to *cis*-dichlorobis(triphenylphosphine) platinum(II) **249**, where close correspondence was found between directly measured values for the $T_1(^{195}Pt)$ by inversion recovery compared with indirectly determined values generated from our spin-state satellite exchange method. We have also applied our method to two Ag(I)-bisphosphine metal complexes reported in chapter 3, where we have obtained values for the longitudinal relaxation times of silver in both cases and found how these values can be used to correlate to the geometrical properties of these complexes; with symmetrical tetrahedral complex **226** giving rise to a larger T_1-relaxation time constant contrasted with less symmetrical trigonal-planar complex **225**. It is generally assumed that the T_1 of silver is typically of the order of thousands of seconds, largely because in the literature, T_1s of Ag have been measured for simple, isolated salts and not for complexes of silver. It is demonstrated in this work that this assumption is not always true and that the geometrical properties of the ligand affect the T_1 of the metal significantly. We envisage broad applications of this method for determining the T_1 of other insensitive transition-metal nuclei.

6. Experimental

6.1 General Experimental

6.1.1 Solvents and Reagents

Bulk solutions were evaporated under reduced pressure using a Büchi rotary evaporator. All solvents were commercially supplied or dried by filtration through activated alumina (powder ~150 mesh, pore size 58 Å, basic, Sigma-Aldrich) columns. Petroleum ether refers to the fraction collected between 30-40 °C. Ethyl diazoacetate **171** was obtained as a 15% wt solution in toluene from Sigma Aldrich. Chloroform was obtained from Sigma Aldrich as a 2.5 L winchester containing 0.5-1.0% ethanol as a stabiliser. It was extracted using water, basified over K_2CO_3, distilled and stored over 4 Å molecular sieves. (*R*)-DM-SEGPHOS **196** was obtained from STREM chemicals.

6.1.2 Chromatography

Reactions were monitored by thin layer chromatography (TLC) using Merck silica gel 60 F254 plates and visualised by fluorescence quenching under UV light. In addition, TLC plates were stained with aq. basic potassium permanganate solution or vanillin solution as appropriate. Flash column chromatography was carried out on VWR 60 silica gel (40 - 63 µm) using technical grade solvents that were used as supplied. **Enantiomeric excesses** were determined using high performance liquid chromatography (HPLC) performed on an Agilent Technologies 1260 Infinity series -168- machine (column and solvent conditions are reported with the appropriate compound).

6.1.3 Spectroscopy

^{1}H, ^{13}C, ^{19}F and ^{31}P NMR spectra were recorded using Bruker DPX-200, Bruker DPX-400, Bruker DQX-400, Bruker AVIII400, Bruker AVC-500 and Bruker DRX-500 spectrometers. Chemical shifts (δ) are given in parts per million (ppm), and coupling constants (*J*) are given in Hertz (Hz). The ^{1}H NMR spectra are reported as follows: ppm, (multiplicity, coupling constants, number of protons). Low resolution mass spectra were recorded on a Waters LCT premier XE Micromass spectrometer (ESI) operating in positive and negative ionisation mode. **High resolution mass spectra** (HRMS, accurate mass) 190 were recorded on a Bruker daltonios MicroTOF mass spectrometer. **IR spectra** (IR) were recorded on a Bruker Tensor 27 FT-IR spectrometer as a thin film on a diamond ATR module. Only selected absorption maxima (vmax) are reported in wavenumbers (cm^{-1}). Optical rotations were recorded using a Perkin Elmer 341 polarimeter; $[\alpha]_D^T$ values are reported in 10-1 deg cm^2 g1; concentrations (c) are quoted in g/100 mL; D refers to the D-line of sodium (589 nm); Temperatures (T) are given in degrees Celsius (°C). (+) and (–) compound number prefixes indicate the sign of the optical rotation. Enantiomeric excesses were determined by HPLC analysis on an Agilent 1200 Series instrument using

a chiral stationary phase column specified in the individual experiment or by GC analysis on an Agilent 7820A instrument employing a chiral stationary phase column specified in the individual experiment and by comparing the samples with the appropriate racemic mixtures.

6.1.4 Naming of Compounds

All compound names were generated using ACD Labs 12.0 following IUPAC nomenclature.

6.1.5 X-Ray Crystallographic Data

Single crystal X-ray diffraction data were collected at 150 °K using an Enraf-Nonius KCCD diffractometer or an Oxford Diffraction SuperNova diffractometer. The crystal structures of complex **226** was solved with SIR92 and refined with CRYSTALS including the Flack x parameter (where appropriate) under the guidance of Dr. A. L. Thompson of the University of Oxford Chemical Crystallography department. Crystallographic data is provided in the appendices.

6.1.6 Melting Points

Melting points (MP) were recorded in degrees Celsius (°C), using a Leica Galen III hot-stage microscope apparatus and are reported uncorrected.

6.2 Experimental for Chapter 2

6.2.1 Synthesis and Characterization of Catalysts and Precursors

General Procedure A for Reduction of Amino Acids

According to a literature procedure[56], to a solution of sodium borohydride (2.4 equiv) in THF was added the amino acid (1.0 equiv). The reaction mixture was cooled to 0 °C and a solution of iodine (1.0 equiv) in THF was added dropwise over 30 minutes after which the reaction was warmed to room temperature and then refluxed for 18 h. After refluxing, the reaction mixture was allowed to cool to room temperature. MeOH was then added in a dropwise manner until a clear solution was formed and stirring was maintained for 30 min before the volatiles were removed *in vacuo* to reveal a white paste. The white paste was dissolved in a 20% KOH solution (50 mL) and the resulting solution was stirred for 3 hours. The organic phase was extracted (3 × 100 mL) with CH_2Cl_2, the collected organics were washed with brine and then dried over $MgSO_4$ and volatiles removed *in vacuo*. The resulting crude material was dissolved in CH_2Cl_2 and triethylamine (1.18 equiv) was added before the reaction was cooled to 0 °Cafter which Boc_2O (1.18 equiv) was added and stirring was maintained for 1 hour at 0 °C and an additional 8 hours at room temperature. The reaction mixture was washed with water (50 mL), brine and then dried over $MgSO_4$ and the volatiles removed *in vacuo*. The crude residue was purified by FCC using 40% EtOAc/petroleum ether.

tert-Butyl N-[(2S)-1-hydroxy-3,3-dimethylbutan-2-yl]carbamate **123**

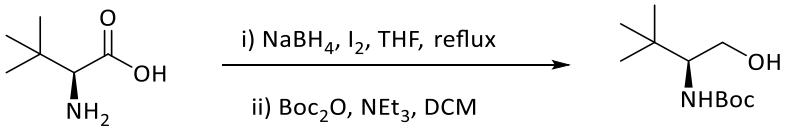

Prepared according to General Procedure A on a 38.1 mmol scale to afford the title compound as a colourless solid in 60% yield (4.81 g).

$[\alpha]_D^{25}$ -3.2 (c=1.0, $CHCl_3$) (lit **$[\alpha]_D^{25}$** - 5.5 (c = 1.0, $CHCl_3$)[122];

MP 105 – 107 °C (lit. 105 °C)[122];

^{1}H NMR (400 MHz, $CDCl_3$) δ 4.71 (br.s, 1H, CHNHC=O), 3.70-3.94 (m, 1H, $CHCH_AH_BOH$), 3.40-3.62 (m, 2H, $CHCH_AH_BOH$), 2.50 (br.,s, 1H, CH_2OH), 1.47 (s, 9H, $OC(CH_3)_3$), 0.96 (s, 9H, $CHC(CH_3)_3$);

^{13}C NMR (100 MHz, $CDCl_3$) δ 157.2 (C=O), 79.5 ($OC(CH_3)_3$), 63.1 ($CHCH_2OH$), 61.0 (CHNHC=O), 33.6 ($CHC(CH_3)_3$), 28.3 ($OC(CH_3)_3$), 26.8 ($CHC(CH_3)_3$).

All data reported is in agreement with those published in literature.[123]

tert-Butyl N-[(2S)-1-(1,3-dioxo-2,3-dihydro-1H-isoindol-2-yl)-3,3-dimethylbutan-2-yl]carbamate **124**

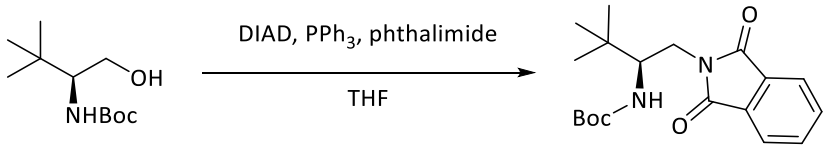

According to a literature procedure[124], to a solution of alcohol **123** (6.08g, 28 mmol, 1.0 equiv), phthalimide (4.12 g, 28 mmol, 1.0 equiv) and triphenylphosphine (7.34 g, 28 mmol, 1.0 equiv) in THF (174 mL) was added DIAD (6.0 mL, 30.8 mmol, 1.1 equiv) at 0 °C. The reaction mixture was allowed to warm to room temperature where stirring was maintained for 72 hours. The volatiles were removed *in vacuo*. Purification by FCC using 20% EtOAc/petroleum ether afforded the title compound in 80% yield (7.76 g).

$[\alpha]_D^{25}$ +37.4 (c=0.95, $CHCl_3$), lit **$[\alpha]_D$** +48.7 (c = 0.46, $CHCl_3$)[122];

MP 148 – 150 °C (lit. 146 – 147 °C)[122];

^{1}H NMR (400 MHz, $CDCl_3$) δ 7.78 (dd, *J* = 5.3, 2.9 Hz, 2H, ArH), 7.65 (dd, *J* = 5.0, 2.9 Hz, 2H, ArH), 4.47 (d, *J* = 10.6 Hz, 1H, CHNHC=O), 3.78-3.86 (m, 2H, CHNHC=O and $CHCH_AH_BN$),), 3.57 – 3.68 (m, 1H, $CHCH_AH_BN$), 1.09 (s, 9H, $OC(CH_3)_3$), 1.02 (s, 9H, $CHC(CH_3)_3$);

^{13}C NMR (100 MHz, $CDCl_3$) δ 168.4 (NC(=O)C), 156.0 (NC(=O)O), 133.7 (ArCH), 132.1 (ArC), 123.1 (ArCH), 78.9 ($OC(CH_3)_3$), 57.4 (CHNHC=O), 38.6 ($CHCH_2N$), 33.6 ($CHC(CH_3)_3$), 27.9 ($OC(CH_3)_3$), 26.4 ($CHC(CH_3)_3$). All data reported is in agreement with those published in literature.[122]

tert-Butyl N-[(2S)-1-amino-3,3-dimethylbutan-2-yl]carbamate **125**

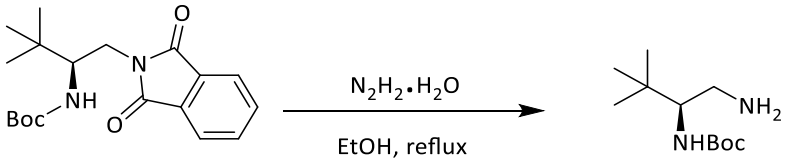

According to a literature procedure[124] to a solution of **124** (8.71 g, 25 mmol, 1.0 equiv) in EtOH (130 mL) under a N_2 atmosphere at room temperature was added hydrazine monohydrate (8.24 mL, 170

mmol, 6.8 equiv). The reaction mixture was heated to reflux and stirred for 5 h. The reaction was then cooled to room temperature and filtered. The precipitate was washed with CH_2Cl_2 (3 × 100 mL), and the filtrate was concentrated *in vacuo*. The crude product was purified by FCC (CH_2Cl_2/MeOH = 9/1) to afford the title compound as a colourless solid in 90% yield (4.86 g).

$[\alpha]_D^{23}$ +7.88 (c = 0.99, $CHCl_3$), lit. **$[\alpha]_D$** + 9.80 (c = 0.48, $CHCl_3$)[122];

MP 82 – 84 °C (lit. 84 °C)[122];

^{1}H NMR (400 MHz, $CDCl_3$) δ 4.42 (d, *J* = 10.4 Hz, 1H, CHNHC=O), 3.34 (td, *J* = 10.4, 3.1 Hz, 1H, CHNHC=O), 2.97 (dd, *J* = 13.5, 3.0 Hz, 1H, $CHCH_AH_BNH_2$), 2.48 – 2.35 (m, 1H, $CHCH_AH_BNH_2$), 1.58 (br. s, 2H, $CHCH_2NH_2$), 1.45 (s, 9H, $OC(CH_3)_3$), 0.90 (s, 9H, $CHC(CH_3)_3$);

^{13}C NMR (100 MHz, $CDCl_3$) δ 156.9 (C=O), 79.2 ($OC(CH_3)_3$). 62.2 (CHNHC=O), 42.2 ($CHCH_2NH_2$), 34.2 ($CHC(CH_3)_3$), 28.4 ($OC(CH_3)_3$), 26.5 ($CHC(CH_3)_3$). All data reported is in agreement with those published in literature.[122]

1-(1H-Imidazole-1-sulfonyl)-1H-imidazole **127**

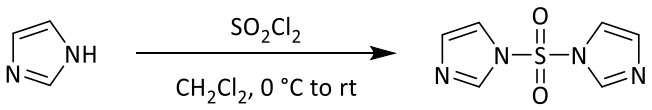

According to a literature procedure[125] to a solution of imidazole **126** (11.2g, 164.5 mmol, 4.7 equiv) in CH_2Cl_2 (80 mL) under an N_2 atmosphere at 0 °C was added sulfuryl chloride (2.84 mL, 35 mmol, 1.0 equiv) dropwise. The reaction mixture was then allowed to warm to room temperature and was stirred overnight. The inorganics were removed by filtration and the resulting filtrate was concentrated *in vacuo*. The crude product was recrystallized from refluxing isopropanol to afford the title compound as a colourless solid in 80% yield (5.60 g).

MP 143 – 145 °C (lit. 143 – 144 °C)[120];

^{1}H NMR (DMSO-d_6, 400 MHz) δ 8.50 (s, 2 H, ArH), 7.92 (s, 2 H, ArH), 7.24 (s, 2 H, ArH);

^{13}C NMR (400 MHz, $CDCl_3$) δ 136.5 (ArCH), 132.5 (ArCH), 117.4 (ArCH). All data reported is in agreement with those published in literature.[125]

1-(1H-Imidazole-1-sulfonyl)-3-methyl-1H-imidazol-3-ium **128**

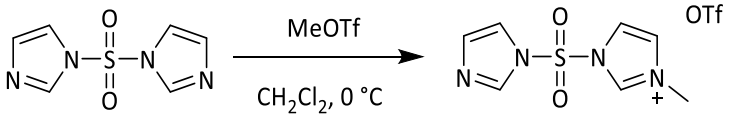

According to a literature procedure[125] to a solution of **127** (13.40 g, 67.6 mmol, 1.11 equiv) in CH_2Cl_2 (134 mL) under an N_2 atmosphere at 0°C was added methyl triflate (7.0 mL, 60.9mmol, 1.0 equiv) dropwise. The reaction mixture was stirred at 0 °C for 2.5 hours after which the reaction mixture was filtered and dried under high vacuum to afford the title compound in 97% yield (20.23 g).

^{1}H NMR (D_2O, 400 MHz) δ 9.87 (s, 1H, ArH), 8.44 (s, 1H, ArH), 8.10 (s, 1H, ArH), 7.72 (s, 1H, ArH), 7.65 (s, 1H, ArH), 7.20 (s, 1H, ArH), 3.94 (s, 3H, NCH_3);

^{13}C NMR (D_2O, 100 MHz) δ 138.9 (ArCH), 131.8 (ArCH), 126.0 (ArCH), 120.6 (ArCH), 118.8 (ArCH), 37.1 (NCH_3). All data reported is in agreement with those published in literature.[125]

1H-Imidazole-1-sulfonyl azide **129**

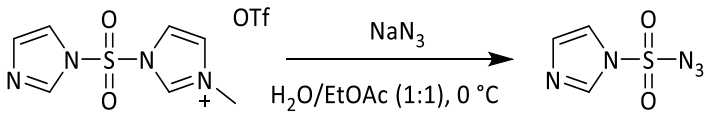

According to a literature procedure[125], a solution of **128** (13.6 g, 37.5 mmol, 1.0 equiv) was made in H_2O/EtOAc (1 : 1 v/v) (24 mL). Under an N_2 atmosphere at 0 °C was added sodium azide (2.93 g, 45 mmol, 1.2 equiv) and the mixture was allowed to stir for 2 hours at 0 °C. The mixture was then diluted with H_2O (59 mL) and EtOAc (59 mL). The organic phase was extracted and the aqueous phase was back extracted with EtOAc (2 × 30 mL). The combined organics were dried with $MgSO_4$, filtered and due to its likely instability was used immediately, without any further purification in the next step.

tert-Butyl N-[(2S)-1-azido-3,3-dimethylbutan-2-yl]carbamate **82**

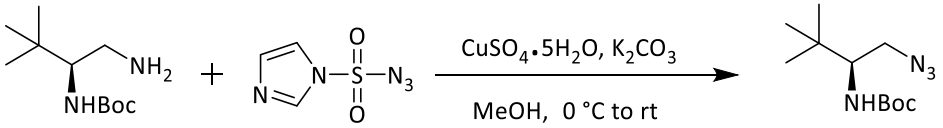

To amine **125** (6.48 g, 30 mmol, 1.2 equiv) under an N_2 atmosphere at 0 °C was added a pre-dissolved solution of **129** (5.40 g, 25 mmol, 1.0 equiv) in MeOH (118 mL). Potassium carbonate (5.87 g, 42.5 mmol, 1.7 equiv) and coppersulfate pentahydrate (124.1 mg, 2 mol%) was added and the reaction mixture was stirred at 0 °C for 30 minutes before warming to room temperature where the mixture was allowed to stir overnight. The volatiles were removed under a stream of N_2 and the crude mixture was dissolved in H_2O/Et_2O (1 : 1 v/v, 400 mL). The organic phase was extracted followed by a brine wash and dried over $MgSO_4$ and concentrated *in vacuo*. Purification by FCC using 10% Et_2O/petroleum ether afforded the title compound as a white solid in 62% yield (3.76 g).

MP 62 – 64 °C;

^{1}H NMR (400 MHz, $CDCl_3$) δ 4.53 (d, *J* = 10.0 Hz, 1H, CHN<u>H</u>C=O), 3.69 – 3.55 (m, 1H, C<u>H</u>NHC=O), 3.47 (dd, *J* = 12.6, 4.0 Hz, 1H, CHC<u>H</u>$_A$CH$_B$N$_3$), 3.22 (dd, *J* = 12.6, 4.5 Hz, 1H, CHCH$_A$C<u>H</u>$_B$N$_3$), 1.46 (s, 9H, OC(C<u>H</u>$_3$)$_3$), 0.93 (s, 9H, CHC(C<u>H</u>$_3$)$_3$);

^{13}C NMR (400 MHz, $CDCl_3$) δ 155.8 (C=O), 79.5 (OC(C<u>H</u>$_3$)$_3$), 58.2 (<u>C</u>HNHC=O), 52.0 (CH<u>C</u>H$_2$N$_3$), 34.2 (CH<u>C</u>(CH$_3$)$_3$), 28.4 (OC(<u>C</u>H$_3$)$_3$), 26.6 (CHC(<u>C</u>H$_3$)$_3$). All data reported is in agreement with those published in literature.[42]

General Procedure B (coupling of Boc-azide to isothiocyanate)

To the *N*-Boc protected azide (1.0 equiv) was added TFA (12.6 equiv) dropwise at 0 °C under an N_2 atmosphere. The mixture was stirred for 2 h at room temperature and deprotection was confirmed by TLC against the starting material. The mixture was then concentrated under a N_2 stream. The mixture was then diluted with an Et_2O/H_2O (1 : 1, v/v) solution and the pH was adjusted to 14 by adding solid NaOH at 0 °C. The organic phase was extracted with Et_2O twice and the combined organics were washed with brine and dried over $MgSO_4$, filtered and concentrated *in vacuo*. The crude mixture was diluted with 14 mL of THF and 3,5-bis(trifluoromethylphenyl)isothiocyanate (1.10 equiv) was added and stirring was maintained for 12 hours before the mixture was concentrated *in* vacuo. Purification was performed by FCC using 20% EtOAc/petroleum ether.

3-[(2S)-1-Azido-3,3-dimethylbutan-2-yl]-1-[3,5-bis(trifluoromethyl)phenyl]thiourea **83**

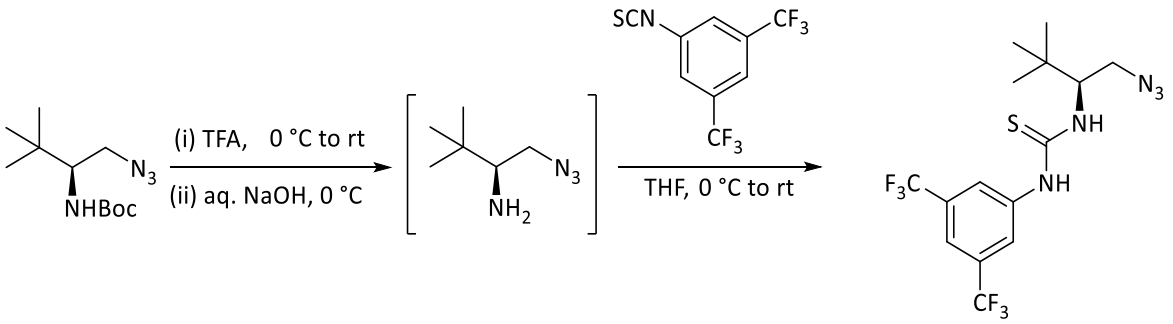

Prepared according to General Procedure B on a 4.13 mmol scale to afford the title compound as a white solid in 51% yield (870 mg).

$[\alpha]_D^{23}$ -14.6 (c=1.4, $CHCl_3$);

MP 163 – 165 °C (lit. 164 – 166 °C);

^{1}H NMR (400 MHz, CD_3OD) δ 8.25 (s, 2H, ArH), 7.63 (s, 1H, ArH), 4.74 (br.s, 1H, CHNHC=S), 3.63 (dd, *J* = 12.9, 3.9 Hz, 1H, $CHCH_ACH_BN_3$), 3.43 (dd, *J*=12.9, 3.9 Hz, $CHCH_ACH_BN_3$), 1.04 (s, 9H, $CHC(CH_3)_3$);

^{13}C NMR ($CDCl_3$, 100 MHz) δ 184.1 (C=S), 143.4 (ArCNH), 133.0 (q, J_{CF} = 33.5 Hz, $ArCCF_3$), 124.9 (q, J_{CF} = 272.0 Hz, $ArCF_3$) 123.8 (ArCH), 118.0 (ArCH), 62.8 (CHNHC=S), 52.7 ($CHCH_2N_3$), 35.8 ($CHC(CH_3)_3$), 27.3 ($CHC(CH_3)_3$). All data reported is in agreement with literature values.[42]

tert-butyl N-[(2S)1-hydroxy-3-phenylpropan-2-yl]carbamate **119**

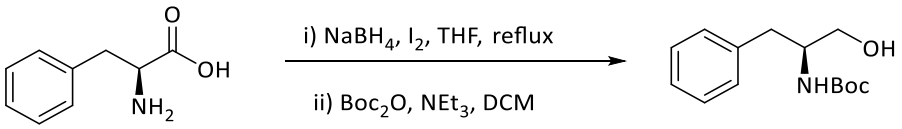

Prepared according to General Procedure A on a 60.5 mmol scale. The crude mixture was used without further purification, quantitative mass return.

^{1}H NMR (400 MHz, $CDCl_3$) δ 7.36 – 7.30 (m, 2H, ArH), 7.28 – 7.21 (m, 3H, ArH), 4.89 (d, *J* = 6.1 Hz, 1H, CHNHC=O), 3.86 (br.s, 1H, CHNHC=O), 3.71 – 3.64 (m, 1H, $CHCH_ACH_BOH$), 3.57 (dd, J = 10.9, 5.2 Hz, 1H, $CHCH_ACH_BOH$), 2.87 (d, *J* = 7.1 Hz, 2H, $CHCH_2Ar$), 1.44 (s, 9H, $OC(CH_3)_3$);

^{13}C NMR (100 MHz, CDCl3) δ 156.1 (C=O), 137.8 (ArC), 129.3 (ArCH), 128.5 (ArCH), 126.5 (ArCH), 79.7 ($OC(CH_3)_3$), 64.3 ($CHCH_2OH$), 53.7 ($CHCH_2OH$), 37.4 ($CHCH_2Ar$), 28.3 ($OC(CH_3)_3$). All data reported is in agreement with literature.[126]

tert-butyl N-{1-[(4-methylbenzenesulfonyl)oxy]-3-phenylpropan-2-yl}carbamate **120**

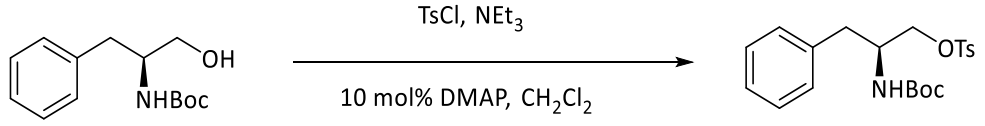

According to a literature procedure[42], a solution of **119** (15.2 g, 60.5 mmol, 1.0 equiv) in 202 mL of CH_2Cl_2 was made. Triethylamine (9.3 mL, 66.6 mmol, 1.1 equiv), DMAP (739 mg, 10 mol%) were then added sequentially.The reaction mixture was cooled to 0 °C and tosyl chloride (12.70g, 66.6 mmol, 1.1 equiv) was added at after which the reaction mixture was allowed to warm to room temperature and allowed to stir at this temperature for 12 hours. Purification by FCC using 20% EtOAc/petroleum ether afforded the title compound in 35% yield (8.49 g).

$[\alpha]_D^{23}$ -8.45 (c=0.93, $CHCl_3$);

MP 69 - 71 °C (lit. 74 °C)[127];

^{1}H NMR (400 MHz, $CDCl_3$) δ 7.84 (d, *J* = 8.3 Hz, 2H, ArH), 7.40 (d, *J* = 8.1 Hz, 2H, ArH), 7.30 – 7.23 (m, 3H, ArH), 7.16 – 7.10 (m, 2H, ArH), 4.81 (d, *J* = 8.5 Hz, 1H, CHNHC=O), 4.14 – 4.01 (m, 2H, CHNHC=O & $CHCH_ACH_BOTs$), 3.94 (dd, *J* = 9.4 Hz, 2.9 Hz, 1H, $CHCH_ACH_BOTs$), 2.92 (dd, *J* = 13.7, 6.2 Hz, 1H, $CHCH_ACH_BAr$), 2.86 – 2.79 (m, 1H, $CHCH_ACH_BAr$), 2.51 (s, 3H, $ArCH_3$), 1.44 (s, 9H, $OC(CH_3)_3$);

^{13}C NMR (100 MHz, $CDCl_3$) δ 155.0 (C=O), 145.0 (ArC), 136.7 (ArC), 132.4 (ArC), 130.0 (ArCH), 129.2 (ArCH), 128.6 (ArCH), 128.0 (ArCH), 126.7 (ArCH), 79.8 ($OC(CH_3)_3$), 70.0 ($CHCH_2OTs$), 50.7 ($CHCH_2Ar$), 37.1 ($CHCH_2Ar$), 28.3 ($OC(CH_3)_3$), 21.7 ($ArCH_3$).

All data is in agreement with those found in literature.[127]

tert-butyl N-[(2S)1-azido-3-phenylpropan-2-yl]carbamate **121**

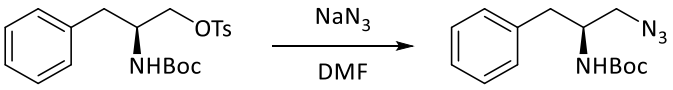

According to a literature procedure[42], under argon DMF (33 mL) was added to **126** (4.00 g, 9.88 mmol, 1.0 equiv). Finally, sodium azide (707 mg, 10.87 mmol, 1.1 equiv) was added to the reaction mixture at 0 °C. The reaction mixture was allowed to warm to rt and stirring was maintained for 12 hours. Purification by FCC using 30% Et_2O/petroleum ether afforded the title compound as a white solid in 63% yield (1.70 g).

$[\alpha]_D^{23}$ -7.36 (c = 1.25, $CHCl_3$);

MP 65 - 67 °C (lit. 60 °C)[42];

^{1}H NMR (400 MHz, $CDCl_3$) δ 7.37 – 7.29 (m, 2H, ArH), 7.28 – 7.15 (m, 3H, ArH), 4.66 (d, J = 8.1 Hz, 1H, CHNHC=O), 3.97 (s, 1H, CHNHC=O), 3.42 (dd, J = 12.4, 4.4 Hz, 1H, $CHCH_ACH_BN_3$), 3.30 (dd, J = 12.3, 4.4 Hz, 1H, $CHCH_ACH_BN_3$), 2.88 (dd, J = 13.2, 7.0 Hz, 1H, $CHCH_ACH_BAr$), 2.78 (dd, J = 13.6, 8.0 Hz, 1H, $CHCH_ACH_BAr$), 1.42 (s, 9H, $OC(CH_3)_3$);

^{13}C NMR (100 MHz, $CDCl_3$) δ 155.3 (C=O), 137.1 (ArC), 129.3 (ArCH), 128.7 (ArCH), 126.7 (ArCH), 80.0 ($OC(CH_3)_3$), 53.1 ($CHCH_2N_3$), 51.3 ($CHCH_2N_3$), 38.1 ($CHCH_2Ar$), 28.3 ($OC(CH_3)_3$).

All data reported is in agreement with those reported in literature.[42]

3-[(2S)1-azido-3-phenylpropan-2-yl]-1-[3,5-bis(trifluoromethyl)phenyl]thiourea **122**

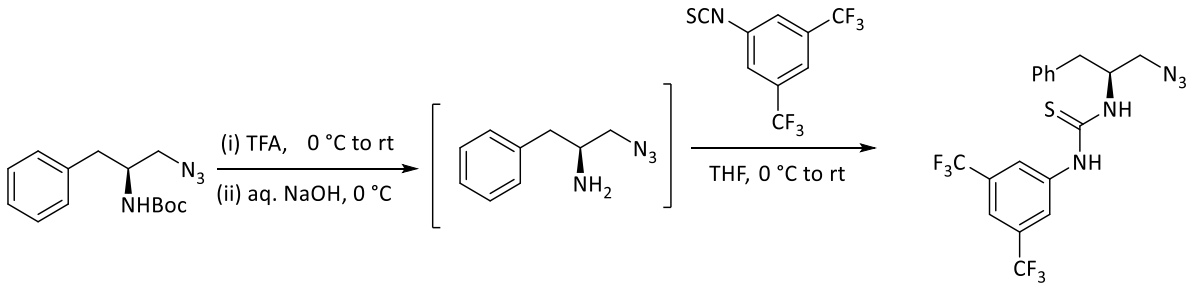

Prepared according to General Procedure B on a 4.13 mmol scale to afford the title compound as a white solid in 74% yield (1.36 g).

$[\alpha]_D^{23}$ +3.2 (*c* = 1.0, $CHCl_3$);

MP 102 – 104 °C (lit. 96 – 98 °C)[42];

^{1}H NMR (400 MHz, $CDCl_3$) δ 8.45 (br. s, 1H, ArNHC=S), 7.74 (s, 1H, $(CF_3)_2ArH$), 7.68 (s, 2H, $(CF_3)_2ArH$), 7.34-7.20 (m, 5H, ArH), 6.25 (br. s, 1H, CHNHC=S), 4.86 (br. s, 1H, CHNHC=S), 3.71 (dd, *J* = 12.4, 4.2 Hz, 1H, $CHCH_ACH_BN_3$), 3.46 (dd, *J* = 12.4, 3.4 Hz, 1H, $CHCH_ACH_BN_3$), 3.05 (dd, *J* = 13.8, 6.5 Hz, 1H, $CHCH_ACH_BAr$), 2.85 (dd, *J* = 13.8, 8.2 Hz, 1H, $CHCH_ACH_BAr$);

^{13}C NMR (100 MHz, $CDCl_3$) δ 180.01 (C=S), 138.22, 136.26, 133.24 (q, J_{CF}=34.3 Hz), 129.10, 129.01, 127.26, 124.20- 124.03 (m), 122.6 (J_{CF} = 272.7 Hz), 121.34, 119.96-119.77 (m), 55.4, 52.3, 37.4.

All data reported is in agreement with those in literature.[42]

9H-fluoren-9-ylmethyl N-[(2S)1-hydroxy-3-methylbutan-2-yl]carbamate **131**

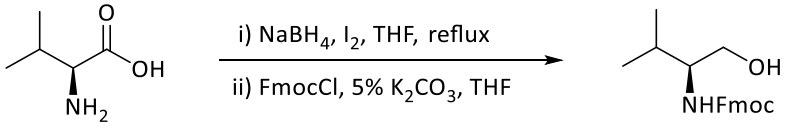

The reduction of (L)-valine **130** was prepared in the same way as is described in General Procedure A on a 2.97 mmol scale. The reduced amino acid was then dissolved in 12.5 mL of a 5% K_2CO_3 solution and cooled to 0 °C. A solution of FmocCl (1.0 g, 3.9 mmol, 1.3 equiv) in THF was added dropwise and the mixture was stirred at room temperature for 2 hours. Purification by FCC using 30% EtOAc/petroleum ether afforded the title compound as a white solid in 83% yield (802 mg).

MP 110 – 112 °C (lit. 107 – 108 °C)[128];

^{1}H NMR (400 MHz, $CDCl_3$) δ 7.76 (d, *J* = 7.5 Hz, 2H, ArH), 7.60 (d, *J* = 7.5 Hz, 2H, ArH), 7.40 (t, *J* = 7.4 Hz, 2H, ArH), 7.31 (td, *J* = 7.4, 1.0 Hz, 2H, ArH), 4.95 (d, *J* = 8.7 Hz, 1H, CHNHC=O), 4.50-4.39 (m, 2H, $CHCH_2OCO$), 4.22 (t, *J* = 6.7 Hz, 1H, $CHCH_2OCO$), 3.73-3.59 (m, 2H, $CHCH_2OH$), 3.55 – 3.35 (m, 1H, $CHCH_2OH$), 2.26 (t, *J* = 5.4 Hz, 1H, $CHCH_2OH$), 1.91-1.80 (m, 1H, $(CH_3)_2CH$), 0.95 (d, *J* = 6.8 Hz, 3H, CH_3CHCH_3), 0.92 (d, *J*=6.8 Hz, 3H, CH_3CHCH_3);

^{13}C NMR (100 MHz, $CDCl_3$) δ 157.2 (C=O), 144.0 (ArC), 141.5 (ArC), 127.8 (ArCH), 127.2 (ArCH), 125.1(ArCH), 120.1 (ArCH), 66.7 ($CHCH_2OCO$), 63.8 ($CHCH_2OCO$), 58.7 ($CHCH_2OH$), 47.5 ($CHCH_2OCO$), 29.3 (CH_3CHCH_3), 19.6 (CH_3CHCH_3), 18.8 (CH_3CHCH_3).

The data reported is in agreement with literature.[128]

9H-fluoren-9-ylmethyl N-[(2S)1-iodo-3-methylbutan-2-yl]carbamate **132**

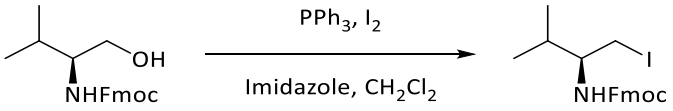

According to a literature procedure[42], a solution of triphenylphosphine (1.84 g, 7.0 mmol, 3.0 equiv) and imidazole (783 mg, 11.5 mmol, 5.0 equiv) in CH_2Cl_2 (11 mL) was made. Iodine (1.78 g, 7.0 mmol, 3.0 equiv) in CH_2Cl_2 was then added at 0 °C dropwise. The mixture was allowed to stir for 30 min before **131** (760 mg, 2.3 mmol, 1.0 equiv) was added. The mixture was allowed to warm to room tempearure and was stirred for an additional 5 hours after which the volatiles were removed *in vacuo* and the crude material was purified by FCC using 10% EtOAc/petroleum ether to afford the title compound as a yellow amorphous solid in 90% yield (900 mg).

$[\alpha]_D^{23}$ +0.56 (c=0.60, $CHCl_3$);

^{1}H NMR (400 MHz, $CDCl_3$) δ 7.78 (d, *J* = 7.5 Hz, 2H), 7.62 (dd, *J* = 7.3, 2.3 Hz, 2H), 7.41 (t, *J* = 7.5 Hz, 2H), 7.33 (t, *J* = 7.4 Hz, 2H), 4.81 (d, *J* = 9.1 Hz, 1H), 4.49-4.39 (m, 2H), 4.25 (t, *J* = 6.8 Hz, 1H), 3.42 (dd, *J* = 10.4, 3.9 Hz, 1H), 3.33 (dd, *J* = 10.4, 4.7 Hz, 1H), 3.26 – 3.10 (m, 1H), 1.87 – 1.72 (m, 1H), 0.95 (d, 6.7 Hz, 3H), 0.94 (d, *J*=6.7 Hz, 3H);

^{13}C NMR (100 MHz, $CDCl_3$) δ 155.9 (C=O), 143.9 (ArC), 141.38 (ArC), 127.7 (ArCH), 127.1 (ArCH), 125.2 (ArCH), 120.0 (ArCH), 66.7 ($CHCH_2OCO$), 56.2 ($CHNHC{=}O$), 47.3 ($CHCH_2OCO$), 32.3 (CH_3CHCH_3), 19.3 (CH_3CHCH_3), 18.4 (CH_3CHCH_3), 13.1 (CH_2I).

All data reported are in agreement with literature values.[129]

9H-fluoren-9-ylmethyl N-[(2S)1-azido-3-methylbutan-2-yl]carbamate **133**

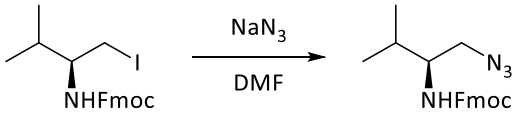

According to a literature procedure[42], **132** (840 mg, 1.93 mmol, 1.0 equiv) was dissolved in 6.5 mL of DMF and sodium azide (251 mg, 3.86 mmol, 2.0 equiv) was added at 0 °C. The reaction mixture was allowed to stir for 9 hours at room temperature after which 10 mL of H_2O was added and the organic phase was extracted with Et_2O. The combined organics were washed with brine and then dried over $MgSO_4$ and concentrated *in vacuo*. The crude material was purified by FCC using 10% EtOAc/petroleum ether to afford the title compound as a white solid in 77% yield (510 mg).

MP 106 – 108 °C;

^{1}H NMR (400 MHz, $CDCl_3$) δ 7.77 (d, *J* = 7.5 Hz, 2H, ArH), 7.60 (d, *J* = 7.5 Hz, 2H, ArH), 7.41 (t, *J* = 7.5 Hz, 2H, ArH), 7.32 (t, *J* = 7.4 Hz, 2H, ArH), 4.78 (d, *J* = 9.4 Hz, 1H, CHNHC=O), 4.45 (d, *J* = 6.9 Hz, 2H, $CHCH_2OCO$), 4.24 (t, *J* = 6.9 Hz, 1H, $CHCH_2OCO$), 3.61-3.54 (m, 1H, CHNHC=O), 3.45 (d, *J* = 4.8 Hz, 2H, $CHCH_2N_3$), 1.90 – 1.75 (m, *J* = 6.9 Hz, 1H, CH_3CHCH_3), 0.96 (d, *J* = 6.9 Hz, 3H, CH_3CHCH_3), 0.93 (d, *J* = 6.9 Hz, 3H, CH_3CHCH_3);

^{13}C NMR (100 MHz, $CDCl_3$) δ 156.1 (C=O), 143.8 (ArC), 141.3 (ArC), 127.7 (ArCH), 127.1 (ArCH), 125.0 (ArCH), 120.0 (ArCH), 66.7 ($CHCH_2OCO$), 56.2 ($CHNHC{=}O$), 53.0 ($CHCH_2N_3$), 47.3 ($CHCH_2OCO$), 29.7 (CH_3CHCH_3), 19.5 (CH_3CHCH_3), 18.5 (CH_3CHCH_3). The data reported is in agreement with those published in literature.[42]

tert-butyl N-[(2S)-1-hydroxy-3-methylbutan-2-yl]carbamate **135**

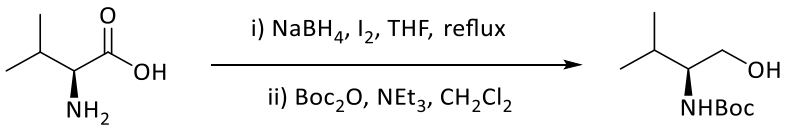

Prepared according to General Procedure A on a 31 mmol scale to afford the title compound as a colourless oil in 69% yield (4.35 g).

^{1}H NMR (400 MHz, $CDCl_3$) δ 4.66 (br. s, 1H), 3.74-3.66 (m, 1H), 3.63-3.56 (m, 1H), 3.47-3.39 (m, 1H), 2.43 (br. s, 1H), 1.92 – 1.77 (m, 1H), 1.44 (s, 9H), 0.95 (d, *J* = 7.0 Hz, 3H), 0.93(d, *J*=7.0 Hz, 3H);

^{13}C NMR (100 MHz, $CDCl_3$) δ 156.8, 79.4, 63.2, 59.2, 29.2, 28.4, 19.5, 18.5.

All data reported is in agreement with literature.[130]

tert-butyl N-[(2S)-3-methyl-1-[(4-methylbenzenesulfonyl)oxy]butan-2-yl]carbamate **136**

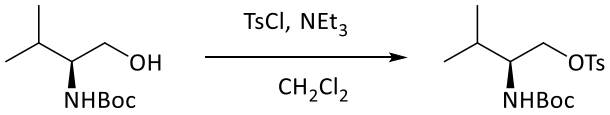

According to a literature procedure[42], **135** (812 mg, 4 mmol, 1.0 equiv) was dissolved in 13 mL of CH_2Cl_2 under argon and triethylamine (0.61 mL, 4.4 mmol, 1.1 equiv) was added. The reaction mixture was cooled to 0 °C and tosyl chloride (839 mg, 4.4 mmol, 1.1 equiv) was added in the minimum amount of CH_2Cl_2. The reaction mixture was warmed to room temperature and was allowed to stir for 24 hours after which H_2O was added and the organic phase was extracted. The combined organics were washed with brine and dried over $MgSO_4$ and then concentrated *in vacuo* before purification by FCC using 10% EtOAc/petroleum ether to afford the title compound as a white solid in 64% yield (903 mg).

MP 67 – 69 °C (lit. 75-76 °C)[131];

^{1}H NMR (400 MHz, $CDCl_3$) δ 7.77 (d, *J* = 8.3 Hz, 2H, Ar<u>H</u>), 7.34 (d, *J* = 8.1 Hz, 2H, Ar<u>H</u>), 4.59 (d, *J* = 9.1 Hz, 1H, CHN<u>H</u>C=O), 4.07 (dd, *J* = 9.8, 3.6 Hz, 1H, CHC<u>H</u>$_A$CH$_B$OTs), 4.01 (dd, *J* = 9.8, 3.6 Hz, 1H, CHCH$_A$C<u>H</u>$_B$OTs), 3.55-3.43 (m, 1H, C<u>H</u>CH$_A$CH$_B$OTs), 2.44 (s, 3H, ArCH$_3$), 1.90 – 1.72 (m, 1H, CH$_3$C<u>H</u>CH$_3$), 1.39 (s, 9H, OC(C<u>H</u>$_3$)$_3$), 0.92 (d, *J*=6.8 Hz, 3H, C<u>H</u>$_3$CHCH$_3$), 0.88 (d, *J* = 6.7 Hz, 3H, CH$_3$CHC<u>H</u>$_3$);

^{13}C NMR (100 MHz, $CDCl_3$) δ 155.4 (C=O), 145.0 (ArC), 132.5 (ArC), 129.9 (ArCH), 127.9 (ArCH), 79.5 ($OC(CH_3)_3$), 70.1 ($CHCH_2OTs$), 54.7 ($CHCH_2OTs$), 28.9 (CH_3CHCH_3), 28.3 ($OC(CH_3)_3$), 21.6 ($ArCH_3$), 19.2 (CH_3CHCH_3), 18.6 (CH_3CHCH_3);

LRMS (ES+) mass calculated for $[M+Na]^+$ 380.1, found 380.1. All data reported agree with literature values.[131]

tert-butyl N-[(2S)-1-azido-3-methylbutan-2-yl]carbamate **137**

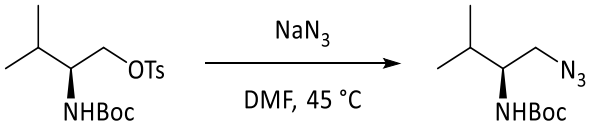

According to a literature procedure[42], compound **136** (860 mg, 2.4 mmol, 1.0 equiv) was dissolved in 8 mL of DMF under Argon. Sodium azide (172 mg, 2.6 mmol, 1.08 equiv) was added at 0 °C and the mixture was allowed to stir for 12 hours at room temperature. The reaction mixture was then diluted with H_2O (8 mL) and the organic phase was extracted twice using Et_2O. The combined organics were washed with brine, dried over $MgSO_4$, filtered and then concentrated *in vacuo*. Purification by FCC using 10% Et_2O/petroleum ether afforded the title compound as a white amorphous solid in 51% yield (283 mg).

^{1}H NMR (400 MHz, $CDCl_3$) δ 4.55 (d, *J* = 7.3 Hz, 1H, CHNHC=O), 3.56-3.47 (m, 1H, $CHCH_ACH_BN_3$), 3.45-3.27 (m, 2H, $CHCH_2N_3$), 1.89 – 1.73 (m, 1H, CH_3CHCH_3), 1.45 (s, 9H, $OC(CH_3)_3$), 0.94 (d, *J* = 7.0 Hz, 3H, CH_3CHCH_3), 0.92 (d, *J* = 7.0 Hz, 3H, CH_3CHCH_3);

^{13}C NMR (100 MHz, $CDCl_3$) δ 155.4 (C=O), 79.4 ($OC(CH_3)_3$), 55.5 ($CHCH_2N_3$), 53.0 ($CHCH_2N_3$), 29.7 (CH_3CHCH_3), 28.3 $OC(CH_3)_3$), 19.4 (CH_3CHCH_3), 18.3 (CH_3CHCH_3). All data reported is in agreement with the literature.[132]

3-[(2S)-1-azido-3-methylbutan-2-yl]-1-[3,5-bis(trifluoromethyl)phenyl]thiourea **138**

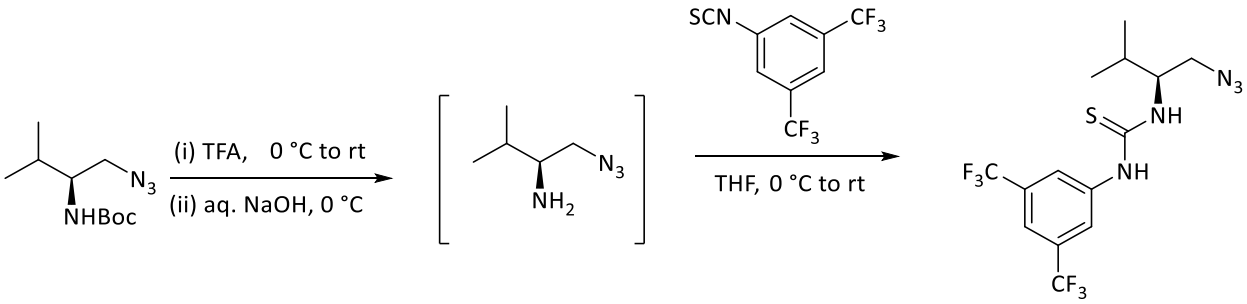

Prepared according to General Procedure B on a 1.08 mmol scale to afford the title compound as a white solid in 61% yield (262 mg).

$[\alpha]_D^{23}$ -4.26 (*c* = 0.92, $CHCl_3$).

MP 118 – 120 °C (lit. 112 – 115 °C)[42];

^{1}H NMR (400 MHz, $CDCl_3$) δ 8.29 (br. s, 1H, ArNHC=S), 7.80 (s, 2H, ArH), 7.74 (s, 1H, ArH), 6.21 (br. s, 1H, CHNHC=S), 4.40 (br. s, 1H, CHNHC=S), 3.77 (dd, *J* = 12.6, 4.2 Hz, 1H, $CHCH_ACH_BN_3$), 3.59 (dd, *J* = 12.6, 4.2 Hz, 1H, $CHCH_ACH_BN_3$), 1.99 – 1.84 (m, 1H, CH_3CHCH_3), 1.28 (d, 6.8 Hz, 3H, CH_3CHCH_3), 0.99 (d, 6.8 Hz, 3H, CH_3CHCH_3);

^{13}C NMR (100 MHz, $CDCl_3$) δ 180.6 (C=S), 138.5 (ArC), 133.3 (q, *J*=34.3 Hz, $ArCCF_3$), 123.9 (q, J_{CF}=3.8 Hz, ArCH), 122.7(q, *J*=272.7 Hz, $ArCF_3$), 119.8-119.6 (m, ArCH), 60.0 (CHNHC=S), 52.0 ($CHCH_2N_3$), 29.7 (CH_3CHCH_3), 19.3 (CH_3CHCH_3), 19.0 (CH_3CHCH_3);

^{19}F NMR (377 MHz, $CDCl_3$) δ -63.1.

All data reported is in agreement with the literature.[42]

General Procedure C for the *in situ* Generation of Iminophosphorane Catalysts

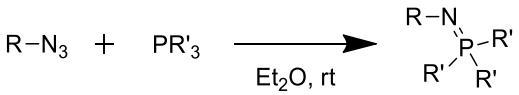

To the corresponding organoazide (0.020 mmol, 1.0 equiv) and phosphine (0.020 mmol, 1.0 equiv) under an argon atmosphere was added Et_2O (0.1 mL), and the reaction mixture was stirred at room temperature for 24 h. The iminophosphorane product was confirmed by LRMS and TLC, and the volatiles were removed under a N_2 stream to yield the crude product, which was used as a catalyst without further purification.

General Procedure D Synthesis of *N*-sulfinyl thiourea hydrogen-bond donor

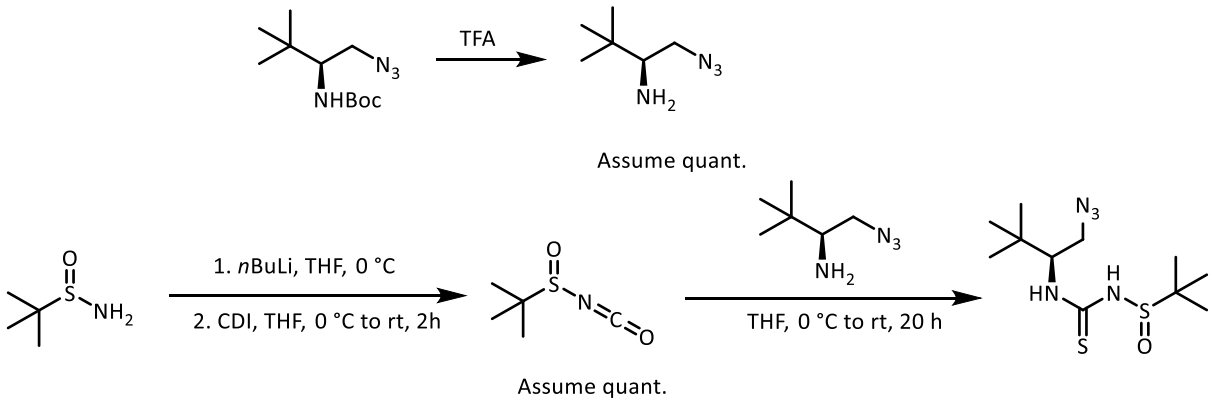

According to a literature procedure[58], a solution of sulfinamide (73 mg, 0.60 mmol, 1.0 equiv) was made in dry THF (6.0 mL, 0.1 M). This was then cooled to 0 °C upon which *n*BuLi (0.38 mL, 0.60 mmol, 1.0 equiv) was added dropwise over a period of 10 minutes. A solution of carbonyl diimidazole (97 mg, 0.60 mmol, 1.0 equiv) was made in a separate flask using the minimum amount of THF, which was then cooled to 0 °C. The solution of CDI was then added dropwise to the sulfonamide anion and the mixture was stirred for 20 minutes at 0 °C. The ice bath was then removed and the mixture was allowed to warm to room temperature whereupon stirring was continued for 2 hours. A solution of aminoazide (85.2 mg, 0.60 mmol, 1.0 equiv) was made in THF (0.60 mL) and this was added dropwise to the primary reaction vessel. The mixture was stirred for an overnight period upon which the reaction was quenched with acetic acid (34 µL in 0.60 mL of THF). The reaction mixture was then concentrated *in vacuo*. The crude residue was then purified by FCC using 2% MeOH/CH_2Cl_2.

(S)-N-(((S)-1-azido-3,3-dimethylbutan-2-yl)carbamothioyl)-2-methylpropane-2-sulfinamide **161a**

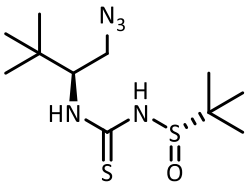

Prepared according to General Procedure D to afford the title compound as a white solid in 63% yield (115 mg).

$[\alpha]_D^{25}$ -29.79(c=1.0, $CHCl_3$);

MP 194-196 °C;

^{1}H NMR (400 MHz, $CDCl_3$) δ 7.64 (s, 1H, NHC=S), 6.11 (d, *J* = 9.7 Hz, 1H, CHNHC=S), 3.79 (td, *J* = 8.9, 3.5 Hz, 1H, CHNHC=S), 3.43 (dd, *J* = 12.7, 3.6 Hz, 1H, $CHCH_ACH_BN_3$), 3.20 (dd, *J* = 12.7, 8.7 Hz, 1H, $CHCH_ACH_BN_3$), 1.29 (s, 9H, $OC(CH_3)_3$), 0.95 (s, 9H, $S(O)C(CH_3)_3$);

^{13}C NMR (100 MHz, $CDCl_3$) δ 154.67 (C=S), 58.60 (C<u>H</u>CH_2N_3), 57.33 (S(O)<u>C</u>$(CH_3)_3$), 52.13 (CH<u>C</u>H_2N_3), 34.06 (CH<u>C</u>$(CH_3)_3$), 26.81 (S(O)C(<u>C</u>$H_3)_3$), 22.16 (CHC(<u>C</u>$H_3)_3$);

IR ν_{max}/cm^{-1} 3326, 2964, 2099, 1707, 1649, 1546, 1473.

<u>(R)-N-(((S)-1-azido-3,3-dimethylbutan-2-yl)carbamothioyl)-2-methylpropane-2-sulfinamide **161b**</u>

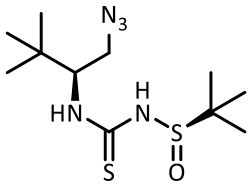

Prepared according to General Procedure D to afford the title compound as a white solid in 65% yield (119 mg).

$[\alpha]_D^{25}$ +40.12 (c=0.86, $CHCl_3$);

MP 152-154 °C;

^{1}H NMR (400 MHz, $CDCl_3$) δ 7.64 (s, 1H, N<u>H</u>C=S), 6.11 (d, *J* = 9.7 Hz, 1H, CHN<u>H</u>C=S), 3.79 (td, *J* = 8.9, 3.5 Hz, 1H, C<u>H</u>NHC=S), 3.43 (dd, *J* = 12.7, 3.6 Hz, 1H, CHC<u>H</u>$_A$C$H_B$$N_3$), 3.20 (dd, *J* = 12.7, 8.7 Hz, 1H, CHCH_AC<u>H</u>$_B$$N_3$), 1.29 (s, 9H, OC(C<u>H</u>$_3)_3$), 0.95 (s, 9H, S(O)C(C<u>H</u>$_3)_3$);

^{13}C NMR (100 MHz, $CDCl_3$) δ 154.67 (C=S), 58.60 (C<u>H</u>CH_2N_3), 57.33 (S(O)<u>C</u>$(CH_3)_3$), 52.13 (CH<u>C</u>H_2N_3), 34.06 (CH<u>C</u>$(CH_3)_3$), 26.81 (S(O)C(<u>C</u>$H_3)_3$), 22.16 (CHC(<u>C</u>$H_3)_3$);

IR ν_{max}/cm^{-1} 3326, 2964, 2099, 1707, 1649, 1546, 1473.

Synthesis of *N*-diphenylphosphinoyl ketimines 139a, 139b and 139i

General Procedure E for the synthesis of *N*-DPP ketimines

To a solution of NH_2OH•HCl (1.5 equiv) and NaOAc (1.5 equiv.) in EtOH/H_2O (1:1, 1.8 M) was added the corresponding ketone (1.0 equiv) at rt, and the reaction mixture refluxed for 20 h. After cooling to rt, the reaction mixture was stored at - 20 °C for 24 h. The precipitated oxime was filtered, washed with cold ethanol, vacuum dried and used directly without further purification (in some cases, extraction with CH_2Cl_2 of the aqueous phase after evaporation of the ethanol was performed and the crude oxime used directly without further purification in the next step). To a solution of crude oxime (1.0 equiv) in CH_2Cl_2/*n*-hexane (1 : 1, 0.3 M) under an inert atmosphere at -45 °C was added triethylamine (1.1 equiv) and stirred for 10 min. Subsequently, chlorodiphenylphosphine (1.1 equiv.)

was added dropwise over 20 min *via* a syringe pump. After stirring at -45 °C for 1 h and at rt for 16 h, the reaction mixture was filtered and the filter cake was washed with 1 : 1 Et_2O : CH_2Cl_2. The filtrate was collected and concentrated *in vacuo* (temperature of H_2O bath below 20 °C). The resulting crude residue was triturated using the minimum amount of Et_2O to reveal a white solid which was filtered and further purified by FCC (50% EtOAc/petroleum ether mixtures with 2% NEt_3).

P,*P*-Diphenyl-*N*-[(1*E*)-1-phenylethylidene]phosphinic amide **139a**

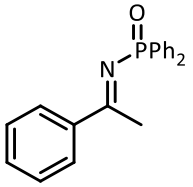

Synthesised according to General Procedure E from acetophenone on a 50 mmol scale to afford the title compound as a white solid in 45% yield (7.1 g).

MP 130 – 132 °C (lit. 128 – 130 °C)[133];

^{1}H NMR (400 MHz, $CDCl_3$) δ 8.10 - 8.06 (m, 6 H), 7.65 - 7.40 (m, 9 H), 2.95 (d, *J*=2.0 Hz, 3 H);

^{13}C NMR (100 MHz, $CDCl_3$) δ 181.4 (d, J_{PC}=7.9 Hz), 139.3 (d, J_{PC}=23.4 Hz), 134.5 (d, J_{PC}=131.0 Hz), 132.4, 131.5 (d, J_{PC}=9.6 Hz), 131.3 (d, J_{PC}=3.2 Hz), 128.35 128.3 (d, J_{PC}=12.0 Hz), 127.8, 22.9 (d, J_{PC}=12.8 Hz);

^{31}P NMR (162 MHz, $CDCl_3$) δ 18.9.

All data reported is in agreement with the literature.[134]

P,*P*-diphenyl-*N*-[(1*E*)-1-(3-Methoxyphenyl)ethylidene]phosphinic amide **139b**

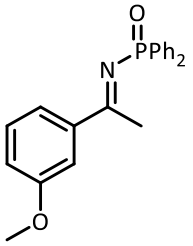

Synthesised according to General Procedure E from 3-methoxy acetophenone on a 6.10 mmol scale to afford the title compound as an amorphous white solid in 32% yield (681 mgs).

^{1}H NMR (400 MHz, $CDCl_3$) δ 8.10 - 7.89 (m, 4H), 7.72 - 7.63 (m, 2H), 7.52 - 7.37 (m, 7H), 7.15 - 7.10 (m, 1H), 3.89 (s, 3H), 2.95 (d, *J* = 2.0 Hz, 3H);

^{13}C NMR (100 MHz, $CDCl_3$) δ 181.5 (d, J_{PC}=8.0 Hz), 159.7, 141.0 (d, J_{PC}=24.0 Hz), 134.8 (d, J_{PC}=131.0 Hz), 131.6 (d, J_{PC}=8.8 Hz), 131.5 (d, J_{PC}=3.2 Hz), 129.6, 128.5 (d, J_{PC}=12.8 Hz), 120.6, 117.8, 113.5, 55.5, 23.2 (d, J_{PC}=12.8 Hz);

^{31}P NMR (162 MHz, $CDCl_3$) δ 20.1.

All data reported is in agreement with the literature.[135]

P,*P*-Diphenyl-*N*-[1-(3,5-bis(trifluoromethyl)phenyl)ethylidene]phosphinic amide **139i**

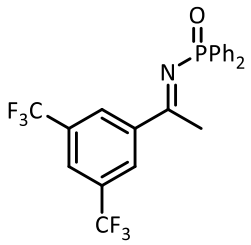

Synthesised according to General Procedure E on a 3.70 mmol scale to afford the title compound as a white solid in 47% yield (765 mgs).

MP 125 – 127 °C (lit. 120 – 121 °C)[42];

^{1}H NMR (400 MHz, $CDCl_3$) δ 7.99 – 7.92 (m, 4H), 7.65 – 7.59 (m, 1H), 7.49 – 7.39 (m, 6H), 7.25 (d, *J* = 3.5 Hz, 1H), 6.56 (dd, *J* = 3.5, 1.7 Hz, 1H), 2.80 (d, *J* = 2.0 Hz, 3H);

^{13}C NMR (100 MHz, $CDCl_3$) δ 178.1 (d, J_{PC} = 7.1 Hz), 141.3 (d, J_{PC} = 24.6 Hz), 133.5 (d, J_{PC} = 130.9 Hz), 132.1 (q, J_{FC} = 33.8 Hz), 131.9 (d, J_{PC} = 2.5 Hz), 131.5 (d, J_{PC} = 9.3 Hz), 128.6 (d, J_{PC} = 12.7 Hz), 127.7 (br s), 125.3–125.6 (m, 1C), 123.0 (q, J_{FC} = 272.8 Hz), 22.9 (d, J_{PC} = 11.8 Hz);
^{31}P NMR (162 MHz, $CDCl_3$) δ 21.5.
All data reported is in agreement with the literature.[42]

General Procedure F for the racemic synthesis of phospha-Mannich adducts

To a solution of the ketimine (0.20 mmol, 1.0 equiv) in Et_2O (0.4 mL) was added sequentially diethyl phosphite **90** (26 µL, 0.20 mmol, 1.0 equiv) and triisopropyl-Verkade's Superbase **141** (6.0 mg, 0.020 mmol, 0.10 equiv) at rt. Stirring was maintained for 3 h or until TLC analysis indicated disappearance of starting materials. The reaction mixture was purified by flash column chromatography [petroleum ether to petroleum ether/EtOAc 1 : 2, EtOAc then EtOAc : MeOH 9 : 1] to afford the desired *rac*-phospha-Mannich addition product in yields ranging from 85 – 95%.

General Procedure G for the enantioselective ketimine phospha-Mannich reaction

To a solution of the ketimine (0.40 mmol, 2.0 equiv) and pre-formed catalyst **84** (as described in General Procedure C) (14.7 mg, 0.02 mmol, 0.10 equiv) in Et_2O (4.0 mL) under an argon atmosphere was added diethyl phosphite **90** (26 µL, 0.20 mmol, 1.0 equiv) at rt. Stirring was maintained for 24 h whereupon the reaction mixture was purified by flash column chromatography [petroleum ether to petroleum ether/EtOAc 1 : 2, EtOAc then EtOAc : MeOH 9 : 1] to afford the desired phospha-Mannich addition product.

Diethyl {(1S)-1-[(diphenylphosphoryl)amino]-1-phenylethyl}phosphonate **140a**

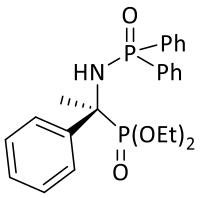

Synthesised according to General Procedure G using ketimine **139a** (128 mg, 0.40 mmol, 2.0 equiv) to afford the title compound as a colourless solid in 99% yield (91 mg) and 58% ee [determined by HPLC, Chiralpak OG, hexane/isopropanol = 95/5, 1 mL/min, λ = 220 nm, t (minor) = 31.17 min, t (major) = 37.34 min].

$[\alpha]_D^{25}$ = -17.6(*c* = 1.0, $CHCl_3$);

^{1}H NMR ($CDCl_3$, 500 MHz) δ 1.03 (t, *J* = 7.0 Hz, 3 H), 1.25 (t, *J* = 7.0 Hz, 3 H), 1.82 (d, J_{PH} = 17.0 Hz, 3 H), 3.53 (ddq, *J* = 10.0, 7.0, 7.0 Hz, 1 H), 3.81 (ddq, *J* = 10.0, 7.0, 7.0 Hz, 1 H), 4.03 - 4.20 (m, 3 H), 7.18 - 7.30 (m, 5 H), 7.31 - 7.47 (m, 4 H), 7.51 (dd, *J* = 7.5, 1.5 Hz, 2 H), 7.55 - 7.64 (m, 2 H), 7.82 - 7.91 (m, 2 H);

^{13}C NMR ($CDCl_3$, 125 MHz) δ 16.4 (d, J_{PC} = 5.7 Hz), 16.6 (d, J_{PC} = 5.7 Hz), 20.6 ('t', J_{PC} = 5.2 Hz), 58.6 (dd, J_{PC} = 154.5, 1.9 Hz), 63.6 (d, J_{PC} = 7.6 Hz), 63.9 (d, J_{PC} = 7.6 Hz), 127.1, 127.1, 127.6, 127.7, 128.2, 128.2, 128.5, 128.6, 128.6, 131.7. 131.8, 132.0, 134.1 (d, J_{PC} = 126.8 Hz), (d, J_{PC} = 129.7 Hz), 141.4;

^{31}P NMR ($CDCl_3$, 162 MHz) δ 20.1 (J_{PP} = 29.3 Hz), 24.8 (J_{PP} = 29.3 Hz); **MP** 124-126°C;

IR ν_{max}/cm^{-1} 3394, 2984, 1671.4, 1439, 1392, 1238, 1205, 1122, 1048, 1020, 971, 830, 757, 725, 698;

HRMS (ESI+) calcd. for $C_{24}H_{29}NNaO_4P_2$ 480.1464, found 480.1454.

Diethyl [(1S)-1-[(diphenylphosphoryl)amino]-1-(4-methoxyphenyl)ethyl]phosphonate **140b**

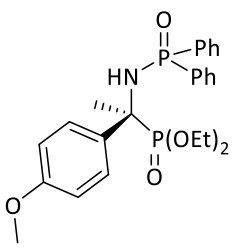

Synthesised according to General Procedure G using ketimine **139b** (140 mg, 0.40 mmol, 2.0 equiv) to afford the title compound as an amorphous colourless solid in 90% yield (88 mg) and 62% ee [determined by HPLC, Chiralpak AD-H, hexane/isopropanol = 80/20, 1 mL/min, λ = 220 nm, t (minor) = 14.26 min, t (major) = 15.04 min].

$[\alpha]_D^{25}$ = -15.9 (*c* = 0.42, $CHCl_3$);

^{1}H NMR ($CDCl_3$, 500 MHz) δ 1.12 (t, *J* = 7.0 Hz, 3 H), 1.32 (t, *J* = 7.0 Hz, 3 H), 1.86 (d, *J* = 17.0 Hz, 3 H), 3.57 - 3.67 (m, 1 H), 3.81 (s, 3 H), 3.88 (ddq, *J* = 10.0, 7.0, 7.0 Hz, 1 H), 4.09 - 4.27 (m, 3 H), 6.83 - 6.90 (m, 2 H), 7.28 - 7.34 (m, 2 H), 7.39 - 7.54 (m, 6 H), 7.63 - 7.70 (m, 2 H), 7.89 - 7.96 (m, 2 H);

^{13}C NMR ($CDCl_3$, 125 MHz) δ 16.5 (d, J_{PC} = 5.7 Hz), 16.7 (d, J_{PC} = 4.8 Hz), 20.8 ('t', J_{PC} = 4.8 Hz), 55.4, 58.2 (dd, J_{PC} = 155.0, 2.9 Hz), 63.6 (d, J_{PC} = 7.6 Hz), 63.8 (d, J_{PC} = 7.6 Hz), 113.6 (d, J_{PC} = 2.9 Hz), 128.4, 128.4, 128.5, 128.5, 128.6, 128.6, 131.7, 131.7, 131.8, 131.9 - 131.9, 131.9, 132.0, 134.2 (d, J_{PC} = 126.8 Hz), 134.6 (d, J_{PC} = 129.7 Hz), 159.0 (d, J_{PC} = 1.9 Hz);

^{31}P NMR ($CDCl_3$, 162 MHz) δ 20.2 (J_{PP} = 27.4 Hz), 24.9 (J_{PP} = 27.4 Hz);

IR ν_{max}/cm^{-1} 3396, 2989, 2361, 1595, 1513, 1439, 1391, 1298, 1120, 1023, 972, 724;

HRMS (ESI+) calcd. for $C_{25}H_{32}O_5NP_2$ 488.1750, found 488.1747.

Diethyl [(1S)-1-[(diphenylphosphoryl)amino]-1-(3-methoxyphenyl)ethyl]phosphonate **140c**

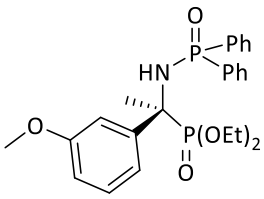

Synthesised according to General Procedure G using ketimine **139c** (140 mg, 0.40 mmol, 2.0 equiv) to afford the title compound as an amorphous colourless solid in >99% yield (97 mg) and 58% ee [determined by HPLC, Chiralpak AD-H, hexane/isopropanol = 80/20, 1 mL/min, λ = 230 nm, t (major) = 8.71 min, t (minor) = 14.54 min].

$[\alpha]_D^{25}$ = -14.9 (*c* = 1.58, $CHCl_3$);

^{1}H NMR ($CDCl_3$, 500 MHz) δ 1.13 (t, *J* = 7.0 Hz, 3 H), 1.32 (t, *J* = 7.0 Hz, 3 H), 1.87 (d, *J* = 17.0 Hz, 3 H), 3.66 (ddq, *J* = 10.0, 8.5, 7.0 Hz, 1 H), 3.79 (s, 3 H), 3.91 (dqq, *J* = 10.0, 7.0, 7.0 Hz, 1 H), 4.08 - 4.26 (m, 3 H), 6.79 - 6.85 (m, 1 H), 7.13 - 7.16 (m, 1 H), 7.17 - 7.22 (m, 1 H), 7.23 - 7.34 (m, 3 H), 7.38 - 7.53 (m, 4 H), 7.64 - 7.72 (m, 2 H), 7.89 - 7.98 (m, 2 H);

^{13}C NMR ($CDCl_3$, 125 MHz) δ 16.4 (d, J_{PC} = 5.7 Hz), 16.6 (d, J_{PC} = 4.8 Hz), 20.7 ('t', J_{PC} = 4.8 Hz), 55.4, 58.7 (dd, J_{PC} = 153.5, 1.9 Hz), 63.6 (d, J_{PC} = 7.6 Hz), 63.8 (d, J_{PC} = 7.6 Hz), 113.0 (d, J_{PC} = 2.9 Hz), 113.3 (d, J_{PC} = 4.8 Hz), 119.6 (d, J_{PC} = 4.8 Hz), 128.4, 128.5, 128.5, 128.6, 129.1 (d, J_{PC} = 1.9 Hz), 131.7, 131.7, 131.8, 131.9, 131.9, 132.0, 134.2 (d, J_{PC} = 126.8 Hz), 134.4 (d, J_{PC} = 129.7 Hz), 143.1, 159.4 (d, J_{PC} = 1.9 Hz);

^{31}P NMR ($CDCl_3$, 162 MHz) δ 20.1 (d, J_{PP} = 27.4 Hz), 24.6 (d, J_{PP} = 27.4 Hz);

IR ν_{max}/cm^{-1} 3395, 2986, 1597, 1439, 1392, 1293, 1121, 1020, 973, 725, 698;

HRMS (ESI+) calcd. for $C_{25}H_{32}O_5NP_2$ 488.1750, found 488.1747.

Diethyl [(1S)-1-[(diphenylphosphoryl)amino]-1-(2-methoxyphenyl)ethyl]phosphonate **140d**

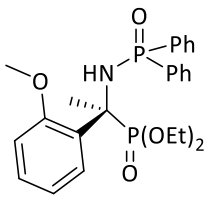

Synthesised according to General Procedure G using ketimine **139d** (140 mg, 0.40 mmol, 2.0 equiv) to afford the title compound as an amorphous colourless solid in 78% yield (76 mg) and 41% ee [determined by HPLC, Chiralpak IA, hexane/isopropanol = 95/5, 1 mL/min, λ = 220 nm, t (minor) = 16.17 min, t (major) = 20.06 min].

$[\alpha]_D^{25}$ = -2.17 (*c* = 1.52, $CHCl_3$);

^{1}H NMR ($CDCl_3$, 500 MHz) δ (ppm): 1.05 (t, *J* = 7.0 Hz, 3 H), 1.33 (t, *J* = 7.0 Hz, 3 H), 1.93 (d, J_{PH} = 16.0 Hz, 3 H), 3.55 - 3.63 (m, 1 H), 3.77 (s, 3 H), 3.86 (ddq, *J* =10.0, 7.0, 7.0 Hz, 1 H), 4.13 - 4.30 (m, 2 H), 5.98 (dd, *J* = 9.0, 1.5 Hz, 1 H), 6.92 ('t', *J* = 7.5 Hz, 1 H), 6.97 (d, *J* = 8.0 Hz, 1 H), 7.17 ('dt', *J* = 8.0, 2.0 Hz, 1 H), 7.24 - 7.31 (m, 3 H), 7.35 - 7.41 (m, 1 H), 7.41 - 7.52 (m, 3 H), 7.61 - 7.67 (m, 2 H), 7.90 - 8.01 (m, 2 H);

^{13}C NMR ($CDCl_3$, 125 MHz) δ (ppm): 16.4 (d, J_{PC} = 5.7 Hz), 16.7 (d, J_{PC} = 5.7 Hz), 21.3 (t, J_{PC} = 5.2 Hz), 56.0, 59.4 (dd, J_{PC} = 159.3, 3.8 Hz), 63.1 (d, J_{PC} = 6.7 Hz), 63.5 (d, J_{PC} = 7.6 Hz), 112.8 (d, J_{PC} = 2.9 Hz), 121.2, 128.3, 128.4, 128.5, 128.7, 128.8, 129.0, 129.4, 129.5, 131.4, 131.5, 131.6, 131.6, 131.9, 131.9, 135.1 (d, J_{PC} = 130.7 Hz), 135.2 (dd, J_{PC} = 124.9, 1.9 Hz), 158.8 (d, J_{PC} = 3.8 Hz);

^{31}P NMR ($CDCl_3$, 162 MHz) δ (ppm): 20.1 (d, J_{PP} = 31.3 Hz), 23.7 (d, J_{PP} = 31.3 Hz);

IR ν_{max}/cm^{-1} 3354, 2982, 1595, 1493, 1391, 1278, 1119, 1023, 971, 785, 754;

HRMS (ESI+) calcd. for $C_{25}H_{32}O_5NP_2$ 488.1750, found 488.1747.

Diethyl {(1S)-1-(4-chlorophenyl)-1-[(diphenylphosphoryl)amino]ethyl}phosphonate **140e**

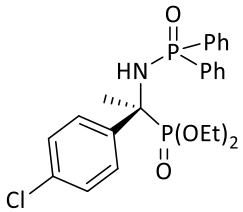

Synthesised according to General Procedure G using ketimine **139e** (141 mg, 0.40 mmol, 2.0 equiv) to afford the title compound as an amorphous colourless solid in >99% yield (98 mg) and 54% ee [determined by HPLC, Chiralpak OG, hexane/isopropanol = 95/5, 1 mL/min, λ = 220 nm, t (minor) = 30.68 min, t (major) = 38.40 min].

$[\alpha]_D^{25}$ = -15.9 (*c* = 0.98, $CHCl_3$);

^{1}H NMR ($CDCl_3$, 500 MHz) δ (ppm): 1.14 (t, *J* = 7.0 Hz, 3H), 1.32 (t, *J* = 7.0 Hz, 3 H), 1.86 (d, *J* = 17.0 Hz, 3 H), 3.70 (ddq, *J* = 10.0, 8.5, 7.0, Hz, 1 H), 3.92 (dqq, *J* = 10.0, 7.0, 7.0 Hz, 1 H), 4.10 - 4.25 (m, 3 H), 7.28 - 7.36 (m, 4 H), 7.41 - 7.48 (m, 3 H), 7.49 - 7.55 (m, 3 H), 7.61 - 7.70 (m, 2 H), 7.88 - 7.98 (m, 2 H);

^{13}C NMR ($CDCl_3$, 125 MHz) δ (ppm): 16.4 (d, J_{PC} = 5.7 Hz), 16.6 (d, J_{PC} = 5.7 Hz), 20.9 ('t', J_{PC} = 4.8 Hz), 58.4 (dd, J_{PC} = 154.5, 2.9 Hz), 63.7, 64.0 (d, J_{PC} = 7.6 Hz), 128.3, 128.3, 128.6, 128.6, 128.7, 128.7, 131.7, 131.9, 131.9, 132.0, 132.0, 134.0 (d, J_{PC} = 126.8 Hz), 133.7 (d, J_{PC} = 2.9 Hz), 134.3 (d, J_{PC} = 129.7 Hz), 140.1;

^{31}P NMR ($CDCl_3$, 162 MHz) δ (ppm): 20.3 (d, J_{PP} = 29.3 Hz), 24.3 (d, J_{PP} = 29.3 Hz);

IR ν_{max}/cm^{-1} 3391, 2986, 2359, 1593, 1494, 1439, 1392, 1278, 1121, 1020, 972, 721;

HRMS (ESI+) calcd. for $C_{24}{}^{35}ClH_{29}NO_4P_2$ 492.1255, found 492.1254.

Diethyl {(1S)-1-(4-bromophenyl)-1-[(diphenylphosphoryl)amino]ethyl}phosphonate **140f**

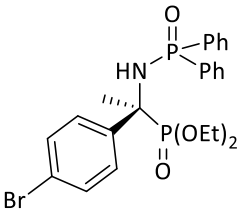

Synthesised according to General Procedure G using ketimine **139f** (159 mg, 0.40 mmol, 2.0 equiv) to afford the title compound as an amorphous colourless solid in 86% yield (92 mg) and 46% ee [determined by HPLC, Chiralpak OG, hexane/isopropanol = 95/5, 1 mL/min, λ = 220 nm, t (minor) = 29.86 min, t (major) = 38.44 min].

$[\alpha]_D^{25}$ = -15.3 (*c* = 1.14, $CHCl_3$);

^{1}H NMR ($CDCl_3$, 500 MHz) δ (ppm): 1.14 (t, *J* = 7.0 Hz, 3 H), 1.31 (t, *J* = 7.0 Hz, 3 H), 1.85 (d, *J* = 17.0 Hz, 3 H), 3.64 - 3.76 (m, 1 H), 3.92 (dqq, *J* = 10.0, 7.0, 7.0 Hz, 1 H), 4.09 - 4.26 (m, 3 H), 7.29 - 7.36 (m, 2 H), 7.39 - 7.48 (m, 7 H), 7.49 - 7.54 (m, 1 H), 7.61 - 7.70 (m, 2 H), 7.87 - 7.99 (m, 2 H);

^{13}C NMR ($CDCl_3$, 125 MHz) δ (ppm): 16.4 (d, J_{PC} = 5.7 Hz), 16.6 (d, J_{PC} = 4.8 Hz), 20.8 ('t', J_{PC} = 4.8 Hz), 58.4 (dd, J_{PC} = 154.5, 2.9 Hz), 63.7 (d, J_{PC} = 7.6 Hz), 64.0 (d, J_{PC} = 6.7 Hz), 121.9 (d, J_{PC} = 2.9 Hz), 128.6, 128.6, 128.6, 128.7, 129.0, 129.0, 131.2, 131.3, 131.6, 131.7, 131.9, 131.9, 132.0, 132.0, 133.9 (d, J_{PC} =126.8 Hz), 134.3 (d, J_{PC} =129.7 Hz), 140.6;

^{31}P NMR ($CDCl_3$, 162 MHz) δ (ppm): 20.3 (d, J_{PP} = 29.3 Hz), 24.2 (d, J_{PP} = 29.3 Hz);

IR ν_{max}/cm^{-1} 3391, 2986, 2360, 1593, 1487, 1439, 1393, 1278, 1121, 1021, 973, 728;

HRMS (ESI+) calcd. for $^{79}BrC_{24}H_{29}NO_4P_2$ $[M+H]^+$ 536.0750, found 536.0749; $^{81}BrC_{24}H_{29}NO_4P_2$ $[M+H]^+$ 538.0729, found 538.1341.

Diethyl {(1S)-1-(4-fluorophenyl)-1-[(diphenylphosphoryl)amino]ethyl}phosphonate **140g**

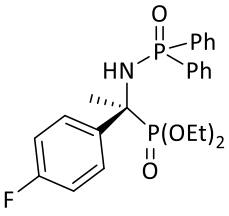

Synthesised according to General Procedure G using ketimine **139g** (135 mg, 0.40 mmol, 2.0 equiv) to afford the title compound as an amorphous colourless solid in 98% yield (93 mg) and 56% ee [determined by HPLC, Chiralpak OG, hexane/isopropanol = 95/5, 1 mL/min, λ = 230 nm, t (minor) = 30.56 min, t (major) = 36.20 min].

$[\alpha]_D^{25}$ = -10.7 (*c* = 1.38, $CHCl_3$);

^{1}H NMR ($CDCl_3$, 500 MHz) δ (ppm): 1.12 (t, *J* = 7.0 Hz, 3 H), 1.31 (t, *J* = 7.0 Hz, 3 H), 1.87 (d, *J* = 17.0 Hz, 3 H), 3.67 (ddq, *J* = 10.0, 8.5, 7.0 Hz, 1 H), 3.84 - 3.97 (m, 1 H), 4.09 - 4.26 (m, 3 H), 6.97 - 7.04 (m, 2 H), 7.28 - 7.35 (m, 2 H), 7.39 - 7.47 (m, 3 H), 7.48 - 7.53 (m, 1 H), 7.53 - 7.58 (m, 2 H), 7.62 - 7.70 (m, 2 H), 7.88 - 7.97 (m, 2 H);

^{13}C NMR ($CDCl_3$, 125 MHz) δ (ppm): 16.3 (d, J_{PC} = 5.7 Hz), 16.5 (d, J_{PC} = 5.7 Hz), 20.9 ('t', J_{PC} = 4.8 Hz), 58.1 (dd, J_{PC} = 154.5, 1.9 Hz), 63.6 (d, J_{PC} = 6.7 Hz), 63.8 (d, J_{PC} = 7.6 Hz), 114.9 (dd, $J_{PC,FC}$ = 21.0, 1.9 Hz), 128.4, 128.5, 128.5, 128.6, 128.9, 128.9, 128.9, 129.0, 129.0, 131.6, 131.7, 131.7, 131.8, 131.9, 133.9 (d, J_{PC} = 126.8 Hz), 134.2 (d, J_{PC} = 130.7 Hz), 136.9 - 137.3 (m), 162.2 (dd, $J_{FC,PC}$ = 247.0, 2.9 Hz);

^{31}P NMR ($CDCl_3$, 162 MHz) δ (ppm): 20.2 (d, J_{PP} = 29.4 Hz), 24.5 (dd, J_{PP} = 29.3, 3.9 Hz);

^{19}F NMR ($CDCl_3$, 377 MHz) δ (ppm): -115.4 - -115.3 (m);

IR ν_{max}/cm^{-1} 3392, 2988, 1602, 1509, 1439, 1392, 1236, 1122, 1020, 973, 726;

HRMS (ESI+) calcd. for $C_{24}H_{29}FNO_4P_2$ $[M+H]^+$ 476.1550, found 476.15481.

Diethyl [(1S)-1-[(diphenylphosphoryl)amino]-1-(pyridin-3-yl)ethyl]phosphonate **140h**

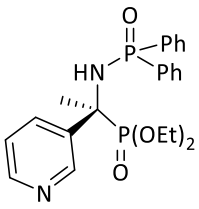

Synthesised according to General Procedure G using ketimine **139h** (128 mg, 0.40 mmol, 2.0 equiv) to afford the title compound as an amorphous colourless solid in >99% yield (91 mg) and 53% ee [determined by HPLC, Chiralpak AD-H, hexane/isopropanol = 80/20, 1 mL/min, λ = 220 nm, t (minor) = 18.16 min, t (major) = 20.40 min].

$[\alpha]_D^{25}$ = -13.5 (*c* = 1.32, $CHCl_3$);

^{1}H NMR ($CDCl_3$, 500 MHz) δ (ppm): 1.09 (t, *J* = 7.0 Hz, 3 H), 1.25 (t, *J* = 7.0 Hz, 3 H), 1.85 (d, *J* = 17.0 Hz, 3 H), 3.71 (ddq, *J* = 10.0, 8.5, 7.0 Hz, 1 H), 3.89 (dqq, *J* = 10.0, 7.0, 7.0 Hz, 1 H), 4.05 - 4.21 (m, 3 H), 7.18

- 7.23 (m, 1 H), 7.23 - 7.29 (m, 2 H), 7.33 - 7.43 (m, 3 H), 7.44 - 7.49 (m, 1 H), 7.56 - 7.65 (m, 2 H), 7.82 - 7.92 (m, 3 H), 8.46 (d, *J* = 4.0 Hz, 1 H), 8.76 (br. s., 1 H);

^{13}C NMR ($CDCl_3$, 125 MHz) δ (ppm): 16.4 (d, J_{PC} = 4.8 Hz), 16.6 (d, J_{PC} = 4.8 Hz), 20.6 ('t', J_{PC} = 4.8 Hz), 57.5 (dd, J_{PC} = 154.5, 1.9 Hz), 63.8 (d, J_{PC} = 7.6 Hz), 64.1 (d, J_{PC} = 7.6 Hz), 122.9, 128.6, 128.7, 131.6, 131.7, 131.9, 132.0, 132.1 (d, J_{PC} = 2.9 Hz), 133.7 (d, J_{PC} = 126.8 Hz), 134.1 (d, J_{PC} = 129.7 Hz), 135.0 (d, J_{PC} = 4.8 Hz), 137.2, 148.6 (d, J_{PC} = 4.8 Hz), 148.7 (d, J_{PC} = 2.9 Hz);

^{31}P NMR ($CDCl_3$, 162 MHz) δ (ppm): δ 20.5 (d, J_{PP} = 29.3 Hz), 23.8 (d, J_{PP} = 29.3 Hz);

IR ν_{max}/cm^{-1} 3401, 2925, 1645, 1590, 1439, 1392, 1237, 1122, 1021, 973, 727;

HRMS (ESI+) calcd. for $C_{23}H_{29}N_2O_4P_2$ 459.1597, found 459.1593.

Diethyl {(1S)-1-[3,5-bis(trifluoromethyl)phenyl]-1-[(diphenylphosphoryl) amino]ethyl}phosphonate

140i

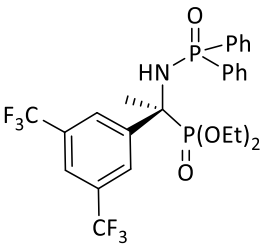

Synthesised according to General Procedure G using ketimine **139i** (182 mg, 0.40 mmol, 2.0 equiv) to afford the title compound as an amorphous colourless solid in >99% yield (118 mg) and 52% ee [determined by HPLC, Chiralpak AD-H, hexane/isopropanol = 90/10, 1 mL/min, λ = 220 nm, t (major) = 5.57 min, t (minor) = 13.52 min].

$[\alpha]_D^{25}$ = -8.8 (*c* = 1.38, $CHCl_3$);

^{1}H NMR ($CDCl_3$, 500 MHz) δ (ppm): 1.17 (t, *J* = 7.0 Hz, 3 H), 1.31 (t, *J* = 7.0 Hz, 3 H), 1.97 (d, *J* = 16.5 Hz, 3 H), 3.81-3.89 (m, 1 H), 3.95-4.03 (m, 1 H), 4.10 - 4.23 (m, 3 H), 7.33 - 7.38 (m, 2 H), 7.42 - 7.53 (m, 3 H), 7.54-7.57 (m, 1 H), 7.60 - 7.69 (m, 2 H), 7.78 (s, 1 H), 7.92 - 7.99 (m, 2 H), 8.08 (s, 2 H);

^{13}C NMR ($CDCl_3$, 125 MHz) δ (ppm): 16.2 (d, J_{PC} = 5.7 Hz), 16.4 (d, J_{PC} = 4.8 Hz), 21.4 ('t', J_{PC} = 4.3 Hz), 58.7 (dd, J_{PC} = 154.5, 1.9 Hz), 63.9 (d, J_{PC} = 7.6 Hz), 64.0 (d, J_{PC} = 7.6 Hz), 121.4 (octet, $J_{PC,FC}$ = 3.5 Hz), 123.4 (q, J_{FC} = 272.8 Hz), 127.7 – 127.9 (m), 128.6, 128.7, 131.1 (qd, $J_{PC,FC}$ = 33.4, 1.9 Hz), 131.2, 131.3, 131.9, 132.0, 132.1 (d, J_{PC} = 9.5 Hz), 132.1 (d, J_{PC} = 9.5 Hz), 133.4 (dd, J_{PC} = 124.9, 1.9 Hz), 133.6 (d, J_{PC} = 129.7 Hz), 144.5;

^{31}P NMR ($CDCl_3$, 162 MHz) δ (ppm): 21.7 (d, J_{PP} = 32.6 Hz), 23.0 (d, J_{PP} = 32.6 Hz);

^{19}F NMR ($CDCl_3$, 377 MHz) δ (ppm): 62.7;

IR ν_{max}/cm^{-1} 3200, 2988, 1439, 1368, 1278, 1241, 1130, 1048, 1022, 975, 754;

HRMS (ESI+) calcd. for $C_{26}H_{28}F_6NO_4P_2$ 594.1392, found 594.13886.

Diethyl {(1S)-1-[(diphenylphosphoryl)amino]-1-phenylpropyl}phosphonate **140j**

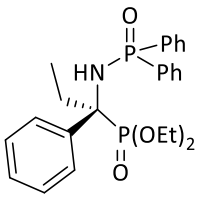

Synthesised according to General Procedure G using ketimine **139j** (133 mg, 0.40 mmol, 2.0 equiv) to afford the title compound as an amorphous colourless solid in >99% yield (94 mg) and 71% ee [determined by HPLC, Chiralpak OD, hexane/isopropanol = 96/4, 1 mL/min, λ = 220 nm, t (minor) = 20.90 min, t (major) = 23.55 min].

$[\alpha]_D^{25}$ = -16.3 (*c* = 0.94, $CHCl_3$);

^{1}H NMR ($CDCl_3$, 400 MHz) δ (ppm): 0.74 (t, *J* = 7.5 Hz, 3 H), 1.12 (t, *J* = 7.0 Hz, 3 H), 1.18 (t, *J* = 7.0 Hz, 3 H), 2.20 – 2.32 (m, 1 H), 2.35 – 2.50 (m, 1 H), 3.71 (t, *J* = 7.5 Hz, 1 H), 3.78 - 4.09 (m, 4 H), 7.07 - 7.48 (m, 9 H), 7.69 - 7.81 (m, 4 H), 7.88 - 8.00 (m, 2 H);

^{13}C NMR ($CDCl_3$, 100 MHz) δ (ppm): 9.8 (d, J_{PC} = 8.1 Hz), 16.8 (d, J_{PC} = 5.1 Hz), 17.0 (d, J_{PC} = 5.1 Hz), 27.3, 63.4 (d, J_{PC} = 7.3 Hz), 63.6 (d, J_{PC} = 7.3 Hz), 65.4 (dd, J_{PC} = 154.1, 3.7 Hz), 127.9 (d, J_{PC} = 2.2 Hz), 128.3, 128.3, 128.5, 128.6, 128.7, 128.9, 129.0, 131.9, 131.9, 132.0, 132.0, 132.1, 132.6, 132.7, 135.1 (d, J_{PC} = 130.6 Hz), 135.4 (d, J_{PC} = 127.7 Hz), 139.7 (t, J_{PC} = 2.2 Hz);

^{31}P NMR ($CDCl_3$, 162 MHz) δ (ppm): 20.0 (d, J_{PP} = 23.5 Hz), 25.1 (d, J_{PP} = 23.5 Hz);

IR ν_{max}/cm^{-1} 3382, 3059, 2980, 1595, 1439, 1390, 1278, 1207, 1120, 1022, 966, 700;

HRMS (ESI+) calcd. for $C_{25}H_{32}NO_4P_2$ 472.1801, found 472.1799.

Determination of Absolute Stereochemical Configuration

Diethyl [(1*S*)-1-amino-1-phenylethyl]phosphonate **163**

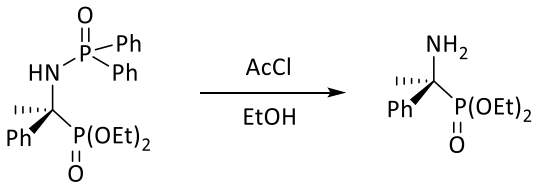

To a solution of HCl in EtOH (5.0 mL) [obtained by the dropwise addition of acetyl chloride (1.5 mL, 21 mmol, 100 equiv) at 0 °C to ethanol] and a solution of **140a** (94 mgs, 0.204 mmol, 1.0 equiv, 58% ee) in EtOH (0.10 mL) was added. The reaction mixture was allowed to warm to room temperature and stirred at this temperature for 30 minutes before warming to 50 °C and stirred for a further 12 h.

The reaction mixture was then concentrated under a stream of N_2. The crude mixture was diluted with dichloromethane and basified to a pH of 10 using saturated aq $NaHCO_3$. The organic phase was extracted with CH_2Cl_2 (×3). The combined organics were washed with brine, dried (Na_2SO_4) and concentrated *in vacuo*. Analysis of the crude reaction mixture by ^{1}H NMR revealed a conversion of 67%. The resulting crude material was purified by FCC using 20% MeOH/EtOAc to afford the title compound **163** and **140a** (26 mg) as an inseparable mixture. Purification by preparative HPLC [Agilent Prep-Sil, 10 µm, 30 cm x 250 mm, 80/20 then 70/30 hexane/isopropanol, 20 mL/min] afforded the title compound **163** as a colourless oil in 14% yield (7 mg).

$[\alpha]_D^{25}$ = -12.1 (*c* = 0.7, EtOH), [lit. $[\alpha]_D^{25}$ = +24.2, (*c* 3.19, EtOH) for (*R*)-**163**, 91% ee],[51] [lit. $[\alpha]_D^{20}$ = +26.4, (*c* 1.23, EtOH) for (*R*)-**163**, 96% ee].[136] From the specific rotation, the absolute configuration was determined to be *S*.

^{1}H NMR ($CDCl_3$, 400 MHz) δ 1.13 (t, *J* = 7.1 Hz, 3H), 1.25 (t, *J* = 7.1 Hz, 3H), 1.70 (d, *J* = 15.8 Hz, 3H), 1.84 (br, 2H), 3.74-3.84 (m, 1H), 3.88-4.06 (m, 3H), 7.26-7.29 (m, 1H), 7.34 (t, *J* = 7.7 Hz, 2H), 7.62-7.64 (m, 2H);

^{13}C NMR ($CDCl_3$, 125 MHz) δ 16.3 (d, *J* = 5.7 Hz), 16.4 (d, *J* = 5.7 Hz), 26.2, 55.2 (d, *J* = 145.9 Hz), 62.6 (d, *J* = 7.6 Hz), 63.0 (d, *J* = 6.8 Hz), 126.5 (d, *J* = 4.8 Hz), 127.2 (d, *J* = 2.8 Hz), 128.1 (d, *J* = 2.8 Hz), 141.1;

^{31}P NMR ($CDCl_3$, 162 MHz) δ 27.9.

Data is consistent with that given in the literature.[51]

6.3 Experimental for Chapter 3

6.3.1 Synthesis of Amidosulfones

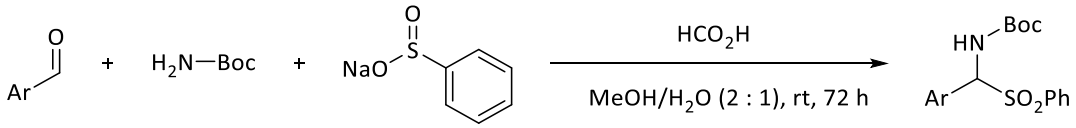

General Procedure H for synthesis of amidosulfones

According to a literature procedure,[78] a mixture of aldehyde (37.5 mmol, 1.5 equiv), Boc-carbamate (2.93 g, 25 mmol, 1.0 equiv) and benzene sulfinic acid sodium salt (8.26 g, 50 mmol, 2.0 equiv) was suspended in MeOH/H_2O (2 : 1, 75 mL). Formic acid (1.9 mL) was then added and the resulting mixture was then stirred for 72 hours at room temperature and the resulting precipitate was filtered off, washing with water and then Et_2O, to yield the desired amidosulfone[xiv] as a white solid.

tert-butyl [(benzenesulfonyl)(phenyl)methyl]carbamate **201a**

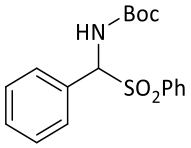

Synthesised according to General Procedure H to afford the title compound as a white solid in 75% yield (6.5 g).

MP 165 – 168 °C (lit. 169 – 170 °C)[137];

^{1}H NMR (400 MHz, $CDCl_3$) δ 7.91 (d, *J* = 7.5 Hz, 2H), 7.67 – 7.61 (m, 1H), 7.57 – 7.50 (m, 2H), 7.47 – 7.37 (m, 5H), 5.99 – 5.85 (m, 2H), 1.25 (s, 9H);

^{13}C NMR (100 MHz, $CDCl_3$) δ 153.62, 136.97, 134.08, 129.98, 129.96, 129.58, 129.17, 129.05, 128.88, 81.35, 74.05, 28.12.

Data is consistent with those reported in literature.[138]

[xiv] **Amidosuflones 201b-n were synthesised by David Barber.**

tert-butyl (naphthalen-2-yl(phenylsulfonyl)methyl)carbamate **201d**

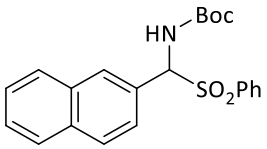

Synthesised according to General Procedure H to afford the title compound as a white solid in 62% yield (6.2 g) after trituration with the minimum amount of Et_2O.

MP 180 – 182 °C (lit. 174.4 – 175 °C)[137];

^{1}H NMR (400 MHz, DMSO-d_6) δ 8.86 (d, *J* = 10.7 Hz, 1H), 8.23 (s, 1H), 7.98 – 7.89 (m, 1H), 7.84 – 7.79 (m, 1H), 7.76 – 7.70 (m, 1H), 7.66 – 7.61 (m, 2H), 7.60 – 7.55 (m, 2H), 6.21 (d, *J* = 10.6 Hz, 1H), 1.18 (s, 9H);

^{13}C NMR (100 MHz, DMSO-d_6) δ 154.1, 137.1, 134.0, 133.1, 132.3, 129.7, 129.2, 129.2, 128.1, 127.8, 127.6, 127.0, 126.6, 79.5, 74.6, 27.9.

tert-butyl [(benzenesulfonyl)(pyridin-3-yl)methyl]carbamate **201k**

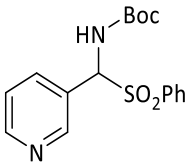

Synthesised according to General Procedure H to afford the title compound as an amorphous white solid in 80% yield (7.0 g).

^{1}H NMR (400 MHz, DMSO-d_6) δ 8.85 (d, *J* = 10.7 Hz, 1H), 8.82 (d, *J* = 2.3 Hz, 1H), 8.62 (dd, *J* = 4.8, 1.6 Hz, 1H), 8.14 (d, *J* = 8.1 Hz, 1H), 7.93 – 7.87 (m, 2H), 7.79 – 7.72 (m, 1H), 7.69 – 7.60 (m, 2H), 7.51 – 7.41 (m, 1H), 6.19 (d, *J* = 10.7 Hz, 1H), 1.18 (s, 9H);

^{13}C NMR (100 MHz, DMSO-d_6) δ 154.0, 150.6, 150.3, 137.1, 136.6, 134.2, 129.2, 129.2, 126.4, 123.3, 79.6, 72.3, 27.8.

6.3.2 Synthesis of *N*-Boc protected Aldimines

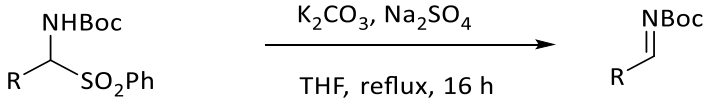

General Procedure I for Synthesis of Aldimines (52a-o)

According to a literature procedure[78], a RBF was charged with amidosulfone (1.0 equiv), potassium carbonate (15.0 equiv) and sodium sulfate (18.0 equiv). Dry THF was added (0.51 *m*M) under argon and the suspension was heated to 70 °C for 16 hours after which the reaction mixture was passed through a thick pad of celite on a glass frit, with washings of CH_2Cl_2. The filtrate was concentrated *in vacuo* to afford the pure aldimine.

tert-butyl [(E)-phenylmethylidene]carbamate **52a**

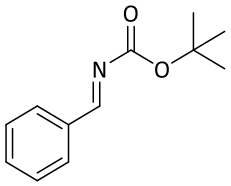

Synthesised according to General Procedure I on a 10 mmol scale to afford the title compound as a clear oil in 98% yield (2.0 g).

^{1}H NMR (400 MHz, $CDCl_3$) δ 8.89 (s, 1 H), 7.91-7.94 (m, 2 H), 7.56-7.59 (m, 1 H), 7.45 - 7.52 (m, 2 H), 1.60 (s, 9 H);

^{13}C NMR (100 MHz, $CDCl_3$) δ 169.9, 162.8, 134.2, 133.7, 130.4, 129.0, 82.5, 28.1.
All data is consistent with those reported in the literature.[139]

tert-butyl [(E)-(thiophen-2-yl)methylidene]carbamate **52b**

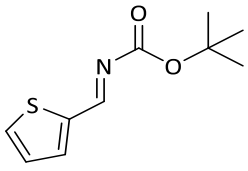

Synthesised according to General Procedure I on a 10 mmol scale to afford the title compound as a yellow amorphous solid in 95% yield (2.0 g).

^{1}H NMR (400 MHz, $CDCl_3$) δ 9.09 (s, 1 H), 7.66 - 7.70 (m, 2 H), 7.18 (dd, *J*=4.7, 3.9 Hz, 1 H), 1.58 (s, 9 H);

^{13}C NMR (100 MHz, $CDCl_3$) δ 163.8, 162.3, 140.4, 137.3, 134.4, 128.5, 82.3, 28.1.

All data is consistent with those reported in the literature.[139]

tert-butyl [(E)-(furan-2-yl)methylidene]carbamate **52c**

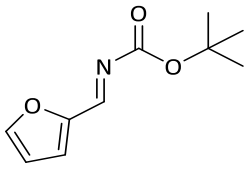

Synthesised according to General Procedure I on a 10 mmol scale to afford the title compound as a yellow oil in 97% yield (1.9 g).

^{1}H NMR (400 MHz, $CDCl_3$) δ 8.78 (s, 1 H), 7.69 (s, 1 H), 7.24 (d, *J*=3.4 Hz, 1 H), 6.61 (dd, *J*=3.4, 1.6 Hz, 1 H), 1.57 (s, 9 H);

^{13}C NMR (100 MHz, $CDCl_3$) δ 162.1, 157.4, 150.7, 148.1, 121.3, 113.0, 82.1, 27.8;

All data is consistent with those reported in the literature.[139]

tert-butyl [(E)-(naphthalen-2-yl)methylidene]carbamate **52d**

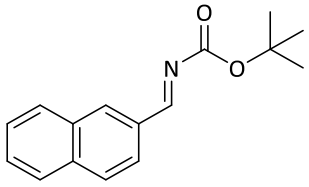

Synthesised according to General Procedure I on a 10 mmol scale to afford the title compound as a white amorphous solid in 98% yield (2.5 g).

^{1}H NMR (400 MHz, $CDCl_3$) δ 9.06 (s, 1 H), 8.30 (s, 1 H), 8.11 (dd, *J*=8.7, 1.6 Hz, 1 H), 7.86 - 7.99 (m, 3 H), 7.54 - 7.65 (m, 2 H), 1.62 (s, 9 H);

^{13}C NMR (100 MHz, $CDCl_3$) δ 170.0, 162.7, 136.0, 134.2, 132.8, 131.8, 129.2, 128.8, 128.6, 128.0, 126.9, 124.0, 82.3, 27.9.

All data is consistent with those reported in the literature.[139]

tert-butyl [(E)-(4-methoxyphenyl)methylidene]carbamate **52e**

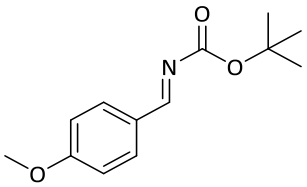

Synthesised according to General Procedure I on a 10 mmol scale to afford the title compound as a white amorphous solid in 94% yield (2.2 g).

^{1}H NMR (400 MHz, $CDCl_3$) δ 8.89 (s, 1 H), 7.90 (d, *J*=8.7 Hz, 2 H), 6.97 (d, *J*=8.7 Hz, 2 H), 3.89 (s, 3 H), 1.59 (s, 9 H);

^{13}C NMR (100 MHz, $CDCl_3$) δ 169.8, 164.1, 162.8, 132.5, 126.9, 114.3, 81.8, 55.5, 27.9.

All data is consistent with those reported in the literature.[139]

tert-butyl [(E)-(2-methoxyphenyl)methylidene]carbamate **52f**

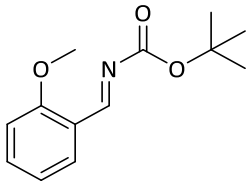

Synthesised according to General Procedure I on a 10 mmol scale to afford the title compound as a clear oil in 94% yield (2.2 g).

^{1}H NMR (400 MHz, $CDCl_3$) δ ppm 9.38 (s, 1 H), 8.12 (dd, *J*=7.8, 1.7 Hz, 1 H), 7.54-7.50 (m, 1 H), 6.90 - 7.04 (m, 2 H), 3.91 (s, 3 H), 1.59 (s, 9 H);

^{13}C NMR (100 MHz, $CDCl_3$) δ 165.6, 163.0, 160.7, 134.9, 128.1, 122.3, 120.5, 111.0, 81.6, 55.3, 27.7.

All data reported is in accordance with literature values.[137]

tert-butyl [(E)-(3-methylphenyl)methylidene]carbamate **52g**

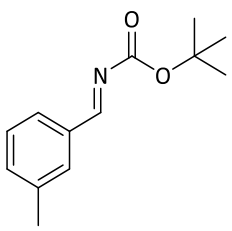

Synthesised according to General Procedure I on a 10 mmol scale to afford the title compound as a clear oil in 96% yield (2.1 g).

^{1}H NMR (400 MHz, $CDCl_3$) δ 8.87 (s, 1 H), 7.79 (s, 1 H), 7.71 - 7.66 (m, 1 H), 7.40 - 7.36 (m, 2 H), 2.41 (s, 3 H), 1.60 (s, 9 H);

^{13}C NMR (100 MHz, $CDCl_3$) δ 170.1, 162.8, 138.7, 134.4, 134.0, 130.1, 128.7, 128.0, 82.1, 27.9, 21.1.

All data reported is in agreement with the literature.[140]

tert-butyl [(E)-(4-methylphenyl)methylidene]carbamate **52h**

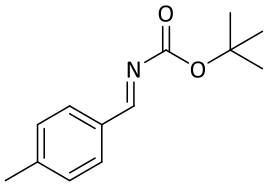

Synthesised according to General Procedure I on a 10 mmol scale to afford the title compound as a clear oil in 96% yield (2.1 g).

^{1}H NMR (400 MHz, $CDCl_3$) δ 8.89 (s, 1 H), 7.82 (d, *J*=8.1 Hz, 2 H), 7.29 (d, *J* = 8.1 Hz), 2.43 (s, 3 H), 1.60 (s, 9 H);

^{13}C NMR (100 MHz, $CDCl_3$) δ 170.2, 163.0, 144.8, 131.7, 130.5, 129.8, 82.3, 28.1, 22.0.

All data is consistent with those reported in the literature.[139]

tert-butyl [(E)-(2-chlorophenyl)methylidene]carbamate **52i**

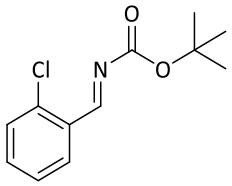

Synthesised according to General Procedure I on a 10 mmol scale to afford the title compound as a clear oil in 92% yield (2.2 g).

^{1}H NMR (400 MHz, $CDCl_3$) δ 9.29 (s, 1 H), 8.20 (dd, *J*=7.9, 1.3 Hz, 1 H), 7.51 - 7.42 (m, 2 H), 7.40 7.31 (m, 1 H), 1.60 (s, 9 H);

^{13}C NMR (100 MHz, $CDCl_3$) δ 165.7, 162.4, 137.9, 135.1, 134.2, 130.2, 129.1, 127.1, 82.6, 27.9.

All data reported is in agreement with the literature.[140]

tert-butyl [(E)-(4-fluorophenyl)methylidene]carbamate **52j**

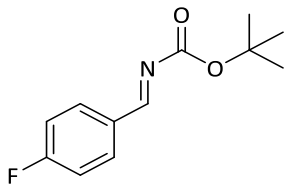

Synthesised according to General Procedure I on a 10 mmol scale to afford the title compound as a white amorphous solid in 94% yield (2.1 g).

^{1}H NMR (400 MHz, $CDCl_3$) δ 8.86 (s, 1 H), 7.93-7.97 (m, 2H), 7.17 (t, *J*=8.6 Hz, 2 H), 1.60 (s, 9 H);

^{13}C NMR (100 MHz, $CDCl_3$) δ 168.6, 167.5, 164.9, 162.6, 132.8, 132.7, 130.6, 116.5, 116.3, 82.6, 28.1.

All data is consistent with those reported in the literature.[139]

tert-butyl [(E)-(pyridin-3-yl)methylidene]carbamate **52k**

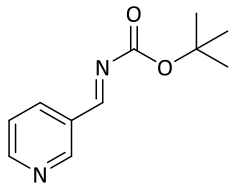

Synthesised according to General Procedure I on a 10 mmol scale to afford the title compound as a white solid in 97% yield (2.0 g).

MP 152 – 154 °C;

^{1}H NMR (400 MHz, $CDCl_3$) δ 9.03 (d, *J*=1.5 Hz, 1 H), 8.90 (s, 1 H), 8.78 (dd, *J* = 4.7, 1.7 Hz, 1 H), 8.31 (dt, *J* = 7.9, 1.9 Hz, 1 H), 7.47 - 7.41 (m, 1 H), 1.61 (s, 9 H);

^{13}C NMR (100 MHz, $CDCl_3$) δ 166.9, 162.2, 154.1, 152.5, 136.0, 130.0, 124.1, 83.0, 28.0.

All data is consistent with those reported in the literature.[139]

tert-butyl [(E)-(3-bromophenyl)methylidene]carbamate **52l**

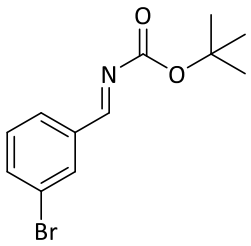

Synthesised according to General Procedure I on a 10 mmol scale to afford the title compound as a clear oil in 95% yield (2.7 g).

^{1}H NMR (400 MHz, $CDCl_3$) δ 8.79 (s, 1 H), 8.12 (t, *J*=1.6 Hz, 1 H), 7.80 (d, *J*=7.8 Hz, 1 H), 7.66 - 7.72 (m, 1 H), 7.37 (t, *J*=7.8 Hz, 1 H), 1.60 (s, 9 H);

^{13}C NMR (100 MHz, $CDCl_3$) δ 168.0, 162.3, 136.4, 136.2, 132.4, 130.5, 129.2, 123.3, 82.8, 28.1.
All data is consistent with those reported in the literature.[139]

tert-butyl [(E)-(naphthalen-1-yl)methylidene]carbamate **52m**

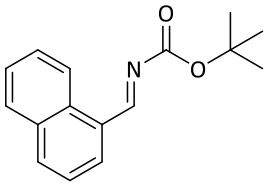

Synthesised according to General Procedure I on a 10 mmol scale to afford the title compound as a white amorphous solid in 94% yield (2.4 g).

^{1}H NMR (400 MHz, $CDCl_3$) δ 9.56 (s, 1 H), 8.93 (d, J=8.6 Hz, 1 H), 8.20 (dd, J=7.2, 1.1 Hz, 1 H), 8.07 (d, J=8.1 Hz, 1 H), 7.92 (d, J=8.1 Hz, 1 H), 7.64 - 7.70 (m, 1 H), 7.55 - 7.61 (m, 2 H), 1.64 (s, 9 H);

^{13}C NMR (100 MHz, $CDCl_3$) δ 169.2, 163.0, 134.5, 133.9, 132.1, 132.0, 129.5, 129.0, 128.3, 126.7, 125.3, 124.1, 82.4, 28.2.
All data is consistent with those reported in the literature.[139]

tert-butyl [(E)-(4-chlorophenyl)methylidene]carbamate **52n**

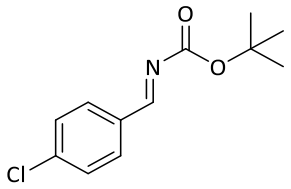

Synthesised according to General Procedure I on a 10 mmol scale to afford the title compound as a clear oil in 96% yield (2.3 g).

^{1}H NMR (400 MHz, $CDCl_3$) δ 8.84 (s, 1 H), 7.87 (d, *J*=8.5 Hz, 2 H), 7.46 (d, *J*=8.5 Hz, 2 H), 1.60 (s, 9 H);

^{13}C NMR (100 MHz, CDCl3) δ 168.3, 162.3, 139.8, 132.5, 131.3, 129.3, 82.5, 27.9.

All data reported is in agreement with the literature.[140]

tert-butyl [(E)-cyclohexylmethylidene]carbamate **52o**

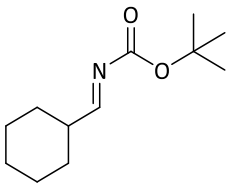

According to a literature procedure,[79] a RBF was charged with cesium carbonate (1.64 g, 10.0 mmol, 10 equiv) and under vacuum the solid was dried using a heat gun. Once cool, dry CH_2Cl_2 (10 mL) was added under argon followed by the addition of *N*-(tert-butoxycarbonyl)–α-(phenylsulfonyl)cyclohexylamine **202** (351 mgs, 1.0 mmol, 1.0 equiv) in one portion. The reaction mixture was stirred at room temperature for 10 hours until disappearance of the amidosulfone starting material was observed by TLC, after which the reaction mixture was cooled to 0 °C and diluted with pre-cooled hexane (10 mL). The organic layer was washed with water (2 × 10 mL) and brine (10 mL) and subsequently dried over sodium sulfate. The volatiles were removed *in vacuo* to afford the title compound as a clear oil in 98% yield (207 mgs).

^{1}H NMR (400 MHz, $CDCl_3$) δ 8.16 (s, 1H), 2.36 – 2.26 (m, 1H), 1.94 – 1.84 (m, 2H), 1.82 – 1.74 (m, 3H), 1.72 – 1.65 (m, 1H), 1.52 (s, 9H), 1.36 – 1.25 (m, 4H);

^{13}C NMR (100 MHz, $CDCl_3$) δ 178.4, 161.8, 81.0, 48.14, 28.1, 27.9, 27.8, 27.7, 27.4, 25.3, 25.2.

All data reported is in agreement with literature values.[79]

6.3.3 Synthesis and characterization of adducts 191a-o

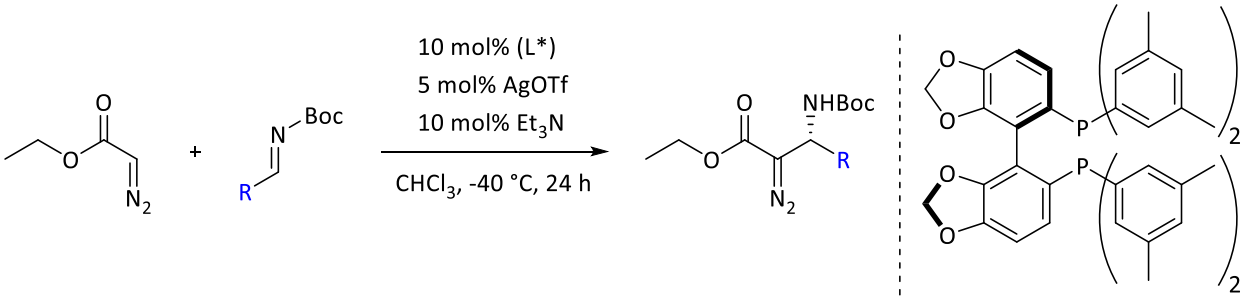

General Procedure J for reaction on 0.10 mmol scale

A reaction tube was charged with silver triflate (1.3 mgs, 0.005 mmol, 5 mol%,) and (*R*)-(+)-5,5'-Bis[di(3,5-xylyl)phosphino]-4,4'-bi-1,3-benzodioxole **196** (7.2 mgs, 0.010 mmol, 10 mol%). Anhydrous chloroform (0.4 mL, 0.167 *m*M) was added under an atmosphere of argon. The resulting mixture was stirred for 1 hour at room temperature after which triethylamine (1.4 µL, 0.010 mmol, 10 mol%) was added and a faint yellow solution was produced after 15 min of stirring at room temperature. The aldimine was then added (0.10 mmol, 1.0 equiv) in $CHCl_3$ (0.2 mL) and the reaction mixture was cooled to -40 °C and stirred at this temperature for 30 min. Electron-rich aldimines produced a bright yellow colour on addition, no colour change was observed on addition of electron-deficient aldimines. Ethyl diazoacetate **171** (0.1 mL, 0.12 mmol, 1.2 equiv, 15% in toluene), which had been pre-cooled was finally added. After a 24 h period, the reaction mixture was passed through a short pad of silica on a glass frit, eluting with diethyl ether. The filtrate was then concentrated *in vacuo* and purified immediately *via* FCC (15 mL of silica) eluting with 10% Et_2O/Petroleum ether to yield the desired compound[xv] as either a yellow oil or yellow solid.

ethyl (3R)-3-{[(tert-butoxy)carbonyl]amino}-2-diazo-3-phenylpropanoate **191a**

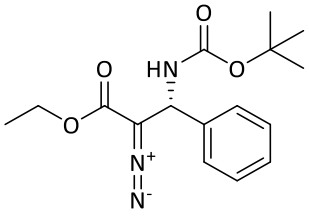

Prepared according to General Procedure J using aldimine **52a** (20.5 mgs, 0.10 mmol) to afford the title compound in 77% isolated yield as a yellow solid (25 mg) and 97% ee [determined by HPLC, Chiralpak AS-H, hexane/isopropanol = 95/5, 1 mL/min, λ = 220 nm, t (minor) = 12.36 min, t (major) = 16.64 min].

MP 78-80°C;

$[\alpha]_D^{25}$ = +27.3 (*c* = 1.0, $CHCl_3$);

[xv] **The quaternary α-carbon cannot be seen by ^{13}C-NMR.**

^{1}H NMR (400 MHz, $CDCl_3$) δ 7.41 - 7.27 (m, 5 H, ArH), 5.66 (d, *J* = 6.6 Hz, 1 H, CHNHC=O), 5.43 (br. s, 1 H, CHNHC=O), 4.21 (q, *J*=7.3 Hz, 2 H, CH_2CH_3), 1.46 (s, 9 H, $OC(CH_3)_3$), 1.25 (t, *J*=7.2 Hz, 3 H, CH_2CH_3);

^{13}C-NMR (100 MHz, $CDCl_3$), δ 165.9 (OC=O), 154.9 (NC(=O)OC), 139.1 (ArC), 128.9 (ArCH), 128.0 (ArCH), 126.2 (ArCH**)**, 80.4 ($OC(CH_3)_3$), 61.0 (CH_2CH_3), 51.2 (CHNHC=O), 28.3 ($OC(CH_3)_3$), 14.4 (CH_2CH_3);

IR ν_{max}/cm^{-1} 3346, 2978, 2095, 1697, 1497, 1167;

HRMS (ESI+): calcd for $C_{16}H_{21}N_3O_4$ $[M+Na]^+$ 319.1532, found 342.1422.

ethyl (3S)-3-{[(tert-butoxy)carbonyl]amino}-2-diazo-3-(thiophen-2-yl)propanoate **191b**

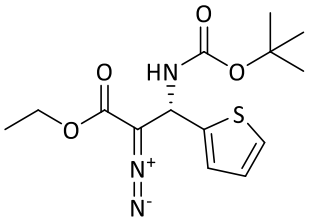

Prepared according to General Procedure J using aldimine **52b** (21.1 mgs, 0.10 mmol) to afford the title compound in 81% isolated yield as a yellow oil (27 mg), and 97% ee [determined by HPLC, Chiralpak AD-H, hexane/isopropanol = 95/5, 1 mL/min, λ = 220 nm, t (minor) = 11.57 min, t (major) = 16.81 min].

$[\alpha]_D^{25}$ = +8.6 (*c* = 1.1, $CHCl_3$);

^{1}H-NMR(400 MHz, $CDCl_3$) δ 7.28-7.21 (m, ArH), 7.01 – 6.94 (m, 2 H, ArH), 5.87 (d, *J*=7.9 Hz, 1 H, CHNHC=O), 5.49 (br. s., 1 H, CHNHC=O), 4.25 (q, *J*=7.1 Hz, 2 H, CH_2CH_3), 1.47 (s, 9 H, $OC(CH_3)_3$), 1.27 (t, *J*=7.1 Hz, 3 H, CH_2CH_3);

^{13}C-NMR (100 MHz, $CDCl_3$), δ 165.7 (OC=O), 154.7 (NC(=O)OC), 143.3 (ArC), 127.2 (ArCH), 125.3 (ArCH), 124.9 (ArCH), 80.7 ($OC(CH_3)_3$), 61.2 (CH_2CH_3), 48.1 (CHNHC=O), 28.4 ($OC(CH_3)_3$), 14.5 (CH_2CH_3);

HRMS (ESI+): calcd for $C_{14}H_{19}N_3O_4S$ 348.0989 $[M+Na]^+$, found 348.0987.

All data reported is consistent with those found in the literature.[141]

ethyl (3S)-3-{[(tert-butoxy)carbonyl]amino}-2-diazo-3-(furan-2-yl)propanoate **191c**

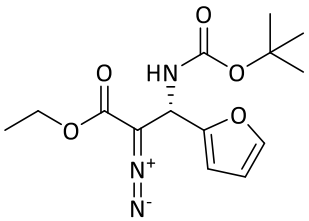

Prepared according to General Procedure J using aldimine **52c** (19.5 mgs, 0.10 mmol) which afforded the desired compound in 70% isolated yield as a yellow oil (22 mg) and 98% ee [determined by HPLC, Chiralpak AD-H, hexane/isopropanol = 95/5, 1 mL/min, λ = 220 nm, t (minor) = 9.44 min, t (major) = 13.75 min].

$[\alpha]_D^{25}$ = +12.0 (*c* = 1.0, $CHCl_3$).

^{1}H-NMR(400 MHz, $CDCl_3$) δ 7.36 (s, 1 H, ArH), 6.37 - 6.31 (m, 1 H, ArH), 6.28 (d, J = 3.1 Hz, 1H, ArH), 5.70 (d, *J*=7.6 Hz, 1 H, CHNHC=O), 5.39 (br. s, 1 H, CHNHC=O), 4.23 (q, *J*=7.2 Hz, 2 H, CH_2CH_3), 1.46 (s, 9 H, $OC(CH_3)_3$), 1.26 (t, *J*=7.1 Hz, 3 H, CH_3CH_2);

^{13}C-NMR (100 MHz, $CDCl_3$) δ 165.7 (O<u>C</u>=O), 154.8 (N<u>C</u>(=O)OC), 151.3 (Ar<u>C</u>), 142.6 (Ar<u>C</u>H), 110.7 (Ar<u>C</u>H), 107.2 (Ar<u>C</u>H), 80.7 (O<u>C</u>(CH_3)$_3$), 61.2 (<u>C</u>$H_2$$CH_3$), 46.2 (<u>C</u>HNHC=O), 28.4 (OC(<u>C</u>H_3)$_3$), 14.6 (CH_2<u>C</u>H_3);

HRMS (ESI+): calcd for $C_{14}H_{19}N_3O_5$ 332.1217 $[M+Na]^+$, found 332.1216.

All data reported is consistent with those found in the literature.[141]

<u>ethyl (3R)-3-{[(tert-butoxy)carbonyl]amino}-2-diazo-3-(naphthalen-2-yl)propanoate **191d**</u>

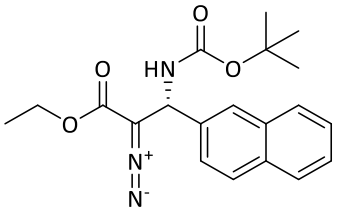

Prepared according to the General Procedure J using aldimine **52d** (25.5 mgs, 0.10 mmol) which afforded the desired compound in 81% isolated yield as an amorphous, yellow solid (29 mg) and 98% ee. [determined by HPLC, Chiralpak AD-H, hexane/isopropanol = 95/5, 1 mL/min, λ = 220 nm, t (minor) = 14.66 min, t (major) = 18.32 min].

$[\alpha]_D^{25}$ = +22.9 (*c* = 1.1, $CHCl_3$);

^{1}H-NMR (400 MHz, $CDCl_3$) δ 7.93-7.77 (m, 4 H, Ar<u>H</u>), 7.55 - 7.41 (m, 3 H, Ar<u>H</u>), 5.84 (d, *J*=7.5 Hz, 1 H, C<u>H</u>NHC=O), 5.50 (br. s, 1 H, CHN<u>H</u>C=O), 4.23 (q, *J*=7.1 Hz, 2 H, C<u>H</u>$_2$$CH_3$), 1.47 (s, 9 H, OC(C<u>H</u>$_3$)$_3$), 1.25 (t, *J*=7.1 Hz, 3 H, CH_2C<u>H</u>$_3$);

^{13}C-NMR (100 MHz, $CDCl_3$) δ 166.1 (O<u>C</u>=O), 155.1 (N<u>C</u>(=O)OC), 136.6 (Ar<u>C</u>), 133.4 (Ar<u>C</u>), 133.1 (Ar<u>C</u>), 129.0 (Ar<u>C</u>H), 128.2 (Ar<u>C</u>H), 127.8 (Ar<u>C</u>H), 126.6 (Ar<u>C</u>H), 126.4 (Ar<u>C</u>H), 125.1 (Ar<u>C</u>H), 124.3 (Ar<u>C</u>H), 80.6 (O<u>C</u>(CH_3)$_3$), 61.2 (<u>C</u>$H_2$$CH_3$), 51.6 (<u>C</u>HNHC=O), 28.5 (OC(<u>C</u>H_3)$_3$), 14.5 (CH_2<u>C</u>H_3);

IR ν_{max}/cm^{-1} 3342, 2978, 2093, 1695, 1506, 1392, 1164.

HRMS (ESI+): calcd for $C_{20}H_{23}N_3O_4$ $[M+Na]^+$ 392.1577, found 392.1581.

<u>ethyl (3R)-3-{[(tert-butoxy)carbonyl]amino}-2-diazo-3-(4-methoxyphenyl)propanoate **191e**</u>

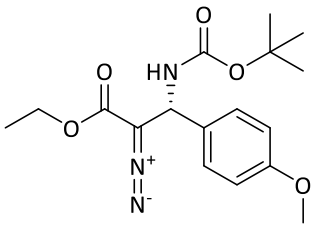

Prepared according to the General Procedure J using aldimine **52e** (23.5 mgs, 0.10 mmol) to afford the title compound in 80% isolated yield as a yellow solid (28 mg) and 98%ee [determined by HPLC, Chiralpak AD-H, hexane/isopropanol = 95/5, 1 mL/min, λ = 220 nm, t (major) = 25.17, t (minor) = 27.78 min].

MP 68-70°C;

$[\alpha]_D^{25}$ = +12.3 (*c* = 1.3, $CHCl_3$).

^{1}H-NMR (400 MHz, $CDCl_3$) δ 7.28 (d, *J* = 8.6 Hz, 2H, ArH), 6.90 (d, *J*=8.6 Hz, 2H, ArH), 5.62 (d, *J*=7.3 Hz, 1H, CHNHC=O), 5.32 (br.s, 1H, CHNHC=O), 4.25 (q, *J*=7.1 Hz, 2H, CH_2CH_3), 3.80 (s, 3H, $ArOCH_3$), 1.45 (s, 9H, $(OC(CH_3)_3)$), 1.27 (t, *J*=7.1 Hz, 3H, CH_2CH_3);

^{13}C-NMR (100 MHz, $CDCl_3$) δ 166.0 (OC=O), 159.3 ($ArCOCH_3$), 154.8 (NC(=O)OC), 131.2 (ArC), 127.4 (ArCH), 114.2 (ArCH), 80.3 ($OC(CH_3)_3$), 61.0 (**C**H_2CH_3), 55.3 ($ArOCH_3$), 50.7 (CHNHC=O), 28.3 ($OC(CH_3)_3$), 14.4 (CH_2CH_3);

IR ν_{max}/cm^{-1} 3352, 2978, 2092, 1692, 1511, 1162;

HRMS (ESI+): calcd for $C_{17}H_{23}N_3O_5$ $[M+Na]^+$ 372.1530, found 372.1532.

ethyl (3R)-3-{[(tert-butoxy)carbonyl]amino}-2-diazo-3-(2-methoxyphenyl)propanoate **191f**

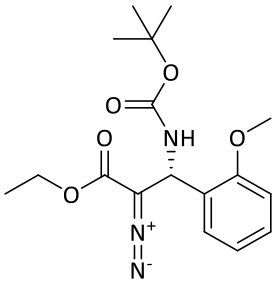

Prepared according to the General Procedure J using aldimine **52f** (23.5 mgs, 0.10 mmol) to afford the title compound in 86% isolated yield as a yellow oil (30 mg) and 96% ee [determined by HPLC, Chiralpak AD-H, hexane/isopropanol = 95/5, 1 mL/min, λ = 220 nm, t (major) = 16.29 min, t (minor) = 19.79 min].

$[\alpha]_D^{25}$ = +4.5 (*c* =1.2, $CHCl_3$);

^{1}H-NMR (400 MHz, $CDCl_3$) δ 7.37 - 7.23 (m, 2 H, ArH), 6.98 - 6.88 (m, 2 H, ArH), 5.83 (br. s., 2 H, CHNHC=O & CHNHC=O), 4.17 (q, *J*=7.1 Hz, 2 H, CH_2CH_3), 3.87 (s, 3 H, $ArOCH_3$), 1.46 (s, 9 H, $OC(CH_3)_3$), 1.23 (t, *J*=7.1 Hz, 3 H, CH_2CH_3);

^{13}C-NMR (100 MHz, $CDCl_3$) δ 166.3 (OC=O), 156.8 (ArC), 154.8 (NC(=O)OC)), 129.2 (ArCH), 128.4 (ArCH), 127.4 (ArC), 120.8 (ArCH), 110.7 (ArCH), 80.2 ($OC(CH_3)_3$), 60.9 (CH_3CH_2), 55.4 ($ArOCH_3$), 47.8 (CHNHC=O), 28.4 ($OC(CH_3)_3$), 14.5 (CH_2CH_3);

IR ν_{max}/cm^{-1} 3353, 2976, 2093, 1695, 1602, 1491, 1392, 1165.

HRMS (ESI+): calcd for $C_{17}H_{23}N_3O_5$ $[M+Na]^+$ 372.1527, found 372.1530.

ethyl (3R)-3-{[(tert-butoxy)carbonyl]amino}-2-diazo-3-(3-methylphenyl)propanoate **191g**

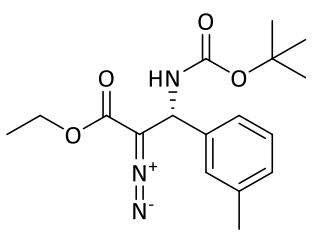

Prepared according to the General Procedure J using aldimine **52g** (21.9 mgs, 0.10 mmol) to afford the title compound in 75% isolated yield as a yellow oil (25 mg) and 98% ee [determined by HPLC, Chiralpak AD-H, hexane/isopropanol = 95/5, 1 mL/min, λ = 220 nm, t (major) = 14.42 min, t (minor) = 15.84 min].

$[\alpha]_D^{25}$=+22.3 (*c* = 1.0, $CHCl_3$);

^{1}H-NMR (400 MHz, $CDCl_3$) δ 7.46-7.33 (m, 1 H, ArH), 7.31-7.16 (m, 3 H, ArH), 5.74 (d, *J*=7.3 Hz, 1 H, CHNHC=O), 5.47 (br. s., 1 H, CHNHC=O), 4.33 (q, *J*=7.1 Hz, 2 H, CH_3CH_2), 2.47 (s, 3 H, $ArCH_3$), 1.57 (s, 9 H, $OC(CH_3)_3$), 1.37 (t, *J*=7.1 Hz, 3 H, CH_2CH_3);

^{13}C-NMR (100 MHz, $CDCl_3$) δ 166.1 (OC=O), 155.0 (NC(=O)OC), 139.2 ArC), 138.8 (ArC), 129.0 (ArCH), 128.9 (ArCH), 127.0 (ArCH), 123.3 (ArCH), 80.5 ($OC(CH_3)_3$) , 61.1 (CH_3CH_2), 51.3 (CHNHC=O), 28.5 ($OC(CH_3)_3$), 21.6 ($ArCH_3$), 14.5 (CH_2CH_3);

IR ν_{max}/cm^{-1} 3351, 2979, 2093, 1698, 1491, 1368, 1163;

HRMS (ESI+): calcd for $C_{17}H_{23}N_3O_4$ $[M+Na]^+$ 356.1577, found 356.1581.

ethyl (3R)-3-{[(tert-butoxy)carbonyl]amino}-2-diazo-3-(4-methylphenyl)propanoate **191h**

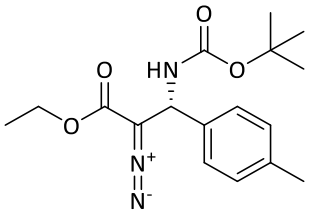

Prepared according to the General Procedure J using aldimine **52h** (21.9 mgs, 0.10 mmol) to afford the title compound as a yellow solid in 70% isolated yield (22 mg) and 98% ee [determined by HPLC, Chiralpak AD-H, hexane/isopropanol = 95/5, 1 mL/min, λ = 220 nm, t (major) = 15.67 min, t (minor) = 16.86 min].

MP 74-76°C;

$[\alpha]_D^{25}$ = +13.1 (*c* =1.3, $CHCl_3$).

^{1}H-NMR (400 MHz, $CDCl_3$) δ 7.23 (d, *J*=8.1 Hz, 2 H, ArH), 7.16 (d, *J*=8.1 Hz, 2 H, ArH), 5.62 (d, *J*=7.5 Hz, 1 H, CHNHC=O), 5.35 (br. s., 1 H, CHNHC=O), 4.21 (q, *J*=7.2 Hz, 2 H, CH_2CH_3), 2.33 (s, 3 H, $ArCH_3$), 1.45 (s, 9 H, $OC(CH_3)_3$), 1.25 (t, *J*=7.1 Hz, 3 H, CH_2CH_3);

^{13}C NMR (100 MHz, $CDCl_3$) δ 166.1 (OC=O), 155.0 (NC(=O)OC), 137.9 (ArC), 136.3 (ArC), 129.7 (ArCH), 126.2 (ArCH), 80.3 ($OC(CH_3)_3$), 61.1 (CH_2CH_3), 50.9 (CHNHC=O), 28.5 ($OC(CH_3)_3$), 21.2 ($ArCH_3$), 14.6 (CH_2CH_3);

IR ν_{max}/cm^{-1} 3353, 2978, 2093, 1697, 1512, 1392, 1167.

HRMS (ESI+): calcd for $C_{17}H_{23}N_3O_4$ $[M+Na]^+$ 356.1581. found 356.1581.

ethyl (3R)-3-{[(tert-butoxy)carbonyl]amino}-3-(2-chlorophenyl)-2-diazopropanoate **191i**

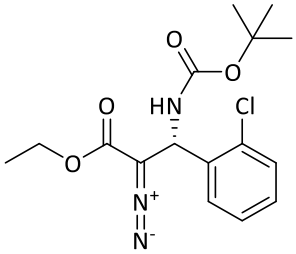

Prepared according to the General Procedure J using aldimine **52i** (23.9 mgs, 0.10 mmol) to afford the title compound in 80% isolated yield (28 mg) and 94% ee [determined by HPLC, Chiralpak AD-H, hexane/isopropanol = 95/5, 1 mL/min, λ = 220 nm, t (major) = 16.74 min, t (minor) = 19.41 min].

$[\alpha]_D^{25}$ = +104.9 (*c* =1.0, $CHCl_3$);

^{1}H NMR (400 MHz, $CDCl_3$) δ 7.47 (d, *J*=7.3 Hz, 1 H, ArH), 7.38 (dd, *J*=7.6, 1.4 Hz, 1 H, ArH), 7.32 - 7.21 (m, 2 H, ArH), 5.94 (d, *J*=7.7 Hz, 1 H, CHNHC=O), 5.74 (br. s, 1 H, CHNHC=O), 4.37 - 4.01 (m, 2 H, CH_2CH_3), 1.44 (s, 9 H, $OC(CH_3)_3$), 1.23 (t, *J*=7.1 Hz, 3 H, CH_2CH_3);

^{13}C-NMR (100 MHz, $CDCl_3$) δ 166.0 (OC=O), 154.8 (NC(=O)OC), 136.8 (ArC), 132.8 (ArC), 130.1 (ArCH), 129.2 (ArCH), 128.2 (ArCH), 127.1 (ArCH), 80.5 ($OC(CH_3)_3$), 61.3 (CH_2CH_3), 49.34 (CHNHC=O), 28.59 ($OC(CH_3)_3$), 14.65 (CH_2CH_3);

IR ν_{max}/cm^{-1} 3343, 2977, 2360, 2096, 1698, 1476, 1169.

HRMS (ESI+): calcd for $C_{16}H_{20}ClN_3O_4$ $[M+Na]^+$ 376.1036, found 376.1035.

ethyl (3R)-3-{[(tert-butoxy)carbonyl]amino}-2-diazo-3-(4-fluorophenyl)propanoate **191j**

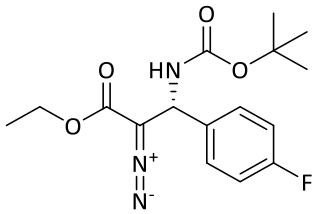

Prepared according to the General Procedure J using aldimine **52j** (22.3 mgs, 0.10 mmol) which afforded the title compound in 76% isolated yield as a yellow solid (25 mg) and 96% ee. [determined by HPLC, Chiralpak AD-H, hexane/isopropanol = 95/5, 1 mL/min, λ = 220 nm, t (major) = 15.31 min, t (minor) = 17.15 min].

MP 82-86°C;

$[\alpha]_D^{25}$ = +29.5(*c* =1.1, $CHCl_3$);

^{1}H-NMR (400 MHz, $CDCl_3$) δ ppm 7.34-7.31 (m, 2 H, ArH), 7.06-7.02 (m, 2 H, ArH), 5.64 (d, *J*=7.4 Hz, 1 H, CHNHC=O), 5.41 (br. s, 1 H, CHNHC=O), 4.22 (q, *J*=7.1 Hz, 2 H, CH_2CH_3), 1.45 (s, 9 H, $OC(CH_3)_3$), 1.25 (t, *J*=7.1 Hz, 3 H, CH_2CH_3);

^{13}C-NMR (100 MHz, $CDCl_3$) δ 165.79 (O**C**=O), 163.6 & 161.1 (d, J_{CF} = 247.2 Hz, ArCF), 154.9 (NC(=O)OC), 134.9 (ArC), 127.9 (ArCH), 127.9 (ArCH), 115.8 (ArCH), 115.6 (ArCH), 80.5 ($OC(CH_3)_3$), 61.1 (CH_2CH_3), 50.8 (CHNHC=O), 28.3 ($OC(CH_3)_3$), 14.4 (CH_2CH_3);

^{19}F-NMR δ -114.30;

IR ν_{max}/cm^{-1} 3346, 2980, 2095, 1694, 1509, 1158.

ethyl (3R)-3-{[(tert-butoxy)carbonyl]amino}-2-diazo-3-(pyridin-3-yl)propanoate **191k**

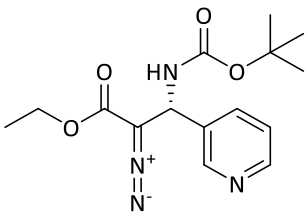

Prepared according to the General Procedure J using aldimine **52k** (20.6 mgs, 0.10 mmol) to afford the title compound as a yellow oil in 88% isolated yield and 92% ee [determined by HPLC, Chiralpak AD-H, hexane/isopropanol = 95/5, 1 mL/min, λ = 220 nm, t (minor) = 36.21 min, t (major) = 45.04 min].

[α]$_D^{25}$ = +33.8 (*c* =0.145, $CHCl_3$);

^{1}H-NMR (500 MHz, $CDCl_3$) δ 8.62 (d, *J*=1.9 Hz, 1 H, ArH), 8.54 (d, *J*=3.8 Hz, 1 H, ArH), 7.73-7.65 (m, 1 H, ArH), 7.29 (dd, *J*=7.9, 4.8 Hz, 1 H, ArH), 5.70 (br. s., 1 H, CHNHC=O & CHNHC=O), 4.16 - 4.27 (m, 2 H, CH_2CH_3), 1.45 (s, 9 H, $OC(CH_3)_3$), 1.25 (t, *J* = 7.1 Hz, 3 H, CH_2CH_3);

^{13}C NMR (126 MHz, $CDCl_3$) δ 165.8 (OC=O), 155.0 (NC(=O)OC), 149.4 (ArCH), 148.2 (ArCH), 135.0 (ArC), 134.1 (ArCH), 123.6 (ArCH), 80.9 ($OC(CH_3)_3$), 61.4 (CH_2CH_3), 49.6 (CHNHC=O), 28.4 ($OC(CH_3)_3$), 14.5 (CH_2CH_3);

IR ν_{max}/cm^{-1} 3338, 2979, 2925, 2094, 1695, 1513, 1392, 1166;

HRMS (ESI+): calcd for $C_{15}H_{20}N_4O_4$ $[M+H]^+$ 321.1557, found 321.1559.

ethyl (3R)-3-(3-bromophenyl)-3-{[(tert-butoxy)carbonyl]amino}-2-diazopropanoate **191l**

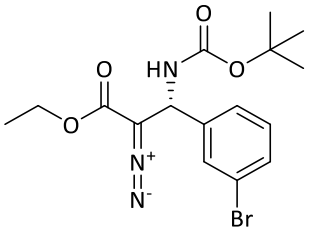

Prepared according to the General Procedure J using aldimine **52l** (28.4 mgs, 0.10 mmol) to afford the title compound as a yellow oil in 72% isolated yield (28 mg) and 95% ee [determined by HPLC, Chiralpak AS-H, hexane/isopropanol = 95/5, 1 mL/min, λ = 220 nm, t (minor) = 9.65 min, t (major) = 13.11 min].

[α]$_D^{25}$ = +30.5 (*c* =1.3 , $CHCl_3$);

^{1}H-NMR(400 MHz, $CDCl_3$) δ 7.53 (s, 1 H, ArH), 7.46 (d, *J*=7.8 Hz, 1 H, ArH), 7.18 - 7.36 (m, 2 H, ArH), 5.67 (d, *J*=7.6 Hz, 1 H, CHNHC=O), 5.48 (br. s, 1 H, CHNHC=O), 4.18-4.40 (m, 2H, CH_2CH_3), 1.49 (s, 9 H, $OC(CH_3)_3$), 1.27 (t, *J*=7.1 Hz, 3 H, CH_2CH_3);

^{13}C NMR (100 MHz, $CDCl_3$) δ 165.8 (O<u>C</u>=O), 155.0 (N<u>C</u>(=O)OC), 141.6 (Ar<u>C</u>), 131.3 (Ar<u>C</u>H), 130.5 (Ar<u>C</u>H), 129.5 (Ar<u>C</u>H), 125.0 (Ar<u>C</u>H), 123.0 (Ar<u>C</u>), 80.8 (O<u>C</u>(CH_3)$_3$), 61.3 ($\underline{C}H_2CH_3$), 50.9 (<u>C</u>HNHC=O), 28.4 (OC($\underline{C}H_3$)$_3$), 14.5 ($CH_2\underline{C}H_3$);

IR ν_{max}/cm^{-1} 3341, 2980, 2095, 1695, 1571, 1475, 1369, 1163;

HRMS (ESI+): calcd for $C_{16}H_{20}BrN_3O_4$ $[M+Na]^+$ 420.0530, found 420.0529.

<u>ethyl (3R)-3-{[(tert-butoxy)carbonyl]amino}-2-diazo-3-(naphthalen-1-yl)propanoate **191m**</u>

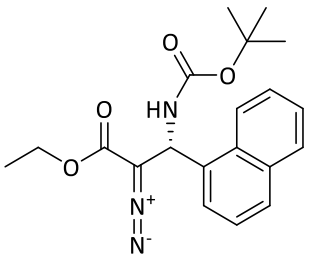

Prepared according to General Procedure J using aldimine **52m** (25.5 mgs, 0.10 mmol) to afford the title compound in 84% isolated yield as a yellow oil (31 mg) and 96% ee [determined by HPLC, Chiralpak AD-H, hexane/isopropanol = 95/5, 1 mL/min, λ = 220 nm, t (major) = 21.15 min, t (minor) = 22.85 min].

$[\alpha]_D^{25}$= +46.5 (*c* = 1.4, $CHCl_3$);

^{1}H-NMR (400 MHz, $CDCl_3$) δ 8.02 (d, *J*=8.3 Hz, 1 H, Ar<u>H</u>), 7.88 (d, *J*=7.9 Hz, 1 H, Ar<u>H</u>), 7.82 (d, *J*=8.2 Hz, 1 H, Ar<u>H</u>), 7.60 - 7.49 (m, 3 H, Ar<u>H</u>), 7.48 - 7.42 (m, 1 H, Ar<u>H</u>), 6.43 (d, *J*=7.0 Hz, 1 H, C<u>H</u>NHC=O), 5.30 (br. s., 1 H, CHN<u>H</u>C=O), 4.25 (q, *J*=7.1 Hz, 2 H, $C\underline{H}_2CH_3$), 1.44 (br. s., 9 H, OC($C\underline{H}_3$)$_3$), 1.26 (t, *J*=7.1 Hz, 3 H, $CH_2C\underline{H}_3$);

^{13}C-NMR (100 MHz, $CDCl_3$), δ 165.8 (O<u>C</u>=O), 154.9 (N<u>C</u>(=O)OC), 134.3 (Ar<u>C</u>), 134.2 (Ar<u>C</u>), 130.4 (Ar<u>C</u>), 129.2 (Ar<u>C</u>H), 129.1 (Ar<u>C</u>H), 127.0 (Ar<u>C</u>H), 126.2 (Ar<u>C</u>H), 125.3 (Ar<u>C</u>H),), 123.8 (Ar<u>C</u>H), 122.9 (Ar<u>C</u>H), 80.6 ((O<u>C</u>(CH_3)$_3$), 61.3 ($\underline{C}H_2CH_3$), 48.1 (<u>C</u>HNHC=O), 28.4 (OC($\underline{C}H_3$)$_3$), 14.6 ($\underline{C}H_3CH_2$);

IR ν_{max}/cm^{-1} 3341, 2978, 2094, 1694, 1510, 1368, 1165.

HRMS (ESI+): calcd for $C_{20}H_{23}N_3O_4$ $[M+Na]^+$ 392.1577, found 392.1581.

<u>ethyl (3R)-3-{[(tert-butoxy)carbonyl]amino}-3-(4-chlorophenyl)-2-diazopropanoate **191n**</u>

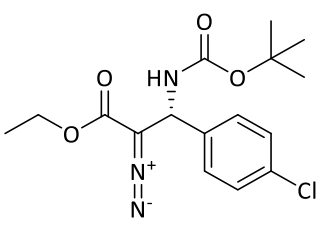

Prepared according to the General Procedure J using aldimine **52n** (23.9 mgs, 0.10 mmol) to afford the title compound in 60% isolated yield as a yellow solid (19 mg) and 96% ee. [determined by HPLC, Chiralpak AD-H, hexane/isopropanol = 95/5, 1 mL/min, λ = 220 nm, t (major) = 15.42 min, t (minor) = 17.49 min].

MP 88-92 °C;

$[\alpha]_D^{25}$ = +32.4 (*c* = 0.75, $CHCl_3$);

^{1}H NMR (400 MHz, $CDCl_3$) δ 7.34 (d, *J*=8.5 Hz, 2 H, ArH), 7.30 (d, *J*=8.5 Hz, 2 H, ArH), 5.63 (d, *J*=7.7 Hz, 1 H, CHNHC=O), 5.42 (br. s., 1 H, CHNHC=O), 4.33 - 4.13 (m, 2 H, CH_2CH_3), 1.45 (s, 9 H, $OC(CH_3)_3$), 1.25 (t, *J*=7.1 Hz, 3 H, CH_2CH_3);

^{13}C-NMR (100 MHz, $CDCl_3$) δ 165.9 (OC=O), 155.0 (NC(=O)OC), 137.9 (ArC), 134.0 (ArC), 129.2 (ArCH), 127.8 (ArCH), 80.7 ($OC(CH_3)_3$), 61.3 (CH_3CH_2), 51.0 (CHNHC=O), 28.4 ($OC(CH_3)_3$), 14.5 (CH_2CH_3);

IR ν_{max}/cm^{-1} 3343, 2876, 2931, 2095, 1695, 1491, 1392, 1166;

HRMS (ESI+): calcd for $C_{16}H_{20}ClN_3O_4$ $[M+Na]^+$ 376.1035, found 376.1036.

ethyl (3R)-3-((tert-butoxycarbonyl)amino)-3-cyclohexyl-2-diazopropanoate **191o**

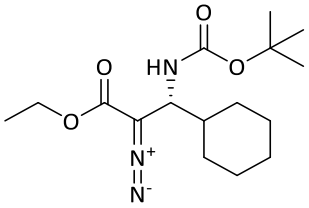

Prepared according to the General Procedure J using aldimine **52o** (42.2 mgs, 0.20 mmol) to afford the title compound as a yellow oil in 72% isolated yield (47 mg) and 29% ee [determined by HPLC, Chiralpak AS-H, hexane/isopropanol = 95/5, 1 mL/min, λ = 220 nm, t (major) = 8.88 min, t (minor) = 13.77 min].

$[\alpha]_D^{25}$ = +2.2 (*c* =1.1 , $CHCl_3$);

^{1}H NMR (500 MHz, $CDCl_3$) δ 5.27 – 5.08 (m, 1H, CHNHC=O), 4.22 (q, *J* = 7.3, 6.2 Hz, 2H, CH_2CH_3), 4.12-4.04 (m, 1H, CHNHC=O), 1.94 – 1.61 (m, 6H), 1.43 (s, 9H), 1.27 (t, *J* = 7.1 Hz, 3H), 1.23-1.12 (m, 3H), 1.05-0.94 (m, 2H);

^{13}C NMR (126 MHz, $CDCl_3$) δ 205.17 (OC=O), 155.52 (NC(=O)OC),, 79.79 ($OC(CH_3)_3$),, 60.85 (CH_2CH_3), 53.86 (CHNHC=O), 41.40 (CHCH(NH)), 30.24 (CH_2), 29.99 (CH_2), 29.84 (CH_2), 28.49 ($OC(CH_3)_3$), 28.37 (CH_2), 26.29 (CH_2), 14.58 (CH_2CH_3);

IR ν_{max}/cm^{-1} 3348.5, 2928.3, 2854.0, 2360.9, 2089.4, 1696.5, 1498.0, 1170.5;

HRMS (ESI+): calcd for $C_{16}H_{27}N_3O_4$ $[M+H]^+$ 348.1899, found 348.1901.

General Procedure K for reaction on 5.0 mmol scale

A reaction tube was charged with silver triflate (12.8 mg, 0.05 mmol, 0.01 equiv) and **196** (72 mg, 0.1 mmol, 0.02 equiv). Under an atmosphere of argon, $CHCl_3$ (2.0 mL) was added and the resulting mixture was stirred for 30 minutes at room temperature. Triethylamine (28 µL, 0.20 mmol, 0.04 equiv) was added to produce a yellow coloured solution of catalyst. Aldimine **52a** (1.0 g, 5.0 mmol) was then

added in $CHCl_3$ (4.0 mL) to produce a brightly coloured yellow solution, after which 4Å molecular sieves were added. The resulting mixture was cooled to -40 ˚C and kept at this temperature for 30 minutes whereupon ethyl diazoacetate (5.2 mL, 6.0 mmol, 1.2 equiv) was added. After 48 h, the reaction was quenched by passing it through a short pad of silica on a glass frit, eluting with diethyl ether. The volatiles were removed *in vacuo* and the resulting yellow crude oil was purified by FCC using 10% diethyl ether/petroleum ether to afford the desired diazo adduct **191a** as a yellow solid (1.28 g) in 81% yield and 96% ee determined by chiral HPLC.

Synthesis of Racemates

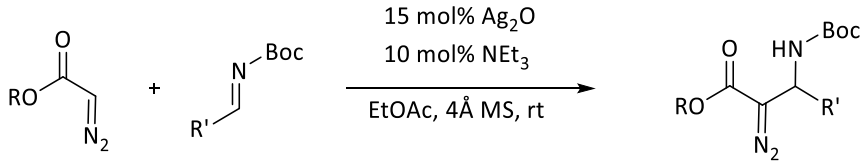

A RBF was charged with aldimine (0.1 mmol, 1.0 equiv), Ag_2O (3.5 mg, 0.015 mmol, 0.15 equiv) followed by 4 Å molecular sieves. Ethyl acetate (1.0 mL) was added under an atmosphere of argon. Triethylamine (1.4 µL, 0.01 mmol, 0.10 equiv) was added and the resulting suspension was stirred for 10 minutes. The diazoester was then added (1.2 equiv) in 0.2 mL of ethyl acetate. Stirring was maintained for a 24 h period after which the reaction mixture was filtered through a pad of celite on a glass frit, eluting with ethyl acetate. The filtrate was concentrated *in vacuo* and purified by FCC.[xvi]

6.3.4 Diazoacetate examples 209a-c

N,N-ditosylhydrazine **205**

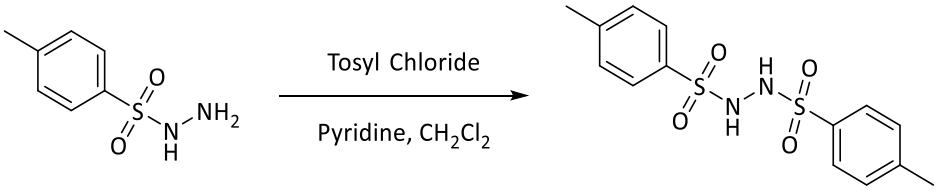

According to a literature procedure[81], a 500 mL flask was charged with tosyl chloride (5.7g, 30 mmol, 1.5eq) and tosyl hydrazide **203** (3.7 g, 20 mmol, 1.0 equiv) and a magnetic stirrer bar. The solids were suspended in anhydrous CH_2Cl_2 (20 mL) and cooled to 0 °C in an ice bath. Pyridine (2.4 mL, 30 mmol, 1.5 equiv) was added in CH_2Cl_2 (20 mL) over a period of 10 minutes. The reaction mixture was allowed to slowly warm to room temperature whereupon stirring was maintained for 3 hours. Diethyl ether (20 mL) was then added, which resulted in the formation of a heavy precipitate. The precipitate was

[xvi] **This protocol for synthesizing racemates is scalable to 5.0 mmol scale.**

broken up with a spatula and transferred to a (100 mL) beaker equipped with a magnetic stirrer bar. Water (20 mL) was added first and then diethyl ether (20 mL) and the mixture was stirred for a further 20 minutes. The suspension was then filtered on a Büchner funnel, where the solid was left to dry for 5 minutes. The solid was then transferred to 250 mL RBF and was suspended in methanol (70 mL). The mixture was then refluxed for 3 hours after which the solution was cooled slowly, crystals of product slowly precipitated out and was collected by filtration with washings of Et_2O. This afforded the desired product in 81% isolated yield (5.50 g) as a white solid.

MP 204 – 206 °C (lit. 210-212 °C)[78];

^{1}H NMR (400 MHz, DMSO-d_6) δ 9.58 (s, 2H, SO_2NH), 7.65 (d, *J* = 8.3 Hz, 4H, ArH), 7.39 (d, *J* = 8.1 Hz, 4H, ArH), 2.40 (s, 6H, $ArCH_3$);

^{13}C NMR (100 MHz, DMSO-d_6) δ 143.5, 135.5, 129.5, 127.8, 21.1.

All data reported is in agreement with the literature[81].

Allyl bromoacetate **208a**

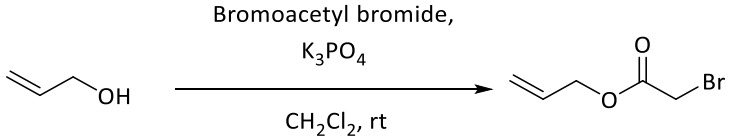

According to a literature procedure[142], a 50 mL RBF was charged with bromoacetyl bromide **207** (0.56 mL, 6.6 mmol, 1.5 equiv) and dry CH_2Cl_2 (15 mL) was added under argon. Allyl alcohol (0.30 mL, 4.4 mmol, 1.0 equiv) was then added and potassium phosphate tribasic (2.3 g, 11 mmol, 2.5 equiv) was added in one portion and the resulting suspension was stirred for 3 hours at room temperature after which the reaction mixture was quenched with water, the organics extracted with CH_2Cl_2 and the combined organics were dried over Na_2SO_4. Removal of volatiles *in vacuo* afforded crude **208a** which was used directly in the next step.

General Procedure L for synthesising α-bromoacetates using $NaHCO_3$ as a base

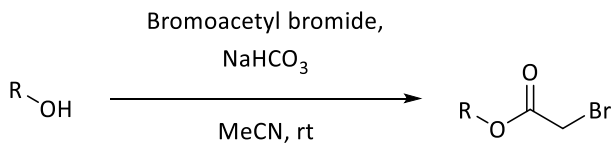

According to a literature procedure[143], alcohols **206b-c** (1.0 equiv) and $NaHCO_3$ were dissolved in acetonitrile (0.2 *m*M) and bromoacetyl bromide **207** (1.5 equiv) was added dropwise at 0 °C. The reaction was stirred for 10 minutes at 0 °C before being quenched with water. The organics were

extracted with CH_2Cl_2 (× 3). The combined organics were dried over Na_2SO_4 before being concentrated *in vacuo*. Pure bromoacetates were then obtained by passing the crude reaction mixture through a short pad of silica eluting with 10% Et_2O/petroleum ether.

Benzyl bromoacetate **208b**

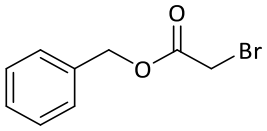

Prepared according to General Procedure L from benzyl alcohol on 10 mmol scale. The title compound was isolated in 99% yield (2.27g) as an orange oil.

^{1}H NMR (400 MHz, $CDCl_3$) δ 7.44 – 7.34 (m, 5H), 5.21 (s, 2H), 3.88 (s, 2H);

^{13}C NMR (100 MHz, $CDCl_3$) δ 167.2, 135.1, 128.8, 128.8, 128.6, 68.1, 26.0.

All data reported is in agreement with the literature[143].

Phenyl 2-bromoacetate **208c**

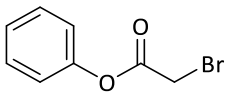

Prepared according to General Procedure L from Phenol on a 10 mmol scale. The title compound was isolated in 20% yield (446 mg) as a pale yellow oil.

^{1}H NMR (400 MHz, $CDCl_3$) δ 7.44 – 7.38 (m, 2H), 7.30 – 7.24 (m, 1H), 7.20 – 7.06 (m, 2H), 4.06 (s, 2H);

^{13}C NMR ($CDCl_3$, 100 MHz) δ 165.5, 150.4, 129.3,125.8, 121.6, 46.8.

All data reported is in agreement with the literature[142].

General Procedure M for Synthesis of Diazoacetates 209a-c

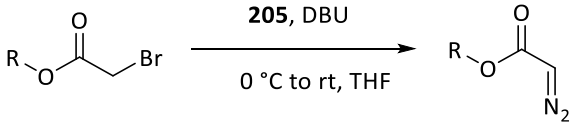

According to a literature procedure[142], bromoacetates **208a-c** (1.0 equiv) and *N,N*-ditosylhydrazine **205** were dissolved in THF (0.4 *m*M) and cooled to 0 °C, after which DBU (2.5 equiv) was then added dropwise. The reaction mixture was allowed to slowly warm to room temperature and was stirred at

this temperature for 30 minutes. The reaction was then quenched with a saturated solution of sodium hydrogen carbonate. The organic phase was extracted (×3) with diethyl ether. The combined organics were washed with brine and dried over sodium sulfate and concentrated *in vacuo*. The crude product was purified by FCC using 10% Et_2O/petroleum ether to afford the product as a yellow oil.

allyl diazoacetate **209a**

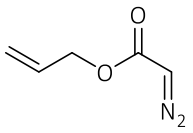

Prepared according to General Procedure M from crude **208a**. The title compound was isolated in quantitative yield (554 mgs) as a yellow oil.

^{1}H NMR (400 MHz, $CDCl_3$) δ 6.00 – 5.87 (m, 1H), 5.36 – 5.22 (m, 2H), 4.77 (s, 1H), 4.66 (d, *J* = 5.7 Hz, 2H);

^{13}C NMR ($CDCl_3$, 100 MHz) δ 46.5, 65.7, 118.6, 132.5, 166.8.

All data reported is in agreement with literature.[144]

Benzyl diazoacetate **209b**

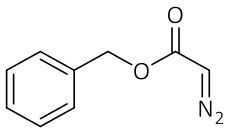

Prepared according to General Procedure M from **208b** on a 5.0 mmol scale to afford the title compound in 84% yield (742 mgs) as a yellow oil.

^{1}H NMR (400 MHz, Chloroform-*d*) δ 7.40 – 7.31 (m, 5H), 5.21 (s, 2H), 4.80 (s, 1H);

^{13}C NMR ($CDCl_3$, 100 MHz) δ 166.5, 135.8, 128.5, 128.2, 128.1, 66.3, 51.8.

All data reported is in agreement with literature[142].

2-diazo-1-phenylethan-1-one **209c**

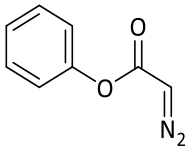

Prepared according to General Procedure M from **208c** on 2.0 mmol scale to afford the title compound in 69% yield (222 mg) as a yellow oil.

^{1}H NMR (400 MHz, $CDCl_3$) δ 7.42 – 7.35 (m, 2H), 7.28 – 7.21 (m, 1H), 7.17 – 7.11 (m, 2H), 5.00 (s, 1H);

^{13}C NMR (100 MHz, $CDCl_3$) δ 166.6, 75.9, 53.7, 25.3.

All data reported is in agreement with literature.[142] .

6.3.5 Synthesis of adducts 210a-c

prop-2-en-1-yl (3R)-3-{[(tert-butoxy)carbonyl]amino}-2-diazo-3-phenylpropanoate **210a**

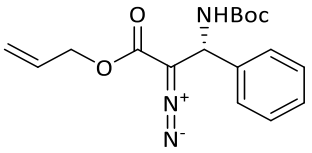

Prepared according to General Procedure G on a 0.20 mmol scale, using diazoacete **209a** (30 mg, 0.24 mmol, 1.2 equiv) to afford the title compound in 79% isolated yield as a yellow oil (52 mgs) and in 94% ee [determined by HPLC, Chiralpak AS-H, hexane/isopropanol =90/10, 1 mL/min, λ = 220 nm, t (minor) = 9.77 min, t (major) = 13.83 min].

$[\alpha]_D^{25}$ = +30.0 (*c* = 1.2, $CHCl_3$);

^{1}H-NMR (500 MHz, $CDCl_3$) δ 7.40 - 7.28 (m, 5 H, ArH), 5.93-5.85 (m, 1 H, $CH_2CH{=}CH_2$), 5.68 (br. s., 1 H, CHNHC=O), 5.37 (br. s, 1 H, CHNHC=O), 5.31 - 5.18 (m, 2 H, $CH_2CH{=}CH_2$), 4.72 - 4.60 (m, 2 H, $CH_2CH{=}CH_2$), 1.45 (s, 9 H, $OC(CH_3)_3$);

^{13}C-NMR (126 MHz, $CDCl_3$) δ 165.7 (OC=O), 155.0 (NC(=O)OC), 139.0 (ArC), 132.1 ($CH_2CH{=}CH_2$), 129.0 (ArCH), 128.2 (ArCH), 126.3 (ArCH), 118.4 ($CH_2CH{=}CH_2$), 80.5 ($OC(CH_3)_3$), 65.6 ($CH_2CH{=}CH_2$), 51.3 (CHNHC=O), 28.4 ($OC(CH_3)_3$);

IR ν_{max}/cm^{-1} 3323, 2095, 1720, 1495, 1114;

HRMS (ESI+): calcd for $C_{17}H_{21}N_3O_4$ $[M+Na]^+$ 354.1424, found 354.1426.

benzyl (3R)-3-{[(tert-butoxy)carbonyl]amino}-2-diazo-3-phenylpropanoate **210b**

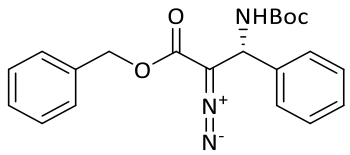

Prepared according to General Procedure G on a 0.20 mmol scale, using diazoacetate **209b** (42 mg, 0.24 mmol, 1.2 equiv) to afford the title compound in 72% isolated yield as a yellow oil (55 mgs) and in 92% ee [determined by HPLC, Chiralpak IA, hexane/isopropanol =95/5, 1 mL/min, λ = 220 nm, t (major) = 25.56 min, t (minor) = 32.25 min].

$[\alpha]_D^{25}$ = +21.9(*c* = 1.1, $CHCl_3$);

^{1}H-NMR (400MHz, $CDCl_3$) δ 7.40 - 7.27 (m, 10 H, ArH), 5.70 (br. s, 1 H, CHNHC=O), 5.42 (br. s, 1 H, NHCH), 5.27 - 5.15 (m, 2 H, $ArCH_2O$), 1.45 (s, 9 H, $(OC(CH_3)_3)$);

^{13}C-NMR (126 MHz, $CDCl_3$) δ 165.8 (OC=O), 155.0 (NC(=O)OC), 139.0 (ArC), 135.9 (ArC), 129.0 (ArCH), 128.7 (ArCH), 128.4 (ArCH), 128.2 (ArCH), 128.1 (ArCH), 126.3 (ArCH), 80.5 ($OC(CH_3)_3$), 66.7 ($ArCH_2O$), 51.3 (CHNHC=O), 28.4 ($OC(CH_3)_3$);

IR ν_{max}/cm^{-1} 3349, 2094, 1690, 1453, 1165;

HRMS (ESI+): calcd for $C_{21}H_{23}N_3O_4$ $[M+Na]^+$ 404.1580, found 404.1578.

(3R)-3-{[(tert-butoxy)carbonyl]amino}-2-diazo-3-phenylpropanoate **210c**

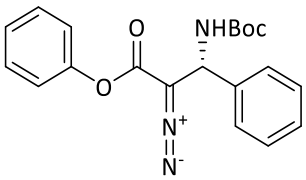

Prepared according to General Procedure G on a 0.20 mmol scale, using diazoacetate **209c** (39 mg, 0.24 mmol, 1.2 equiv) to afford the title compound in 64% isolated yield as a pale yellow solid (47 mgs) and in 88% ee [determined by HPLC, Chiralpak AS-H, hexane/isopropanol =95/5, 1 mL/min, λ = 220 nm, t (major) = 16.75 min, t (minor) = 22.32 min].

MP 102-104 °C;

$[\alpha]_D^{25}$ = +29.0 (*c* = 1.1, $CHCl_3$);

^{1}H-NMR 400 MHz, $CDCl_3$) δ 7.49-7.30 (m, 7 H, ArH), 7.24 - 7.19 (m, 1 H, ArH), 7.11 (d, *J*=6.2 Hz, 2 H, ArH), 5.76 (br. s, 1 H, CHNHC=O), 5.48 (br. s, 1 H, CHNHC=O), 1.48 (s, 9 H, $(OC(CH_3)_3)$);

^{13}C-NMR (126 MHz, $CDCl_3$) δ 164.2 (OC=O), 155.1 (NC(=O)OC), 150.4 (ArC), 138.9 (ArC), 129.5 (ArCH), 129.1 (ArCH), 128.4 (ArCH), 126.4 (ArCH), 125.9 (ArCH), 121.7 (ArCH), 80.7 ($OC(CH_3)_3$), 51.5 (CHNHC=O), 28.4 ($OC(CH_3)_3$);

IR ν_{max}/cm^{-1} 3327, 2097, 1718, 1453, 1137;

HRMS (ESI+): calcd for $C_{20}H_{21}N_3O_4$ $[M+Na]^+$ 390.1424, found 390.142.

6.3.6 Derivatisation of the Mannich adduct

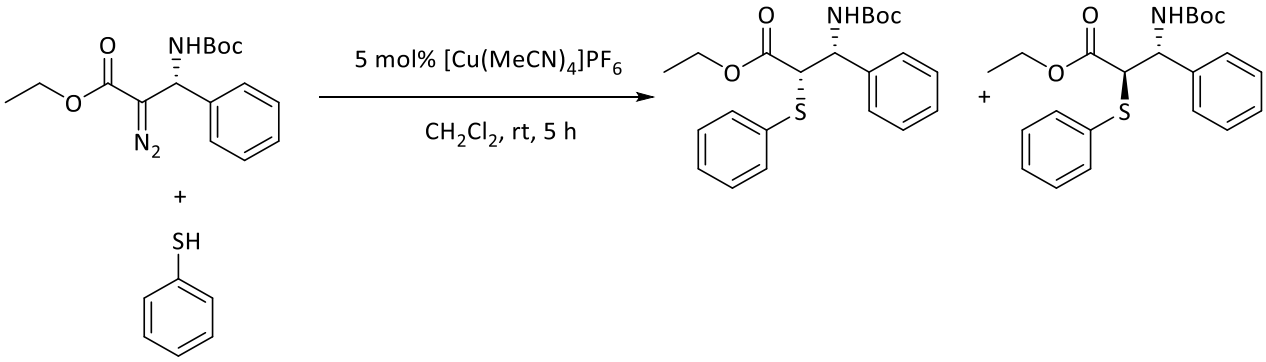

A reaction tube was charged with copper tetrakisacetonitrile hexafluorophosphate (3.8 mg, 0.01 mmol, 0.05 equiv) and dry dichloromethane (2.0 mL) was added under argon. Thiophenol was added in one portion (20 µL, 0.20 mmol, 1.0 equiv) to produce a cloudy solution. Mannich adduct **191a** (64 mg, 0.20 mmol, 1.0 equiv) was subsequently added dropwise in dichloromethane (1.0 mL). The reaction mixture was stirred at room temperature for 5 hours after which the reaction was quenched by passing it through a small pad of silica on a glass frit. The resulting filtrate was collected and concentrated *in vacuo* and the crude residue was purified by FCC using 10% diethyl ether/petroleum ether.

ethyl (2S,3R)-3-((tert-butoxycarbonyl)amino)-3-phenyl-2-(phenylthio)propanoate **213a**

Syn-**213a** obtained in 16% isolated yield (12.8 mg) as a white solid and in 60% ee [determined by HPLC, Chiralpak IA, hexane/isopropanol =90/10, 1 mL/min, λ = 220 nm, t (major) = 13.30 min, t (minor) = 14.93 min].

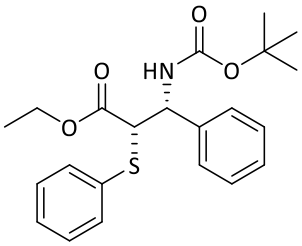

MP 60-62 °C;

[α]$_D^{25}$ = +14.2 (*c* = 1.2, $CHCl_3$);

^{1}H NMR (400 MHz, $CDCl_3$) δ 7.54 – 7.46 (m, 2H, ArH), 7.33 – 7.27 (m, 8H, ArH), 5.88 (d, *J* = 10.6 Hz, 1H, CHNHC=O), 5.48 (dd, *J* = 10.6, 5.8 Hz, 1H, CHNHC=O), 4.31 – 4.10 (m, 2H, CH_2CH_3), 3.99 (d, *J* = 5.8 Hz, 1H, CHSAr), 1.30 (s, 9H, $OC(CH_3)_3$), 1.26 (t, *J* = 7.1 Hz, 3H, CH_2CH_3);

^{13}C NMR (126 MHz, $CDCl_3$) δ 171.8 (OC=O), 154.4 (NC(=O)OC), 134.2 (ArCH), 129.4 (ArCH), 129.2 (ArCH), 128.8 (ArCH), 128.6 (ArCH), 128.3 (ArCH), 127.6 (ArCH), 80.1 ($OC(CH_3)_3$), 61.8 (CHNHC=O), 61.5 (CH_2CH_3), 56.0 (CHSAr), 28.3 ($OC(CH_3)_3$), 14.2 (CH_2CH_3);

IR ν_{max}/cm^{-1} 3353, 3032, 2979, 2931, 1718;

HRMS (ESI+): calcd for $C_{22}H_{27}NO_4S$ $[M+Na]^+$ 424.1553, found 424.1555.

ethyl (2R,3R)-3-((tert-butoxycarbonyl)amino)-3-phenyl-2-(phenylthio)propanoate **213b**

Anti-**213b** obtained in 34% isolated yield (27.1 mg) as a white solid and in 72% ee [determined by HPLC, Chiralpak IA, hexane/isopropanol =90/10, 1 mL/min, λ = 220 nm, t (major) = 20.25 min, t (minor) = 27.90 min].

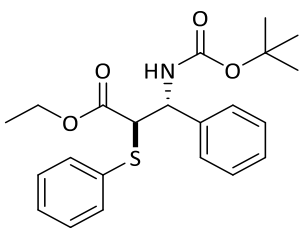

MP 64-66 °C;

$[\alpha]_D^{25}$ = +45.3 (*c* = 1.0, $CHCl_3$);

^{1}H NMR (400 MHz, $CDCl_3$) δ 7.52 – 7.48 (m, 2H, ArH), 7.39 – 7.27 (m, 8H, ArH), 5.68 (t, *J* = 10.2 Hz, 1H, CHNHC=O), 4.64 (d, *J* = 10.6 Hz, 2H, CHNHC=O), 4.30 – 4.11 (m, 2H, CH_2CH_3), 3.89 (d, *J* = 9.8 Hz, 1H, CHSAr), 1.32 – 1.21 (m, 12H, $OC(CH_3)_3$ & CH_2CH_3);

^{13}C NMR (126 MHz, $CDCl_3$) δ 170.96 (OC=O), 154.15 (NC(=O)OC), 135.1 (ArCH), 134.48 (ArCH), 132.0 (ArC), 129.1 (ArCH), 129.0 (ArCH), 128.7 (ArCH), 128.12 (ArCH), 80.17 ($OC(CH_3)_3$), 61.53 (CH_2CH_3), 60.72 (CHNHC=O), 57.68 (CHSAr), 28.22 ($OC(CH_3)_3$), 14.21 (CH_2CH_3);

IR ν_{max}/cm^{-1} 3353, 3032, 2979, 2931, 1718;

HRMS (ESI+): calcd for $C_{22}H_{27}NO_4S$ $[M+Na]^+$ 424.1553, found 424.1552.

ethyl (2Z)-3-[(tert-butoxycarbonyl)amino]-3-phenylprop-2-enoate **214**

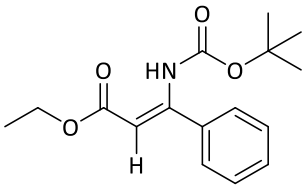

^{1}H NMR (400 MHz, $CDCl_3$) δ 8.06 (d, *J* = 12.0 Hz, 1H), 7.50 – 7.41 (m, 2H), 7.39 – 7.28 (m, 3H), 6.59 (br.s, 1H), 4.21 (q, *J* = 7.1 Hz, 2H), 1.47 (s, 9H), 1.27 (d, *J* = 7.2 Hz, 3H);

^{13}C NMR (126 MHz, $CDCl_3$) δ 171.81, 167.13, 134.18, 130.07, 129.13, 128.82, 128.08, 80.09, 60.64, 28.21, 14.51;

IR ν_{max}/cm^{-1} 3424.9, 3330.2, 3060.3, 2927.4, 2359.2, 1738.2, 1707.1, 1641.3, 1230.2, 1145.6;

HRMS (ESI+): calcd for $C_{16}H_{21}NO_4$ $[M+H]^+$ 292.1543, found 292.1544.

ethyl (2Z)-3-[(tert-butoxycarbonyl)amino]-2-phenylprop-2-enoate **220**

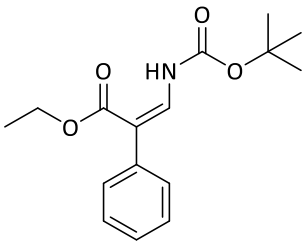

^{1}H NMR (400 MHz, $CDCl_3$) δ 9.91 (br.s, 1H), 7.70 – 7.13 (m, 6H), 4.29 – 4.15 (m, 2H), 1.50 (s, 9H), 1.27 (t, *J* = 7.2 Hz, 3H);

^{13}C NMR (126 MHz, $CDCl_3$) δ 171.9, 168.8, 140.4, 136.8, 129.6, 128.1, 127.0, 82.0, 60.7, 28.3, 14.4;

IR ν_{max}/cm^{-1} 3424.9, 3330.2, 3060.3, 2927.4, 2359.2, 1738.2, 1707.1, 1641.3, 1230.2, 1145.6;

HRMS (ESI+): calcd for $C_{16}H_{21}NO_4$ $[M+Na]^+$ 314.1368, found 314.1363.

ethyl (3S)-3-{[(tert-butoxy)carbonyl]amino}-3-phenylpropanoate **211**

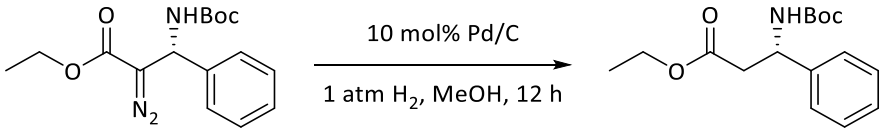

According to a literature procedure[66], a flask was charged with diazo-adduct **191a** (100 mg, 0.30 mmol) and palladium on carbon (10 mg, 10 wt% of **191a**). Dry methanol (1.25 mL) was added under argon. The flask was flushed with argon 3 times by alternating vacuum and argon filling with a balloon. The argon balloon was replaced with H_2 and stirred at room temperature for 12 hours. The palladium catalyst was then removed by filtration through a pad of celite® on a glass frit, eluting with methanol. The filtrate was then concentrated *in vacuo* and purified directly by FCC eluting with 10% diethyl ether/petroleum ether, which furnished the desired compound as a colourless crystalline solid (66 mg), 75% isolated yield, 96% ee [determined by HPLC, Chiralpak OD, hexane/isopropanol = 95/5, 1 mL/min, λ = 220 nm, t (minor) = 15.81 min, t (major) = 19.28 min]. Absolute stereochemistry was deduced on comparison to literature data for the same compound.[145]

MP 76-80 °C;

$[\alpha]_D^{25}$ = -32.7 (*c* = 1.1, EtOAc) [lit. $[\alpha]_D^{20}$ = -31.6 (*c* = 1.0, EtOAc) for *S*-**211**, on comparison with literature data of same compound[145];

^{1}H NMR (400 MHz, $CDCl_3$) δ 7.41 - 7.17 (m, 5 H, ArH), 5.50 (br. s., 1 H, CHNHC=O), 5.10 (br. s., 1 H, CHNHC=O), 4.06 (q, *J*=7.3 Hz, 2 H, CH_2CH_3), 2.99 - 2.70 (m, 2 H, $CHCH_AH_BC(O)O$), 1.41 (br. s., 9 H, $OC(CH_3)_3$), 1.15 (t, *J*=7.1 Hz, 3 H, CH_2CH_3);

^{13}C NMR (100 MHz, $CDCl_3$) δ ppm 171.0 (OC=O), 155.1 (NC(=O)OC), 141.2 (ArC), 128.6 (ArCH), 127.5 (ArCH), 126.2 (ArCH), 79.7 ($OC(CH_3)_3$), 60.7 (CH_2CH_3), 51.3 ($CHCH_aH_bC(O)O$), 41.1 ($CHCH_AH_BC(O)O$), 28.4 ($OC(CH_3)_3$), 14.1(CH_2CH_3);

IR ν_{max}/cm^{-1} 3352, 2978, 2930, 2358, 1728, 1497, 1167.

All data reported is in agreement with the literature[145].

1-tert-butyl 4-ethyl (4S,5R)-4-benzyl-5-phenyl-4,5-dihydro-1H-1,2,3-triazole-1,4-dicarboxylate **221**

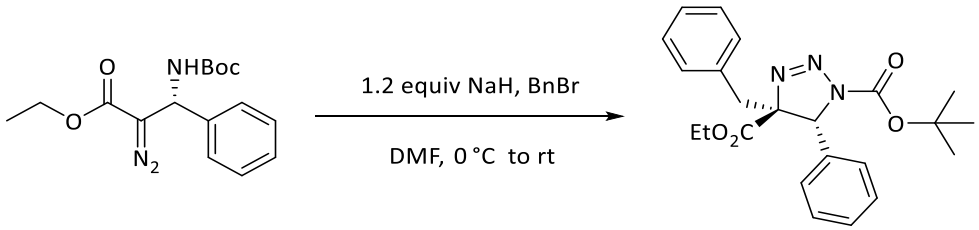

According to a literature procedure[93], a RBF was charged with sodium hydride (19.1 mg, 0.48 mmol, 1.2 equiv) and cooled to 0 °C under an atmosphere of argon. Dry *N, N*-dimethylformamide was then added (1.0 mL). Diazo adduct **191a** (128 mg, 0.4 mmol, 1.0 equiv) and benzyl bromide (58 µL, 0.48 mmol, 1.2 equiv) were then added in a dropwise manner in DMF (0.44 mL) and the mixture was stirred for 15 min. The resulting suspension was allowed to warm to room temperature and stirred for 30 minutes. A saturated solution of ammonium chloride (2 mL) was then added to produce a yellow suspension and the organic phase was extracted using ethyl acetate, dried over Na_2SO_4 and concentrated *in vacuo*. Purification by FCC using 20 % diethyl ether/petroleum ether afforded the title compound in 79% isolated yield as a white solid (129 mg) as a single diastereoisomer, 96% ee [determined by HPLC, Chiralpak IA, hexane/isopropanol =95/5, 1 mL/min, λ = 220 nm, t (major) = 15.79 min, t (minor) = 19.12 min].

MP 160-162°C;

$[\alpha]_D^{25}$ = +103.6 (*c* = 0.9, $CHCl_3$);

^{1}H NMR ^{1}H NMR (500 MHz, $CDCl_3$) δ 7.42 - 7.19 (m, 8 H, ArH) 7.05 (br. s., 2 H, ArH) 4.80 (s, 1 H, CHCN(C=O)) 3.57 - 3.72 (m, 2 H, CH_2CH_3) 3.54 (d, *J* = 14.0 Hz, 1 H, $ArCH_AH_BCN$) 3.25 (d, *J* = 14.0 Hz, 1 H, $ArCH_AH_BCN$) 1.27 (s, 9 H, $OC(CH_3)_3$) 0.83 (t, *J*=7.2 Hz, 3 H, CH_2CH_3);

^{13}C NMR (126 MHz, $CDCl_3$) δ 167.2 (O<u>C</u>=O), 148.9 (N<u>C</u>(=O)OC), 136.7 (Ar<u>C</u>), 133.4 (Ar<u>C</u>), 130.6 (Ar<u>C</u>H), 128.5 (Ar<u>C</u>H), 128.4 (Ar<u>C</u>H), 128.3 (Ar<u>C</u>H), 127.6 (Ar<u>C</u>H), 126.8 (Ar<u>C</u>H), 95.0 ($ArCH_aH_b\underline{C}$), 83.4 (O<u>C</u>$(CH_3)_3$), 62.9 (<u>C</u>HCN(C=O)), 61.8 (<u>C</u>H_2CH_3), 43.1 ($Ar\underline{C}H_aH_bCN$), 27.8 (OC(<u>C</u>$H_3)_3$), 13.5 ($CH_2\underline{C}H_3$);

IR ν_{max}/cm^{-1} 2978, 2358, 1738, 1498, 1336, 1149.

Relative configuration was assigned based on analogy.[93]

All data reported is in agreement with the literature.[93]

<u>ethyl (2R,3R)-3-{[(tert-butoxy)carbonyl]amino}-2-hydroxy-3-phenylpropanoate **223**</u>

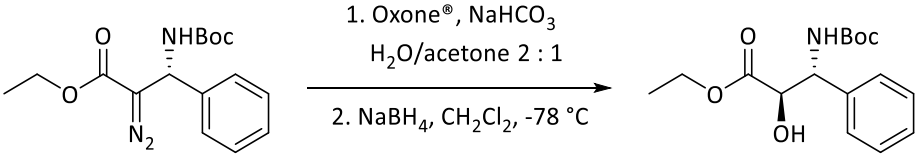

(97% ee)

8:1 dr (*anti:syn*)

According to a literature procedure[65], Oxone® (154 mg, 0.50 mmol, 5.0 equiv) was suspended in acetone/H_2O (3.0 mL : 1.5 mL). Sodium hydrogencarbonate was then added (168 mg, 2.0 mmol, 20 equiv) and stirred for 15 min at room temperature, after which the resulting mixture was cooled to 0 °C. Diazo adduct **191a** (32mg, 0.1 mmol, 1.0 equiv) was then added in 3.0 mL of dichloromethane over a period of 5 minutes. The mixture was then allowed to warm to room temperature and stirred at this temperature for 5 hours. Upon completion, the reaction mixture was diluted with water (3 mL) and extracted with dichloromethane (3 × 5 mL). The organic phase was washed with brine and dried over sodium sulfate and concentrated *in vacuo*. The resulting clear oil was re-dissolved in dry dichloromethane (2.5 mL) under argon which was then cooled to -78 °C. Sodium borohydride (8.7 mg, 0.23 mmol, 2.25 equiv) was then added in one portion. The reaction mixture was allowed to warm to room temperature slowly. After 27 hours, the reaction was quenched with sat. NH_4Cl and extracted with dichloromethane (3 × 5 mL). The combined organics were dried over sodium sulfate and concentrated *in vacuo*. Purification by FCC using 10% diethyl ether /petroleum ether afforded the title compound in 58% isolated yield (18 mgs) as a white, crystalline solid with a 8:1 d.r. (*anti* : *syn*).

Major diastereoisomer:

^{1}H NMR (400 MHz, $CDCl_3$) δ 7.34 - 7.12 (m, 5 H, Ar<u>H</u>), 5.61 (d, *J*=8.3 Hz, 1 H, CHN<u>H</u>C=O), 5.10 (d, *J* =6.4 Hz, 1 H, C<u>H</u>NHC=O), 4.57 (br.s. 1H, C<u>H</u>OH), 4.09 - 4.17 (m, 2 H, C<u>H</u>$_2$CH$_2$), 2.90 (d, *J*=6.4 Hz, 1 H, CHO<u>H</u>), 1.43 (s, 9 H, OC(C<u>H</u>$_3)_3$), 1.24 (t, *J*=7.1 Hz, 3 H, $CH_2C\underline{H}_3$);

^{13}C NMR (100 MHz, $CDCl_3$) δ ppm 172.0 (O<u>C</u>=O), 155.1 (N<u>C</u>(=O)OC), 136.9 (Ar<u>C</u>), 128.5 (Ar<u>C</u>H), 128.2 (Ar<u>C</u>H), 127.5 (Ar<u>C</u>H), 80.0 (O<u>C</u>$(CH_3)_3$), 73.3 (<u>C</u>HOH), 62.2 ($\underline{C}H_2CH_3$), 56.7 (<u>C</u>HNHC=O), 28.3 (OC($\underline{C}H_3)_3$), 14.1 ($CH_2\underline{C}H_3$). All data reported is in agreement with the literature.[141]

Proved to be impossible to separate diastereoisomers by FCC.

<u>ethyl (2E,3R)-3-{[(tert-butoxy)carbonyl]amino}-2-hydrazinylidene-3-phenylpropanoate **224**</u>

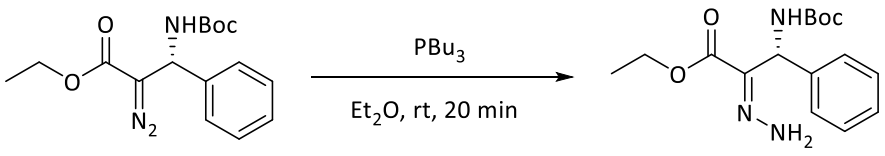

According to a literature procedure[146], diazo adduct **191a** (32 mg, 0.10 mmol) was dissolved in diethyl ether (0.1 mL) under argon. Tributylphosphine (75 μL, 3 equiv) was added in one portion. The resulting mixture was stirred at room temperature for 20 minutes upon which the mixture turned from a yellow solution to clear. The reaction mixture was diluted with ethyl acetate and washed with saturated sodium hydrogen carbonate solution and brine. The organic phase was dried over sodium sulfate and concentrated *in vacuo*. Purification by FCC using 50% ethyl acetate/petroleum ether to afford the title compound in 88% isolated yield (27 mgs) as a clear oil and 96% ee [determined by HPLC, Chiralpak AD-H, hexane/isopropanol =80/20, 1 mL/min, λ = 220 nm, t (major) = 7.48 min, t (minor) = 8.37 min].

$[\alpha]_D^{25}$ = -38.2 (*c* = 1.3, $CHCl_3$);

^{1}H NMR (500 MHz, $CDCl_3$) δ 7.35 - 7.32 (m, 2 H, Ar<u>H</u>), 7.28 - 7.25 (m, 3 H, Ar<u>H</u>), 6.65 (br. s., 2 H, C=NN$\underline{H}_2$), 6.07 (d, *J*=9.5 Hz, 1 H, CHN<u>H</u>C=O), 6.00 (br. s., 1 H, C<u>H</u>NHC=O), 4.16-4.24 (m, 2 H, $C\underline{H}_2CH_3$), 1.46 (s, 9 H, OC($C\underline{H}_3)_3$), 1.24 (t, *J* = 7.1 Hz, 3 H, $CH_2C\underline{H}_3$);

^{13}C NMR (126 MHz, $CDCl_3$) δ ppm 164.2 (O<u>C</u>=O), 156.1(N<u>C</u>(=O)OC), 138.5 (<u>C</u>=N-NH_2), 137.8 (Ar<u>C</u>), 128.8 (Ar<u>C</u>H), 127.6 (Ar<u>C</u>H), 125.5 (Ar<u>C</u>H), 80.4 (O<u>C</u>$(CH_3)_3$), 61.2 ($\underline{C}H_2CH_3$), 47.4 (<u>C</u>HNHC=O), 28.3 (OC($\underline{C}H_3)_3$), 14.1 ($\underline{C}H_2CH_3$);

IR ν_{max}/cm^{-1} 3410, 3300, 3236, 2979, 2932, 1696, 1495, 1167;

HRMS (ESI+): calcd for $C_{16}H_{24}N_3O_4$ $[M+Na]^+$ 344.15824, found 344.1581.

5,10,15,20-tetraphenyl-21H,23H-porphine cobalt(II) **219**

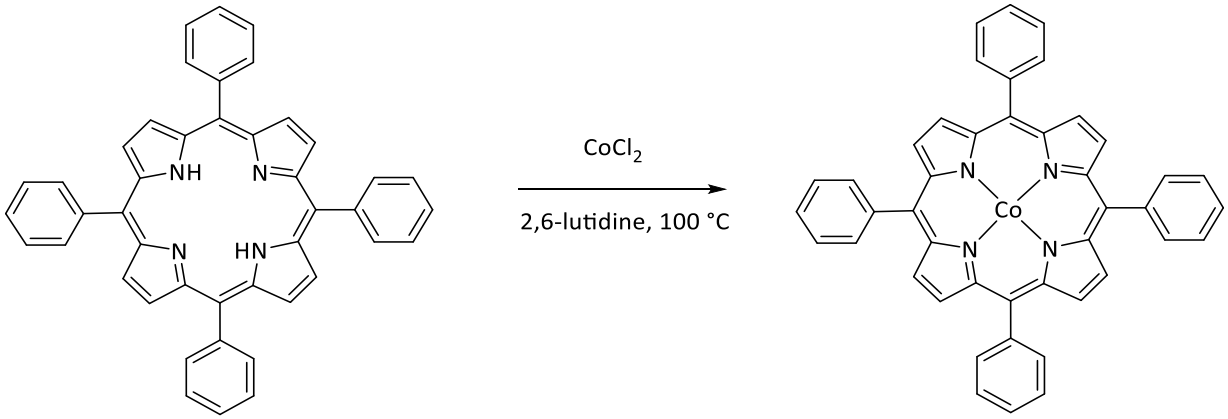

According to a literature procedure[147], free base TPP porphyrin (31 mgs, 0.05 mmol, 1.0 equiv) and anhydrous $CoCl_2$ (65 mgs, 0.50 mmol, 10 equiv) were placed in an oven dried microwave vial. Dry THF (4.0 mL) was added under argon followed by addition of 2,6-lutidine (29 µL, 0.25 mmol, 5.0 equiv). The microwave vial was then sealed and the mixture was heated to 100 °C for 15 hours after which the reaction mixture was allowed to cool and diluted with EtOAc and washed with water (×3). The organic phase was collected and concentrated *in vacuo* to reveal a red powder. This was then purified by FCC using 50% EtOAc/petroleum ether to yield the desired complex in 99% yield (33 mgs) as a dark red solid.

NMR data for this complex was unattainable due to large chemical shifts, characteristic of paramagnetic complexes. Complex **219** was characterised by UV-Vis spectra.

UV–vis (CH_2Cl_2), λmax nm (log ε): 415 (5.18), 529 (4.07).

All data reported is in agreement with the literature.[148]

6.3.7 Mechanistic Studies

A 5 mL RBF was charged with silver triflate (2.6 mgs, 0.01 mmol) and (*R*)-(+)-5,5'-Bis[di(3,5-xylyl)phosphino]-4,4'-bi-1,3-benzodioxole **196** (14.4 mgs, 0.020 mmol). $CDCl_3$ (0.8 mL) was added under argon and the resulting solution was stirred for 1 hour at room temperature before being transferred to an NMR tube for analysis. Addition of triethylamine (2.8 µL, 0.020 mmol) and aldimine **52a** (41 mgs, 0.20 mmol) followed whereby the sample was resubjected to analysis after each addition.

mono-(*R*)-(+)-5,5'-bis[di(3,5-xylyl)phosphino]-4,4'-bi-1,3-benzodioxoletriflatosilver(I) **225**

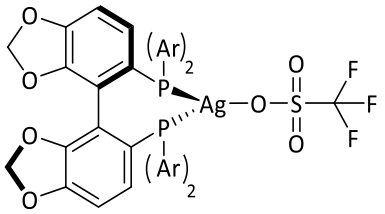

Ar = 3,5-dimethylphenyl

^{31}P NMR (202 MHz, $CDCl_3$) δ 12.46 (dd, *J* = 472.3, 408.5 Hz);

^{19}F NMR (471 MHz, $CDCl_3$) δ -77.83.

bis-(*R*)-(+)-5,5'-bis[di(3,5-xylyl)phosphino]-4,4'-bi-1,3-benzodioxolesilver(I) triflate **226**

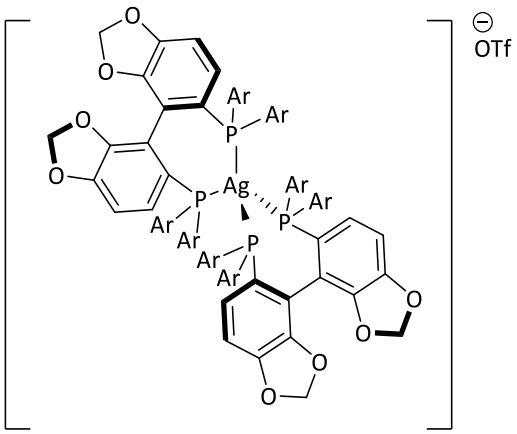

Ar = 3,5-dimethylphenyl

^{31}P NMR (202 MHz, $CDCl_3$) δ 9.10 (dd, *J* = 260.8, 225.2 Hz);

^{19}F NMR (471 MHz, $CDCl_3$) δ -77.83.[xvii]

[xvii] **Value reported is an average of two different fluorine environments.**

Non-linear Effects Study

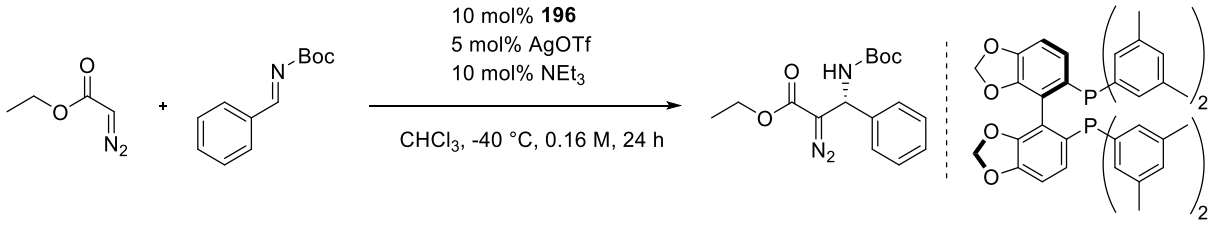

Reactions were performed according to General Procedure J on a 0.20 mmol scale.

Enantiopurity of the catalyst was varied in accordance with the following equation:

$$\%ee\ (cat) = \frac{Major\ ligand\ (R) - Minor\ ligand\ (S)}{Major\ ligand\ (R) + Minor\ ligand\ (S)} \times 100$$

Entry	Major R	Minor S	% ee of ligand	% ee of product
1	1	1	0.00	0
2	2	1	33.33	16
3	3	1	50.00	23
4	4	1	60.00	34
5	9	1	80.00	57
6	1	0	98.00	97

Table 8: Ratios of (*R*)-DM SEGPHOS and (*S*)-DM-SEGPHOS needed to achieve desired enantiomeric excess of major (*R*)-ligand.

%ee	Major R	Minor S	M[R] /mg	M[S]/mg	tot/mg
10	1.22	1	7.92	6.48	14.40
20	1.50	1	8.64	5.76	14.40
30	1.86	1	9.36	5.04	14.40
40	2.33	1	10.08	4.32	14.40
50	3.00	1	10.80	3.60	14.40
60	4.00	1	11.52	2.88	14.40
70	5.67	1	12.24	2.16	14.40
80	9.00	1	12.96	1.44	14.40
90	19.00	1	13.68	0.72	14.40

Table 9: Amounts of (*R*)-DM SEGPHOS and (*S*)-DM-SEGPHOS to achieve the desired enantiopurity of ligand for a 0.20 mmol scale reaction.

6.4 Experimental for Chapter 4

6.4.1 Procedure for Synthesis of Mannich Adduct using BEMP

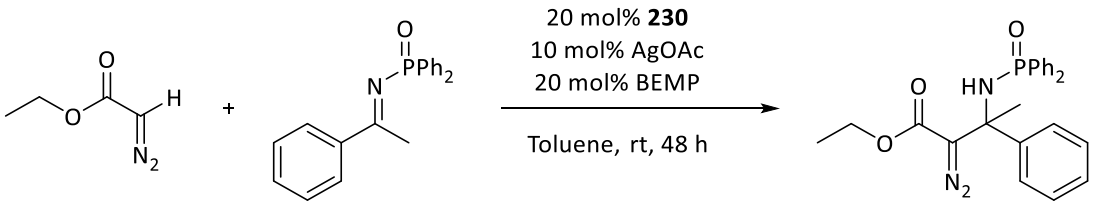

ethyl 2-diazo-3-((diphenylphosphoryl)amino)-3-phenylbutanoate **227**

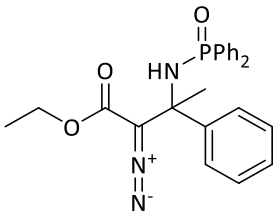

A 5 mL RBF was charged with silver acetate (3.3 mg, 0.020 mmol, 10 mol%) and aminophosphine ligand **230** (25 mg, 0.040 mmol, 20 mol%). Toluene was added under argon (1.0 mL) and stirred at room temperature for 30 minutes. BEMP was added using a microsyringe (12.0 µL, 0.040 mmol, 20 mol%) and then the ketimine **139a** (64.0 mg, 0.2 mmol, 1.0 equiv) as a solid in one portion. Finally, ethyl diazoacetate **171** was added (0.22 mL, 0.24 mmol, 1.2 equiv) and stirred at room temperature for 48 hours after which the reaction was quenched by passing through a short pad of silica on a glass frit and with washings of dichloromethane. The filtrate was concentrated *in vacuo* and purified by FCC with 30% EtOAc/petroleum ether to obtain the title compound as a yellow amorphous solid in 26% yield (23 mg) and 40% ee [determined by HPLC, Chiralpak AD-H, hexane/isopropanol = 90/10, 1 mL/min, λ = 220 nm, t (major) = 18.48 min, t (minor) = 25.85 min].

$[\alpha]_D^{25}$ = +20.0 (*c* = 1.0, $CHCl_3$);

^{1}H NMR (500 MHz, CD_3OD) δ 7.93 – 7.80 (m, 2H, ArH), 7.76 – 7.70 (m, 2H, ArH), 7.52 – 7.46 (m, 4H, ArH), 7.46 – 7.38 (m, 4H, ArH), 7.25 (t, *J* = 8.5, 7.2 Hz, 2H, ArH), 7.20 – 7.11 (m, 1H, ArH), 3.99 – 3.86 (m, 2H, CH_2CH_3), 1.56 (s, 3H, NHCCH_3), 1.08 – 0.99 (m, 3H, CH_2CH_3);

^{13}C NMR (126 MHz, CD_3OD) δ 167.7, 148.0 (d, *J* = 7.5 Hz), 135.2 (d, *J* = 131.6 Hz), 134.9 (d, *J* = 127.0 Hz), 133.4 (d, *J* = 2.8 Hz), 133.3 (d, *J* = 2.8 Hz), 132.8 (d, *J* = 9.8 Hz), 132.5 (d, *J* = 10.1 Hz), 129.9, 129.8, 129.6, 128.5, 126.4, 62.0, 60.3 (d, *J* = 2.8 Hz), 29.4 (d, *J* = 3.4 Hz), 14.6;

^{31}P NMR (202 MHz, CD_3OD) δ 22.61;

IR ν_{max}/cm^{-1} 2924, 2088, 1682, 1439, 1305;

HRMS (ESI+): calcd for $C_{24}H_{24}N_3O_3P$ $[M+Na]^+$ 456.1448, found 456.1440.

6.4.2 Synthesis of Racemate

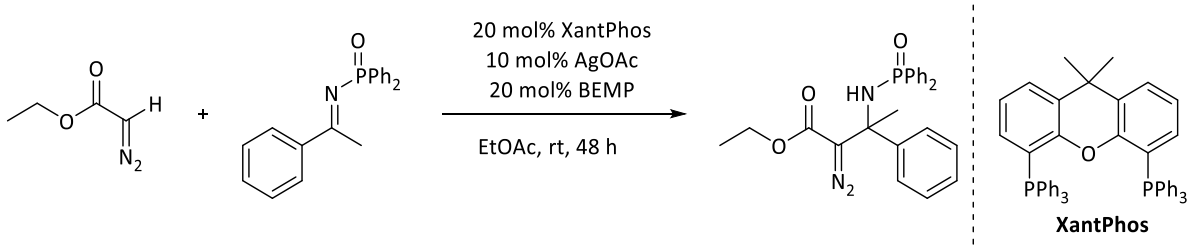

A reaction tube was charged with silver acetate (3.3 mg, 0.02 mmol, 10 mol%) and XantPhos ligand (23 mg, 0.04 mmol, 20 mol%). Ethyl acetate (1.0 mL) was added under argon and the mixture was stirred for 30 minutes at room temperature upon which the reaction mixture turned cloudy. TMG (5 µL, 0.04 mmol, 20 mol%) was then added and the mixture was stirred for a further 15 minutes at room temperature. Ketimine **139a** (64 mg, 0.2 mmol, 1.0 equiv) was then added in one portion and finally ethyl diazoacetate was added (0.22 mL, 0.24 mmol, 1.2 equiv). The reaction mixture was stirred at room temperature for 48 hours. The reaction was quenched by dilution with dichloromethane (1.0 mL) and the reaction mixture was passed through a pad of silica on a glass frit, eluting with EtOAc. The filtrate was concentrated *in vacuo* and purified by FCC, eluting with 30% EtOAc/petroleum ether to obtain racemic **227** in 35% yield (30 mgs) as a yellow amorphous solid.

tert-butyl hydrazinecarboxylate **235**

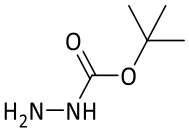

According to a literature procedure[149], a 500 mL flask was charged with hydrazine monohydrate (16.3g, 260 mmol, 2.3 equiv) followed by addition of isopropanol (50 mL). A solution of Boc anhydride (25 g, 115 mmol, 1.0 equiv) in 25 mL of isopropanol was added *via* a cannula. The resulting mixture was allowed to warm to room temperature and stirred for 2 hours after which the solvent was removed and the crude residue was dissolved in CH_2Cl_2 and dried over Na_2SO_4. The CH_2Cl_2 was removed *in vacuo* and the resulting residue was recrystallized from hexane to afford the desired compound in 80% yield (12.06 g) as a crystalline white solid.

MP 39 – 41 °C (lit. 36-38 °C)[150];

^{1}H NMR (400 MHz, $CDCl_3$) δ 5.97 (s, 1H), 3.67 (s, 2H), 1.44 (s, 9H);

^{13}C NMR (100 MHz, $CDCl_3$) δ 158.2, 80.6, 28.5;

All data reported is in agreement with the literature.[127]

tert-butyl (triphenyl-λ^5-phosphanylidene)carbamate **236**

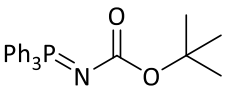

According to a literature procedure[151], Boc-hydrazine **235** (5g, 38 mmol, 1.0 equiv) was dissolved in acetic acid (15 mL) and water (30 mL). The resulting solution was then cooled to 0 °C and $NaNO_2$ (2.90 g, 41.8 mmol, 1.1 equiv) was added portionwise over 15 minutes, evolution of dinitrogen gas was observed. The resulting mixture was then stirred for 30 minutes at 0 °C after which the organics were extracted with Et_2O (2×50 mL). The combined organics were washed with H_2O (40 mL), brine (40 mL) and dried over Na_2SO_4. The resulting solution of Boc-azide in (100 mL) of Et_2O was transferred to a 250 mL RBF. Triphenylphosphine (10g, 38 mmol, 1.0 equiv) was added portionwise at 0 °C under vigorous stirring. The resulting white solid was collected by vacuum filtration and washed with Et_2O. This afforded the title compound in 71% yield over two steps as a white solid (9.10 g).

MP 155-157 °C (lit. 148 °C)[148];

^{1}H NMR (400 MHz, $CDCl_3$) δ 7.77 – 7.69 (m, 6H), 7.57 – 7.50 (m, 3H), 7.48 – 7.40 (m, 6H), 1.36 (s, 9H);

^{13}C NMR (100 MHz, $CDCl_3$) δ 161.4, 133.2 (d, *J* = 9.6 Hz), 132.2 (d, *J* = 2.6 Hz), 129.2 (d, *J* = 100.8 Hz), 128.6 (d, *J* = 12.1 Hz), 78.0 (d, *J* = 2.4 Hz), 28.4;

^{31}P NMR (162 MHz, $CDCl_3$) δ 20.37.

All data reported is in agreement with the literature.[128]

tert-butyl (Z)-(2,2,2-trifluoro-1-phenylethylidene)carbamate **238**

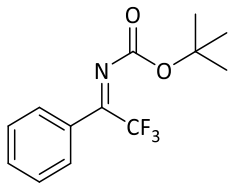

According to a literature procedure[152], a Schlenk tube was charged with trifluoroacetophenone (2.7 mL, 19 mmol, 1.0 equiv) and compound **236** (8.0 g, 21 mmol, 1.1 equiv). Dry toluene was then added (4.0 mL) under argon. The Schlenk tube was fitted with a condenser and the resulting suspension was heated to 120 °C for 18 hours. The reaction mixture was then cooled and hexane was added. The precipitated triphenylphosphine oxide was filtered off by passing the mixture through a glass frit containing a thin pad of celite. The filtrate was concentrated *in vacuo* and purified by FCC using 5% Et_2O/petroleum ether to afford the desired compound in 60% yield (4.2 g) as a clear oil.

^{1}H NMR (400 MHz, $CDCl_3$) δ 7.65 – 7.52 (m, 3H), 7.50 – 7.43 (m, 2H), 1.39 (s, 9H);

^{13}C NMR (100 MHz, $CDCl_3$) δ 158.29, 131.95, 129.10, 128.66, 127.94, 84.10, 27.77;

^{19}F NMR (376 MHz, $CDCl_3$) δ -71.40.

(E)-4-methyl-N-(1-phenylethylidene)benzenesulfonamide **243**

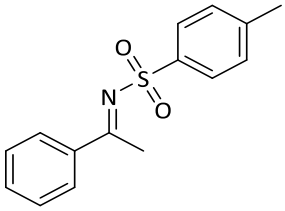

According to a literature procedure[104], a microwave vial was charged with sulphonamide **242** (85.5 mg, 0.5 mmol, 1.0 equiv), AuClJohnPhos (5.3 mg, 0.01 mmol, 2 mol%) and silver triflate (10 mg, 0.04 mmol, 8 mol%). Dry toluene (2.0 mL) was added under argon. Finally, phenylacetylene (166 µL, 1.5 mmol, 3 equiv) was added after which the rubber septum was replaced with a microwave cap and the tube was sealed. The resulting suspension was heated at 100 °C for 9 hours. The reaction mixture was quenched with saturated sodium hydrogencarbonate solution. The organics were extracted with EtOAc (3 × 10 mL), dried over sodium sulfate and concentrated *in vacuo*. The crude mixture was purified by FCC 10% EtOAc/petroleum ether to afford the desired compound as an orange solid in 89% yield (120 mgs).

MP 84 – 86 °C (lit. 80 - 82 °C)[104];

^{1}H NMR (400 MHz, $CDCl_3$) δ 7.96 – 7.86 (m, 4H), 7.58 – 7.49 (m, 1H), 7.46 – 7.37 (m, 2H), 7.35 (d, *J* = 8.1 Hz, 2H), 2.99 (s, 3H), 2.45 (s, 3H);

^{13}C NMR (126 MHz, $CDCl_3$) δ 180.00, 143.68, 138.84, 137.73, 133.31, 129.62, 128.76, 128.43, 127.25, 21.75, 21.33;

Data reported is consistent with literature values.[104]

2,2,2-trifluoroethyl 3-oxobutanoate **247**

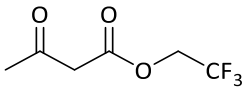

According to a literature procedure[105], a 50 mL RBF was charged with 2,2,2-trifluoroethanol (3.6 mL, 50 mmol, 1.0 equiv) and 2,2,6-trimethyl-4H-1,3-dioxin-4-one (6.6 mL, 50 mmol, 1.0 equiv) and 10 mL of toluene under argon. The flask was fitted with a condenser and heated to 150 °C for 6 hours upon which acetone was liberated. The toluene was then removed *in vacuo* and the product purified by FCC using 5% Et_2O/petroleum ether to afford the desired compound in 66% yield (6.0 g) as an orange oil.

^{1}H NMR (400 MHz, $CDCl_3$) δ 4.53 (q, *J* = 8.4 Hz, 2H), 3.57 (s, 2H), 2.28 (s, 3H);

^{13}C NMR (100 MHz, $CDCl_3$) δ 199.2, 165.6, 61.0 (q, *J* = 37.0 Hz), 49.4, 30.3;

^{19}F NMR (376 MHz, $CDCl_3$) δ -73.8.

Data reported is consistent with literature values[85].

2,2,2-trifluoroethyl diazoacetate **248**

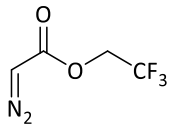

According to a literature procedure[105], a solution of trifluoroacetoacetate **247** (1.8g, 10 mmol, 1.0 equiv) was made in acetonitrile (12 mL), where triethylamine (1.8 mL, 13 mmol, 1.3 equiv) was added. The reaction mixture was cooled to 0 °C using an ice bath whereupon a solution of tosyl azide (1.7 mL, 11 mmol, 1.1 equiv) in acetonitrile (12 mL) was added dropwise. The reaction mixture was allowed to warm to room temperature and stirred at this temperature for 10 hours, after which most of the acetonitrile was removed *in vacuo*. The crude was taken up in Et_2O (60 mL) and washed with a 5% KOH solution. To the organic phase was added a further portion of 5% KOH solution (50 mL) and this was stirred for 1 hour at room temperature. The organic phase was separated, dried over Na_2SO_4 and concentrated *in vacuo*. The crude residue was purified under vacuum distillation whereupon residual acetonitrile was removed. This afforded the desired compound in 20% yield (340 mgs) as a yellow oil.

^{1}H NMR (400 MHz, $CDCl_3$) δ 4.90 (s, 1H), 4.54 (q, *J* = 8.4 Hz, 2H);

^{19}F NMR (376 MHz, $CDCl_3$) δ -74.21.

Data reported is consistent with literature values.[105]

6.4.3 Synthesis of *p*-methoxy Lithium Phenoxide

According to a literature procedure[153], a reaction tube was charged with *para*-methoxyphenol (62.1 mg, 0.50 mmol) and dried under vacuum for 10 minutes. Dry THF (4.7 mL) was added under argon and the resulting solution was cooled to 0 °C. At this temperature, *n*BuLi (200 µL, 0.50 mmol, 2.5 M in *n*-hexane) was then added and the solution was stirred at 0 °C for 1 hour to give a colourless (0.1 M) solution of Li(OC_6H_4-*p*-OMe). This was used immediately.

6.5 Experimental for Chapter 5

NMR Spectroscopy

NMR data were collected using a Bruker AVANCE III HD 400 MHz equipped with a bbo probe, Bruker AVANCE III HD 500MHz equipped with a bbfo probe, a Bruker AVANCE III HD 600 MHz with a bbo probe. Low VT experiments were carried out on the Bruker AVANCE III HD 500 MHz over the range 203−298 K as stated using a Bruker liquid nitrogen evaporator VT system. Samples were dissolved in dry CD_2Cl_2, and $CDCl_3$ characterized by $^{31}P\{^1H\}$, 2D ^{31}P-$^{31}P\{^1H\}$-COSY (modified with proton decoupling, Bruker pulse cosygppgqf using gradient pulses for selection and ^{31}P-$^{31}P\{^1H\}$ NOESY/EXSY spectra phase sensitive with f2 decoupling throughout t1 and t2 acquisition were collected using standard pulse programs (90-t1-90-τm-90-Acq), with mixing times of 1ms-10secs at the temperatures and in the solvents stated. For each data set, 8 or16 transients were acquired for each of the 256 increments with 2K datapoints per spectrum, using a recovery time of 2 s. Data were processed typically as 1K × 1K data points using shifted squared-sinebell apodization windows. Typical sample ^{195}Platinum concentrations for T_1 analyses were 0.05 mM and for Ag complexes based on silver(I) triflate were 0.04 mM. Probe temperature calibrations were performed using neat methanol samples containing a trace of HCl below ambient) using either BCU II fridge module at 233K or liquid nitrogen evaporator attachment at 203 K.

^{31}P-$^{31}P\{^1H\}$ T_1 Relaxation times were measured using the standard inversion-recovery sequence t1ir (180_–t_1–90_–acquire) in which t_1 was varied from 5 ms to 10 s. Proton decoupling was applied during the acquisition period. Data were Fourier-transformed into 2 K data points using a 2 Hz line broadening function. Relaxation times were calculated using the T_1 dynamics module in Topsin 3.5.

^{195}Pt T_1 Relaxation times, T_1 Relaxation times were measured using the standard inversion-recovery sequence t1ir (180_–t_1–90_–acquire) in which t_1 was varied from 1 ms to 300 ms. Data were Fourier-transformed into 2 K data points using a 2 Hz line broadening function. Relaxation times were calculated using the T_1 dynamics module in Topsin 3.5.

6.5.1 Measurement of T_1-relaxation Time Constants using Inversion Recovery

Cis-dichlorobis(triphenylphosphine) platinum(II) **249**

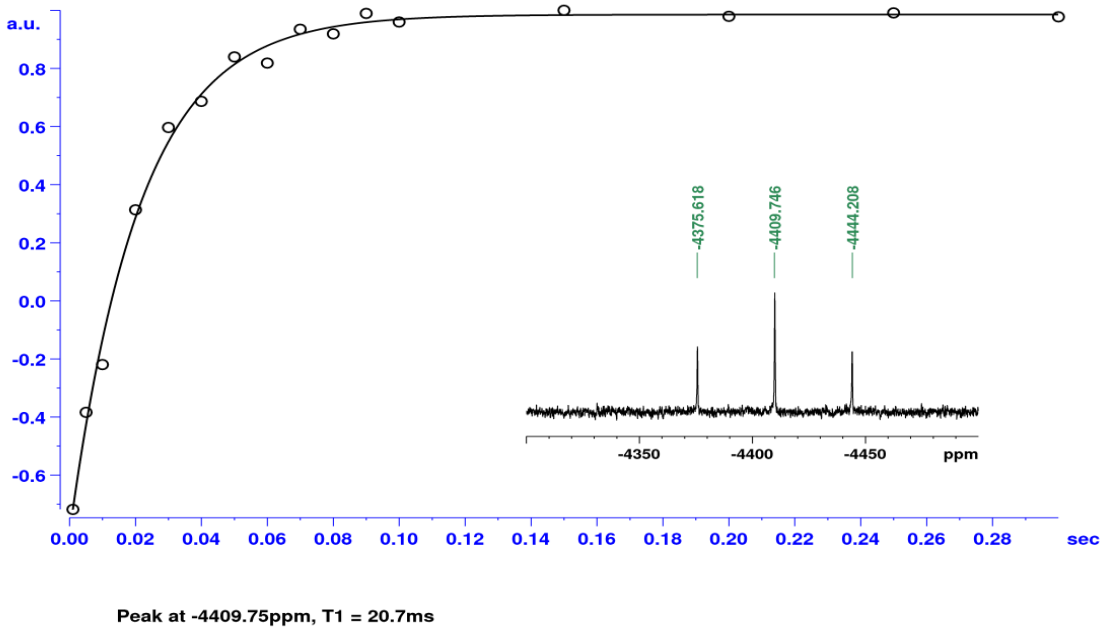

Figure 38: ^{195}Pt T_1 Relaxation measurement using the standard inversion-recovery sequence t1ir (180_–*t*1–90_–acquire) for *Cis*-dichlorobis(triphenylphosphine) platinum(II) on Bruker AVANCE III HD 500MHz.

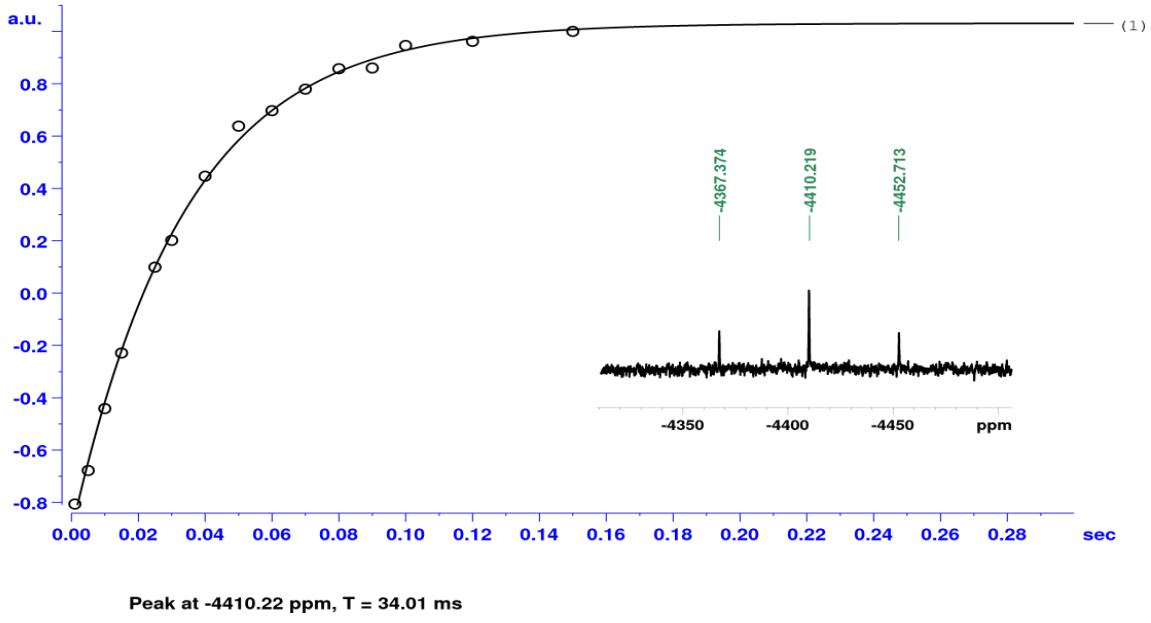

Figure 39: ^{195}Pt T_1 Relaxation measurement using the standard inversion-recovery sequence t1ir (180_–*t*1–90_–acquire) for *Cis*-dichlorobis(triphenylphosphine) platinum(II) on Bruker AVANCE III HD 400MHz.

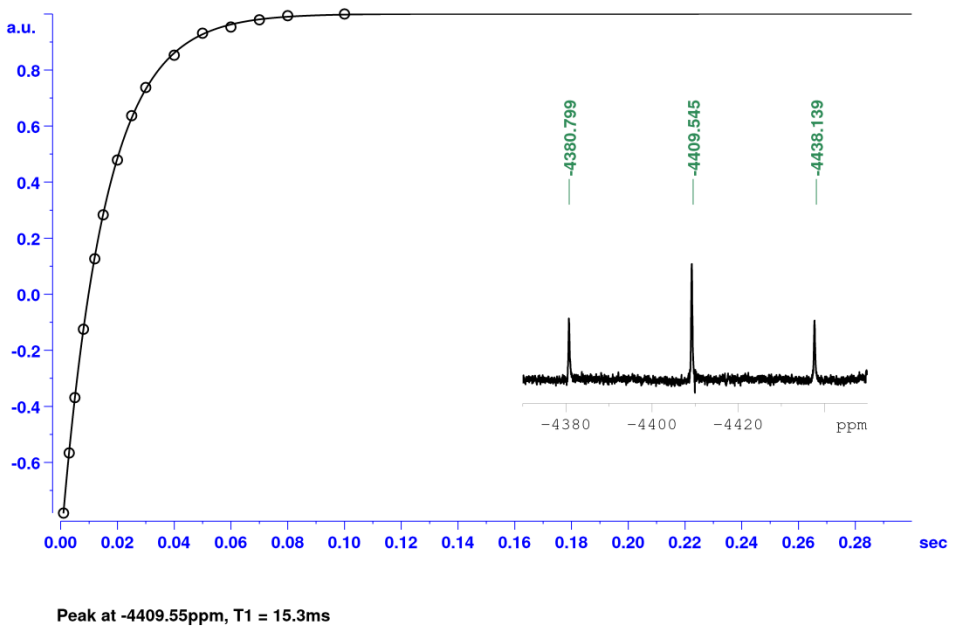

Figure 40:^{195}Pt T_1 Relaxation measurement using the standard inversion-recovery sequence t1ir (180_–*t*1–90_–acquire) for *Cis*-dichlorobis(triphenylphosphine) platinum(II) on Bruker AVANCE III HD 600MHz.

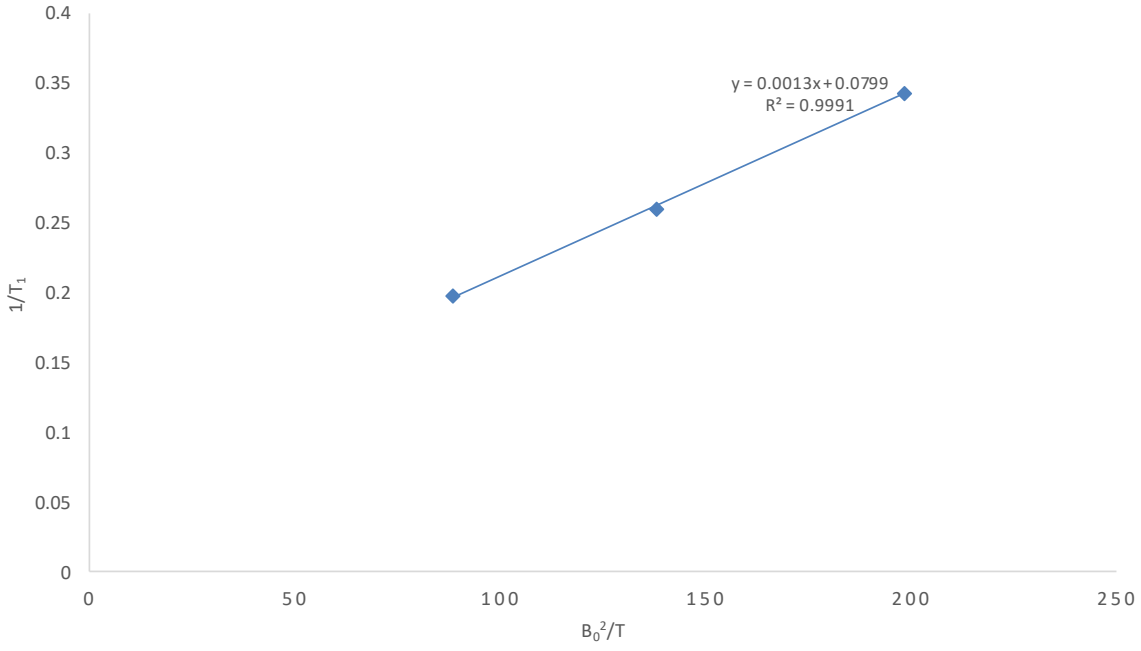

Figure 41: T_1 relaxation dependence of ^{31}P nuclides in complex 249 on the square of the applied magnetic field (B_0^2).

6.5.2 Application of SSSE Method

Cis-dichlorobis(triphenylphosphine) platinum(II) **249**

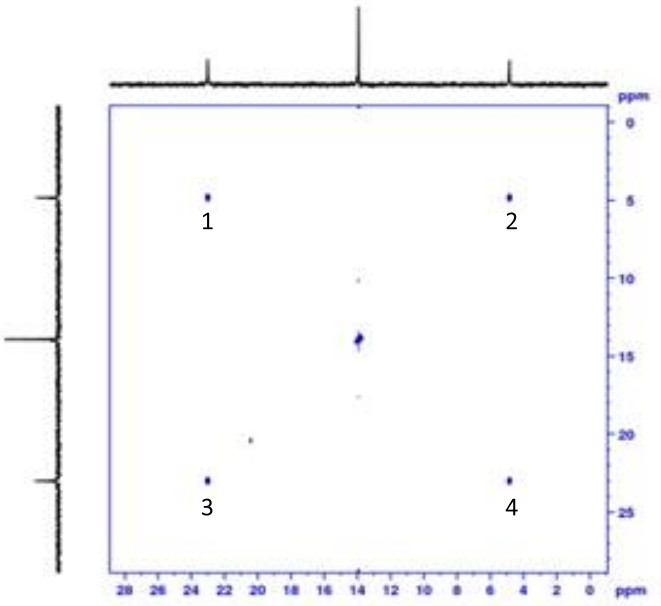

Figure 42: General schematic showing the integral numbering system used for the ^{195}Pt-satellite peaks in the^{31}P-^{31}P-{^{1}H}- EXSY spectrum of 249 (500 MHz). A ratio of integral 1 : Integral 2 was taken ($I_{cross\text{-}peak}/I_{diagonal}$). The same was done for integral 4 with respect to integral 3, which produced an identical result when plotted against mixing time to the former.

tmix/msec	Volume Integral 1	Volume Integral 2	Volume Integral 3	Volume Integral 4	Normalise (1/2)	Normalise (4/3)
0	0	4345700	4409400	0	0	0
1	33288	4200600	4206400	72765	0.007924582	0.01729864
2	167120	4303500	4163800	157360	0.038833508	0.037792401
3	402230	4439100	4500700	159650	0.090610709	0.03547226
4	346260	3970300	4034900	343290	0.087212553	0.085080175
5	412780	4073200	3952000	495450	0.101340469	0.125366903
6	437050	3934000	3910700	462800	0.111095577	0.118341985
7	562260	3989800	4016800	615020	0.140924357	0.15311193
8	682420	3715600	3759200	711980	0.183663473	0.18939668
10	749740	3443500	3483900	718340	0.217726151	0.206188467
12	1009500	3425300	3447100	997750	0.294718711	0.289446201
15	1089700	3258100	3415500	1075700	0.334458734	0.314946567
18	1318600	3323600	3453700	1314300	0.396738476	0.380548397
20	1381200	3160600	3034200	1359600	0.437005632	0.448091754
25	1601600	2935500	2952600	1552700	0.545597002	0.5258755
30	1628400	2538300	2598500	1639400	0.641531734	0.630902444

Table 10: Raw data showing volume integrals of ^{195}Pt-satellite cross peaks (1,4) normalised against the diagonal peaks (2,3) for *cis*-dichlorobis(triphenylphosphine) platinum(II) ^{195}Pt satellite cross-relaxation measurement using ^{31}P-^{31}P-{^{1}H}-EXSY spectra on a Bruker Avance III HD 500 Mhz.

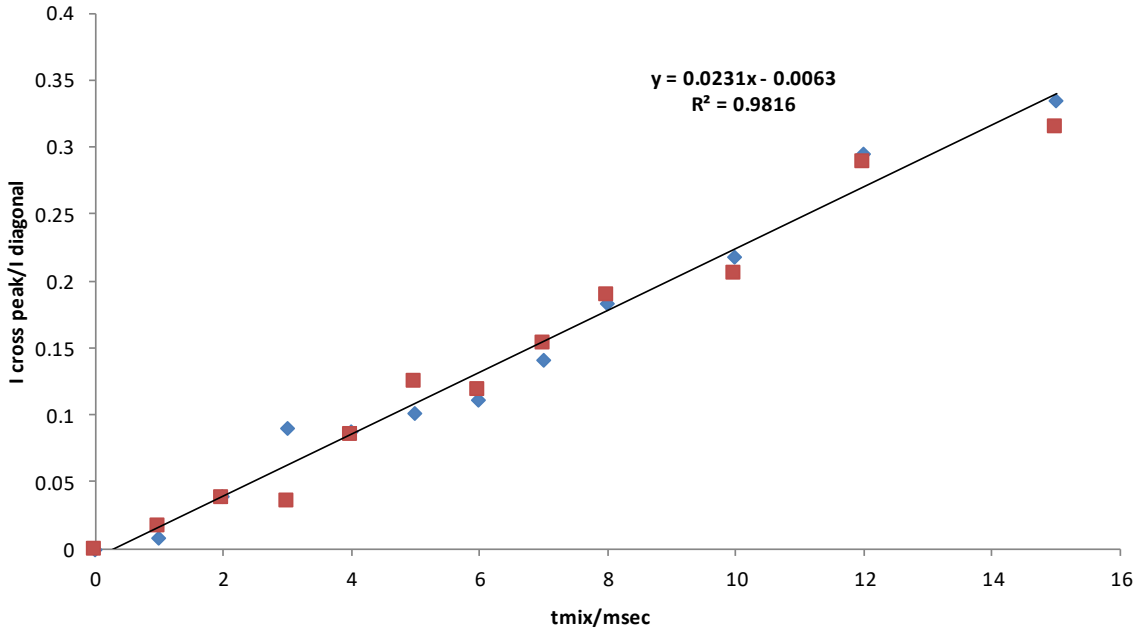

Figure 43: Normalised volume integrals for satellite peak 1 with respect to diagonal peak 2 (blue diamonds) and normalised volume integrals for satellite peak 4 with respect to diagonal peak 3 (red squares) at 500 MHz, data points from t_{mix} = 0 - 15 msec for initial cross-relaxation rate.

tmix/msec	Volume Integral 1	Volume Integral 2	Volume Integral 3	Volume Integral 4	Normalise (1/2)	Normalise (4/3)
0	0	0	0	0	0	0
2	605630	18944000	18460000	498650	0.031969489	0.027012459
5	1510700	17708000	17730000	1335100	0.085311724	0.075301748
6	1718200	18294000	18012000	1761700	0.093921504	0.097807018
8	2304000	17716000	17949000	2313800	0.13005193	0.128909689
10	2201200	16008000	16483000	2422700	0.137506247	0.146981739
12	3288000	17110000	17009000	3254900	0.192168323	0.191363396
15	3440500	15793000	15232000	3612900	0.21784968	0.237191439
20	3973600	14208000	14120000	3905300	0.279673423	0.27657932
25	5029100	14336000	14217000	5555100	0.350802176	0.390736442
30	5410500	13022000	12685000	5513000	0.415489172	0.434607804

Table 11: Raw data showing volume integrals of ^{195}Pt-satellite cross peaks (1,4) normalised against the diagonal peaks (2,3) for *cis*-dichlorobis(triphenylphosphine) platinum(II) ^{195}Pt satellite cross-relaxation measurement using ^{31}P-^{31}P-{^{1}H}-EXSY spectra on a Bruker Avance III HD 400 Mhz.

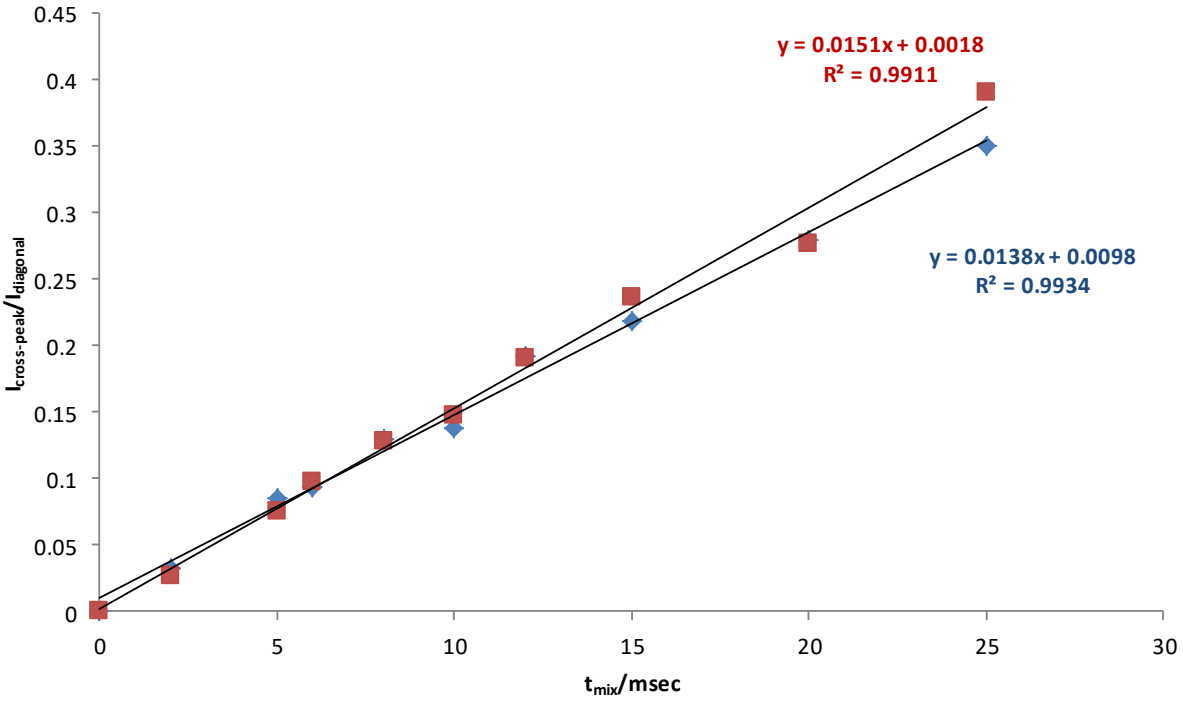

Figure 44: Normalised volume integrals for satellite peak 1 with respect to diagonal peak 2 (blue diamonds) and normalised volume integrals for satellite peak 4 with respect to diagonal peak 3 (red squares) at 400 MHz, data points from tmix= 0 - 25 msec for initial cross-relaxation rate.

tmix/msec	Volume Integral 1	Volume Integral 2	Volume Integral 3	Volume Integral 4	Normalise (1/2)	Normalise (4/3)
0	0	0	0	0	0	0
1	579590	19474000	19308000	799780	0.029762247	0.041422208
2	1461700	19020000	19196000	1387300	0.076850683	0.072270265
4	2327100	19086000	18729000	2459000	0.121927067	0.131293716
6	3456200	18153000	17969000	3542600	0.190392773	0.197150648
8	4334600	17233000	17185000	4315300	0.251529043	0.251108525
10	5068700	16284000	16199000	4994000	0.31126873	0.308290635
12	5645400	15352000	15200000	5876100	0.367730589	0.386585526
15	6730900	14814000	14555000	6601400	0.45436074	0.453548609
20	7771100	13692000	13589000	7721700	0.567565001	0.568231658
25	8742400	12893000	12918000	8668000	0.678073373	0.671001703
30	14119000	18892000	18585000	14131000	0.747353377	0.760344364

Table 12: Raw data showing volume integrals of ^{195}Pt-satellite cross peaks (1,4) normalised against the diagonal peaks (2,3) for *cis*-dichlorobis(triphenylphosphine) platinum(II) ^{195}Pt satellite cross-relaxation measurement using ^{31}P-^{31}P-{^{1}H}-EXSY spectra on a Bruker Avance III HD 600 Mhz.

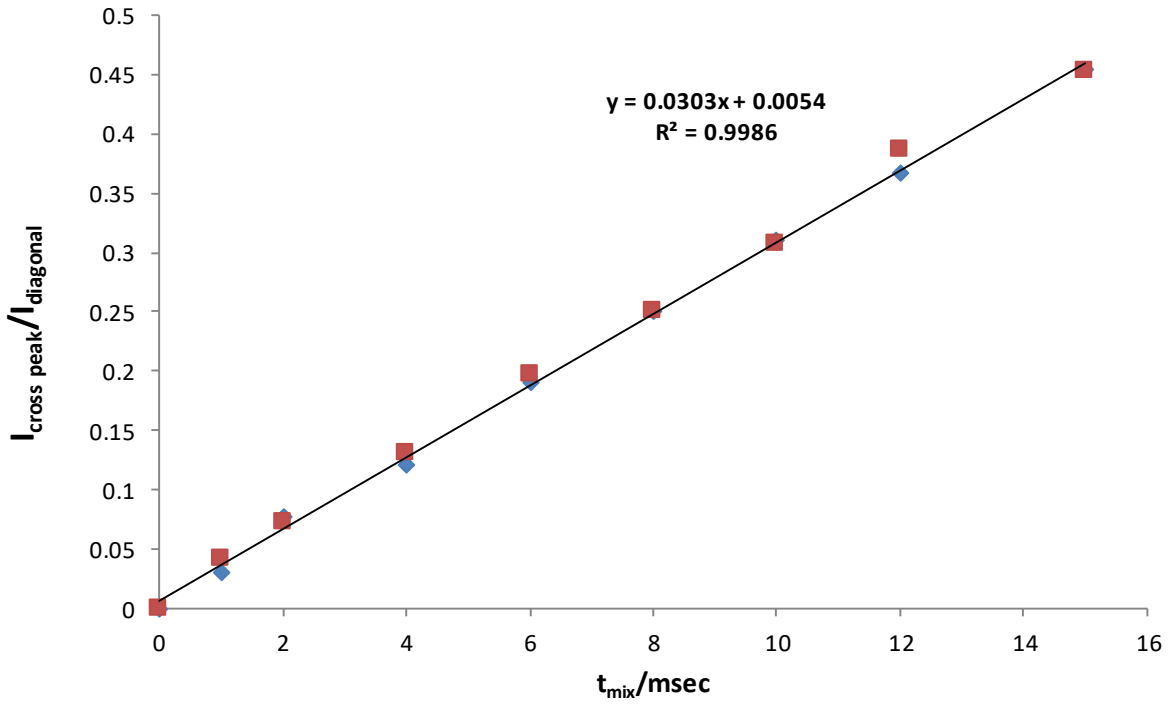

Figure 45: Normalised volume integrals for satellite peak 1 with respect to diagonal peak 2 (blue points) and normalised volume integrals for satellite peak 4 with respect to diagonal peak 3 (red points) at 600 MHz, data points from t_{mix}= 0 - 25 msec for initial cross-relaxation rate.

1-D NMR Spectra for cis-(bistriphenylphosphine) platinum(II) chloride **249**

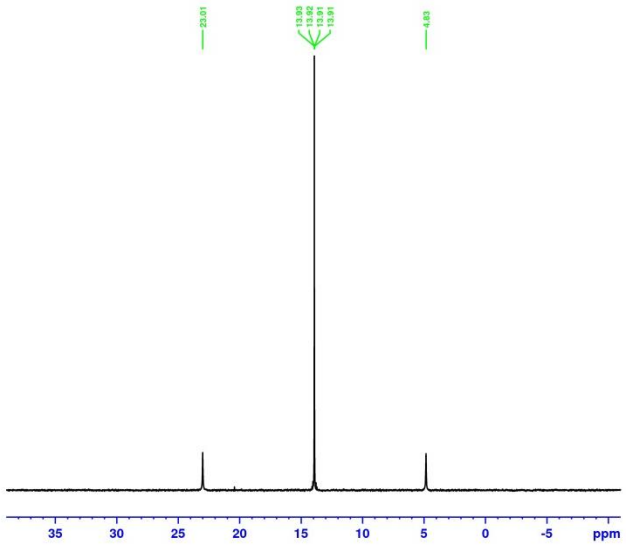

Figure 46: ^{31}P-{^{1}H}-NMR spectrum of *cis*-dichlorobis(triphenylphosphine) platinum(II) (0.05 mM) in CD_2Cl_2 at 298K on a Bruker Avance III 500MHz (LB = 2 Hz).

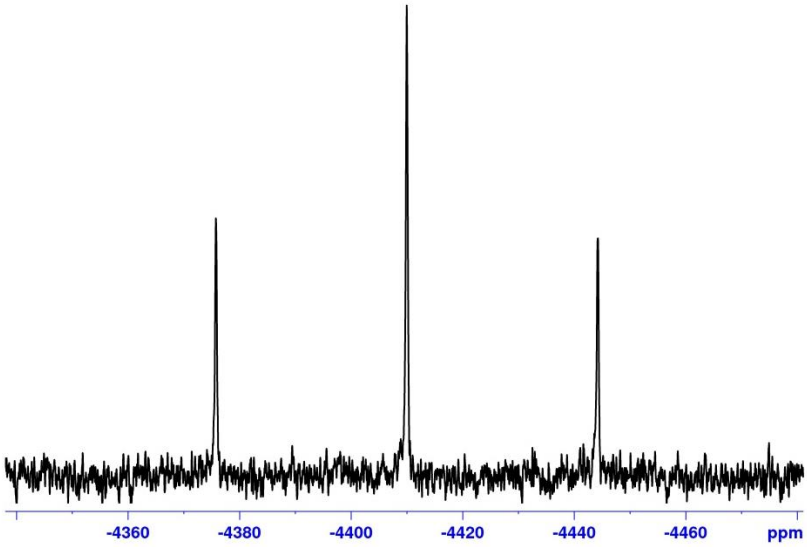

Figure 47: ^{195}Pt NMR Spectrum of *cis*-dichlorobis(triphenylphosphine) platinum(II) (0.05 mM) in CD_2Cl_2 at 298K on a Bruker Avance III 500 MHz (LB =10 Hz).

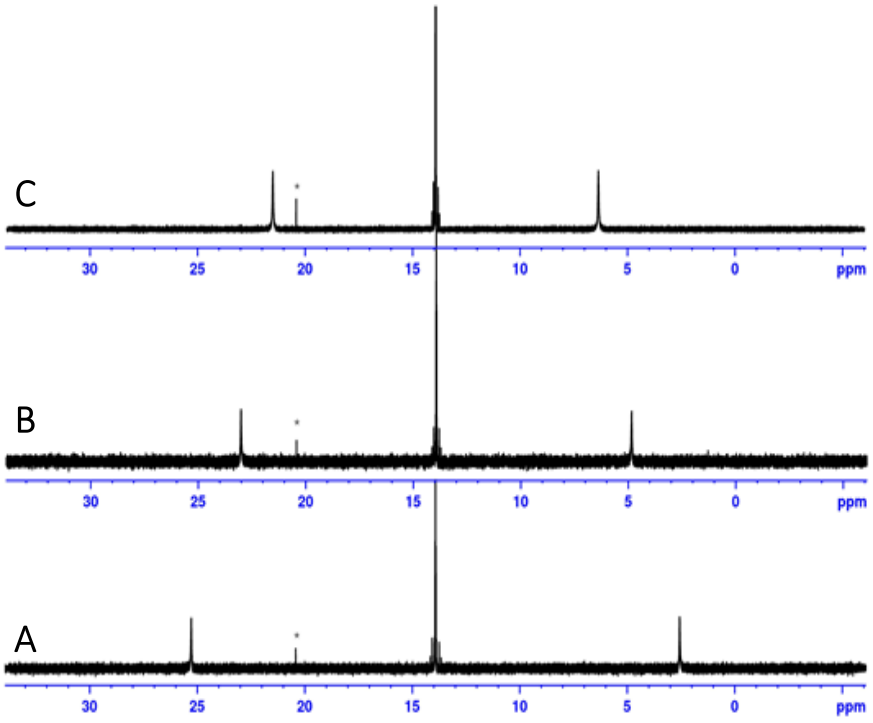

Figure 48: ^{31}P-{^{1}H}-NMR Spectrum of *cis*-dichlorobis(triphenylphosphine) platinum(II) (0.05 mM) in CD_2Cl_2 at 298K (LB = 10 Hz) A at 400MHz, B at 500MHz, C at 600MHz, * impurity.

Silver Complexes **225** and **226**

General Procedure N for preparation of Silver(I) complexes

A 10 mL round bottom flask was charged with silver(I) triflate (9 mg, 0.035 mmol, 1.0 equiv) and (*R*)-(+)-5,5'-Bis[di(3,5-xylyl)phosphino]-4,4'-bi-1,3-benzodioxole **196** (50 mg, 0.07 mmol, 2.0 equiv). Under argon, $CDCl_3$ or CD_2Cl_2 (0.8 mL) was added and the mixture was stirred for 30 minutes at room temperature. The solution was then transferred to an NMR tube for analysis.

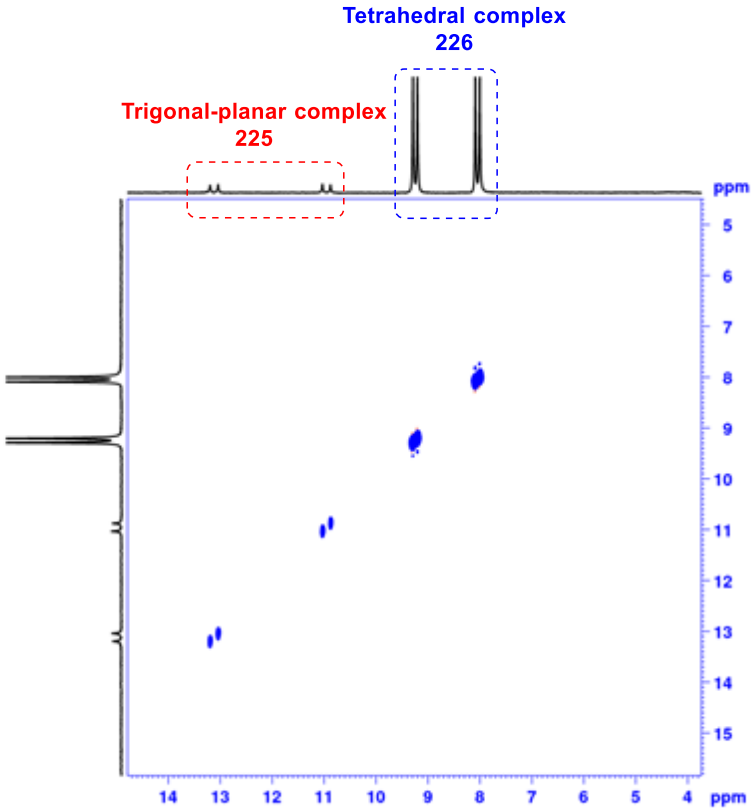

Figure 49: ^{31}P-^{31}P-{^{1}H}-EXSY (500 MHz) spectra of trigonal-planar complex 225 and tetrahedral complex 226. Prepared according to the General Procedure N at 203K; t_{mix} 0-800msec in CD_2Cl_2 (t_{mix}=10 msec).

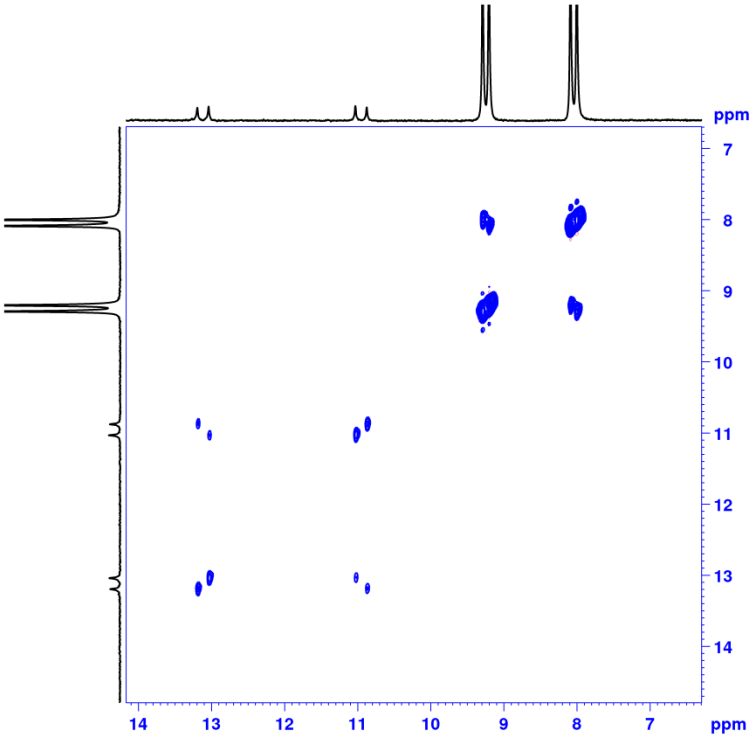

Figure 50: ^{31}P-^{31}P-{^{1}H}-EXSY (500 MHz) spectra of 225 and 226 showing the $^{107/109}$Ag satellite cross-peaks. Prepared according to the General Procedure N at 203K; t_{mix} 0-800msec in CD_2Cl_2 (t_{mix}= 500 msec).

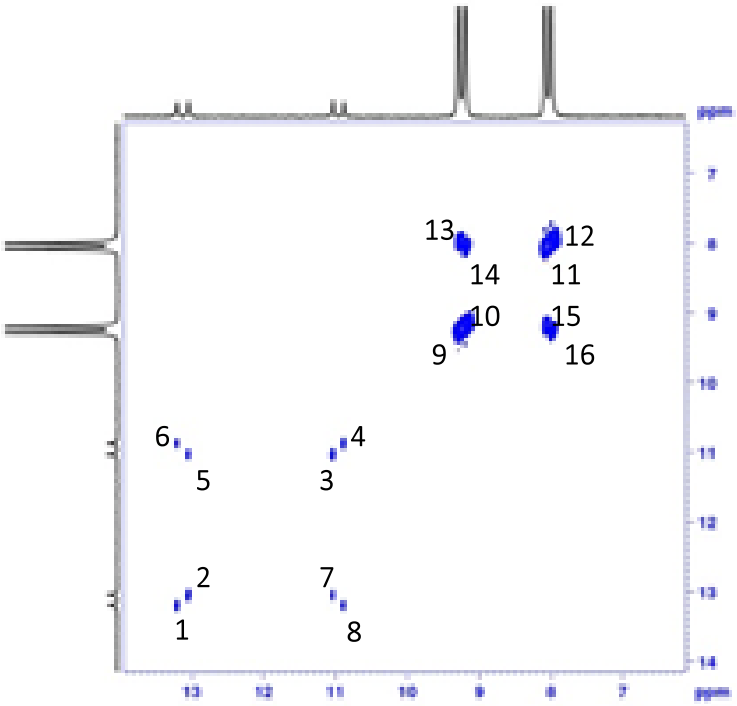

Figure 51: General schematic showing the integral numbering system used for the ^{109}Ag-satellite peaks in the EXSY spectrum. In trigonal-planar complex 225, a ratio of volume integral 6 : volume integral 4 was taken ($I_{cross\text{-}peak}$ / $I_{diagonal}$) for ^{109}Ag satellites and plotted against mixing time. Subsequently, in tetrahedral complex 226, a ratio of volume integral 13 : volume integral 12 was taken ($I_{cross\text{-}peak}/I_{diagonal}$) for ^{109}Ag satellites and plotted against mixing time.

Trigonal-planar complex **225**

tmix/msec	Volume Integral 1	Volume Integral 2	Volume Integral 3	Volume Integral 4	Volume Integral 5	Volume Integral 6	Normalise/^{31}P-^{107}Ag	Normalise/^{31}P-^{109}Ag
50	1134100	1208800	1256700	1132800	64787	66323	0.051553274	0.058547846
75	1053600	1154600	1131400	1095900	89107	86178	0.078758176	0.078636737
100	1013800	1159800	1103300	1014100	80230	123560	0.072718209	0.121842027
200	791510	858410	912070	822820	159470	195130	0.174844036	0.237147857
300	666650	740160	743940	650210	194640	266020	0.261634003	0.409129358
400	521490	578740	610840	507970	232320	245270	0.380328728	0.482843475
500	430290	484870	490730	420910	188070	223610	0.383245369	0.531253712
600	347190	379050	412970	344310	188900	207710	0.457418214	0.6032645
700	302440	349330	329670	326720	230290	234100	0.698547032	0.716515671
800	254250	291110	287430	230060	205640	188880	0.71544376	0.821003217

Table 13: Showing data used to determine initial cross-relaxation rate of ^{109}Ag nucleus using ^{109}Ag satellite cross-relaxation measurement for trigonal-planar complex 225.

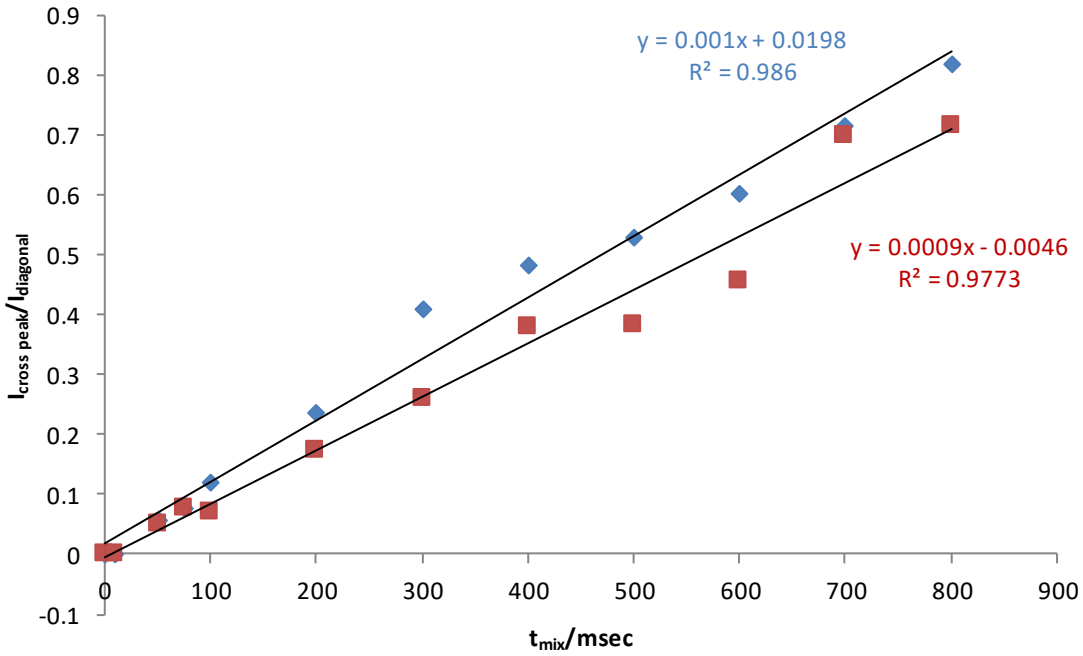

Figure 52: Normalised volume integrals for ^{107}Ag satellite peak 5 with respect to diagonal peak 3 (red squares) and normalised volume integrals for ^{109}Ag satellite peak 6 with respect to diagonal peak 4 (blue diamonds) at 500 MHz, data points from t_{mix} = 0 - 800 msec for initial cross-relaxation rate of trigonal-planar complex 225.

Tetrahedral complex **226**

tmix/msec	Volume Integral 9	Volume Integral 10	Volume Integral 11	Volume Integral 12	Volume Integral 13	Volume Integral 14	Normalise/^{31}P-^{107}Ag	Normalise/^{31}P-^{109}Ag
50	16600000	19200000	18305000	17194000	131760	144370	0.007886916	0.007663138
75	16251000	18047000	17452000	16861000	200280	168600	0.009660784	0.011878299
100	16110000	18306000	17774000	16643000	223890	216310	0.012170024	0.013452503
200	15269000	17922000	16906000	15582000	448880	409600	0.024228085	0.028807599
300	14953000	18409000	15352000	15667000	627770	496780	0.032359302	0.040069573
400	13143000	17249000	15207000	14082000	805150	688820	0.045296245	0.057175827
500	11913000	17097000	11710000	14457000	813750	746140	0.06371819	0.056287612
600	10389000	13510000	10954000	12327000	888150	800150	0.073046376	0.07204916
700	9664300	12454000	10215000	13489000	833790	901950	0.088296623	0.061812588
800	10708000	12470000	12161000	11226000	1086600	902790	0.074236494	0.096793159

Table 14: Data used to determine initial cross-relaxation rate of ^{109}Ag nucleus using ^{109}Ag satellite cross-relaxation measurement for tetrahedral complex 226.

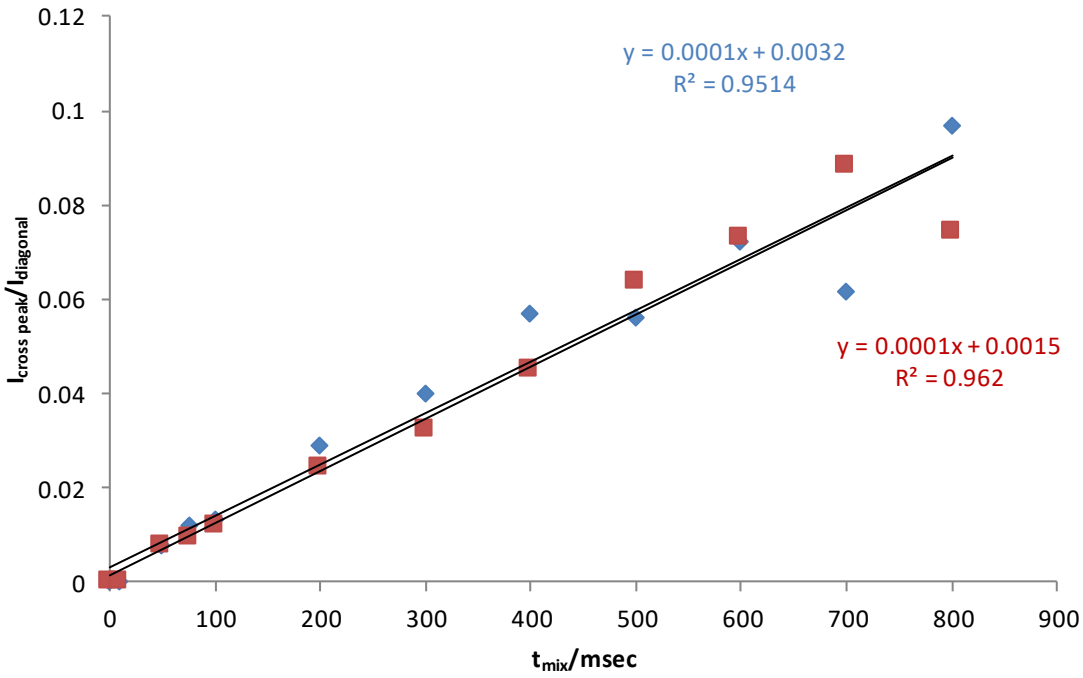

Figure 53: Normalised volume integrals for ^{107}Ag satellite peak 14 with respect to diagonal peak 11 (red squares) and normalised volume integrals for ^{109}Ag satellite peak 13 with respect to diagonal peak 12 (blue diamonds) at 500 MHz, data points from t_{mix}= 0-800 msec for initial cross-relaxation rate of tetrahedral complex 226.

1-D NMR spectra for complexes **225** and **226**

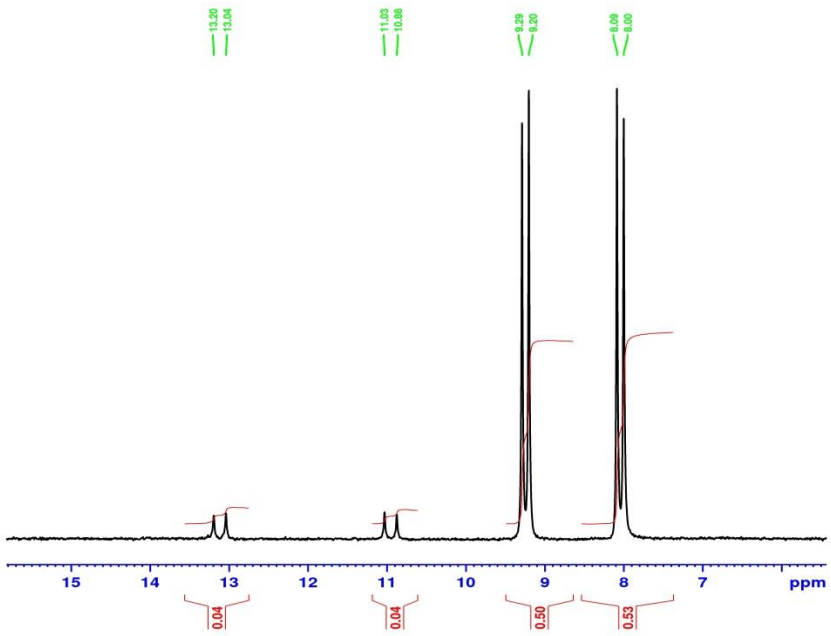

Figure 54: ^{31}P {^{1}H} NMR Spectrum of silver complexes 225 and 226 (0.04 mM) in CD_2Cl_2 at 203K on a Bruker Avance III 500MHz (LB =1Hz).

7. Appendices

7.1 Representative NMR spectra

^{1}H NMR of **140a** (500 MHz, $CDCl_3$)

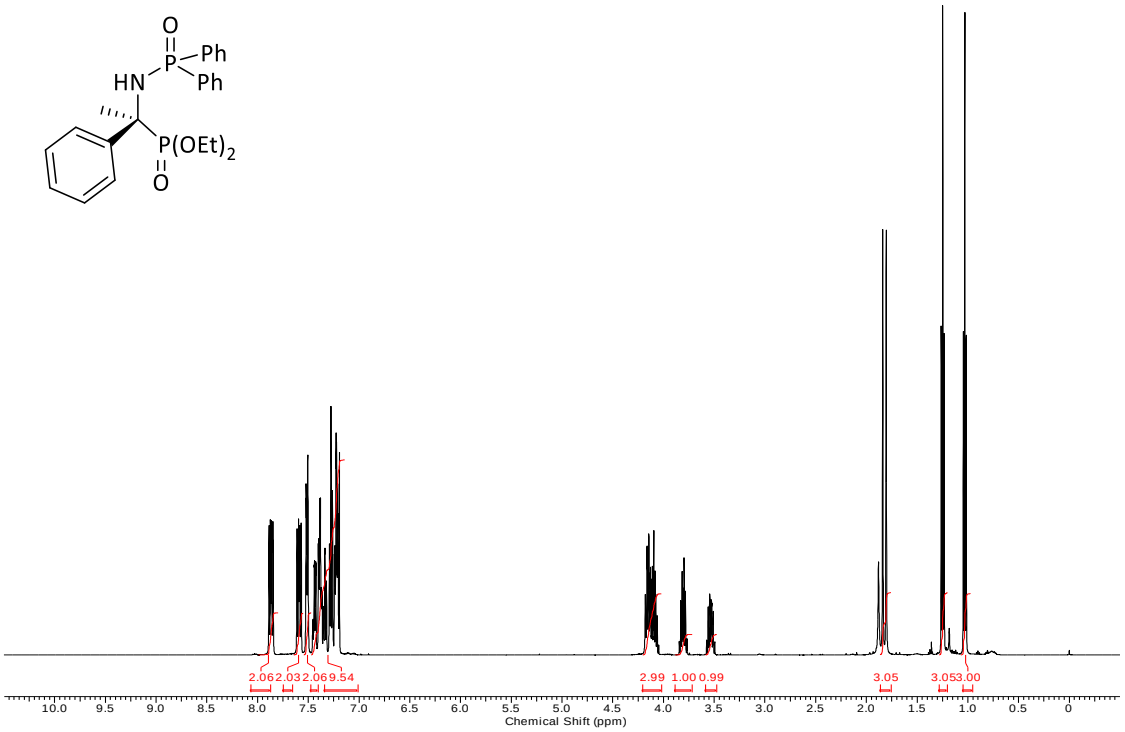

^{13}C NMR of **140a** (125 MHz, $CDCl_3$)

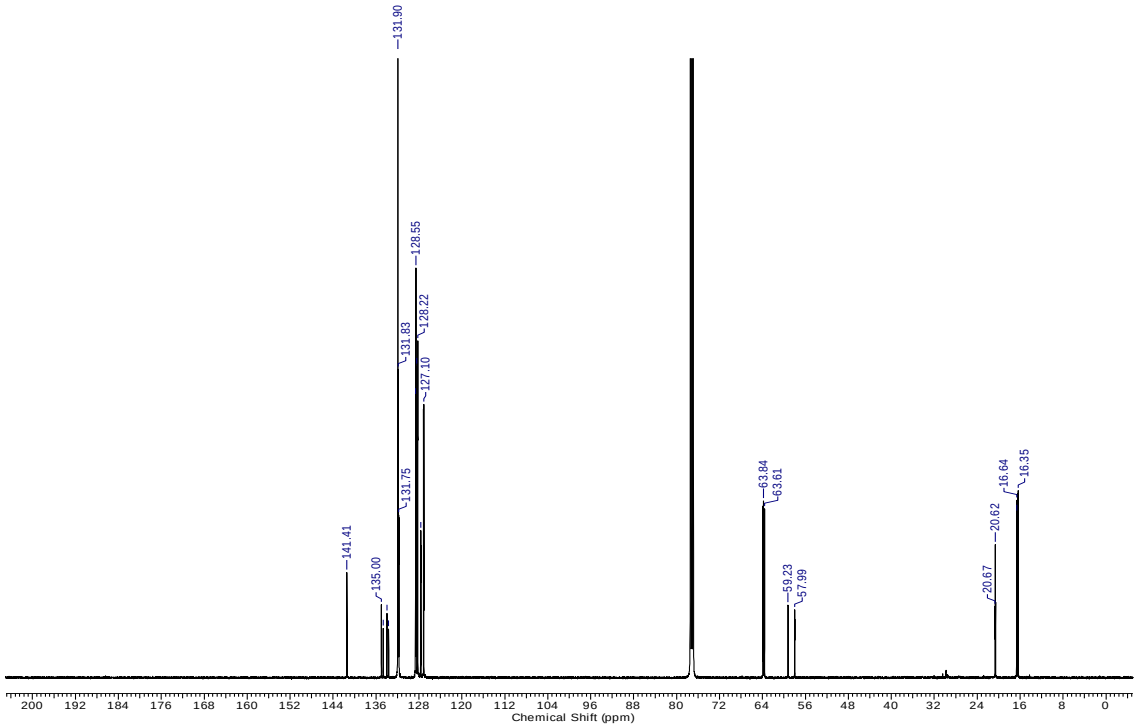

^{1}H NMR of **161a** (400 MHz, $CDCl_3$)

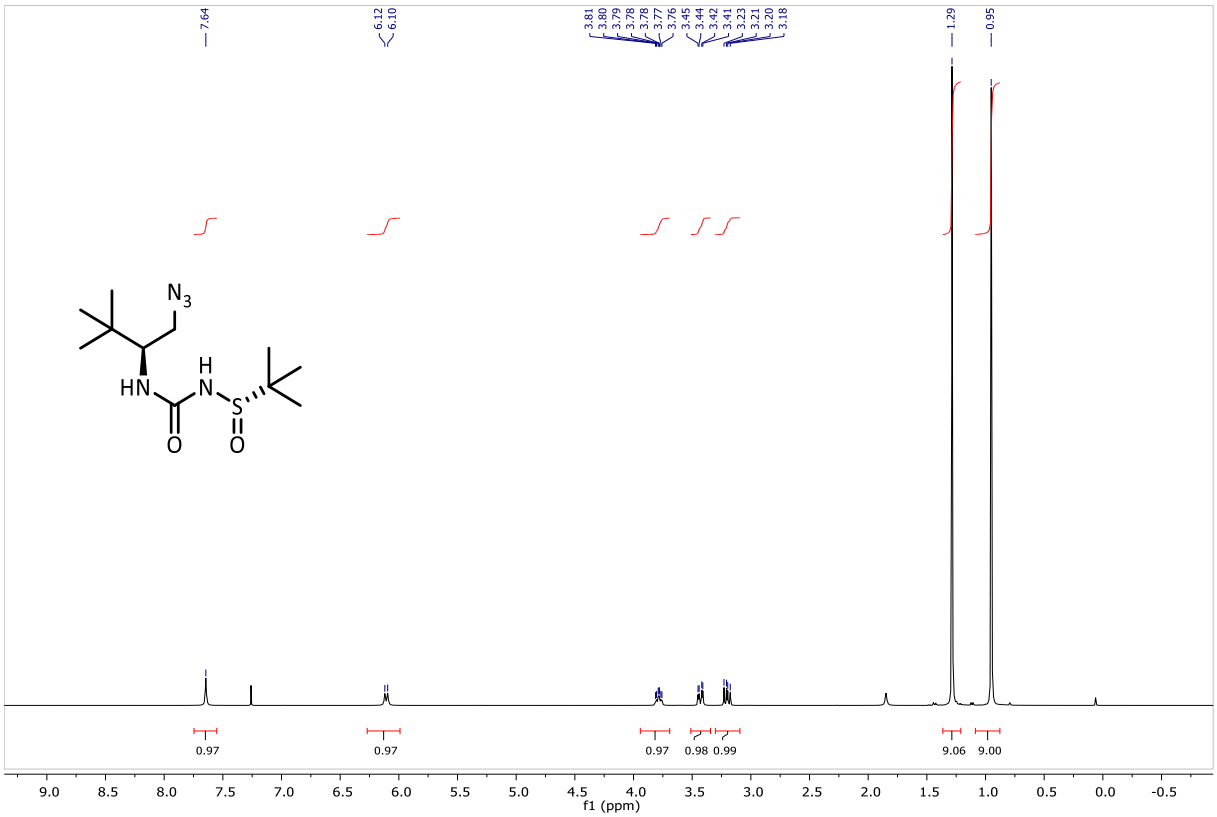

^{13}C NMR of **161a** (100 MHz, $CDCl_3$)

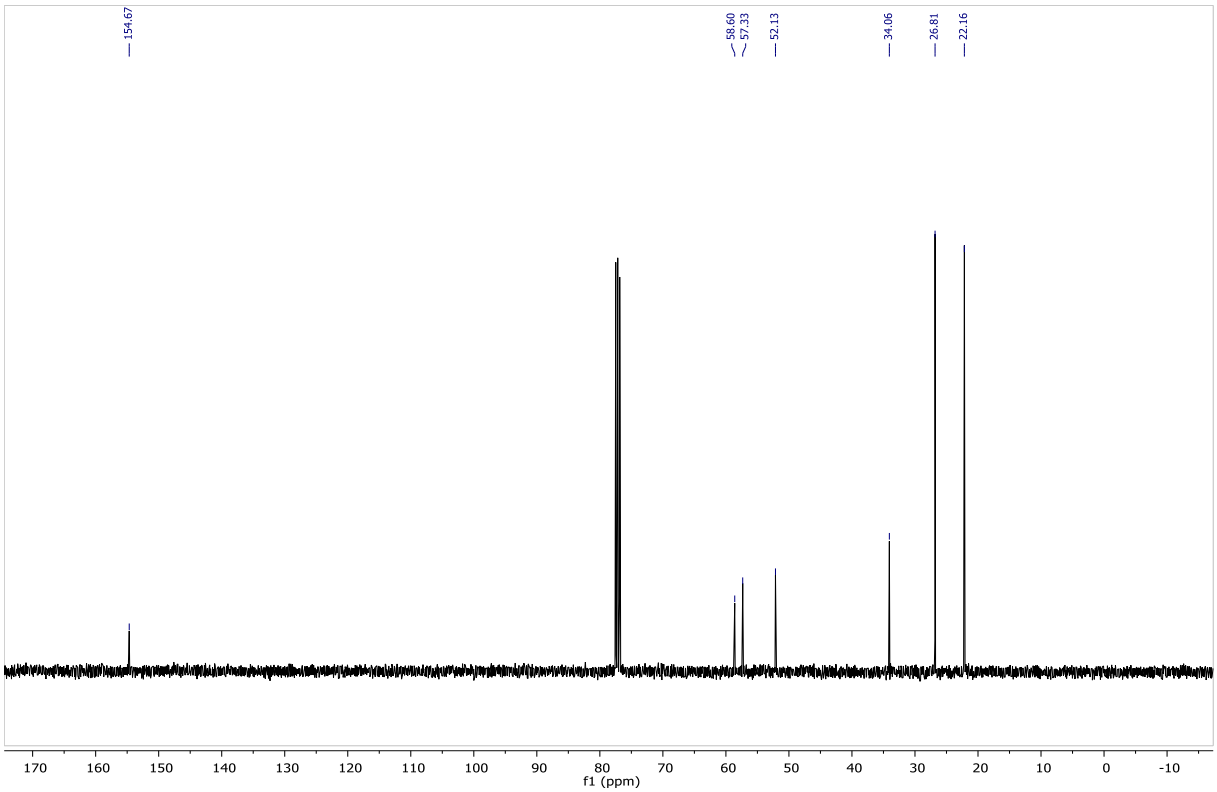

^{1}H-NMR of **191h** (400 MHz)

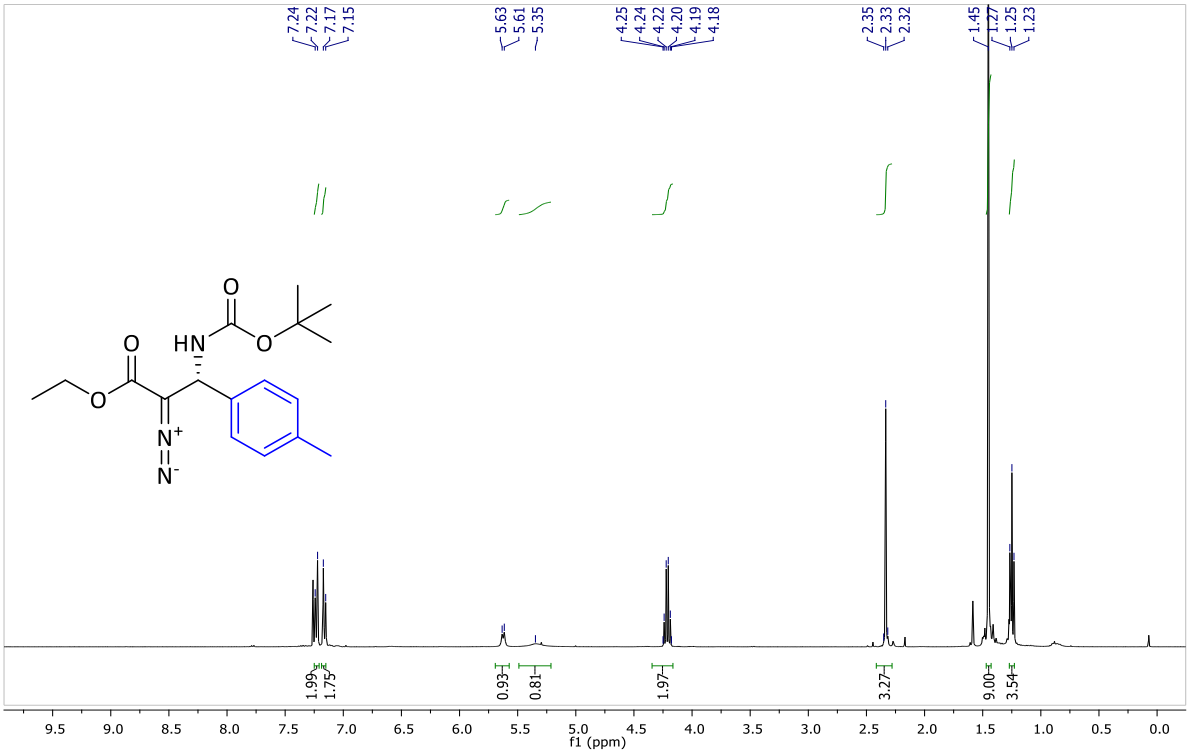

^{13}C-NMR spectrum of **191h** (100 MHz)

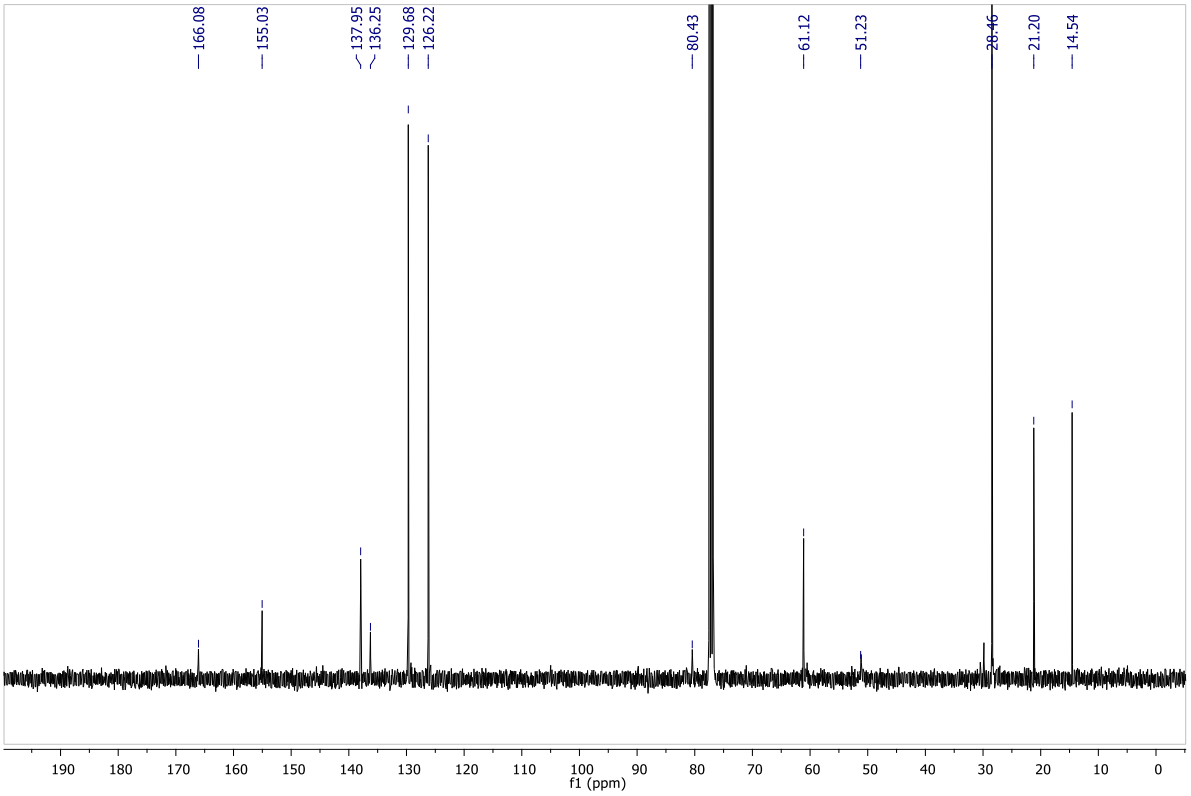

^{1}H-NMR spectrum of **210c** (400 MHz)

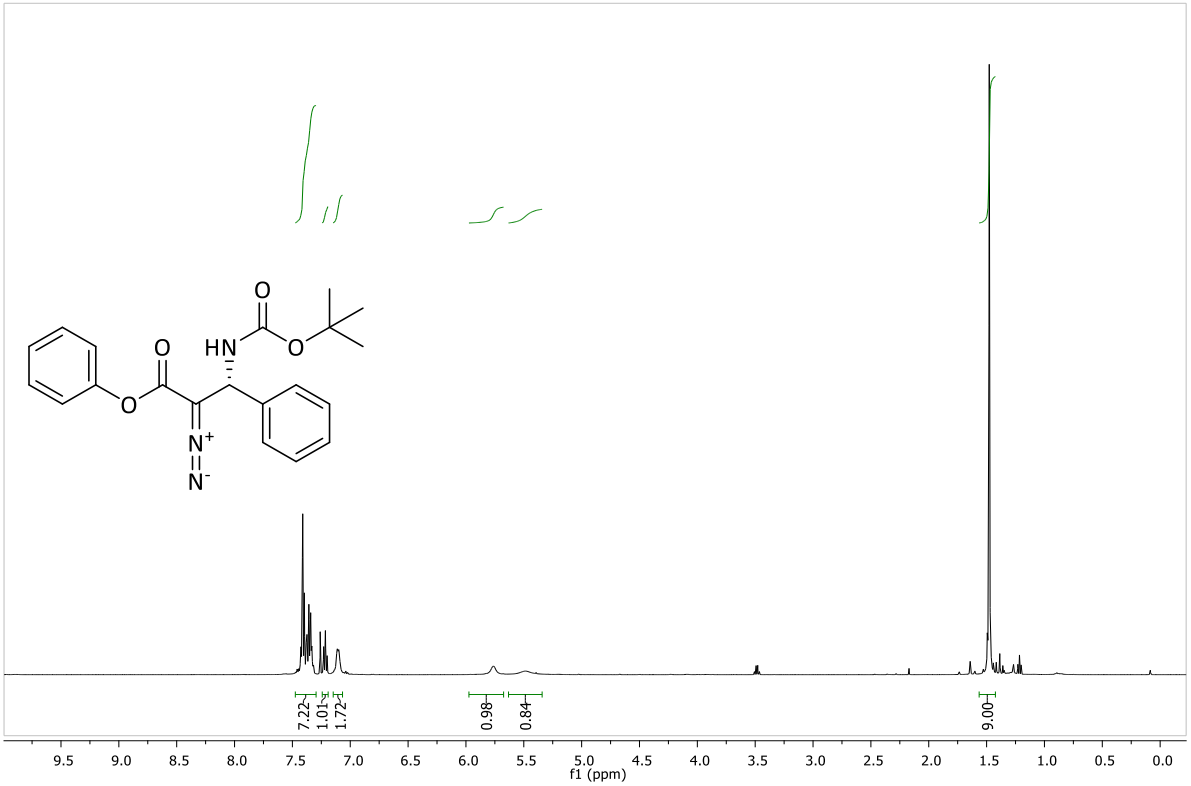

^{13}C-NMR spectrum of **210c** (125MHz)

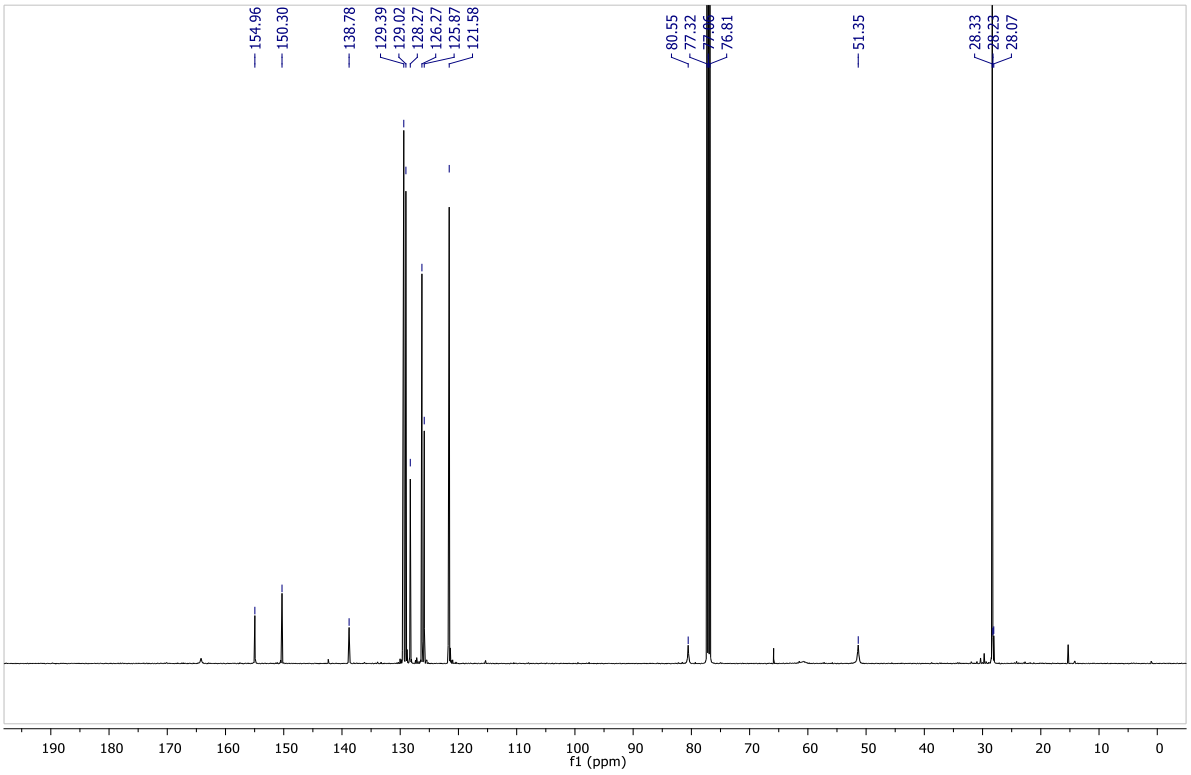

^{1}H-NMR spectrum of **213a** (400 MHz)

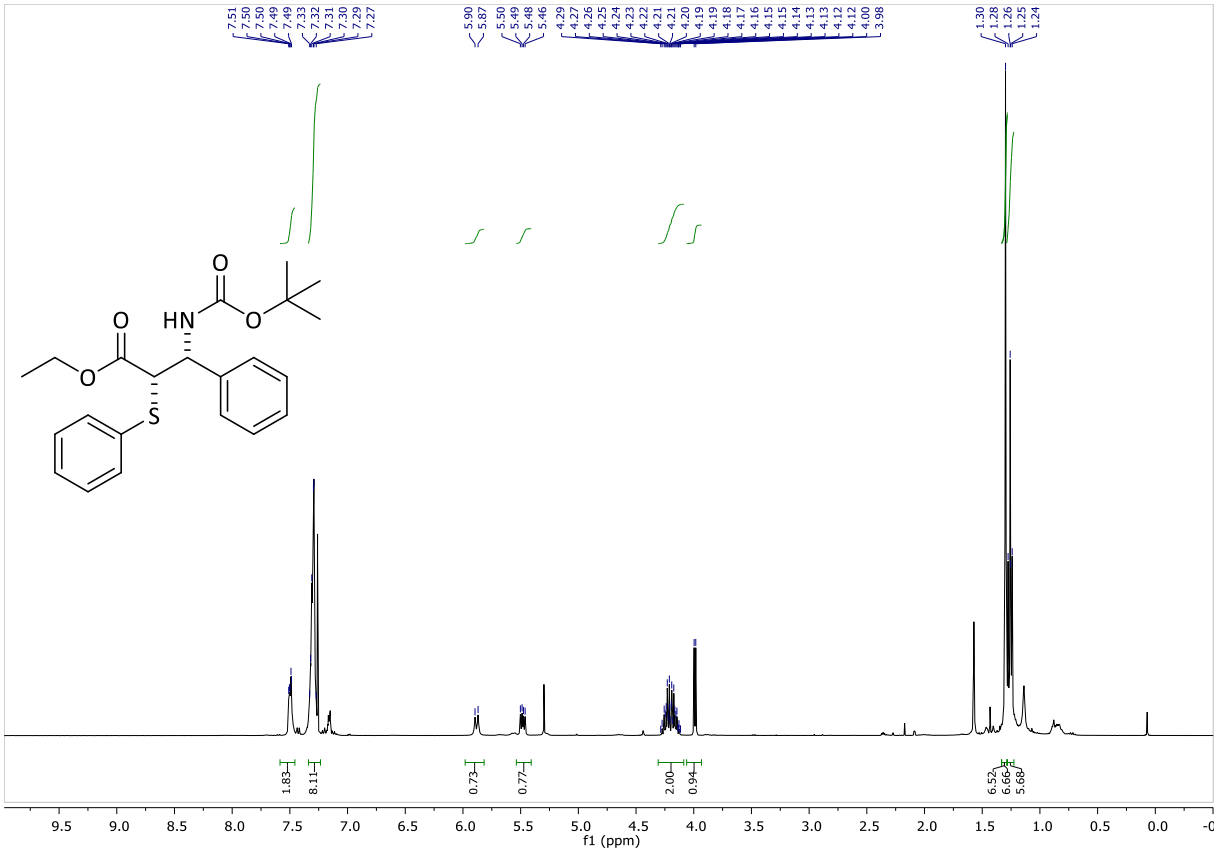

^{13}C-NMR spectrum of **213a** (125 MHz)

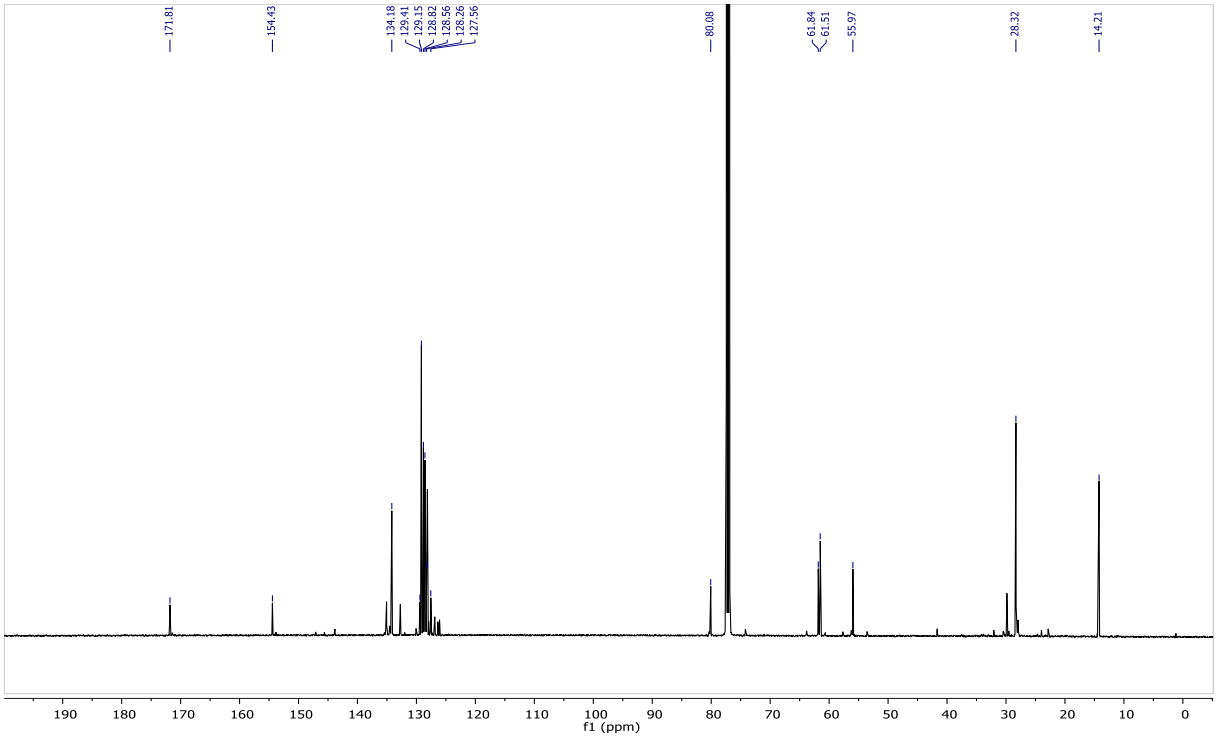

^{1}H-NMR spectrum of **213b** (400 MHz)

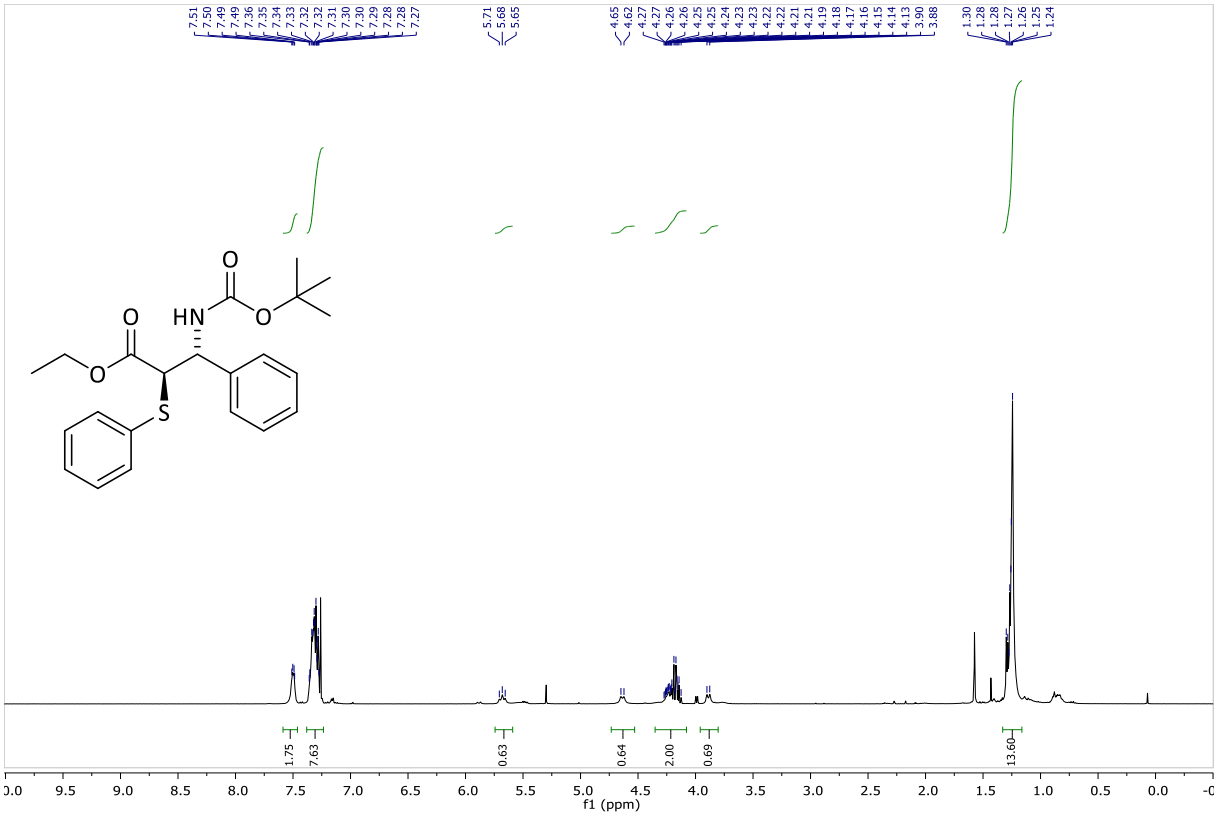

^{13}C-NMR spectrum of **213b** (125 MHz)

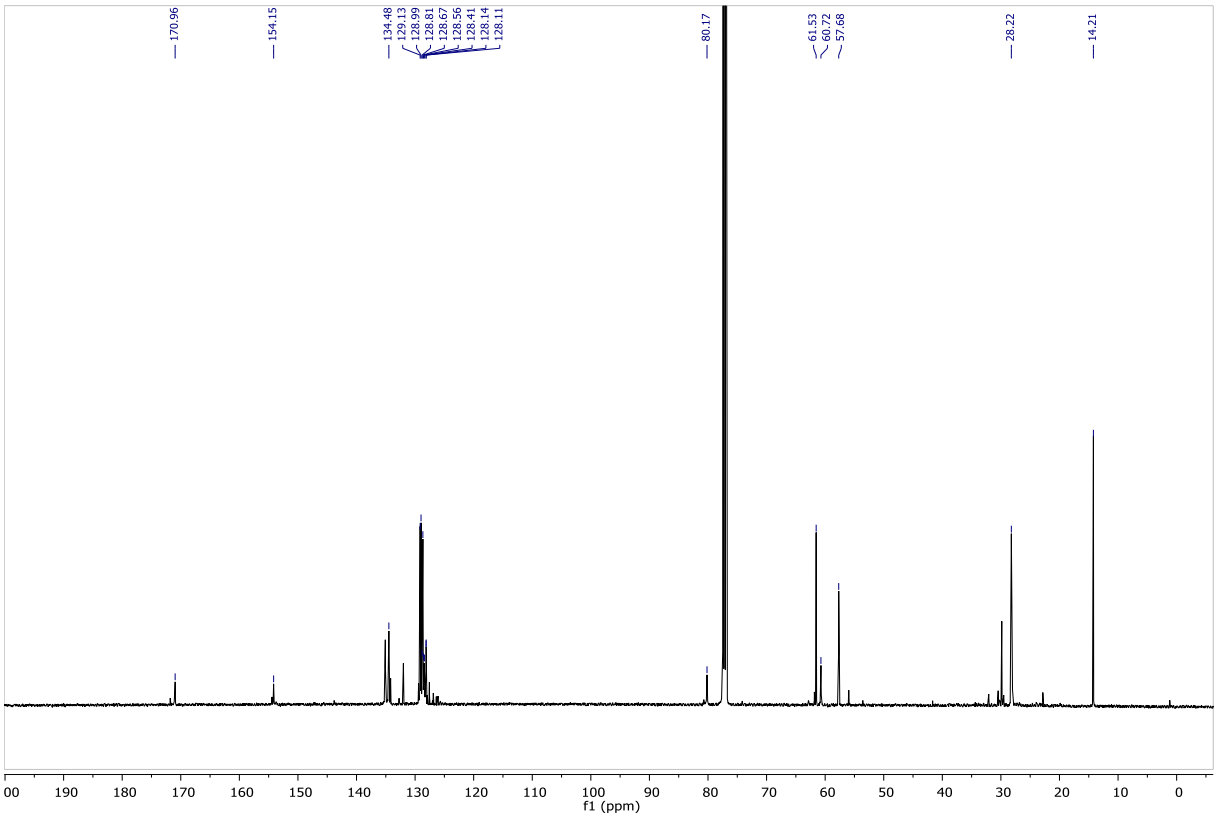

^{1}H-NMR spectrum of **227** (500 MHz)

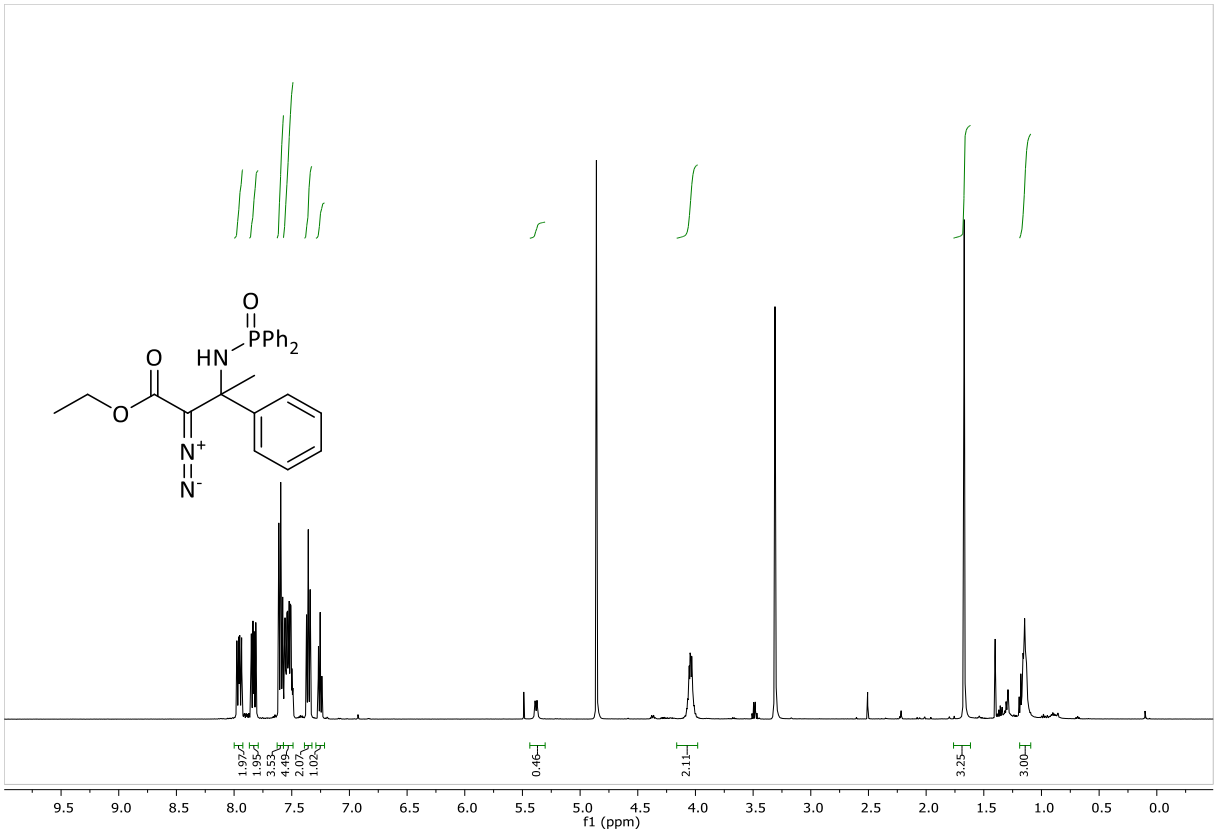

^{13}C-NMR spectrum of **227** (125 MHz)

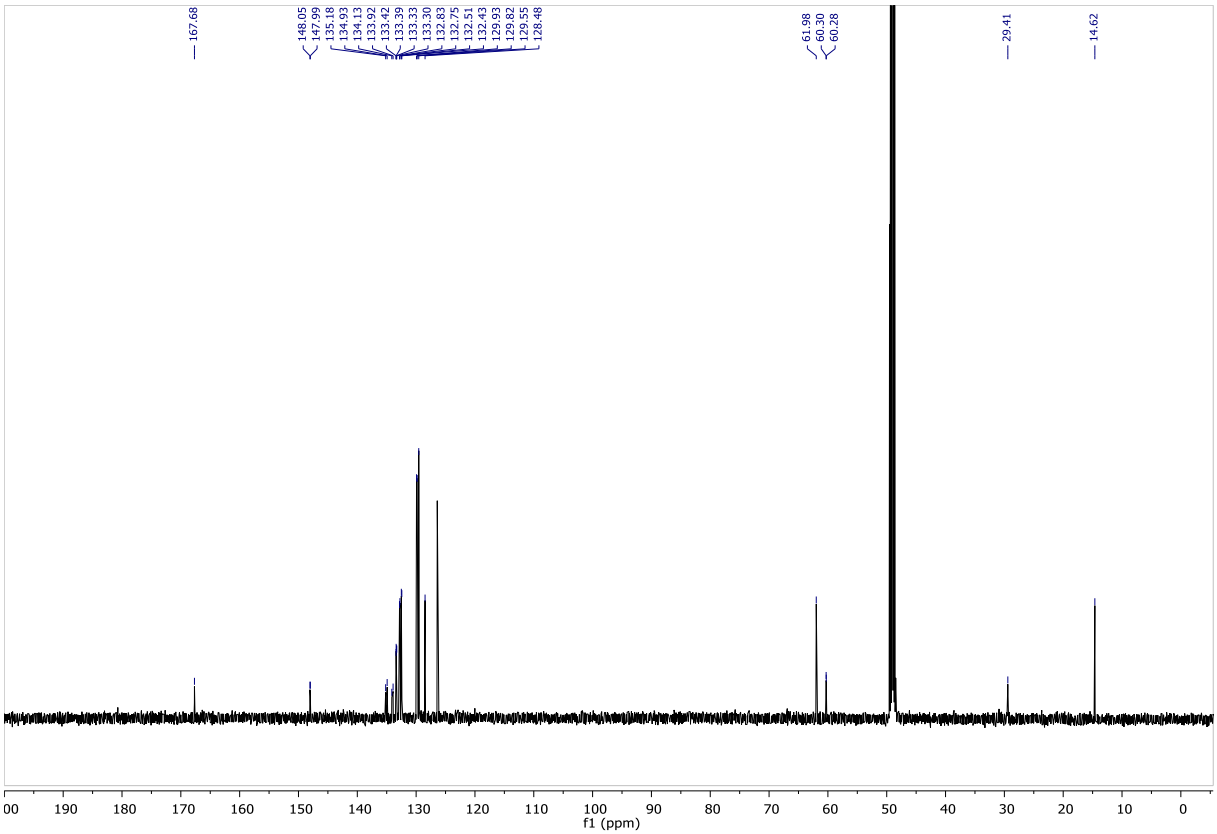

7.2 X-ray Diffraction Data

Single Crystal X-ray structure of Tetrahedral Complex **226**

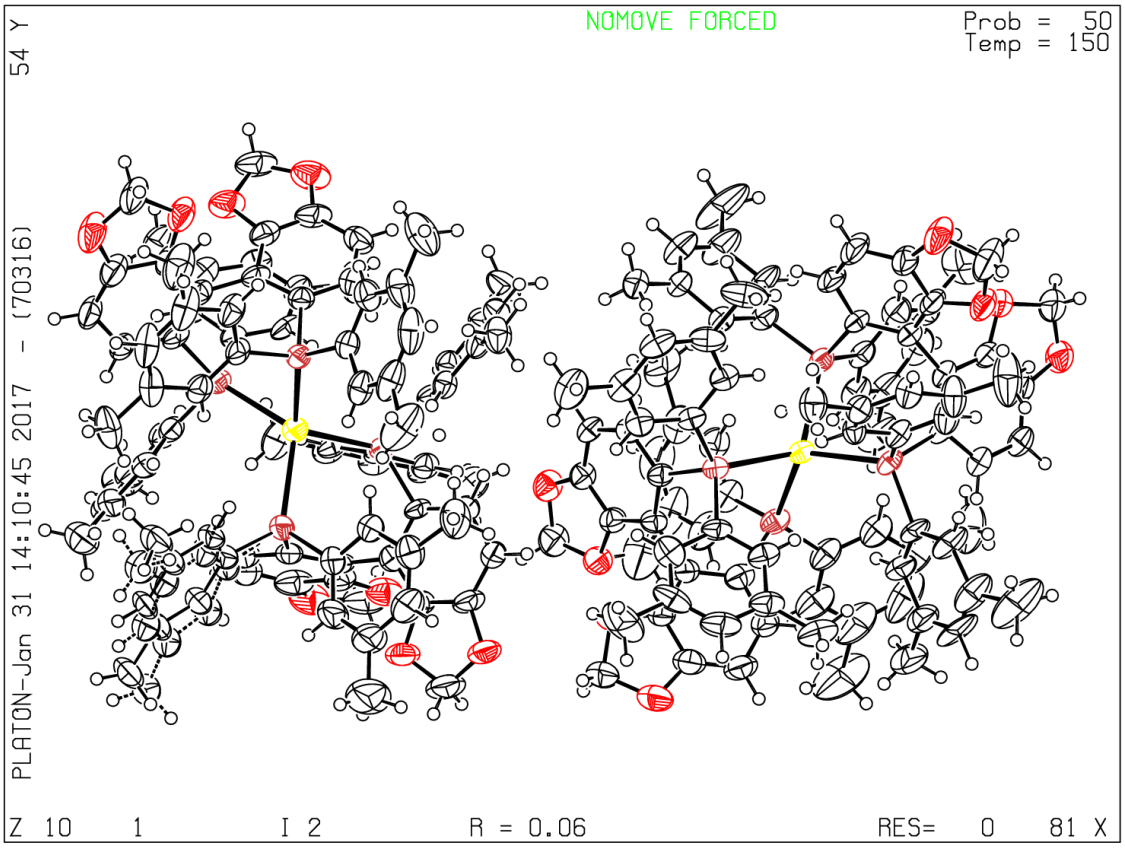

Figure 55: Single Crystal X-ray of complex 226. Triflate counterions have been omitted for clarity.

Crystal data	
Chemical formula	$C_{92}H_{88}AgO_8P_4$
M_r	1553.48
Crystal system, space group	Monoclinic, *I*2
Temperature (K)	150
a, *b*, *c* (Å)	15.7596 (4), 19.9954 (6), 58.7946 (13)
β (°)	92.799 (2)
V (Å³)	18505.2 (4)
Z	8
Radiation type	Cu *K*α
μ (mm⁻¹)	2.79
Crystal size (mm)	0.18 × 0.06 × 0.02

Data collection	
Diffractometer	Oxford Diffraction SuperNova
Absorption correction	Multi-scan *CrysAlis PRO*, (Agilent, 2011)
T_{min}, T_{max}	0.62, 0.95
No. of measured, independent and observed [$I > 2.0\sigma(I)$] reflections	38094, 38098, 28162
R_{int}	0.093
$(\sin\theta/\lambda)_{max}$ (Å^{-1})	0.631
Refinement	
$R[F^2 > 2\sigma(F^2)]$, $wR(F^2)$, S	0.064, 0.168, 0.97
No. of reflections	37943
No. of parameters	1964
No. of restraints	355
H-atom treatment	H-atom parameters constrained
	Method = Modified Sheldrick $w = 1/[\sigma^2(F^2) + (0.04P)^2 + 57.91P]$, where $P = (\max(F_o^2,0) + 2F_c^2)/3$
$\Delta\rho_{max}$, $\Delta\rho_{min}$ (e Å^{-3})	2.27, −1.49

Selected geometric parameters (Å, º)

Ag1—P1	2.5502 (19)	C61—C66	1.400 (9)
Ag1—P2	2.5502 (18)	C62—C63	1.400 (9)
Ag1—P101	2.5419 (17)	C63—C64	1.372 (10)
Ag1—P102	2.5354 (17)	C64—C65	1.373 (9)
Ag2—P201	2.5960 (18)	C64—O67	1.383 (8)
Ag2—P202	2.5406 (18)	C65—C66	1.393 (10)
Ag2—P301	2.5613 (19)	C65—O69	1.370 (9)
Ag2—P302	2.5888 (16)	O67—C68	1.416 (10)
P201—C211	1.834 (7)	C68—O69	1.433 (9)
P201—C221	1.809 (7)	P101—C111	1.857 (6)
P201—C231	1.839 (5)	P101—C121	1.847 (7)
P202—C241	1.850 (7)	P101—C131	1.834 (7)

P202—C251	1.853 (5)	P102—C141	1.832 (7)
P202—C261	1.846 (9)	P102—C151	1.841 (6)
P202—C241	1.850 (7)	P102—C161	1.832 (8)
P202—C261	1.846 (9)	C111—C112	1.380 (12)
P202—C651	1.840 (6)	C111—C116	1.342 (11)
C211—C212	1.425 (9)	C112—C113	1.400 (10)
C211—C216	1.371 (9)	C113—C114	1.348 (15)
C212—C213	1.362 (10)	C113—C117	1.498 (15)
C213—C214	1.406 (11)	C114—C115	1.417 (17)
C213—C217	1.525 (11)	C115—C116	1.405 (12)
C214—C215	1.389 (11)	C115—C118	1.586 (16)
C215—C216	1.385 (10)	C121—C122	1.394 (9)
C215—C218	1.508 (11)	C121—C126	1.361 (11)
C221—C222	1.367 (10)	C122—C123	1.387 (10)
C221—C226	1.428 (10)	C123—C124	1.408 (11)
C222—C223	1.408 (10)	C123—C127	1.498 (10)
C223—C224	1.398 (12)	C124—C125	1.401 (10)
C223—C227	1.489 (11)	C125—C126	1.395 (12)
C224—C225	1.408 (11)	C125—C128	1.510 (13)
C225—C226	1.385 (10)	C131—C132	1.400 (9)
C225—C228	1.506 (11)	C131—C136	1.415 (10)
C231—C232	1.398 (9)	C132—C133	1.392 (10)
C231—C236	1.414 (10)	C133—C134	1.360 (11)
C232—C233	1.400 (10)	C134—C135	1.409 (10)
C233—C234	1.361 (11)	C134—O137	1.378 (9)
C234—C235	1.391 (11)	C135—C136	1.383 (10)
C234—O237	1.370 (8)	C135—O139	1.362 (9)
C235—C236	1.357 (10)	C136—C166	1.475 (9)
C235—O239	1.381 (9)	O137—C138	1.408 (11)
C236—C266	1.496 (10)	C138—O139	1.456 (10)
O237—C238	1.464 (12)	C141—C142	1.396 (11)
C238—O239	1.427 (10)	C141—C146	1.368 (12)
C241—C242	1.367 (11)	C142—C143	1.394 (12)
C241—C246	1.397 (10)	C143—C144	1.350 (16)
C242—C243	1.385 (12)	C143—C147	1.526 (15)
C243—C244	1.395 (14)	C144—C145	1.396 (15)
C243—C247	1.480 (13)	C145—C146	1.407 (11)
C244—C245	1.375 (13)	C145—C148	1.506 (15)
C245—C246	1.402 (11)	C151—C152	1.417 (9)
C245—C248	1.532 (12)	C151—C156	1.386 (11)
C251—C252	1.408 (5)	C152—C153	1.388 (10)

C251—C256	1.385 (5)	C153—C154	1.383 (14)
C252—C253	1.403 (5)	C153—C157	1.517 (11)
C253—C254	1.407 (5)	C154—C155	1.390 (12)
C253—C257	1.510 (6)	C155—C156	1.392 (9)
C254—C255	1.417 (5)	C155—C158	1.490 (11)
C255—C256	1.407 (5)	C161—C162	1.383 (9)
C255—C258	1.496 (7)	C161—C166	1.421 (9)
C261—C262	1.373 (10)	C162—C163	1.385 (11)
C261—C266	1.427 (11)	C163—C164	1.348 (11)
C262—C263	1.387 (13)	C164—C165	1.398 (10)
C263—C264	1.334 (14)	C164—O167	1.391 (10)
C264—C265	1.404 (12)	C165—C166	1.395 (11)
C264—O267	1.383 (12)	C165—O169	1.372 (9)
C265—C266	1.363 (11)	O167—C168	1.405 (11)
C265—O269	1.381 (11)	C168—O169	1.433 (11)
O267—C268	1.404 (13)	P301—C311	1.847 (7)
C268—O269	1.448 (10)	P301—C321	1.835 (8)
C651—C652	1.407 (6)	P301—C331	1.826 (6)
C651—C656	1.387 (6)	P302—C341	1.808 (6)
C652—C653	1.399 (6)	P302—C351	1.835 (8)
C653—C654	1.408 (6)	P302—C361	1.852 (7)
C653—C657	1.508 (7)	C311—C312	1.385 (10)
C654—C655	1.418 (6)	C311—C316	1.384 (11)
C655—C656	1.401 (6)	C312—C313	1.370 (12)
C655—C658	1.501 (7)	C313—C314	1.376 (15)
P1—C11	1.839 (8)	C313—C317	1.522 (12)
P1—C21	1.850 (7)	C314—C315	1.365 (15)
P1—C31	1.845 (8)	C315—C316	1.386 (11)
P2—C41	1.833 (6)	C315—C318	1.513 (14)
P2—C51	1.839 (7)	C321—C322	1.365 (11)
P2—C61	1.848 (7)	C321—C326	1.409 (11)
C11—C12	1.409 (13)	C322—C323	1.432 (11)
C11—C16	1.415 (13)	C323—C324	1.404 (14)
C12—C13	1.417 (12)	C323—C327	1.521 (13)
C13—C14	1.313 (19)	C324—C325	1.356 (15)
C13—C17	1.490 (17)	C325—C326	1.410 (13)
C14—C15	1.42 (2)	C325—C328	1.500 (14)
C15—C16	1.391 (15)	C331—C332	1.398 (10)
C15—C18	1.573 (18)	C331—C336	1.390 (9)
C21—C22	1.373 (10)	C332—C333	1.401 (10)
C21—C26	1.398 (12)	C333—C334	1.378 (12)

C22—C23	1.385 (11)	C334—C335	1.359 (12)
C23—C24	1.387 (15)	C334—O337	1.351 (8)
C23—C27	1.531 (14)	C335—C336	1.397 (10)
C24—C25	1.375 (16)	C335—O339	1.382 (8)
C25—C26	1.378 (13)	C336—C366	1.487 (10)
C25—C28	1.550 (16)	O337—C338	1.414 (12)
C31—C32	1.372 (10)	C338—O339	1.450 (11)
C31—C36	1.421 (11)	C341—C342	1.406 (9)
C32—C33	1.403 (12)	C341—C346	1.376 (11)
C33—C34	1.338 (13)	C342—C343	1.391 (10)
C34—C35	1.399 (10)	C343—C344	1.379 (11)
C34—O37	1.399 (11)	C343—C347	1.510 (9)
C35—C36	1.375 (10)	C344—C345	1.375 (11)
C35—O39	1.366 (10)	C345—C346	1.419 (10)
C36—C66	1.494 (9)	C345—C348	1.504 (12)
O37—C38	1.459 (12)	C351—C352	1.357 (11)
C38—O39	1.448 (9)	C351—C356	1.404 (11)
C41—C42	1.423 (11)	C352—C353	1.387 (12)
C41—C46	1.368 (10)	C353—C354	1.390 (13)
C42—C43	1.378 (11)	C353—C357	1.528 (13)
C43—C44	1.393 (14)	C354—C355	1.393 (14)
C43—C47	1.504 (13)	C355—C356	1.371 (12)
C44—C45	1.382 (14)	C355—C358	1.507 (13)
C45—C46	1.404 (10)	C361—C362	1.396 (10)
C45—C48	1.486 (12)	C361—C366	1.403 (10)
C51—C52	1.434 (10)	C362—C363	1.392 (10)
C51—C56	1.375 (10)	C363—C364	1.350 (13)
C52—C53	1.379 (11)	C364—C365	1.401 (12)
C53—C54	1.385 (13)	C364—O367	1.372 (10)
C53—C57	1.486 (12)	C365—C366	1.364 (10)
C54—C55	1.374 (12)	C365—O369	1.374 (10)
C55—C56	1.414 (10)	O367—C368	1.426 (12)
C55—C58	1.516 (13)	C368—O369	1.430 (10)
C61—C62	1.396 (9)		
P1—Ag1—P2	91.05 (6)	C62—C61—C66	121.4 (6)
P1—Ag1—P101	118.30 (6)	C61—C62—C63	121.6 (6)
P2—Ag1—P101	119.36 (5)	C62—C63—C64	116.4 (6)
P1—Ag1—P102	116.22 (6)	C63—C64—C65	122.0 (6)
P2—Ag1—P102	119.68 (5)	C63—C64—O67	128.4 (6)
P101—Ag1—P102	94.47 (6)	C65—C64—O67	109.5 (6)

P201—Ag2—P202	91.24 (6)	C64—C65—C66	123.1 (7)
P201—Ag2—P301	117.22 (6)	C64—C65—O69	110.5 (6)
P202—Ag2—P301	125.43 (6)	C66—C65—O69	126.4 (6)
P201—Ag2—P302	118.36 (6)	C36—C66—C61	126.2 (6)
P202—Ag2—P302	116.24 (6)	C36—C66—C65	118.5 (6)
P301—Ag2—P302	91.05 (5)	C61—C66—C65	115.3 (6)
Ag2—P201—C211	109.9 (2)	C64—O67—C68	105.5 (5)
Ag2—P201—C221	118.8 (2)	O67—C68—O69	108.8 (6)
C211—P201—C221	104.4 (3)	C68—O69—C65	105.1 (6)
Ag2—P201—C231	115.9 (2)	Ag1—P101—C111	116.8 (3)
C211—P201—C231	103.7 (3)	Ag1—P101—C121	119.8 (2)
C221—P201—C231	102.5 (3)	C111—P101—C121	102.4 (3)
Ag2—P202—C241	116.7 (2)	Ag1—P101—C131	109.8 (2)
Ag2—P202—C251	125.2 (2)	C111—P101—C131	102.9 (3)
C241—P202—C251	94.8 (3)	C121—P101—C131	103.1 (3)
Ag2—P202—C261	99.5 (2)	Ag1—P102—C141	118.3 (2)
C241—P202—C261	107.2 (3)	Ag1—P102—C151	116.6 (2)
C251—P202—C261	113.0 (3)	C141—P102—C151	103.0 (3)
Ag2—P202—C241	116.7 (2)	Ag1—P102—C161	110.2 (2)
Ag2—P202—C261	99.5 (2)	C141—P102—C161	104.9 (4)
C241—P202—C261	107.2 (3)	C151—P102—C161	102.0 (3)
Ag2—P202—C651	132.6 (3)	P101—C111—C112	117.5 (5)
C241—P202—C651	95.0 (4)	P101—C111—C116	121.3 (7)
C261—P202—C651	103.7 (3)	C112—C111—C116	120.9 (7)
P201—C211—C212	118.1 (5)	C111—C112—C113	121.5 (8)
P201—C211—C216	123.2 (5)	C112—C113—C114	116.8 (10)
C212—C211—C216	118.4 (6)	C112—C113—C117	122.3 (10)
C211—C212—C213	121.3 (7)	C114—C113—C117	120.9 (9)
C212—C213—C214	118.3 (7)	C113—C114—C115	123.5 (7)
C212—C213—C217	121.0 (7)	C114—C115—C116	117.0 (8)
C214—C213—C217	120.5 (7)	C114—C115—C118	125.2 (10)
C213—C214—C215	121.8 (7)	C116—C115—C118	117.7 (12)
C214—C215—C216	118.2 (7)	C115—C116—C111	120.3 (10)
C214—C215—C218	120.0 (7)	P101—C121—C122	117.5 (6)
C216—C215—C218	121.8 (7)	P101—C121—C126	121.7 (6)
C215—C216—C211	122.0 (7)	C122—C121—C126	120.8 (7)
P201—C221—C222	121.9 (6)	C121—C122—C123	119.4 (7)
P201—C221—C226	119.7 (5)	C122—C123—C124	119.9 (7)
C222—C221—C226	118.4 (6)	C122—C123—C127	122.5 (7)
C221—C222—C223	123.2 (8)	C124—C123—C127	117.6 (7)
C222—C223—C224	117.1 (7)	C123—C124—C125	120.0 (8)

C222—C223—C227	121.7 (8)	C124—C125—C126	118.4 (8)
C224—C223—C227	121.2 (7)	C124—C125—C128	120.0 (9)
C223—C224—C225	121.7 (7)	C126—C125—C128	121.5 (8)
C224—C225—C226	119.2 (7)	C125—C126—C121	121.3 (7)
C224—C225—C228	119.0 (7)	P101—C131—C132	118.8 (5)
C226—C225—C228	121.8 (7)	P101—C131—C136	121.3 (5)
C221—C226—C225	120.4 (7)	C132—C131—C136	119.9 (7)
P201—C231—C232	122.8 (5)	C131—C132—C133	123.6 (7)
P201—C231—C236	117.6 (5)	C132—C133—C134	116.1 (6)
C232—C231—C236	119.6 (5)	C133—C134—C135	121.5 (7)
C231—C232—C233	121.9 (7)	C133—C134—O137	129.0 (6)
C232—C233—C234	117.4 (7)	C135—C134—O137	109.5 (6)
C233—C234—C235	120.9 (6)	C134—C135—C136	123.1 (7)
C233—C234—O237	129.1 (7)	C134—C135—O139	109.0 (6)
C235—C234—O237	110.0 (7)	C136—C135—O139	127.8 (6)
C234—C235—C236	123.3 (7)	C131—C136—C135	115.5 (6)
C234—C235—O239	109.6 (6)	C131—C136—C166	127.7 (6)
C236—C235—O239	127.0 (7)	C135—C136—C166	116.5 (6)
C231—C236—C235	116.9 (7)	C134—O137—C138	104.8 (6)
C231—C236—C266	123.7 (6)	O137—C138—O139	107.7 (7)
C235—C236—C266	119.2 (7)	C138—O139—C135	104.4 (6)
C234—O237—C238	105.6 (6)	P102—C141—C142	122.4 (6)
O237—C238—O239	107.0 (7)	P102—C141—C146	117.9 (6)
C238—O239—C235	106.4 (7)	C142—C141—C146	119.6 (7)
P202—C241—C242	122.3 (6)	C141—C142—C143	119.4 (9)
P202—C241—C246	117.1 (5)	C142—C143—C144	119.9 (9)
C242—C241—C246	120.6 (7)	C142—C143—C147	120.8 (10)
C241—C242—C243	122.1 (9)	C144—C143—C147	119.3 (9)
C242—C243—C244	116.5 (8)	C143—C144—C145	122.7 (9)
C242—C243—C247	121.2 (10)	C144—C145—C146	116.5 (10)
C244—C243—C247	122.3 (9)	C144—C145—C148	123.6 (9)
C243—C244—C245	123.1 (8)	C146—C145—C148	119.9 (10)
C244—C245—C246	118.9 (8)	C145—C146—C141	121.8 (9)
C244—C245—C248	120.5 (8)	P102—C151—C152	122.4 (6)
C246—C245—C248	120.5 (8)	P102—C151—C156	117.8 (5)
C245—C246—C241	118.5 (7)	C152—C151—C156	119.8 (6)
P202—C251—C252	119.25 (6)	C151—C152—C153	118.6 (8)
P202—C251—C256	119.16 (6)	C152—C153—C154	120.2 (7)
C252—C251—C256	121.45 (6)	C152—C153—C157	118.3 (9)
C251—C252—C253	120.39 (6)	C154—C153—C157	121.4 (8)
C252—C253—C254	116.84 (5)	C153—C154—C155	122.2 (7)

C252—C253—C257	121.38 (6)	C154—C155—C156	117.5 (7)
C254—C253—C257	121.78 (6)	C154—C155—C158	121.7 (7)
C253—C254—C255	123.95 (6)	C156—C155—C158	120.8 (7)
C254—C255—C256	116.88 (5)	C155—C156—C151	121.6 (6)
C254—C255—C258	121.77 (6)	P102—C161—C162	119.7 (5)
C256—C255—C258	121.34 (6)	P102—C161—C166	120.1 (5)
C255—C256—C251	120.46 (6)	C162—C161—C166	120.2 (7)
P202—C261—C262	118.1 (7)	C161—C162—C163	123.5 (7)
P202—C261—C266	120.5 (6)	C162—C163—C164	116.8 (7)
C262—C261—C266	120.8 (9)	C163—C164—C165	121.6 (8)
C261—C262—C263	122.9 (10)	C163—C164—O167	129.0 (7)
C262—C263—C264	117.0 (8)	C165—C164—O167	109.4 (7)
C263—C264—C265	120.9 (9)	C164—C165—C166	123.0 (7)
C263—C264—O267	131.7 (9)	C164—C165—O169	109.4 (7)
C265—C264—O267	107.4 (9)	C166—C165—O169	127.6 (6)
C264—C265—C266	124.3 (9)	C136—C166—C161	127.3 (7)
C264—C265—O269	110.7 (8)	C136—C166—C165	117.4 (6)
C266—C265—O269	124.9 (8)	C161—C166—C165	114.9 (6)
C236—C266—C261	126.6 (7)	C164—O167—C168	105.5 (7)
C236—C266—C265	119.4 (7)	O167—C168—O169	109.4 (8)
C261—C266—C265	113.9 (7)	C168—O169—C165	105.6 (6)
C264—O267—C268	108.2 (7)	Ag2—P301—C311	130.0 (2)
O267—C268—O269	108.0 (8)	Ag2—P301—C321	114.0 (2)
C268—O269—C265	105.0 (7)	C311—P301—C321	98.5 (3)
P202—C651—C652	119.24 (6)	Ag2—P301—C331	99.7 (2)
P202—C651—C656	119.17 (6)	C311—P301—C331	105.7 (3)
C652—C651—C656	121.47 (6)	C321—P301—C331	107.3 (3)
C651—C652—C653	120.39 (6)	Ag2—P302—C341	119.1 (2)
C652—C653—C654	116.83 (5)	Ag2—P302—C351	111.3 (2)
C652—C653—C657	121.38 (6)	C341—P302—C351	104.5 (3)
C654—C653—C657	121.79 (6)	Ag2—P302—C361	117.47 (19)
C653—C654—C655	123.94 (6)	C341—P302—C361	98.6 (3)
C654—C655—C656	116.88 (5)	C351—P302—C361	103.8 (3)
C654—C655—C658	121.78 (6)	P301—C311—C312	116.4 (6)
C656—C655—C658	121.34 (6)	P301—C311—C316	123.7 (5)
C655—C656—C651	120.47 (6)	C312—C311—C316	119.7 (7)
Ag1—P1—C11	120.9 (3)	C311—C312—C313	119.6 (9)
Ag1—P1—C21	113.2 (3)	C312—C313—C314	120.0 (8)
C11—P1—C21	102.6 (3)	C312—C313—C317	119.7 (11)
Ag1—P1—C31	110.6 (2)	C314—C313—C317	120.3 (9)
C11—P1—C31	103.7 (4)	C313—C314—C315	121.4 (8)

C21—P1—C31	104.0 (4)	C314—C315—C316	118.8 (9)
Ag1—P2—C41	113.1 (3)	C314—C315—C318	120.5 (9)
Ag1—P2—C51	120.3 (2)	C316—C315—C318	120.6 (10)
C41—P2—C51	103.5 (3)	C315—C316—C311	120.3 (8)
Ag1—P2—C61	108.9 (2)	P301—C321—C322	118.4 (6)
C41—P2—C61	105.9 (3)	P301—C321—C326	121.0 (6)
C51—P2—C61	104.0 (3)	C322—C321—C326	120.6 (8)
P1—C11—C12	118.0 (6)	C321—C322—C323	120.5 (8)
P1—C11—C16	121.8 (8)	C322—C323—C324	117.1 (9)
C12—C11—C16	120.2 (8)	C322—C323—C327	119.5 (9)
C11—C12—C13	120.0 (10)	C324—C323—C327	123.3 (8)
C12—C13—C14	118.7 (12)	C323—C324—C325	122.9 (8)
C12—C13—C17	119.3 (11)	C324—C325—C326	119.3 (10)
C14—C13—C17	121.9 (10)	C324—C325—C328	120.3 (9)
C13—C14—C15	123.4 (10)	C326—C325—C328	120.4 (11)
C14—C15—C16	119.7 (12)	C325—C326—C321	119.5 (9)
C14—C15—C18	124.9 (12)	P301—C331—C332	117.1 (5)
C16—C15—C18	115.4 (15)	P301—C331—C336	121.7 (5)
C11—C16—C15	117.9 (12)	C332—C331—C336	120.5 (6)
P1—C21—C22	120.4 (6)	C331—C332—C333	122.6 (7)
P1—C21—C26	120.0 (6)	C332—C333—C334	116.3 (7)
C22—C21—C26	119.5 (7)	C333—C334—C335	120.4 (6)
C21—C22—C23	120.5 (9)	C333—C334—O337	126.6 (9)
C22—C23—C24	119.2 (9)	C335—C334—O337	112.9 (7)
C22—C23—C27	119.4 (10)	C334—C335—C336	125.1 (7)
C24—C23—C27	121.3 (8)	C334—C335—O339	108.1 (7)
C23—C24—C25	121.0 (8)	C336—C335—O339	126.8 (7)
C24—C25—C26	119.3 (10)	C335—C336—C331	114.8 (7)
C24—C25—C28	120.6 (10)	C335—C336—C366	117.3 (6)
C26—C25—C28	119.5 (12)	C331—C336—C366	127.9 (6)
C21—C26—C25	120.4 (10)	C334—O337—C338	105.1 (7)
P1—C31—C32	120.5 (6)	O337—C338—O339	107.8 (5)
P1—C31—C36	120.7 (5)	C338—O339—C335	105.5 (7)
C32—C31—C36	118.8 (7)	P302—C341—C342	120.2 (6)
C31—C32—C33	124.0 (8)	P302—C341—C346	121.3 (4)
C32—C33—C34	115.6 (7)	C342—C341—C346	118.5 (6)
C33—C34—C35	123.3 (8)	C341—C342—C343	120.8 (7)
C33—C34—O37	128.5 (8)	C342—C343—C344	118.8 (6)
C35—C34—O37	108.1 (8)	C342—C343—C347	118.2 (7)
C34—C35—C36	121.0 (8)	C344—C343—C347	123.0 (7)
C34—C35—O39	111.0 (7)	C343—C344—C345	122.8 (7)

C36—C35—O39	127.9 (6)	C344—C345—C346	117.3 (7)
C31—C36—C35	117.2 (6)	C344—C345—C348	122.7 (7)
C31—C36—C66	125.4 (6)	C346—C345—C348	119.9 (7)
C35—C36—C66	117.4 (7)	C345—C346—C341	121.8 (6)
C34—O37—C38	105.2 (7)	P302—C351—C352	123.6 (6)
O37—C38—O39	106.1 (7)	P302—C351—C356	118.4 (6)
C38—O39—C35	105.1 (6)	C352—C351—C356	117.8 (8)
P2—C41—C42	121.8 (6)	C351—C352—C353	122.7 (8)
P2—C41—C46	119.1 (6)	C352—C353—C354	118.1 (8)
C42—C41—C46	119.1 (6)	C352—C353—C357	121.0 (9)
C41—C42—C43	119.8 (8)	C354—C353—C357	120.8 (9)
C42—C43—C44	119.5 (8)	C353—C354—C355	121.0 (8)
C42—C43—C47	120.5 (10)	C354—C355—C356	118.4 (9)
C44—C43—C47	120.0 (8)	C354—C355—C358	120.7 (9)
C43—C44—C45	121.8 (7)	C356—C355—C358	120.8 (9)
C44—C45—C46	117.9 (8)	C351—C356—C355	121.8 (8)
C44—C45—C48	121.1 (7)	P302—C361—C362	122.5 (5)
C46—C45—C48	120.9 (9)	P302—C361—C366	117.7 (5)
C45—C46—C41	121.8 (8)	C362—C361—C366	119.8 (6)
P2—C51—C52	121.6 (5)	C361—C362—C363	122.2 (7)
P2—C51—C56	119.0 (6)	C362—C363—C364	117.5 (8)
C52—C51—C56	119.4 (6)	C363—C364—C365	120.6 (8)
C51—C52—C53	119.5 (8)	C363—C364—O367	129.3 (9)
C52—C53—C54	120.0 (8)	C365—C364—O367	110.1 (8)
C52—C53—C57	120.9 (9)	C364—C365—C366	123.2 (8)
C54—C53—C57	119.2 (8)	C364—C365—O369	109.4 (7)
C53—C54—C55	121.6 (7)	C366—C365—O369	127.4 (7)
C54—C55—C56	119.2 (8)	C336—C366—C361	124.8 (6)
C54—C55—C58	122.0 (8)	C336—C366—C365	118.4 (7)
C56—C55—C58	118.8 (9)	C361—C366—C365	116.5 (7)
C55—C56—C51	120.3 (8)	C364—O367—C368	105.5 (7)
P2—C61—C62	117.0 (5)	O367—C368—O369	109.2 (7)
P2—C61—C66	121.3 (5)	C368—O369—C365	105.7 (7)

7.3 ^{1}H-^{1}H-EXSY Spectrum of ^{13}C-labelled NaOAc in D_2O at 298 K showing SSSE cross peaks of ^{13}C nuclides (t_{mix} = 5 sec, 500 MHz)

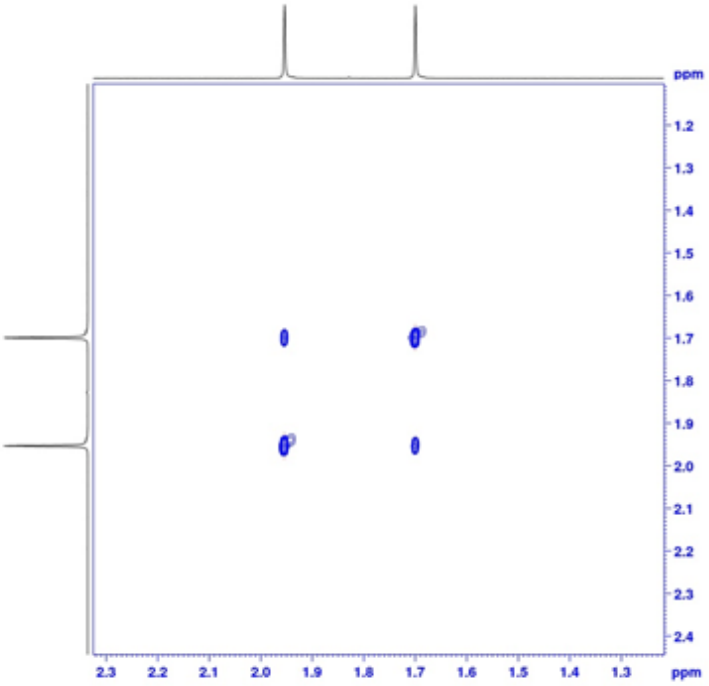

7.4 ^{1}H-^{1}H-EXSY Spectrum of EtOH in $CDCl_3$ at 298 K showing SSSE cross peaks of ^{13}C nuclides (t_{mix} = 5 sec, 500 MHz)

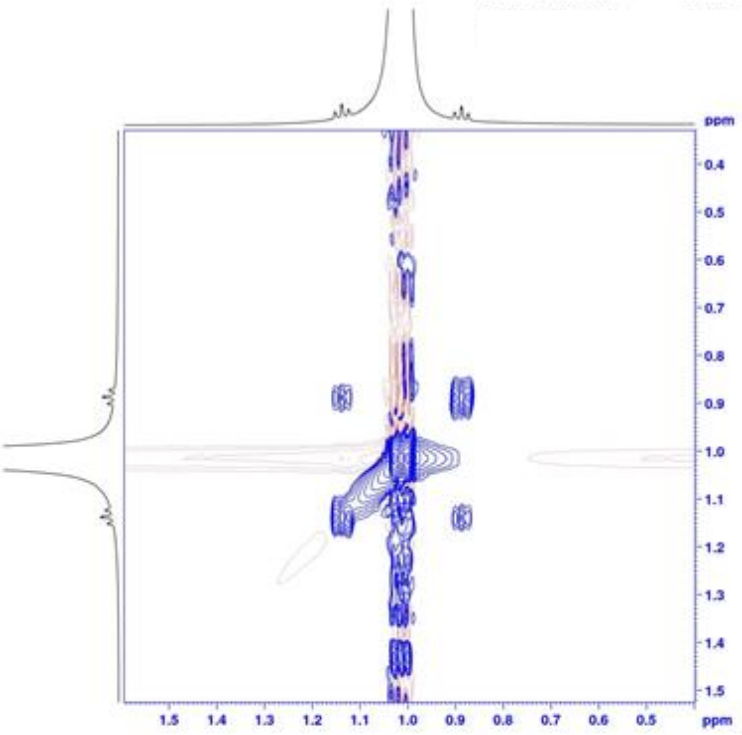

8. References

(1) Strohmann, C.; Gessner, V. H. *J. Am. Chem. Soc.* **2008**, *130*, 11719–11725.

(2) Tomioka, K.; Inoue, I.; Shindo, M.; Koga, K. *Tetrahedron Lett.* **1991**, *32*, 3095–3098.

(3) Soai, K.; Hatanaka, T.; Miyazawa, T. *J.Chem.Soc.,chem.commun.* **1992**, 1097–1098.

(4) Denmark, S. E.; Nakajima, N.; Nicaise, O. J. *J. Am. Chem. Soc.* **1994**, *116*, 8797–8798.

(5) Reich, H. J.; Green, D. P.; Medina, M. A.; Goldenberg, W. S.; Gudmundsson, B. O.; Dykstra, R. R.; Phillips, N. H. *J. Am. Chem. Soc.* **1998**, *120*, 7201–7210.

(6) Hoffmann, D.; Collum, D. B. *J. Am. Chem. Soc.* **1998**, *120*, 5810–5811.

(7) Kizirian, J. C.; Cabello, N.; Pinchard, L.; Caille, J. C.; Alexakis, A. *Tetrahedron* **2005**, *61*, 8939–8946.

(8) Perron, Q.; Alexakis, A. *Tetrahedron: Asymmetry* **2007**, *18*, 2503–2506.

(9) Fujihara, H.; Nagai, K.; Tomioka, K. *J. Am. Chem. Soc.* **2000**, *122*, 12055–12056.

(10) Soeta, T.; Nagai, K.; Fujihara, H.; Kuriyama, M.; Tomioka, K. *J. Org. Chem.* **2003**, *68*, 9723–9727.

(11) Wang, M. C.; Liu, L. T.; Hua, Y. Z.; Zhang, J. S.; Shi, Y. Y.; Wang, D. K. *Tetrahedron: Asymmetry* **2005**, *16*, 2531–2534.

(12) Cote, A.; Boezio, A. A.; Charette, A. B. *Proc. Natl. Acad. Sci. U. S. A.* **2004**, *101*, 5405–5410.

(13) Porter, J. R.; Traverse, J. F.; Hoveyda, A. H.; Snapper, M. L.; College, B.; Hill, C. *J. Am. Chem. Soc.* **2001**, *123*, 984–985.

(14) Akullian, L. C.; Porter, J. R.; Traverse, J. F.; Snapper, M. L.; Hoveyda, A. H. *Adv. Synth. Catal.* **2005**, *347*, 417–425.

(15) Hayashi, T.; Ishigedani, M. *J. Am. Chem. Soc.* **2000**, *122*, 976–977.

(16) Hayashi, T.; Kawai, M.; Tokunaga, N. *Angew. Chemie - Int. Ed.* **2004**, *43*, 6125–6128.

(17) Tokunaga, N.; Otomaru, Y.; Okamoto, K.; Ueyama, K.; Shintani, R.; Hayashi, T. *J. Am. Chem. Soc.* **2004**, *126*, 13584–13585.

(18) Jagt, R. B. C.; Toullec, P. Y.; Geerdink, D.; De Vries, J. G.; Feringa, B. L.; Minnaard, A. J. *Angew. Chemie - Int. Ed.* **2006**, *45*, 2789–2791.

(19) Wei, C.; Li, C. *J. Am. Chem. Soc.* **2002**, *124*, 5638–5639.

(20) Nakamura, K.; Nakamura, H.; Yamamoto, Y. *J. Org. Chem.* **1999**, *64*, 2614–2615.

(21) Riant, O.; Hannedouche, J. *Org. Biomol. Chem.* **2007**, *5*, 873–388.

(22) Kumagai, N.; Shibasaki, M. *Bull. Chem. Soc. Jpn.* **2015**, *88*, 503–517.

(23) Wada, R.; Shibuguchi, T.; Makino, S.; Oisaki, K.; Kanai, M.; Shibasaki, M. *J. Am. Chem. Soc.* **2006**, *128*, 7687–7691.

(24) Sibi, M. P. *Tetrahedron* **2002**, *58*, 7991–8035.

(25) Konishi, M.; Nishio, M.; Saitoh, K.; Miyaki, T.; Oki, T.; Kawaguchi, H. *J. Antibiot. (Tokyo).* **1989**, *42*, 1749–1755.

(26) Harbut, M. B.; Velmourougane, G.; Dalal, S.; Reiss, G.; Whisstock, J. C.; Onder, O.; Brisson, D.; McGowan, S.; Klemba, M.; Greenbaum, D. C. *Proc. Natl. Acad. Sci. U. S. A.* **2011**, *108*, E526–E534.

(27) Von Nussbaum, F.; Spiteller, P.; Rüth, M.; Steglich, W.; Wanner, G.; Gamblin, B.; Stievano, L.; Wagner, F. E. *Angew. Chemie - Int. Ed.* **1998**, *37*, 3292–3295.

(28) Crews, P.; Manes, L. V; Boehler, M. *Tetrahedron Lett.* **1986**, *27*, 2797–2800.

(29) Ishitani, H.; Ueno, M.; Kobayashi, S. *J. Am. Chem. Soc.* **1997**, *119*, 7153–7154.

(30) Kobayashi, S.; Ishitani, H.; Ueno, M. *J. Am. Chem. Soc.* **1998**, *120*, 431–432.

(31) Josephsohn, N. S.; Snapper, M. L.; Hoveyda, A. H. *J. Am. Chem. Soc.* **2004**, *126*, 3734–3735.

(32) Trost, B. M.; Jaratjaroonphong, J.; Reutrakul, V. *J. Am. Chem. Soc.* **2006**, *128*, 2778–2779.

(33) List, B.; Pojarliev, P.; Biller, W. T.; Martin, H. J. *J. Am. Chem. Soc.* **2002**, *124*, 827–833.

(34) Notz, W.; Sakthivel, K.; Bui, T.; Zhong, G.; Barbas, C. F. *Tetrahedron Lett.* **2001**, *42*, 199–201.

(35) Cordova, A. *Acc.Chem.Res.* **2004**, *37*, 102–112.

(36) Tillman, A. L.; Ye, J.; Dixon, D. J. *Chem. Commun. (Camb).* **2006**, *44*, 1191–1193.

(37) Yamada, K. I.; Harwood, S. J.; Gröger, H.; Shibasaki, M. *Angew. Chemie - Int. Ed.* **1999**, *38*, 3504–3506.

(38) Xu, X.; Furukawa, T.; Okino, T.; Miyabe, H.; Takemoto, Y. *Chem. - A Eur. J.* **2005**, *12*, 466–476.

(39) Maggi, C. A. *Gen.Pharmac.* **1995**, *26*, 911–944.

(40) Knudsen, K. R.; Jorgensen, K. A. *Org. Biomol. Chem.* **2005**, *3*, 1362–1364.

(41) Udine, U.; Ungheria, V.; Padova, C. N. R.; Uniti, C. S. *Inorg. Chem* **1990**, *29*, 2859–2862.

(42) Núñez, M. G.; Farley, A. J. M.; Dixon, D. J. *J. Am. Chem. Soc.* **2013**, *135*, 16348–16351.

(43) Kaboudin, B.; Moradi, K.; Sardarian, A. R. *Arkivoc* **2007**, *13*, 210–217.

(44) Allen, J. G.; Atherton, F. R.; Hall, M. J.; Hassall, C. H.; Holmes, S. W.; Lambert, R. W.; Nisbet, L. J.; Ringrose, P. S. *Nature* **1978**, *272*, 56–58.

(45) Stowasser, B.; Budt, K. H.; Jian-Qi, L.; Peyman, A.; Ruppert, D. *Tetrahedron Lett.* **1992**, *33*, 6625–6628.

(46) Smith, W. W.; Bartlett, P. A. *J. Am. Chem. Soc.* **1998**, *120*, 4622–4628.

(47) Ordonez, M.; Rojas-Cabrera, H.; Cativiela, C. *Tetrahedron* **2009**, *65*, 17–49.

(48) Pettersen, D.; Marcolini, M.; Bernardi, L.; Fini, F.; Herrera, R. P.; Sgarzani, V.; Ricci, A. *J. Org. Chem.* **2006**, *71*, 6269–6272.

(49) Joly, G. D.; Jacobsen, E. N. *J. Am. Chem. Soc.* **2004**, *126*, 4102–4103.

(50) Saito, B.; Egami, H.; Katsuki, T. *Angew. Chemie* **2005**, *117*, 4676–4678.

(51) Yin, L.; Bao, Y.; Kumagai, N.; Shibasaki, M. *J. Am. Chem. Soc.* **2013**, *135*, 10341.

(52) Nakamura, S.; Hayashi, M.; Hiramatsu, Y.; Shibata, N.; Funahashi, Y.; Toru, T. *J. Am. Chem. Soc.* **2009**, *131*, 18240–18241.

(53) Kumar, A.; Sharma, V.; Kaur, J.; Kumar, V.; Mahajan, S.; Kumar, N.; Chimni, S. S. *Tetrahedron* **2014**, *70*, 7044–7049.

(54) George, J.; Sridhar, B.; Reddy, B. V. S. *Org. Biomol. Chem.* **2014**, *12*, 1595–1602.

(55) Schreiner, P. R.; Wittkopp, A. *Org. Lett.* **2002**, *4*, 217–220.

(56) McKenon, M. J.; Meyers, A. I. *J. Org. Chem.* **1993**, *58*, 3568–3571.

(57) Brown, C.; Hudson, R. F.; Maron, A.; Record, K. A. F. *J. Chem. Soc. Chem. Commun.* **1976**, *4*, 663–664.

(58) Kimmel, K.; Robak, M.; Ellman, J. *J. Am. Chem. Soc.* **2009**, *131*, 8754–8755.

(59) Robertson, G. P.; Farley, A. J. M.; Dixon, D. J. *Synlett* **2016**, *27*, 21–24.

(60) Janesko, B. G.; Fisher, H. C.; Bridle, M. J.; Montchamp, J. L. *J. Org. Chem.* **2015**, *80*, 10025–10032.

(61) Fu, X.; Jiang, Z.; Tan, C.-H. *Chem. Commun. (Camb).* **2007**, 5058–5060.

(62) Cho, B.; Tan, C.-H.; Wong, M. W. *Org. Biomol. Chem.* **2011**, *9*, 4550–4557.

(63) Padwa, A.; Krumpe, K. E. *Tetrahedron* **1992**, *48*, 5385–5453.

(64) Kumaraswamy, G.; Jayaprakash, N. *Tetrahedron Lett.* **2010**, *51*, 6500–6502.

(65) Trost, B. M.; Malhotra, S.; Ellerbrock, P. *Org. Lett.* **2013**, *15*, 440–443.

(66) Uraguchi, D.; Sorimachi, K.; Terada, M. *J. Am. Chem. Soc.* **2005**, *127*, 9360–9361.

(67) Hashimoto, T.; Maruoka, K. *J. Am. Chem. Soc.* **2007**, *129*, 10054–10055.

(68) Lu, Z.; Zhang, Y.; Wulff, W. D. *J. Am. Chem. Soc.* **2007**, *129*, 7185–7194.

(69) Williams, A. L.; Johnston, J. N. *J Am Chem Soc* **2004**, *126*, 1612–1613.

(70) Bew, S. P.; Carrington, R.; Hughes, D.; Liddle, J.; Pesce, P. *Adv. Synth. Catal.* **2009**, *351*, 2579–2588.

(71) Terada, M. *Synthesis (Stuttg).* **2010**, 1929–1982.

(72) Phosphoic, C.; Bearing, A.; Backbone, B.; Katoh, T.; Mori, K.; Kanno, K. *Org. Lett.* **2009**, *11*, 1664–1666.

(73) Juhl, K.; Hazell, R. G.; Jorgensen, K. A. *J. Chem. Soc. Perkin Trans.* **1999**, *1*, 2293–2297.

(74) Bachmann, S.; Fielenbach, D.; Jørgensen, K. A. *Org. Biomol. Chem.* **2004**, *2*, 3044–3049.

(75) Dias, H. V. R.; Browning, R. G.; Polach, S. A.; Diyabalanage, H. V. K.; Lovely, C. J. *J. Am. Chem. Soc.* **2003**, *125*, 9270–9271.

(76) Schollkopf, U.; Rieber, N. *Chem. Ber.* **1969**, *102*, 488–493.

(77) Ortín, I.; Dixon, D. J. *Angew. Chemie - Int. Ed.* **2014**, *53*, 3462–3465.

(78) Kanazawa, A. M.; Denis, J.; Greene, A. E. *J. Org. Chem.* **1994**, *59*, 1238–1240.

(79) Song, J.; Wang, Y.; Deng, L. *J. Am. Chem. Soc.* **2006**, *128*, 6048–6049.

(80) Torna, T.; Shimokawa, J.; Fukuyama, T. *Org. Lett.* **2007**, *9*, 3195–3197.

(81) Kaupang, A. .; Bonge-Hansen, T. *Beilstein J. Org. Chem.* **2013**, *9*, 1407–1413.

(82) Ye, T.; Mckervey, M. A. *Chem. Rev.* **1994**, *94*, 1091–1160.

(83) Ford, A.; Miel, H.; Ring, A.; Slattery, C. N.; Maguire, A. R.; McKervey, M. A. *Chem. Rev.* **2015**, *115*, 9981–10080.

(84) Zhu, S.; Zhou, Q. *Acc. Chem. Res.* **2012**, *45*, 1365–1377.

(85) Shishkov, I. V.; Rominger, F.; Hofmann, P. *Organometallics* **2009**, *28*, 1049–1059.

(86) Chen, Y.; Zhang, X. P. *J. Org. Chem.* **2007**, *72*, 5931–5934.

(87) Ruppel, J. V; Cui, X.; Xu, X.; Zhang, X. P. *Org. Chem. Front.* **2014**, *1*, 515–520.

(88) Dzik, W. I.; Xu, X.; Zhang, X. P.; Reek, J. N. H.; de Bruin, B. *J. Am. Chem. Soc.* **2010**, *132*, 18429–18429.

(89) Bodnar, B. S.; Miller, M. J.; Hall, N. S.; Dame, N. *J. Org. Chem.* **2007**, *72*, 3929–3932.

(90) Kadaba, P. K. *Synthesis (Stuttg).* **1990**, *55*, 5891–5894.

(91) Kadaba, P. K. *J.Med.Chem.* **1988**, *31*, 196–203.

(92) Munk, M. E.; Kim, Y. K. *J Am Chem Soc* **1964**, *86*, 2213–2217.

(93) Kuznetsov, A.; Gulevich, A. V.; Wink, D. J.; Gevorgyan, V. *Angew. Chemie - Int. Ed.* **2014**, *53*, 9021–9025.

(94) Hayashi, Y.; Kinoshita, Y.; Hidaka, K.; Kiso, A.; Uchibori, H.; Kimura, T.; Kiso, Y. *J. Org. Chem.* **2001**, *66*, 5537–5544.

(95) Momiyama, N.; Yamamoto, H. *J. Am. Chem. Soc.* **2004**, *126*, 5360–5361.

(96) Kochi, J. K.; Krusic, J. *J. Am. Chem. Soc.* **1970**, *768*, 4114–4115.

(97) Puchot, C.; Samuel, O.; Dunach, E.; Zhao, S.; Agami, C.; Kagan, H. B. *J. Am. Chem. Soc.* **1986**, *108*, 2353–2357.

(98) Douglas, C. J.; Overman, L. E. *Proc. Natl. Acad. Sci. U. S. A.* **2004**, *101*, 5363–5367.

(99) Yin, L.; Otsuka, Y.; Takada, H.; Mouri, S.; Yazaki, R. *Org. Lett.* **2013**, *15*, 698–701.

(100) de la Campa, R.; Gammack Yamagata, A. D.; Ortín, I.; Franchino, A.; Thompson, A. L.; Odell, B.; Dixon, D. J. *Chem. Commun.* **2016**, *52*, 10632–10635.

(101) Yazaki, R.; Kumagai, N.; Shibasaki, M. *J. Am. Chem. Soc.* **2010**, *132*, 5522–5531.

(102) Appel, R.; Chelli, S.; Tokuyasu, T.; Troshin, K.; Mayr, H. *J. Am. Chem. Soc.* **2013**, *135*, 6579–6587.

(103) Appel, R.; Mayr, H. *J. Am. Chem. Soc.* **2011**, *133*, 8240–8251.

(104) Cui, D. M.; Zheng, J. Z.; Yang, L. Y.; Zhang, C. *Synlett* **2010**, *809*, 809–811.

(105) Mao, H.; Lin, A.; Shi, Y.; Mao, Z.; Zhu, X.; Li, W.; Hu, H.; Cheng, Y.; Zhu, C. *Angew. Chemie - Int. Ed.* **2013**, *52*, 6288–6292.

(106) Newman, M. S.; Beal III, P. F. *J. Am. Chem. Soc.* **1950**, *72*, 5163–5165.

(107) Jeener, J.; Meier, B. H.; Bachmann, P.; Ernst, R. R. *J. Chem. Phys.* **1979**, *71*, 4546–4553.

(108) Cuperlovic, M.; Meresi, G. H.; Palke, W. E.; Gerig, J. T. *J. Magn. Reson.* **2000**, *142*, 11–23.

(109) Quirós, M. T.; Angulo, J.; Muñoz, M. P. *Chem. Commun.* **2015**, *51*, 10222–10225.

(110) Harris, R. K. *Magn. Reson. Chem.* **1998**, *36*, 145–149.

(111) Pregosin, P. S. *Coord. Chem. Rev.* **1982**, *44*, 247–291.

(112) Conn, P.; Hall, L. D.; Preston, A. *Carbohydr. Chem.* **1973**, *29*, 522–524.

(113) Farrar, T. C.; Locker, I. C. *J. Phys. Chem.* **1987**, *87*, 3281–3287.

(114) Berger, S.; Kreissl, F. R.; Grant, D. M.; Roberts, J. D. *J. Am. Chem. Soc.* **1975**, *97*, 1805–1808.

(115) Still, B. M.; Kumar, P. G. A.; Aldrich-Wright, J. R.; Price, W. S. *Chem. Soc. Rev.* **2007**, *36*, 665–686.

(116) Zangger, K.; Armitage, L. M. *Met. Based. Drugs* **1999**, *6*, 239–245.

(117) Freeman, R.; Freeman, R.; Wittekoe.S; Wittekoe.S; Ernst, R. R.; Ernst, R. R. *J. Chem. Phys.* **1970**, *52*, 1529-.

(118) Hogben, H. J.; Krzystyniak, M.; Charnock, G. T. P.; Hore, P. J.; Kuprov, I. *J. Magn. Reson.* **2011**, *208*, 179–194.

(119) Lallemand, J. Y.; Soulié, J.; Chottard, J. C. *J. Chem. Soc. Chem. Commun.* **1980**, 436–438.

(120) Habtemariam, A.; Parkinson, J. A.; Margiotta, N.; Hambley, T. W.; Parsons, S.; Sadler, P. J. *J. Chem. Soc. Dalt. Trans.* **2001**, 362–372.

(121) Penner, G. H.; Liu, X. *Prog. Nucl. Magn. Reson. Spectrosc.* **2006**, *49*, 151–167.

(122) Busacca, C. A.; Grossbach, D.; Spinelli, E. *Tetrahedron:Asymmetry* **2000**, *11*, 1907–1910.

(123) Braghiroli, D.; Bella, M. Di. *Tetrahedron: Asymmetry* **1996**, *7*, 2145–2150.

(124) Liu, H.; Du, D. M. *Adv. Synth. Catal.* **2010**, *352*, 1113–1118.

(125) Ye, H.; Liu, R.; Li, D.; Liu, Y.; Yuan, H.; Guo, W.; Zhou, L.; Cao, X.; Tian, H.; Shen, J.; Wang, P. G. *Org. Lett.* **2013**, *15*, 18–21.

(126) Wu, Y. C.; Zhu, J. *J. Org. Chem.* **2008**, *73*, 9522–9524.

(127) Ohno, H.; Anzai, M.; Toda, A.; Ohishi, S.; Fujii, N.; Tanaka, T.; Takemoto, Y.; Ibuka, T. *J. Org. Chem.* **2001**, *66*, 4904–4914.

(128) Boeijen, A.; Van Ameijde, J.; Liskamp, R. M. J. *J. Org. Chem.* **2001**, *66*, 8454–8462.

(129) Mondal, S.; Fan, E. *Synlett* **2006**, *2*, 306–308.

(130) Jones, R. C. F.; Law, C. C. M.; Elsegood, M. R. J. *Arkivoc* **2013**, *2013*, 81–87.

(131) Saitoh, A.; Uda, T.; Morimoto, T. *Tetrahedron:Asymmetry* **1999**, *10*, 4501–4511.

(132) Bera, S.; Panda, G. *Org. Biomol. Chem.* **2014**, *12*, 3976.

(133) T.Kobayashi, H.Kawate, H.Kakiuchi, H. K. *Bull. Chem. Soc. Jpn.* **1990**, *63*, 1937–1942.

(134) Lipshutz, B. H.; Shimizu, H. *Angew. Chemie - Int. Ed.* **2004**, *43*, 2228–2230.

(135) Chen, Y. J.; Chen, C. *Tetrahedron: Asymmetry* **2008**, *19*, 2201–2209.

(136) Kuliszewska, E.; Hanbauer, M.; Hammerschmidt, F. *Chem. - A Eur. J.* **2008**, *14*, 8603–8614.

(137) Pedrosa, R.; Andrés, J. M.; Ávila, D. P.; Ceballos, M.; Pindado, R. *Green Chem.* **2015**, *17*, 2217–

2225.

(138) Rampalakos, C.; Wulff, W. D. *Adv. Synth. Catal.* **2008**, *350*, 1785–1790.

(139) Wenzel, A. G.; Jacobsen, E. N. *J. Am. Chem. Soc.* **2002**, *124*, 12964–12965.

(140) Karimi, B.; Jafari, E.; Enders, D. *Chem. - A Eur. J.* **2013**, *19*, 10142–10145.

(141) Goodman, C. G.; Do, D. T.; Johnson, J. S. *Org. Lett.* **2013**, *15*, 2446–2449.

(142) Toma, T.; Shimokawa, J.; Fukuyama, T. *Org. Lett.* **2007**, *9*, 10–12.

(143) Ideue, E.; Toma, T.; Shimokawa, J.; Fukuyama, T. *Org. Synth.* **2012**, *89*, 501–509.

(144) Bolsones, M.; Bonge-Hansen, H. T.; Bonge-Hansen, T. *Synlett* **2014**, *25*, 221–224.

(145) Zhao, W.; Lu, Z.; Wulff, W. D. *J. Org. Chem.* **2014**, *79*, 10068–10080.

(146) Benfatti, F.; Yilmaz, S.; Cozzi, P. G. *Adv. Synth. Catal.* **2009**, *351*, 1763–1767.

(147) Chen, Y.; Fields, K. B.; Zhang, X. P. *J. Am. Chem. Soc.* **2004**, *126*, 14718–14719.

(148) Xia, W.; Salmeia, K. A.; Vagin, S. I.; Rieger, B. *Chem. - A Eur. J.* **2015**, *21* (11), 4384–4390.

(149) Bredihhin, A.; Mäeorg, U. *Tetrahedron* **2008**, *64*, 6788–6793.

(150) Pícha, J.; Vanek, V.; Budesínsky, M.; Mladková, J.; Garrow, T. A.; Jiracek, J. *Eur. J. Med. Chem.* **2013**, *65*, 256–275.

(151) Calí, P.; Begtrup, M. *Synthesis (Stuttg).* **2002**, *2002*, 63–66.

(152) WO2011/009943 A1. 2011.

(153) Yazaki, R.; Kumagai, N.; Shibasaki, M. *J. Am. Chem. Soc.* **2010**, *132*, 10275–10277.